Zirconium and Lanthanide Complexes Supported by Chelating Diamido Ligands

by

Paul Eric O'Connor
B.Sc., Mount Allison University, 1999

A Dissertation Submitted in Partial Fulfillment of the
Requirements for the Degree of

DOCTOR OF PHILOSOPHY

in the Department of Chemistry

Supervisor: Dr. David J. Berg

Abstract

A series of zirconium complexes supported by the chelating diamido ligand $(C_6F_5NHCH_2CH_2OCH_2)_2$ (H_2(NOON)) have been prepared. These complexes include (NOON)$Zr(CH_2Ph)_2$, (NOON)$ZrMe_2$, (NOON)$ZrCl_2$, and (NOON)$ZrCl[N(SiMe_3)_2]$. (NOON)$ZrMe_2$ and (NOON)$ZrCl[N(SiMe_3)_2]$ were crystallographically characterized and for all the complexes, the ligand NMR spectra were consistent with a fluxional process occurring in solution. When (NOON)$Zr(CH_2Ph)_2$ was exposed to 435 nm light, a photochemical reaction occurred which resulted in C-F bond activation and the formation of (NOON)ZrF_2 and a metallated dimer. When (NOON)$ZrCl_2$ was treated with MAO, it showed modest activity as an ethylene polymerization catalyst.

A series of zirconium complexes supported by 1,4,8,11-tetraazabicyclo[6.6.2]hexadecane (H_2(CBC)) have been prepared and characterized. (CBC)$Zr(CH_2Ph)N(Bu^t)C(H)$=$CHPh$, (CBC)$Zr(O\text{-}2,6\text{-}C_6H_3Me_2)_2$, (CBC)$Zr(OSi(Bu^t)_2H)_2$, (CBC)$Zr(CH_2SiMe_3)_2$, (CBC)$ZrC_4Ph_4$ were crystallographically characterized and (CBC)$Zr(CH_2Ph)(O\text{-}2,6\text{-}C_6H_3Bu^t_2)$, (CBC)$Zr[\kappa^2(C,O)\text{-}OC_6H_3(6\text{-}Bu^t)(2\text{-}CMe_2CH_2)]$, (CBC)$ZrCl_2$, (CBC)$ZrCl[N(SiMe_3)_2]$ and (CBC)$ZrMe_2$ were fully characterized. Treatment of (CBC)$ZrMe_2$ with MAO does not result in an active ethylene polymerization catalyst. The metallacycle (CBC)ZrC_4Ph_4 reacts with thionyl chloride and dichlorophenylphosphine to yield tetraphenylthiophene oxide and pentaphenylphosphole respectively.

Treatment of $Yb[N(SiMe_3)_2]_2(OEt_2)_2$ with H_2(CBC) results in the sparingly soluble coordination polymer $[(CBC)Yb]_n$ and two byproducts of this reaction were crystallographically characterized. One was the mixed valence salt $\{[(\mu\text{-CBC})Yb]_3(\mu^3\text{-}O)\}^+\{Yb[N(SiMe_3)_2]_3\}^-$, while the other was $\{[(\mu\text{-CBC})Yb]_3(\mu^3\text{-}O)\}^+I^-$. In both cases the cation is a trimer of ytterbium (III) ions bridged by an oxygen and three amido nitrogens from the (CBC) ligand.

Table of Contents

List of Tables

List of Figures

List of Schemes

List of Abbreviations

CBC	1,4,8,11-tetraazabicyclo[6.6.2]hexadecane
Cp	cyclopentadienyl
Cp*	pentamethylcyclopentadienyl
Cy	cyclohexyl
Da	Daltons
DA	generic diamido ligand
DAC	4,13-diaza-18-crown-6
DME	dimethoxyethane
Ln	lanthanide (Y, La-Lu)
MAC	aza-18-crown-6
MAO	methylaluminoxane
NBS	N-bromosuccinimide
NCS	N-chlorosuccinimide
NOON	$(C_6F_5NCH_2CH_2OCH_2)_2$
r.t.	room temperature
THF	tetrahydrofuran
TMS	tetramethylsilane
VT	variable temperature

List of Numbered Compounds

1	$C_6F_5N(H)CH_2CH_2OCH_2CH_2OCH_2CH_2N(H)C_6F_5$
2	$(NOON)Zr(CH_2Ph)_2$
3	$(NOON)ZrCl_2$
4	$(NOON)ZrCl[N(SiMe_3)_2]$
5	$(NOON)ZrMe_2$
6	$[(C_6F_4NCH_2CH_2OCH_2CH_2OCH_2CH_2NC_6F_5)ZrCH_2Ph]_2$
7	$[(NOON)ZrF_2]_n$
8	$[(NOON)Zr(CH_2Ph)]^+[PhCH_2B(C_6F_5)_3]^-$
9	1,4,8,11-tetraazabicyclo[6.6.2]hexadecane
10	$(CBC)Zr(CH_2Ph)_2$
11	$(CBC)Zr(CH_2Ph)N(Bu^t)C(H)=C(H)Ph$
12	$(CBC)Zr(CH_2Ph)(OC_6H_3Bu^t_2)$
13	$(CBC)Zr[\kappa^2(C,O)\text{-}OC_6H_3(6\text{-}Bu^t)(2\text{-}CMe_2CH_2)]$
14	$(CBC)Zr(OSi(Bu^t)_2H)_2$
15	$(CBC)Zr(OC_6H_3Me_2)_2$
16	$(CBC)ZrCl_2$
17	$(CBC)ZrCl[N(SiMe_3)_2]$
18	$(CBC)ZrMe_2$
19	$(CBC)Zr(CH_2SiMe_3)_2$
20	$(CBC)Zr(C_4Ph_4)$
21	$(CBC')Zr(C_4Ph_4H)$

22	tetraphenylthiophene oxide
23	pentaphenylphosphole
24	$\{[(CBC)Yb]_3O\}^+\{Yb[N(SiMe_3)_2]_3\}^-$
25	$\{[(CBC)Yb]_3O\}^+I^-$
26	$[(CBC)Yb]_n$

Acknowledgements

I would like to thank my supervisor Dr. David J. Berg for much guidance, latitude and many fruitful discussions. Also, I would like to thank the other members of the Berg group, past and present, for their help and cooperation.

Several people deserve recognition for their contributions to this work. The crystal structures reported here were solved by Drs. David Berg, Tosha Barclay and Brendan Twamley. Ms. Chris Greenwood carried out the two dimensional NMR spectra refered to here and trained me to operate the NMR instruments. Also, I would like to thank the staff of the electronic, mechanical and glassblowing shops as well as stores and the front office for all the support over the years. Finally, I want to acknowledge the work of several undergraduates who developed the synthesis of the H_2(NOON) ligand and began work on the first project reported here.

Dedication

There are several people who played key roles in the completion of this thesis: my parents, who endured countless hours in museums and the like to encourage my interest in science; my brother, who never let my head get too big; my second set of parents, who made sure I had quiet time away from the lab; and my wife, who loved me unconditionally despite my inner geek. Thanks to all of you for everything leading up to and beyond this achievement.

Chapter 1: Introduction.

1.1 Historical Perspective.

The discovery of ferrocene in 1951 marked the start of a new era in organometallic chemistry.[1,2] The use of cyclopentadienyl as a spectator ligand was rapidly expanded to other transition elements. The success of this class of ligand has been phenomenal. It has been estimated that 80% of the known organometallic species contain a cyclopentadienyl ligand, most either $C_5H_5^-$ (Cp) or $C_5Me_5^-$ (Cp*); however, countless derivatives have been prepared.[3]

The first reported zirconocene, Cp_2ZrCl_2, was reported in 1953 shortly after the discovery of ferrocene.[4] In the subsequent 50 years, an enormous number of zirconium compounds have been reported from Zr (0) to Zr(IV) and Zr(IV) cations.[5-12] Zirconium compounds with one to four cyclopentadienyl ligands are known, although bent metallocenes, Cp_2ZrX_2 are by far the most common and well studied.

By contrast, the first well characterized monomeric zirconium amide, $Zr(NMe_2)_4$ was not reported until 1959.[13] The chemistry of zirconium amides was relatively unexplored compared to that of the zirconium alkyls for the next 30 years largely due to the lower reactivity of the amides. It is this very property that has led to the resurgence in zirconium amido chemistry. The past 10 years have seen the widespread use of diamido spectator ligands to support the metal center, as an alternative to two cyclopentadienyl ligands.

1.2 Applications of Organozirconium Chemistry.

1.2.1 Properties and Uses of Zirconium.

While the lower oxidation states of zirconium (0^6, II^7, and III^8) have been studied, the highest oxidation state (IV)[9-12] is the one that predominates in applied organometallic chemistry. Since zirconium (IV) is d^0, Cotton and Wilkinson describe the ion as ". . . relatively large, highly charged, and spherical, with no partly filled shell to give it stereochemical preferences. Thus it is not surprising that zirconium (IV) compounds exhibit high coordination numbers and a great variety of coordination polyhedra."[14] The relatively large size of zirconium (IV) compared to titanium (IV) (0.72 vs 0.605 Å for six coordinate compounds)[15] accounts for much of the difference in the chemistry between these two elements. Likewise, the comparable size of zirconium and hafnium (IV) (0.72 vs 0.71 Å for six coordinate complexes) accounts for the very similar chemistry of these two ions.

As a consequence of the high charge of zirconium (IV) and its large size, the metal centre is Lewis acidic. This property not only makes organozirconium complexes useful as olefin polymerization catalysts (*vide infra*) but also as Lewis acid catalysts. For example, the Oppenauer oxidation / Meerwein-Ponndorf-Verley reduction allows for the reduction of aldehydes and ketones under mild conditions, even in the presence of C=C bonds conjugated with the C=O moiety.[16]

(1) 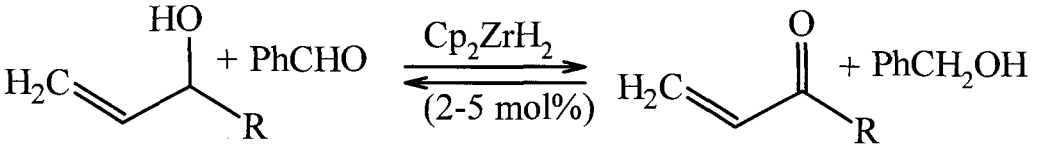

Insertion of unsaturated species such as carbon monoxide, carbon dioxide, alkenes, alkynes, isocyanides, nitriles, isocyanates or sulfur dioxide into the organozirconium moiety has been observed and shows the range of transformations that can occur. $[Cp_2ZrClH]_n$ (Schwartz' reagent) was one of the first organozirconium species to see widespread use in the hydrozirconation of alkenes and alkynes. This furnishes an organozirconium species which can be cleaved directly or subjected to further insertions before the organic group is cleaved from the metal.[17]

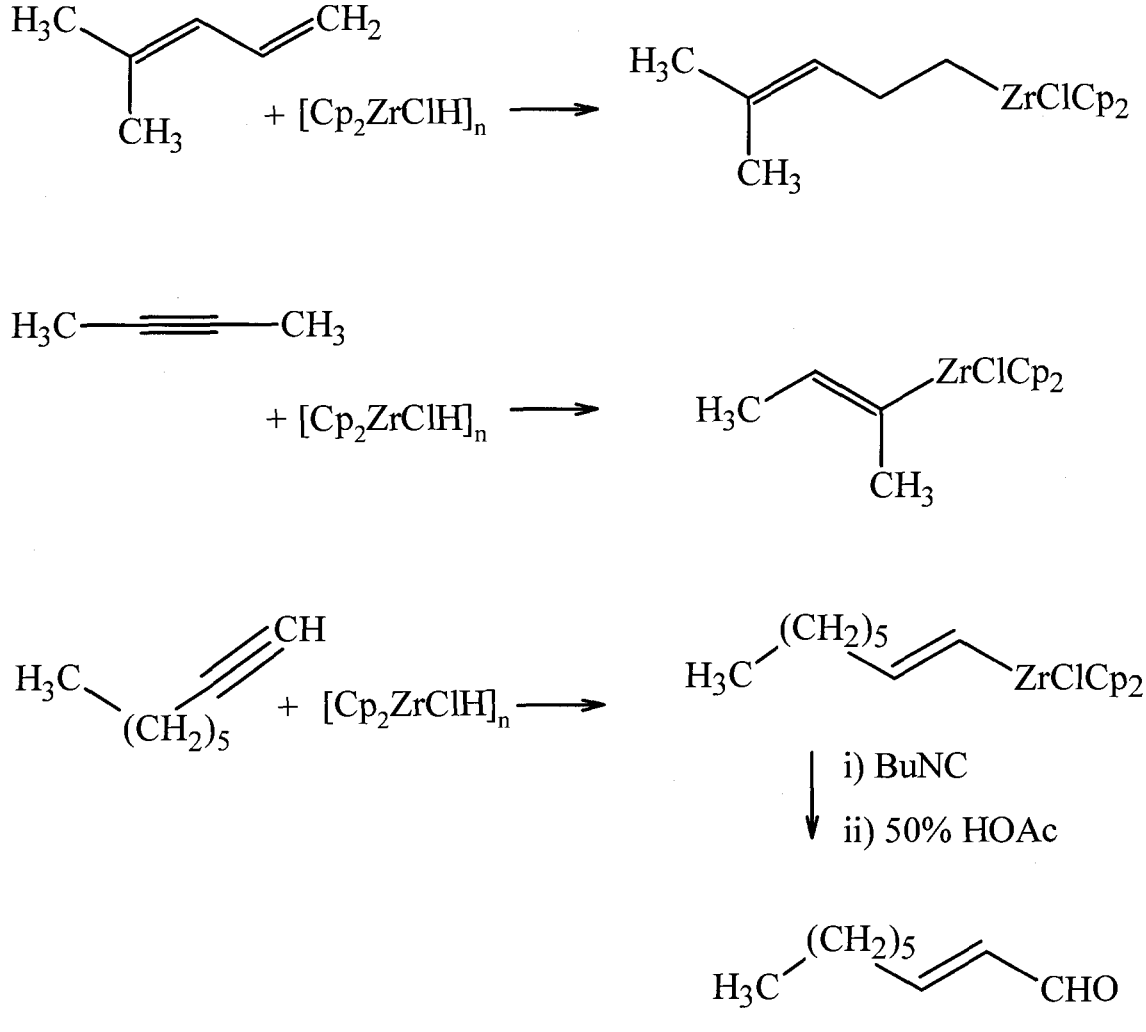

Scheme 1. Hydrozirconation.

Another property that makes organozirconium species so useful is the nucleophilicity of the organic group. In addition to the direct reactions of the metal-carbon bond illustrated below, the organozirconium reagent is also useful as a transfer reagent. The organic group can be transferred stoichiometrically to a main group element such as boron, aluminum, tin, mercury or transferred *in situ* to another transition metal, typically copper, nickel or palladium, for catalytic carbon-carbon bond formation.[17]

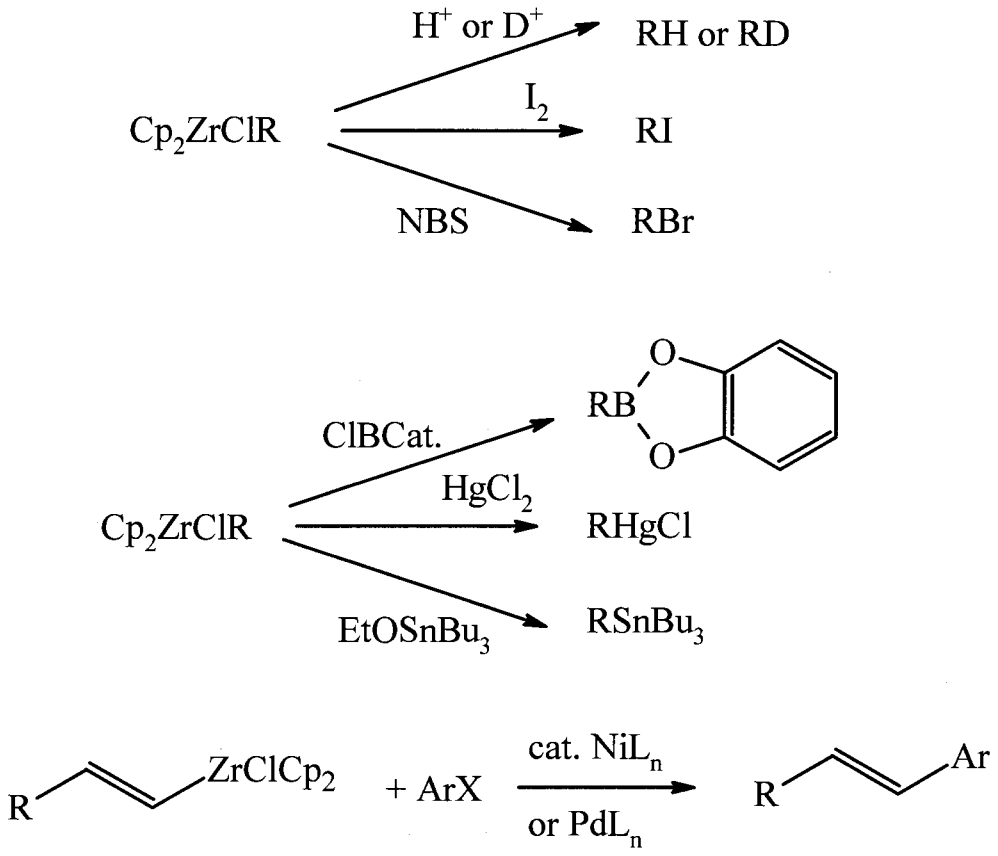

Figure 1. Nucleophilic Reactions.

A third area in which organozirconium chemistry has been exploited is in cyclization reactions. The basicity of the carbon-zirconium bond allows for the formation of benzynes and other metallacylopropenes. These intermediates react with a variety of

unsaturated species[18] and can be used to cyclize substrates.[19] Scheme 2 shows work by Buchwald and coworkers, the synthesis of an intermediate in the preparation of several tetrahydropyrroloquinoline natural products. This strategy relies on the formation of an organometallic species with both an aryl and methyl group bound to zirconium. Loss of methane from this intermediate results in a zirconacyclopropane, a "benzyne", intermediate which can then undergo further insertion reactions.

A similar strategy has been popularized by Negishi and coworkers. In this case, treatment of Cp_2ZrCl_2 with two equivalents of ^nBuLi results in the dialkyl species, which eliminates butane to afford the metallacyclopropane intermediate. These species can then undergo reaction with a number of unsaturated substrates, including organic compounds with conjugated multiple bonds (typically an eneyne) to form a cyclized product. This has been used in the synthesis of several natural products.[20] Moreover, this strategy can also be used to cyclize alkynes to produce a zirconacyclopentadiene. As was outlined above, organozirconium species are nucleophilic and this has been exploited to transfer the metallacycle from zirconium to a wide range of main group elements (Scheme 3).[21] The metallacyclopentadiene may be isolated, or simply generated *in situ* for the one-pot synthesis of the heterocycle.

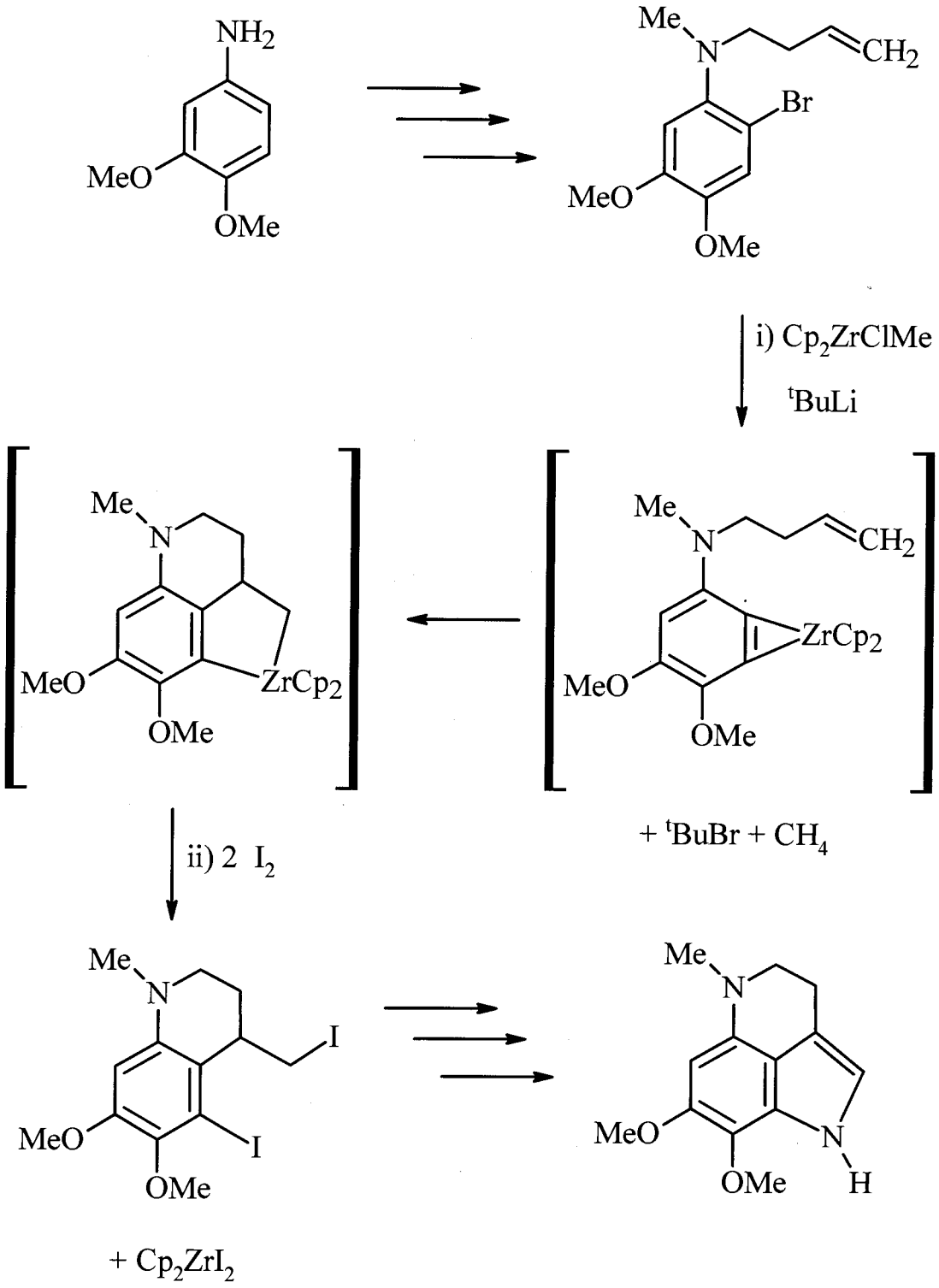

Scheme 2. Synthesis of a Natural Product Intermediate.

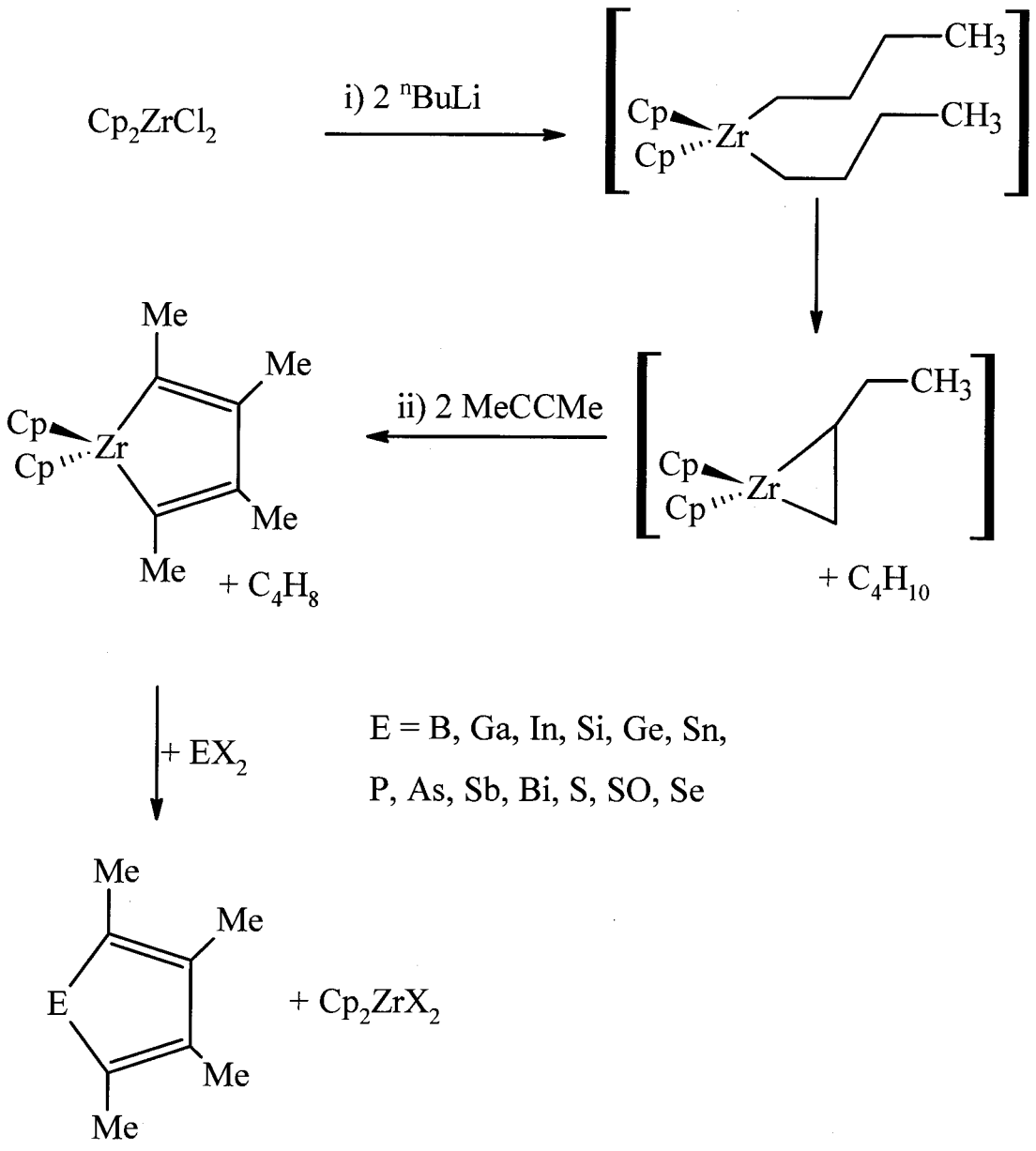

Scheme 3. Synthesis of Heterocycles.

1.2.2 Limitations of Organozirconium Chemistry.

The high Lewis acidity of organozirconium species constrains the solvent choice. Lewis basic solvents such as THF and pyridine are notorious for their coordination to the

metal centre. This can be used to advantage, for example in the solid state zirconium tetrachloride exists as a polymer with chloride bridges between metals, while addition of THF results in $ZrCl_4(THF)_2$ which has greater solubility in aromatic solvents than the polymer. However, the coordinated solvents usually reduce the activity of the catalyst and may be difficult or impossible to remove subsequently, or in the case of pyridine may react with organozirconium bonds to produce the *ortho* metallated species.[22]

Along with being nucleophilic, organozirconium species and zirconium amides are basic; accordingly, they are moisture sensitive, except for those cases where the metal centre is extremely crowded. This is one of the serious limitations of this type of chemistry. All solvents to be used must be rigorously dried - typically distilled from benzophenone-sodium. Also, solvents must be free from acidic protons; in this context that means a pKa greater than about 35. Moreover, these species are oxygen sensitive so an inert atmosphere must be used when handling these compounds.

1.2.3 Olefin Polymerization.

An important industrial aspect of organozirconium chemistry is the production of polyolefins. The scale of world production of polyethylene and polypropylene is staggering. The estimated world demand for polyethylene was 55 million metric tons in 2002 and this is expected to rise to 87 million metric tons by 2010. Likewise, polypropylene demand is expected to rise from 35 million metric tons to 60 million metric tons over the same time period.[23] Canadian production of polyethylene is 4.7 million metric tons and 0.9 million metric tons of polypropylene currently.[24]

In the early 1950's Karl Ziegler discovered that a heterogeneous mixture of aluminum alkyls and group 4 or 5 metal salts would catalyze the polymerization of ethylene under milder conditions than the original radical process. While Karl Ziegler investigated the polymerization of ethylene, Guilio Natta investigated the polymerization of propylene and found that $TiCl_3$ and aluminum alkyls catalyzed the production of polypropylene.[25] This was a breakthrough since α-olefins could not be polymerized by the radical polymerization process used for ethylene. Indeed, Ziegler and Natta were awarded the 1963 Nobel Prize in Chemistry for this work.

Perhaps just as important as the fact that this system was highly active for propylene polymerization was that the polymer produced was isotactic polypropylene (Fig 2). Isotactic polypropylene has a regular ordering of the methyl groups along the polymer backbone, which allows for the polymers to crystallize. This imparts high strength as well as solvent and chemical resistance. By contrast, atactic polypropylene lacks an ordering of the methyl groups, leading to an amorphous structure and consequently poorer physical strength.

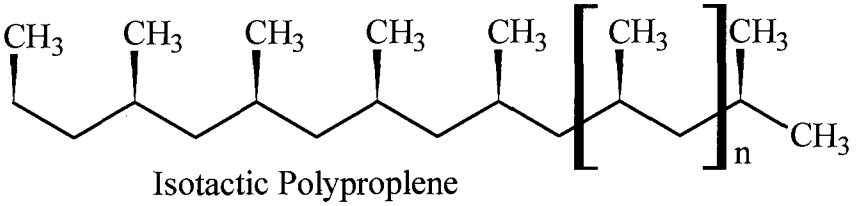

Isotactic Polyproplene

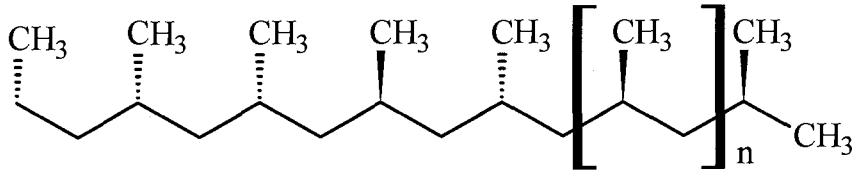

Atactic Polypropylene

Figure 2. Two Types of Polypropylene.

During the late 1970's it was discovered that addition of water to a mixture of titanium or zirconium metallocenes and trimethylaluminum resulted in highly active homogenous olefin polymerization catalysts.[26] This ill-defined aluminum species that results from the partial hydrolysis of trimethylaluminum is known as methylaluminoxane (MAO: roughly $[MeAlO]_n$ n = 6-20)[27,28] MAO does have several advantages: it reacts with any water, it can be used with metallocene dichloride species since it both alkylates and subsequently abstracts the alkyl group to produce the metallocene alkyl cation needed for polymerization. However, it is typically used in 500-10 000 mole equivalents of the group 4 metal, which results in the cost of the MAO being several times that of the other metal. Accordingly, several well defined systems based on boron were developed, which can be used in stoichiometric quantities:

(2) $Cp_2ZrMe_2 + B(C_6F_5)_3 \longrightarrow$ 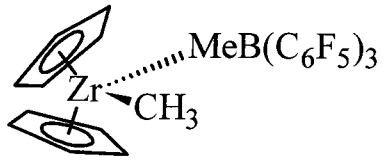

(3) $Cp_2ZrMe_2 + [Ph_3C]^+[B(C_6F_5)_4]^- \longrightarrow$ 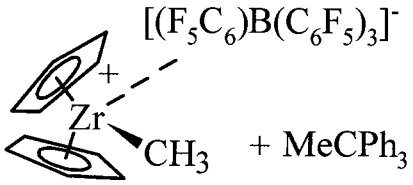

(4) $Cp_2ZrMe_2 + [HNMe_2Ph]^+[B(C_6F_5)_4]^- \longrightarrow$ 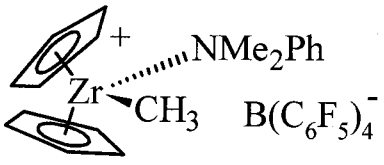

Another strategy that avoided the use of MAO was the use of organolanthanide catalysts. Since Cp^*_2LnR is isoelectric with Cp_2ZrR^+, the organolanthanides do not need

to be activated with an aluminum or borane cocatalyst. Some of these systems have shown incredibly high initial activity for polyethylene production in very short polymerization runs (*ca* 5 seconds), but most show modest activity during longer runs.[29,30]

This discovery of homogenous olefin polymerization catalysts led to an intense research effort to develop new catalysts. Ultimately, the rigid and chiral *ansa* metallocenes (Fig 3) were found to be more than an order of magnitude more active than the best of the heterogeneous catalysts for the production of isotactic polypropylene with group 4 metals.[31] The homogeneity of the active site, relative to the heterogeneous systems, was thought to account for the lower polydispersity of the resulting polymer.

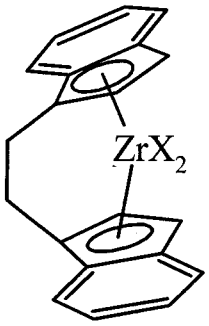

Figure 3. An *Ansa*-Metallocene Catalyst.

The rigid chiral *ansa* metallocenes do have enormous potential, but they have some drawbacks – namely they have limited temperature stability and tend to produce lower molecular weight material under industrial conditions.[26] The solution to this problem has been to replace one of the cyclopentadienyl units in the *ansa* metallocenes with amido donor to give the constrained geometry catalysts (Fig 4), which have been developed by Dow and Exxon.[29]

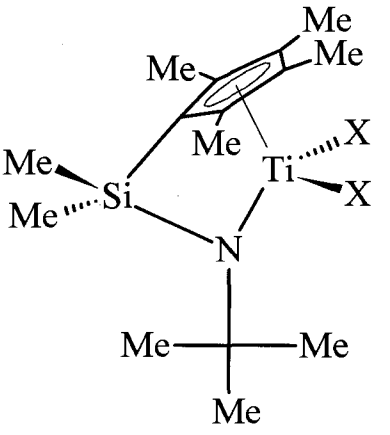

Figure 4. A Constrained Geometry Catalyst.

Not only do these catalysts show better thermal stability than the metallocene systems, but they also produce higher molecular weight material. In ethylene copolymerization, these systems have shown increased incorporation of higher α-olefins into the polymer. In propylene polymerization, the constrained geometry catalysts generally produce the less desirable atactic polypropylene, albeit as very high molecular weight polymer.[26] This remains an area for improvement in these systems.

There have been many major breakthroughs in the development of olefin polymerization systems over the past 50 years. If one traces the progression of the homogeneous catalyst systems (Fig 5), the trend has been from the metallocenes to linked (*ansa*) metallocenes to linked cyclopentadienyl-amido (constrained geometry catalysts). Many different research groups have concluded that the next logical step in this progression may be linked amido-amido ligands (diamides) and numerous new ligands have been developed.

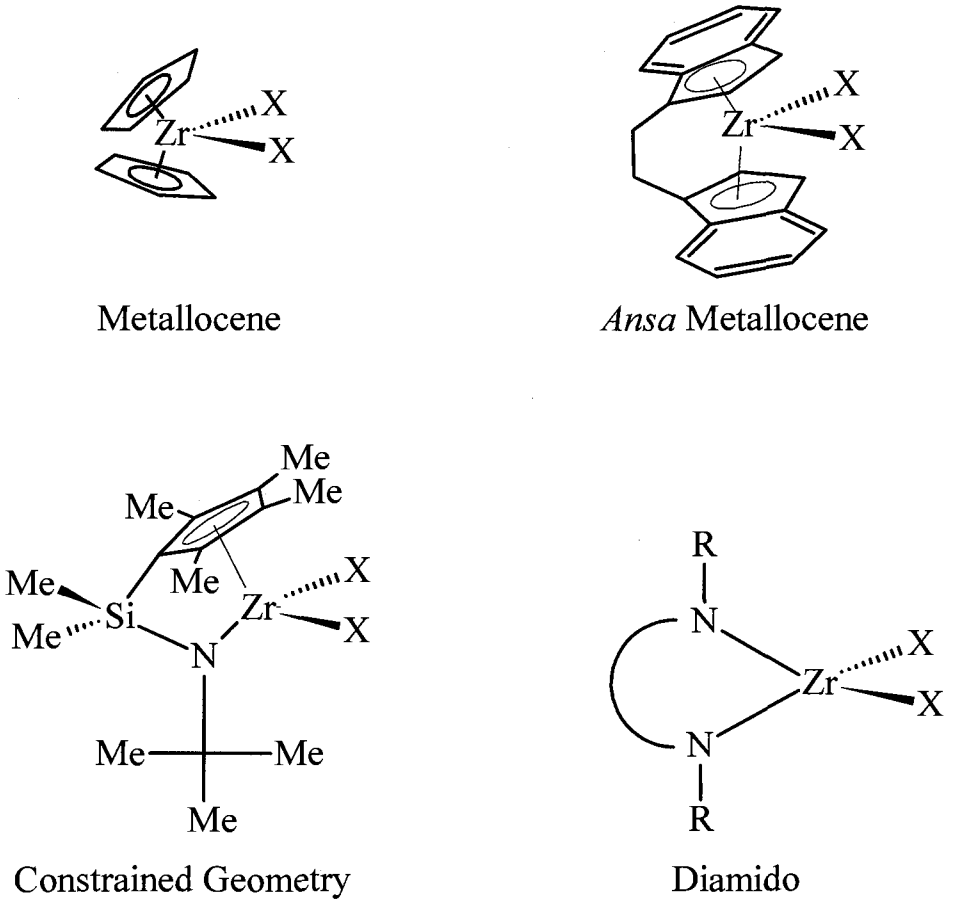

Figure 5. Evolution of Polymerization Catalysts.

1.3 Zirconium Diamido Complexes.

Diamido ligands span a range of sizes and number of additional donors. The smallest are the simple diamides such as $Bu^tNSiMe_2NBu^t$ and in this area research has focused almost exclusively on new olefin polymerization catalysts. The next class have diamides with one additional neutral donor, typically an ether, amine or pyridine although some have phosphines or sulfides. Again in this area the focus has been on developing polymerization catalysts. Finally, the systems that have diamides with two donors or two delocalized anions (porphyrin and tetraazaannulene macrocycles) have been studied. The

focus in this area is more on the stoichiometric reactions: insertions of CO, isocyanides or reduction of dinitrogen although polymerization activity is occasionally reported. The following sections present a selective summary of the nitrogen based ligands that have been successfully used to support zirconium complexes.

1.3.1 Diamides Without Additional Donors.

1.3.1.1 Four-Membered Chelate Rings.

The diamido ligands that form four-membered chelate rings are shown in Fig 6. Burger and coworkers were the first to investigate the diamide ligands in the late 1970's and early 1980's. The focus was on making homoleptic spiro compounds ($\mathbf{DA}_2M$) of group 4 and 14 elements (Fig 7). One consequence of joining two amides together is a reduction in steric shielding of the metal. For example, despite forcing conditions $ZrCl[N(SiMe_3)_2]_3$ does not react with $NaN(SiMe_3)_2$;[32] however, $Zr(\mathbf{L^{II}})_2$ forms readily.[33] In fact, this has often been a problem with many of the diamido (**DA**) ligands (of all chelate sizes) – the spiro compound is formed when zirconium tetrachloride and the lithium salts are mixed, regardless of stoichiometry (Eq 5). These compounds do polymerize ethylene under high pressure, but lack sufficient steric protection of the metal centre. For example, Horton and coworkers studied several cationic complexes with $\mathbf{L^{II}}$. These complexes all suffered from low reactivity and did not catalyse polymerization when followed by NMR. The sterically open cations all had Lewis bases that coordinated more strongly than ethylene - be it coordination of an aryl ring from the benzyl group, coordination of the anion or coordination of NMe_2Ph.[34]

(5) $\quad Li_2(\mathbf{DA}) + ZrCl_4 \text{ (excess)} \rightarrow 0.5\ (\mathbf{DA})_2Zr + 2\ LiCl$

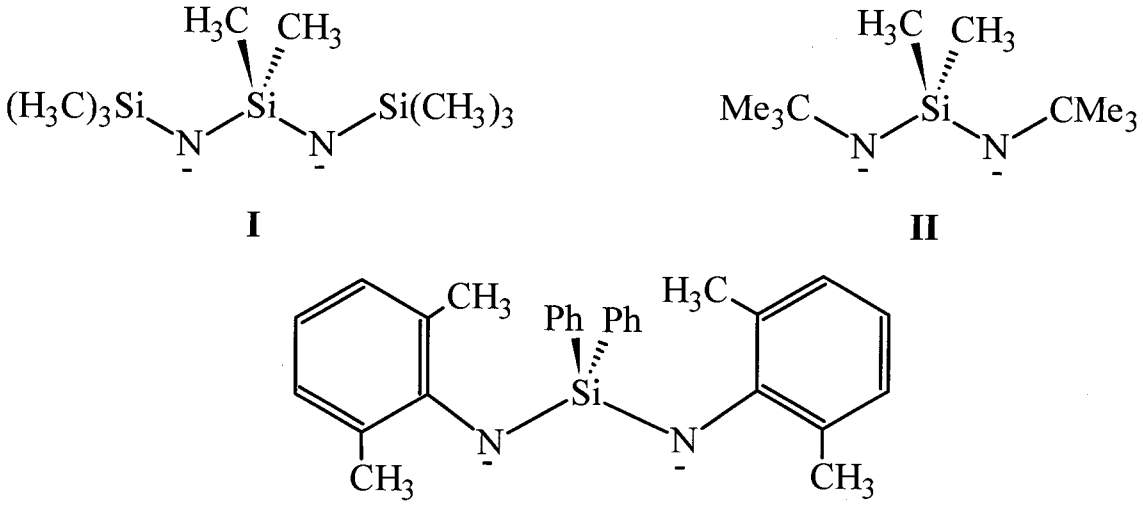

Figure 6. Four-Membered Chelate Rings: I,[35] II,[33,34] III.[36]

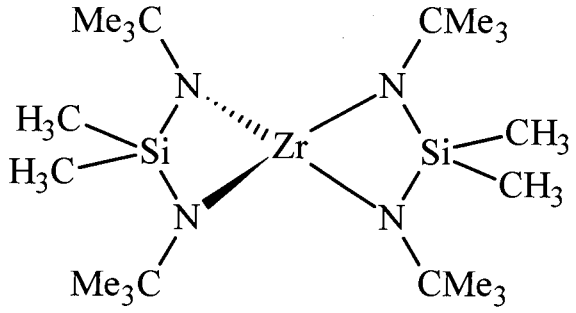

Figure 7. A Spirocyclic Zirconium Complex, $(L^{II})_2Zr$.

1.3.1.2 Five-Membered Chelate Rings.

As outlined in Eq 5, formation of spiro compounds is often a problem with these types of diamido ligands and this was found to be the case with ligands L^{IV}, L^{VIII} and L^{IX} (Fig 8). In the case of $(L^{IX})_2Zr$ it was never tested as an ethylene polymerization catalyst;[37] however, the other two compounds $(L^{IV})_2Zr$ and $(L^{VIII})_2Zr$ were tested.[38,39]

Somewhat surprisingly, when these compounds were treated with excess MAO, ethylene polymerization took place. Presumably, ligand transfer from zirconium to MAO occurred to produce an active $[\mathbf{DA}ZrMe]^+$ species. While the loss of one of the ligands from the spiro compound is a necessary prerequisite for olefin polymerization, it does raise the concern that the second ligand could be transferred, thereby resulting in an unstable or inactive catalyst. This has been modeled with trimethylaluminum and $(\mathbf{L}^{\mathbf{XIIIa}})ZrCl_2$, which react to yield $(\mathbf{L}^{\mathbf{XIIIa}})(AlMe_2)_2$ (Fig 9).[40]

$(\mathbf{L}^{\mathbf{VI}})ZrBz_2$ and $(\mathbf{L}^{\mathbf{VIIb}})ZrCl_2$ are both active ethylene polymerization catalysts. However, they are far from ideal. In the case of the former, the copolymerization with 1-octene yielded high molecular weight material, but the polydispersity was extremely large (38.9). With the latter, the polymer was not studied and the reaction with propylene yielded an oil.

1.3.1.3 Six-Membered Chelate Rings.

One of the early successes of the diamido systems was $(\mathbf{L}^{\mathbf{XIa}})TiMe_2$ which was a highly active catalyst for the living polymerization of 1-hexene at room temperature (Fig 9).[41] When the polymerization was carried out in dichloromethane, the resulting atactic polyhexene had a high molecular weight and narrow polydispersity (M_n > 120 000 $gmol^{-1}$, M_w/M_n 1.07).[30] Treatment of $(\mathbf{L}^{\mathbf{XIa}})TiMe_2$ with $B(C_6F_5)_3$ initially results in abstraction of a methyl group; this species evolves methane and results in transfer of a C_6F_5 ring to titanium.[42] This is a possible deactivation pathway, since the resulting species is inactive as a catalyst and may account for the instability of the active species in the absence of excess monomer.

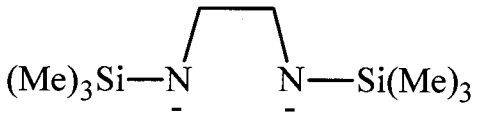

IV

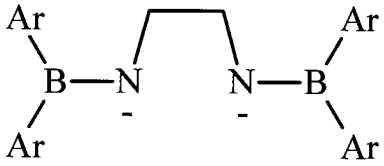

Va Ar = Cy

Vb Ar = Mes

Vc Ar = 2,4,6-$C_6H_2{}^iPr_3$

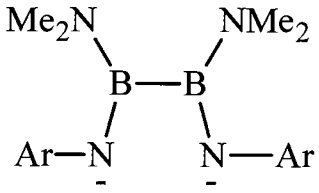

VI Ar = 2,6-$C_6H_3{}^iPr_2$

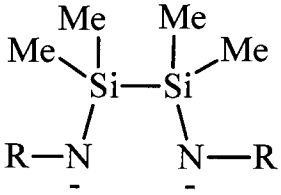

VIIa R = ^{t}Bu

VIIb R = 2,6-$C_6H_3{}^iPr_2$

VIIc R = 4-C_6H_4F

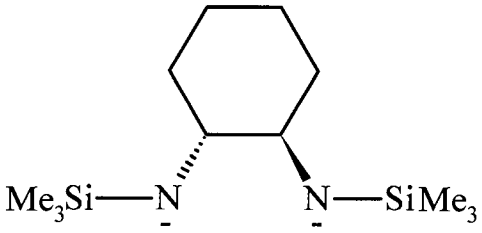

VIII

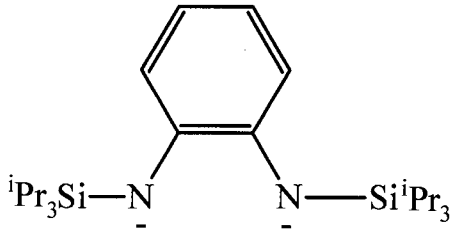

IX

Xa R = ^{i}Pr

Xb R = Np

Figure 8. Five-Membered Chelate Rings: IV,[38] V,[43,44] VI,[45] VII,[46]VIII,[39] IX,[37,47] X.[48,49]

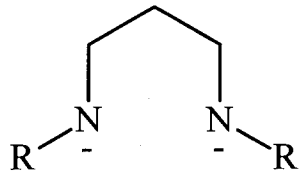

XIa R = 2,6-$C_6H_3{}^iPr_2$

XIb R = 2,6-$C_6H_3Me_2$

XIc R = C_6F_5

XId R = $SiMe_3$

XIe R = Si^iPr_3

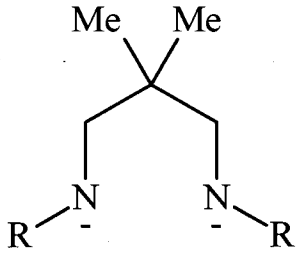

XII R = Si^tBuPh_2

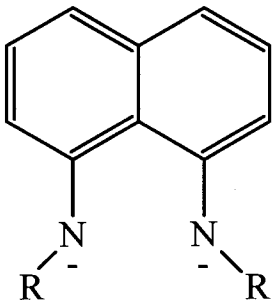

XIIIa R = $SiMe_3$

XIIIb R = Si^iPr_3

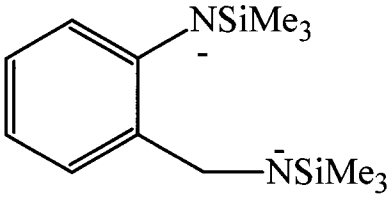

XIV

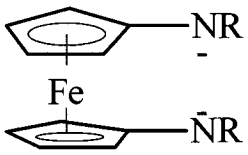

XVa R = $SiMe_3$

XVb R = CH_2Ph

XVc R = Ph

Figure 9. Six-membered Chelate Rings: XI,[22,40,50-53] XII,[54] XIII,[40,55] XIV,[56] XV.[57-59]

In contrast, the zirconium analogue, $(\mathbf{L}^{\mathbf{XIa}})ZrMe_2$ is completely inactive as a catalyst when activated with $B(C_6F_5)_3$. When MAO is used, the resulting polymer is bimodal with both high polymer and oligomers present. This suggests that at least two active species are present in solution. It has also been suggested that in the $(\mathbf{L}^{\mathbf{XIa}})ZrMe_2$ $/B(C_6F_5)_3$ system the anion is strongly bound to the metal centre. This is consistent with larger size of zirconium and is consistent with Schrock's work on zirconium diamido systems bearing additional donors that function as efficient catalysts for 1-hexene polymerization (Section 1.3.2).

1.3.1.4 Larger Chelate Rings.

As one might expect, moving to a larger ligand generally improves the polymerization behaviour of the zirconium catalyst (Fig 10). When the four-membered chelating ligand $(\mathbf{L}^{\mathbf{III}})Zr(NMe_2)_2(NHMe_2)$ and the analogous seven-membered chelating ligand $(\mathbf{L}^{\mathbf{XVI}})Zr(NMe_2)_2$ (Fig 10) were tested under the same conditions, the latter proved to be an active ethylene polymerization catalyst while the former was rapidly deactivated. The difference is a consequence of the smaller bite angle in $\mathbf{L}^{\mathbf{III}}$, the amido nitrogens are part of a four-membered ring; accordingly, the aryl substituents are directed away from the metal. In contrast, the seven membered ring in $\mathbf{L}^{\mathbf{XVI}}$ results in the aryl groups being directed towards the metal centre and providing steric protection to the metal.[36]

$(\mathbf{L}^{\mathbf{XVIII}})ZrX_2$ (X = Cl, Me) is the only example of a diamido system without additional donors that polymerizes α-olefins in a living manner. For a full discussion of the criteria for living polymerization see Coates recent review.[30,60] Some of the key features of living polymerization are a linear increase in number average molecular

weight with increased conversion, narrow polydispersity ($M_w/M_n \approx 1$), complete conversion of all monomer and further chain growth with further monomer addition (if a different monomer is added a block copolymer results). This system has shown activity comparable to that of the Cp_2ZrCl_2/MAO system and the ability to polymerize a range of olefins: ethylene, propylene, 1-hexene, 1-octene and block copolymers of 1-hexene and 1-octene with high activities and relatively narrow polydispersities (1.23-2.35 at 0 and 22°C). Once again, the solid state structure sheds some light on the success of this system; the two aryl groups of the backbone are oriented above and below the ZrN_2 plane and the bulky Si^iPr_3 groups also provide steric protection of the metal centre.

1.3.2 Zirconium Diamido-Donor Complexes.

Like the organozirconium chemistry of the simple diamido ligands, the diamido donor chemistry focuses on olefin polymerization; Schrock and coworkers have published extensively in this area and have reported three different systems for the living polymerization of 1-hexene. These ligands have also been used as supporting systems for interesting organotitanium species such as metallacycles,[61] imides[62] and alkylidenes;[63] however, as might be anticipated from the size difference between these metals, the titanium systems are typically less active than the corresponding zirconium systems for polymerization.

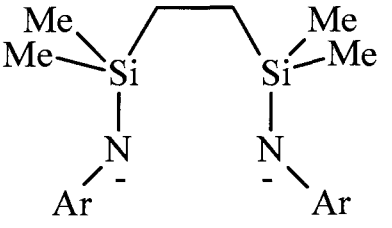

XVI Ar = 2,6-$C_6H_3Me_2$

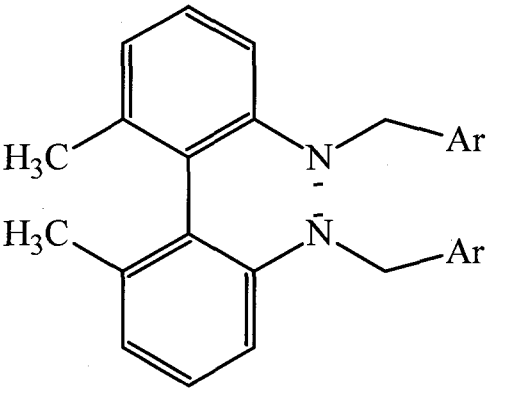

XVIIa Ar = 4-$C_6H_4{}^tBu$

XVIIb Ar = 4-C_6H_4Ph

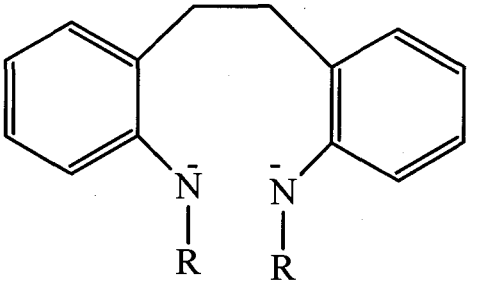

XVIII R = Si^iPr_3

Figure 10. Larger Chelate Rings: XVI,[36] XVII,[64] XVIII.[65]

Almost all the ligand systems in this class are symmetrical, with the neutral donor located between the amido donors. In $\mathbf{L}^{\mathbf{XIX}}$ this is not the case (Fig 11), and one of the byproducts isolated in the synthesis of $(\mathbf{L}^{\mathbf{XIX}})Zr(CH_2CHMe_2)_2$ contained an "ate" complex in which the pendant amino donor was coordinated to magnesium, resulting in $[(\mathbf{L}^{\mathbf{XIX}})Zr(CH_2CHMe_2)_2MgCl_2]_2$. Thus, the pendant donor may not be innocent and may account for the lack of polymerization activity of this system.[66]

Both of the complexes are somewhat unusual in that they both contain alkyls that bear β-hydrogens. However, the Schrock group has repeatedly isolated complexes containing alkyl groups bearing β-hydrogens and this stability of zirconium diamido complexes to β-elimination is more the rule than the exception in this field.[63,66]

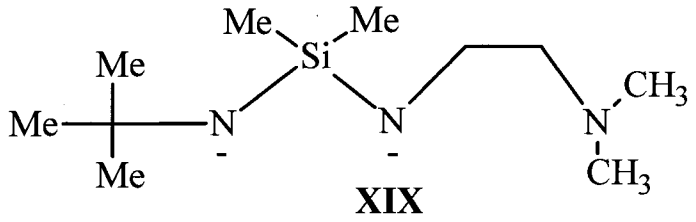

XIX

Figure 11. A Diamido Ligand With a Pendant Donor: XIX.[66]

1.3.2.1 Mixed Diamido-Donor Ligands with Unsaturated Backbones.

The first successful system that Schrock and coworkers reported was $(\mathbf{L}^{\mathbf{XXa}})ZMe_2$/ $[HNMe_2Ph]^+[B(C_6F_5)_4]^-$ (Fig 12). This system was highly active for the polymerization of ethylene and 1-hexene. The resulting atactic polyhexene had an extremely narrow polydispersity (1.02-1.14) and the linear increase of the polymer M_n with increased equivalents of monomer were evidence that the catalyst was living at 0°C.[67,68] All subsequent modifications of this system (ie $\mathbf{L}^{\mathbf{XXb}}$-$\mathbf{L}^{\mathbf{XXh}}$; activity of $\mathbf{L}^{\mathbf{XXIa}}$, $\mathbf{L}^{\mathbf{XXIb}}$ not reported), were inferior as olefin polymerization catalysts. The explanation for this is primarily steric in origin. The bulky ^{t}Bu groups result in a *fac* coordination mode, while the smaller groups result in *mer* geometry (Fig 13). The cations that result from the mer geometry are less crowded and consequently more prone to 2,1 insertion of 1-hexene. This places the bulk of the alkyl group near the metal, making it more prone to β-elimination.

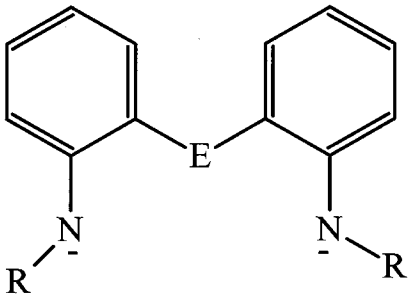

XXa E = O, R = ^{t}Bu

XXb E = O, R = ^{i}Pr

XXc E = O, R = Cy

XXd E = O, R = $SiMe_3$

XXe E = O, R = 0.5 $Me_2SiCH_2CH_2SiMe_2$

XXf E = O, R = Mes

XXg E = S, R = ^{t}Bu

XXh E = S, R = ^{i}Pr

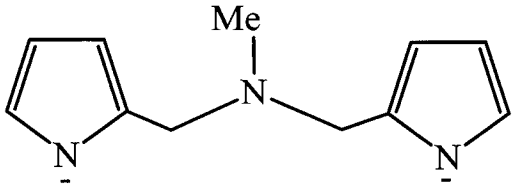

XXII

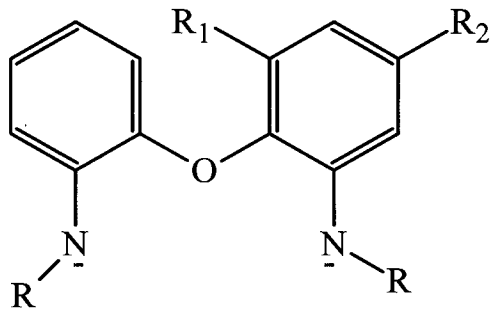

XXIa R = ^{t}Bu, $R_1 = R_2$ = Me

XXIb R = ^{t}Bu, R_1 = Et, R_2 = H

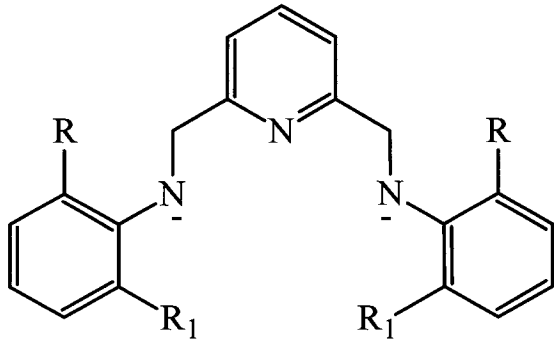

XXIIIa $R = R_1$ = Me

XXIIIb $R = R_1$ = Et

XXIIIc $R = R_1 = {}^{i}$Pr

XXIIId R = H, R_1 = Ph

XXIIIe R = H, $R_1 = {}^{i}$Pr

XXIIIf R = H, $R_1 = {}^{t}$Bu

XXIIIg R = Me, $R_1 = {}^{i}$Pr

XXIIIh Ar = C_6F_5

Figure 12. Mixed Diamido-Donor Ligands with Unsaturated Backbones: XX,[63,67-73] XXI,[69] XXII,[74] XXIII.[51,75-77]

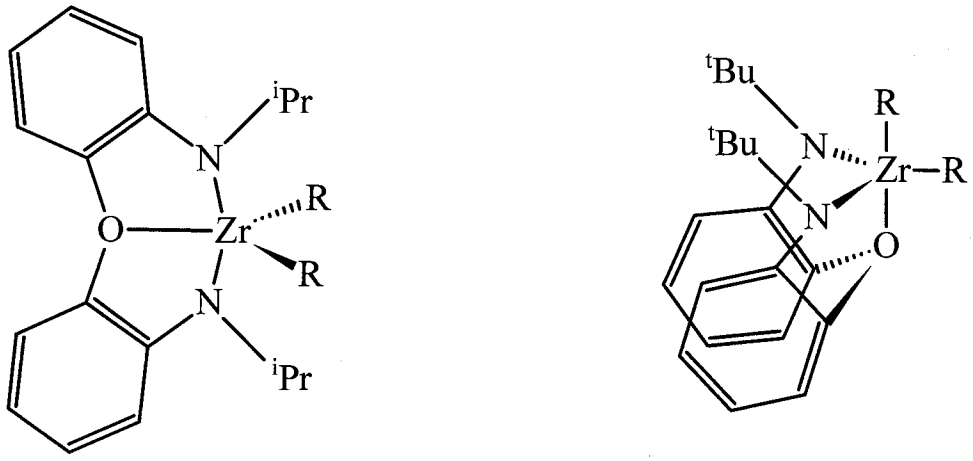

Mer Geometry *Fac* Geometry

Figure 13. Coordination Geometries.

1.3.2.2 Mixed Diamido-Donor Ligands with Saturated Backbones.

Schrock and coworkers found that polymerization using zirconium complexes based on ligands $\mathbf{L}^{\mathbf{XXIVb}}$, $\mathbf{L}^{\mathbf{XXIVc}}$, $\mathbf{L}^{\mathbf{XXIVe}}$ - $\mathbf{L}^{\mathbf{XXIVj}}$ (Fig 14) all suffered from a termination step that did not result in an olefinic end group. Investigation of $(\mathbf{L}^{\mathbf{XXIVb}})ZrMe^{+}$ led to the discovery of *ortho* C-H bond activation in the ligand and this likely accounts for this termination step (Eq 6).[78] Substitution of the troublesome methyl group with the sterically similar chloro substituent allows $(\mathbf{L}^{\mathbf{XXIVa}})ZrMe_2$/ $HNMe_2PhB(C_6F_5)_4$ to function as a living catalyst for the polymerization of 1-hexene. Previously, a similar problem was observed with the closely related trimethylsilyl substituted system $(\mathbf{L}^{\mathbf{XXIVd}})ZrBz_2$/ $B(C_6F_5)_3$ – the putative cationic complex decomposed via CH bond activation (Eq 7)[79] (as did the tetradentate analogue $\mathbf{L}^{\mathbf{XXXIIa}}$, Fig 17).[80]

(6)

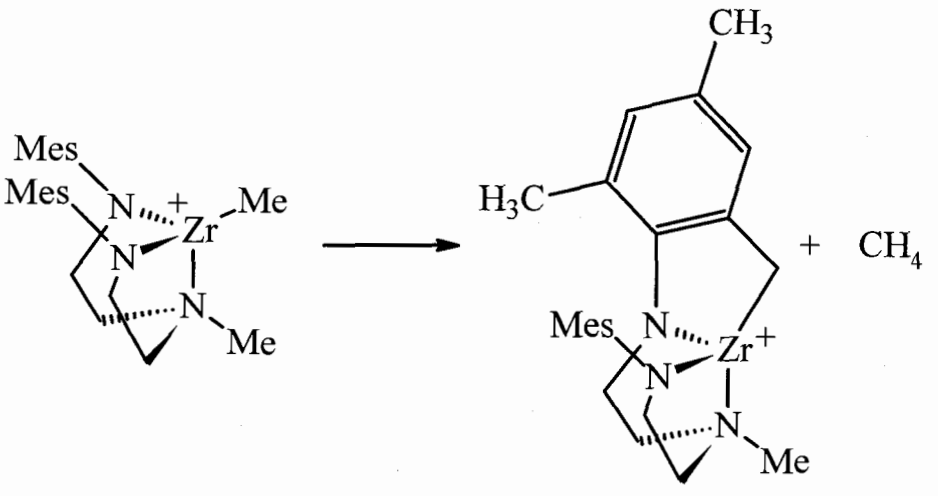

(7)

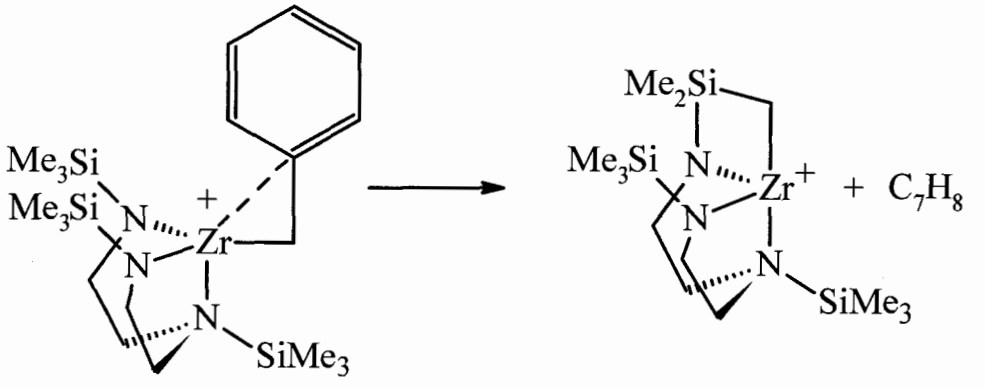

In the previous section much of the reactivity of the complexes could be accounted for by the steric bulk of the substituents on the amido nitrogen. The bulky ^{t}Bu groups in $\mathbf{L}^{\mathbf{XXa}}$ provided supported living polymerization while any smaller substituent was ineffective. The exception to this was the $SiMe_3$ substituent; while the ^{t}Bu analogue was very successful, the $SiMe_3$ analogue $\mathbf{L}^{\mathbf{XXd}}$ was not. In light of these other observations, it seems likely that C-H bond activation may play a role in the instability of the alkyl cation $(\mathbf{L}^{\mathbf{XXd}})ZrMe^{+}$. Given the widespread use of $SiMe_3$ and $Si^{i}Pr_3$ groups, this problem may be quite widespread and the use of these groups in polymerization catalysts should either be avoided or at least approached with a critical eye.

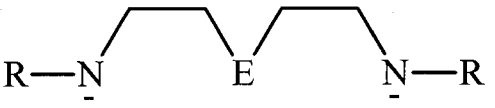

XXIVa E = NMe, R = 2,6-$C_6H_3Cl_2$

XXIVb E = NMe, R = Mes

XXIVc E = NH, R = Mes

XXIVd E = $NSiMe_3$, R = $SiMe_3$

XXIVe E = O, R = 2,6-$C_6H_3Me_2$

XXIVf E = O, R = 2,6-$C_6H_3{}^iPr_2$

XXIVg E = O, R = 2,6-$C_6H_3Et_2$

XXIVh E = O, R = 2-$C_6H_4{}^tBu$

XXIVi E = S, R = 2,6-$C_6H_3Me_2$

XXIVj E = S, R = 2,6-$C_6H_3{}^iPr_2$

XXIVk E= P, R = $SiMe_3$

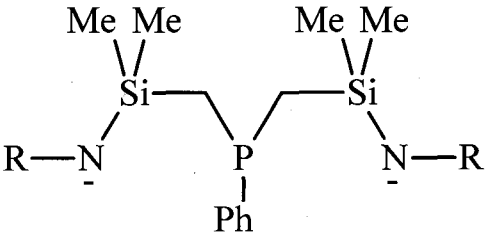

XXV

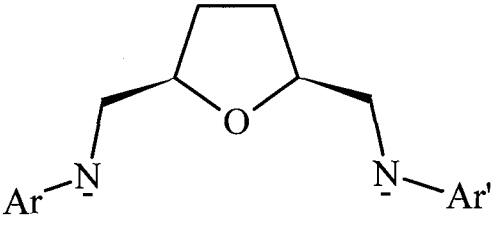

XXVIa Ar = Ar' = 2,6-$C_6H_3Me_2$

XXVIb Ar = 2,6-$C_6H_3Me_2$, Ar' = 2,6-$C_6H_3{}^iPr_2$

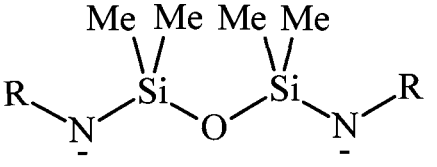

XXVII

Figure 14. Mixed Diamido-Donor Ligands with Saturated Backbones:

XXIV,[78,79,81-87] XXV,[87] XXVI,[88] XXVII.[39]

1.3.2.3 Mixed Tripodal Diamido-Donor Ligands.

The third system studied by Schrock and coworkers involves a tripodal geometry, rather than a linear arrangement of donors (Fig 15). An unusual feature of this system involves the difference in polymerization activity found when the same ligand is used,

but different alkyl groups are bound to the metal. When ($\mathbf{L}^{\mathbf{XXVIIIa}}$)$ZrMe_2$ is activated with $Ph_3CB(C_6F_5)_4$, the system is not a well behaved 1-hexene polymerization catalyst. On the other hand, when ($\mathbf{L}^{\mathbf{XXVIIIa}}$)$Zr^iBu_2$ is activated with $Ph_3CB(C_6F_5)_4$ the system acts as a well behaved and living polymerization catalyst.[60,89] In the former case a dimeric methyl bridged cationic species forms, which does not readily dissociate to yield a catalytically active species (Fig 16). Even addition of excess of THF or DME did not result in cleavage of the dimer, while in the latter the larger isobutyl group prevents this dimerization and allows for a well behaved polymerization of 1-hexene with extremely narrow polydispersity (1.03 at 0°C). Unlike the case with the ligand system $\mathbf{L}^{\mathbf{XXIV}}$, placing chloro substituents on the aniline ring did not improve the activity of this catalyst system, possibly due to interaction of the halide with the metal centre.[90]

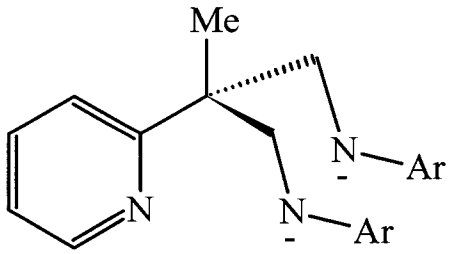

XXVIIIa Ar = Mes

XXVIIIb Ar = 2,4,6-$C_6H_2{}^iPr_3$

XXVIIIc Ar = 2,6-$C_6H_3Cl_2$

XXVIIId Ar = 2,6-$C_6H_3F_2$

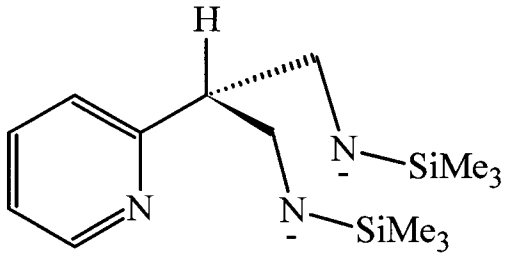

XXIX

Figure 15. Mixed Tripodal Diamido-Donor Ligands: XXVIII,[60,89-91] XXIX.[92]

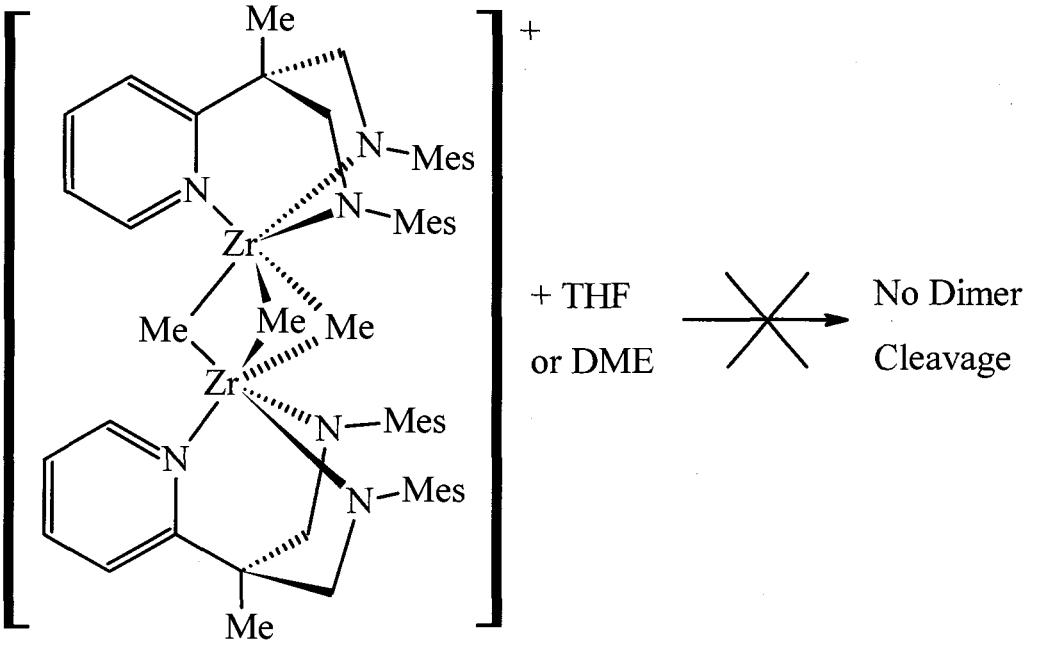

Figure 16. Cationic Dimer.

1.3.3 Zirconium Complexes With Diamido Ligands that Bear Two or More Additional Donors.

With the increased number of donors, the focus in this area is more on the stoichiometric reactions of these complexes (Fig 17). Fryzuk and coworkers have been investigating the reactions of coordinated dinitrogen, which has implications for the production of ammonia. One notable accomplishment involved the use of the "P_2N_2" macrocycle. They have shown that reaction of ($\mathbf{L}^{xxx}$)$ZrCl_2$ with KC_8 in the presence of dinitrogen yields the side-on bound μ-N_2 dimer (Eq 8). The dinitrogen is effectively reduced to N_2^{4-}, but perhaps more importantly, addition of hydrogen did not displace the dinitrogen, but rather reacted with it. This is without precedent and holds promise for further investigation.

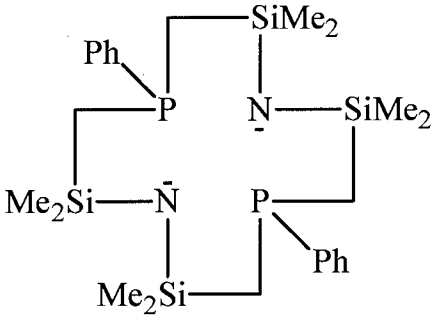

XXX

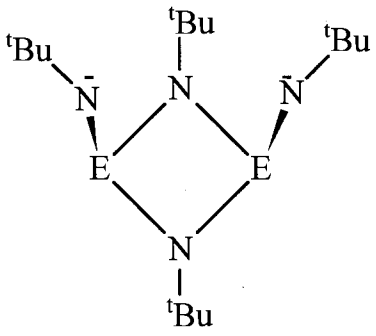

XXXIa E = P

XXXIb E = SiMe

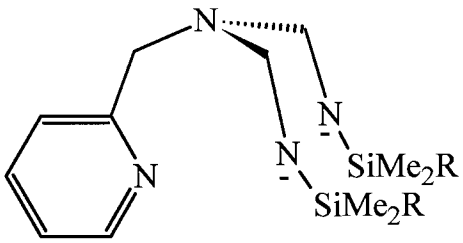

XXXIIa R = Me

XXXIIb R = ^{t}Bu

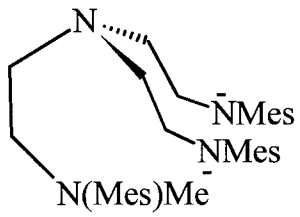

XXXIII

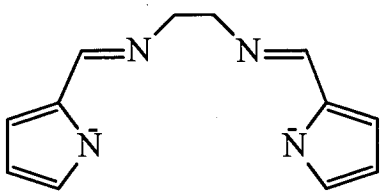

XXXIV

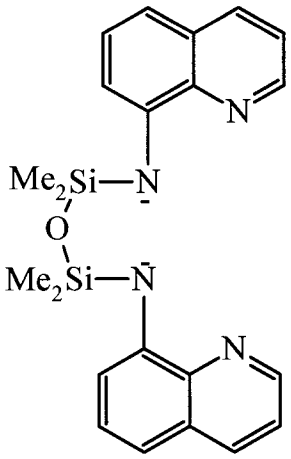

XXXV

Figure 17. Diamido Ligands with Two Or More Donors:

XXX,[93-95] XXXI,[96-98] XXXII,[80,99] XXXIII,[82] XXXIV,[39] XXXV.[39]

(8) 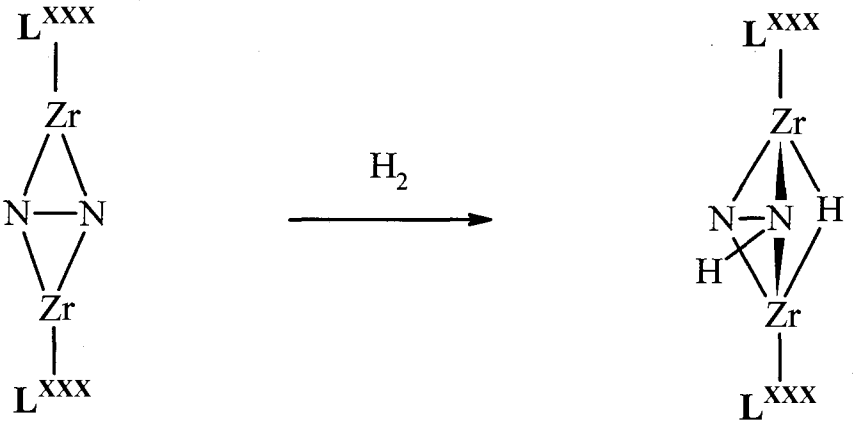

1.3.4 Unsaturated Macrocyclic Diamido Ligands

The size of zirconium precludes it from sitting in the plane of the four nitrogens in any of the ligands $\mathbf{L^{XXXVI}}$-$\mathbf{L^{XL}}$, unlike smaller metals (Fig 18). This has the advantage of forcing the metal out of the pocket resulting in the substituents being *cis* to one another. This geometry has the potential to allow for olefin polymerization; however, while several alkyl cations have been studied,[100,101] only one, supported by $\mathbf{L^{XXXVIIIb}}$, was reported to catalyze ethylene polymerization, albeit with low activity.[102]

As in the previous section, the focus of research in this area has been more on studying the stoichiometric reactions of the zirconium alkyls with unsaturated substrates as a comparison to the zirconium metallocenes. There is one problem that has plagued this area of research. The unsaturated imino functionality is extremely prone to alkyl migration from zirconium to the α-carbon to yield an amido group. This has been observed with ligands $\mathbf{L^{XXXVII}}$,[103] $\mathbf{L^{XXXVIIIa}}$,[104] $\mathbf{L^{XXXVIIIb}}$,[102] and $\mathbf{L^{XXXIX}}$ [105] and a representative example is shown in Eq 9.

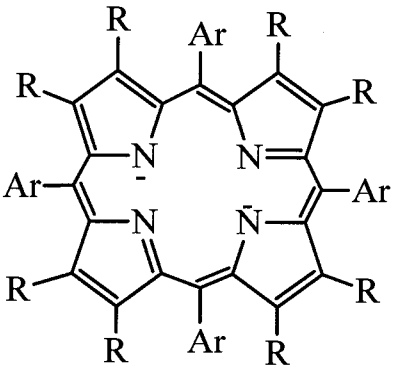

XXXVIa Ar = H, R = Et

XXXVIb Ar = Ph, R = H

XXXVIc Ar = 4-C_6H_4Me, R = H

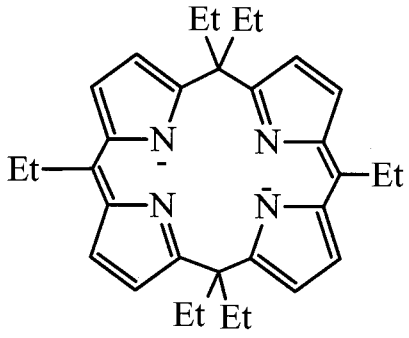

XXXVII

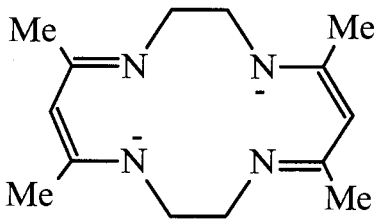

XXXIX

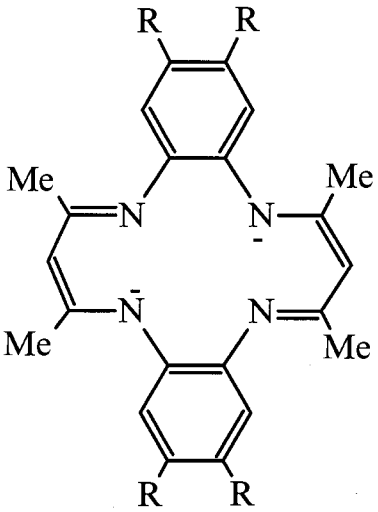

XXXVIIIa R = H

XXXVIIIb R = Me

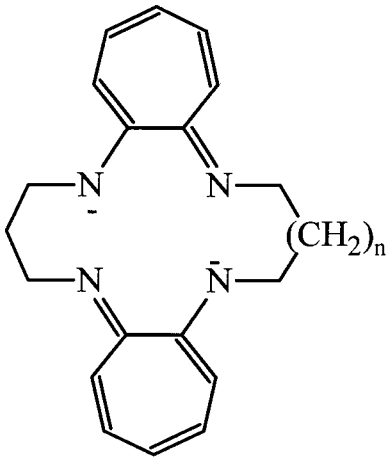

XLa n = 1

XLb n =3

Figure 18. Dianionic N_4 Macrocycles: XXXVI,[106-110] XXXVII,[103] XXXVIII,[100,102,104,111-114] XXXIX,[100,105,115] XL.[101,116,117]

(9) 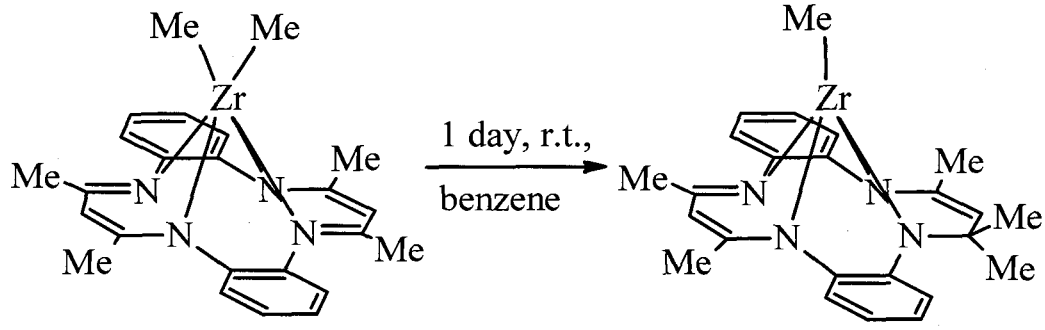

Despite this serious limitation, a number of unusual compounds and reactions have been observed with this class of ligands. In addition to a number of imides supported by the macrocyclic ligands,[110,111] the *bis*-alkyl compounds undergo reactions with unsaturated species that are different from the metallocene counterparts (Eq 10-13). The metallocenes react with one equivalent of carbon monoxide or one equivalent of an isocyanide to form the η^2-acyl or η^2-iminoacyl complex respectively.[118] In contrast, reaction of a macrocyclic (DA)ZrR_2 complex with carbon monoxide can result in migration of both alkyl groups to the carbon to yield the metallaoxirane.[104,119] Reaction with isocyanides again involves migration of both alkyl groups, but in this case it is to two different isocyanides, which can result in the *bis*-η^2-iminoacyl complex[104] or subsequent coupling of the η^2-iminoacyl moieties yields a metallacycle.[116]

Metallocenes

(10) 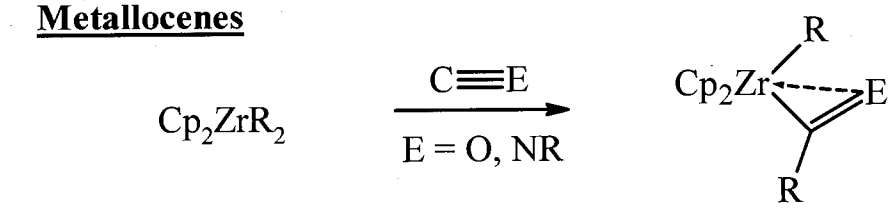

Macrocycles

(11) 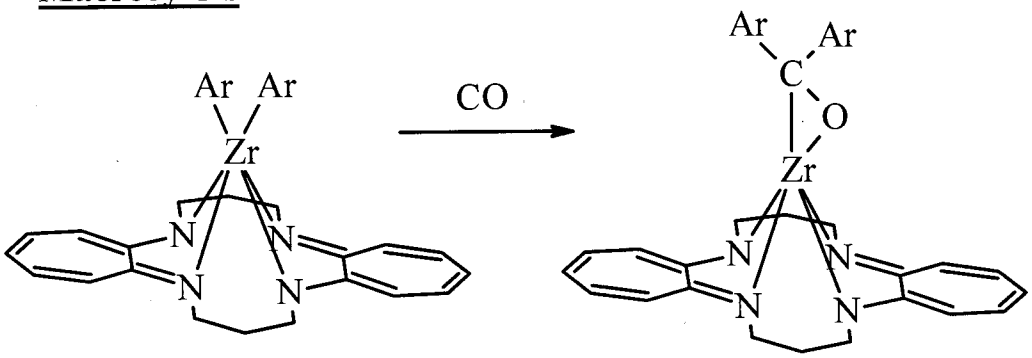

(12) 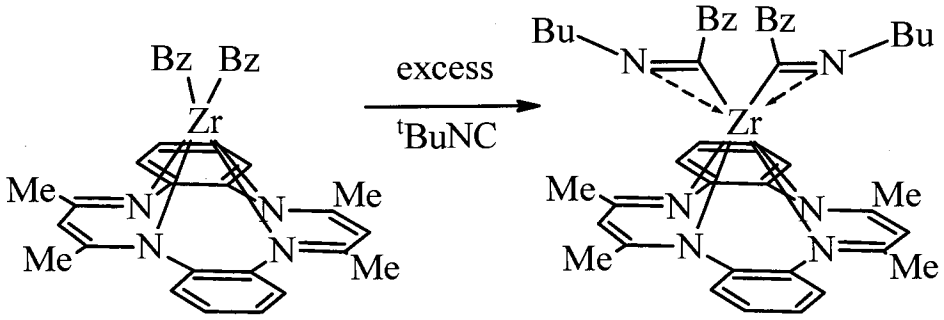

(13) 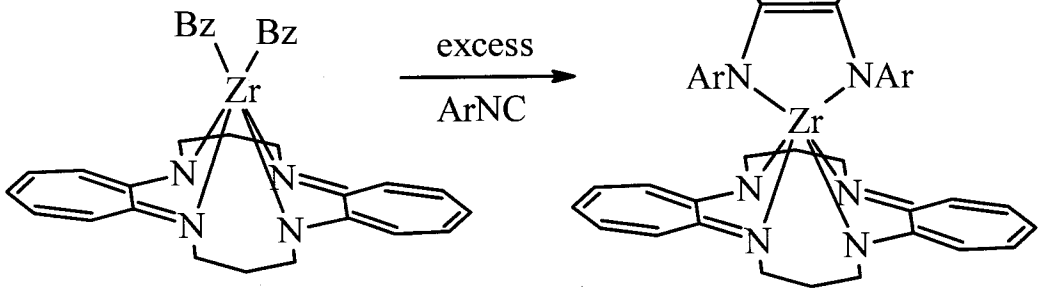

1.4 Scope of This Work

The origin of this work can be traced back to the early 1990's. At that time very little had been reported on the use diamido ligands as ancillary ligands for the early transition metals and lanthanides (the vast majority of ligands $\mathbf{L^{II}}$ through $\mathbf{L^{XL}}$ have been applied to organozirconium chemistry post 1996, although some of the macrocyclic systems were reported earlier). At that time it was unclear what steric and electronic properties of pentamethylcyclopentadienyl made it such a successful ligand for organolanthanide chemistry. Thus began our research program to develop alternative ligand systems for organolanthanide and early transition metal chemistry. The conceptual process involved in developing new ligands is shown in Fig 19.

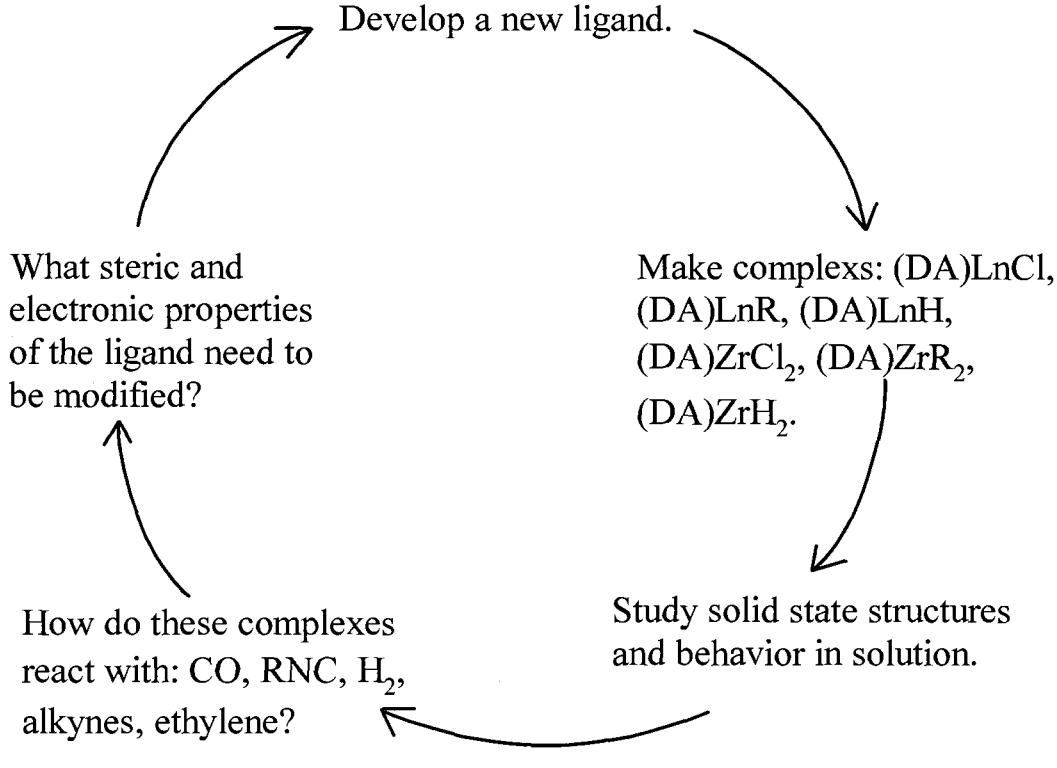

Figure 19. Ligand Development Cycle

The first foray into alternative ligand systems exploited the macrocycle 4,13-diaza-18-crown-6 (DAC). This system was used to support not only organolanthanide chemistry, but also organozirconium chemistry. In the latter case, *bis*-alkyl complexes were formed, but the *cis* and *trans* forms (Scheme 4) were in equilibrium; moreover, these complexes proved unreactive with carbon monoxide and other unsaturated species.[120] This was taken as evidence "that the coordination environment around the metal is extremely congested and reactivity can only be obtained by reducing the steric bulk."[120]

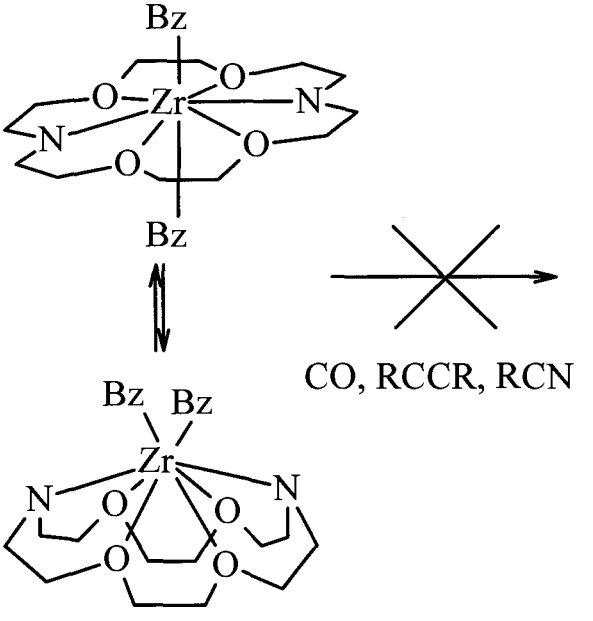

Scheme 4. Reactivity of *Cis* and *Trans* DAC Complexes

This led to the development of $(C_6F_5NHCH_2CH_2OCH_2)_2$, (NOON) as a supporting ligand. In Chapter 2, the synthesis of zirconium complexes supported by NOON will be described. As outlined in Fig 19, the solid state structures and solution behaviour will be described, followed by the reactivity of these complexes with small molecules. One intent of preparing this ligand was to apply it to organolanthanide

chemistry and compare it with the corresponding DAC complexes; however, this proved not to be feasible and no lanthanide complexes were prepared with this ligand. This will be discussed further in Chapter 4.

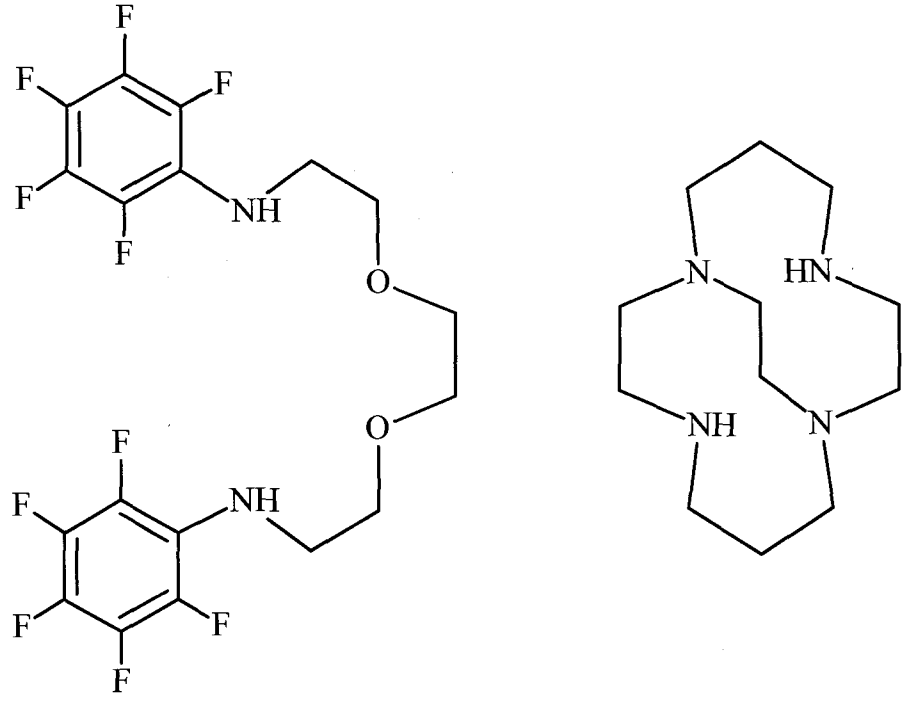

H_2(NOON) H_2(CBC)

Figure 20. Diamido Ligands

The results of the NOON investigation led to the use of 1,4,8,11-tetraazabicyclo[6.6.2]hexadecane (cross-bridged cyclam, H_2(CBC)) as a supporting ligand. Again the synthesis, solid and solution state behaviour, and reactivity of zirconium complexes with CBC will be reported in Chapter 3. The initial investigations of group 3 and lanthanide chemistry supported by CBC will be reported in Chapter 4. Finally, Chapter 5 provides the experimental details for all the work presented here.

Chapter 2. Organozirconium Complexes Supported by a Fluorinated Diamido Ligand

2.1 Introduction

The DAC system was sterically crowded due to the sheer number of ether donors; consequently, removing two of the ether donors from one side of the DAC system gives an acyclic analogue $(C_6F_5NHCH_2CH_2OCH_2)_2$, ($H_2NOON$), which should decrease the steric crowding at the metal centre. The addition of the perfluorophenyl groups to the amido nitrogens should lower the pKa of the amido groups, which should result in less electron density at zirconium and perhaps increased reactivity.

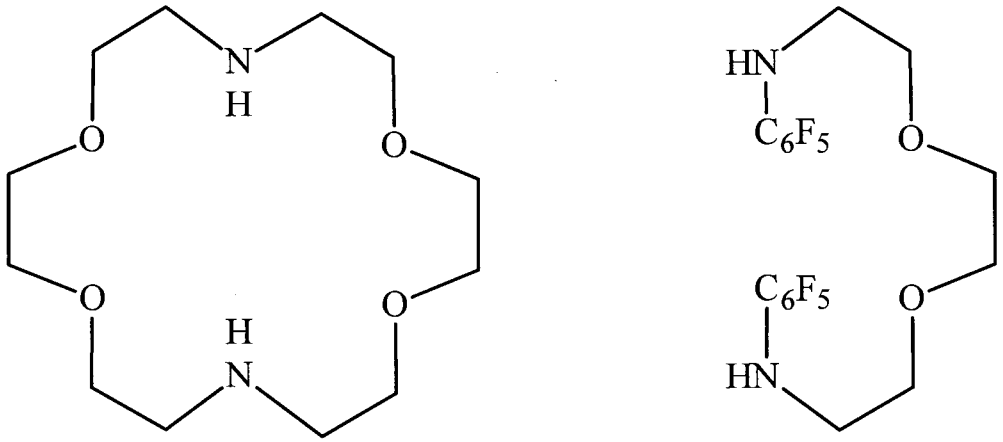

H_2(DAC) (1)

Figure 21. Ligand Evolution.

2.2 Synthesis of Complexes

The H_2(NOON) ligand ($(C_6F_5NHCH_2CH_2OCH_2)_2$, **1**), can be readily synthesized from 1,2-*bis*(2-iodoethoxy)ethane and commercially available pentafluoroaniline in 60% yield (Scheme 5).[121] Excess aniline is required to obtain an acceptable yield, but the excess aniline can be recovered after hydrolysis via vacuum sublimation. The resulting black tar can be recrystallized from hexanes to yield a pale yellow powder in multigram quantities.

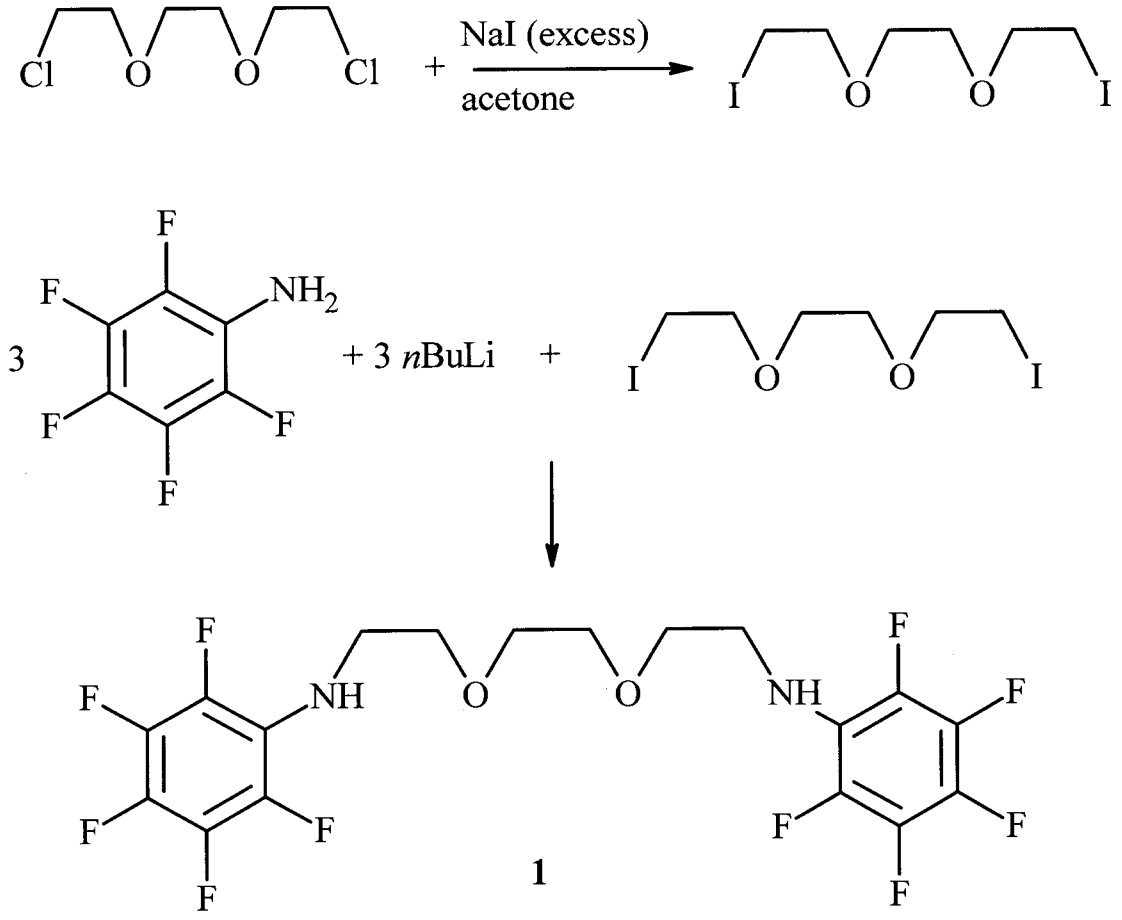

Scheme 5. Synthesis of H_2(NOON), (1)

In our hands, the most reliable and efficient entry into organozirconium chemistry is the direct acid-base reaction of readily prepared homoleptic zirconium compounds with the protio-ligand, H_2(NOON). This method is limited to the homoleptic compounds which are stable at room temperature; in practice this limits this route to $Zr(CH_2Ph)_4$ and $Zr(CH_2SiMe_3)_4$. Other compounds such as $Zr(allyl)_4$ are not stable at room temperature,[5] thereby limiting this approach for practical reasons.

The reaction of tetrabenzylzirconium with H_2(NOON) results in (NOON)$Zr(CH_2Ph)_2$ (**2**) in excellent yield (Eq 14). This compound is a bright yellow powder which is soluble in aromatic solvents and sparingly soluble in aliphatic ones. It is thermally robust, it can be stored at low temperature in the solid state (-30°C) for months without appreciable degradation. In perdeutero-toluene solution, the half-life of **2** is 25 hours at 105°C and this process resulted in the evolution of toluene and the disappearance of the ligand resonances into the baseline.

(14) $H_2NOON + Zr(CH_2Ph)_4 \longrightarrow$ 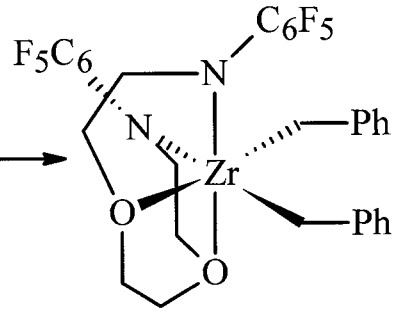 $+ 2\ C_7H_8$

2

A more general route to produce organozirconium species involves the metathesis reaction of a zirconium chloride species with alkyl lithium or Gringnard reagents. Thus, the species (NOON)$ZrCl_2$ (**3**) is a desirable starting material. A straightforward route to

producing this material would be the reaction of Li_2(NOON) with zirconium tetrachloride; however, we were concerned that the isolation of Li_2(NOON) might be hazardous. The potential exists for both intramolecular and intermolecular nucleophilic aromatic substitution reactions to occur between the amido anion and the pentafluorophenyl ring. Since this reaction would produce lithium fluoride as a byproduct, it would likely be exothermic; accordingly, no attempt was made to isolate this compound. Attempts to produce (NOON)$ZrCl_2$ from Li_2(NOON) or K_2(NOON) generated *in situ* and zirconium tetrachloride were unsuccessful. This may be due in part to the nucleophilic aromatic substitution side reaction, as well as the possibility of forming insoluble "ate" complexes - lithium chloride being retained in the metal's coordination sphere. However, the key problem with this approach is the extremely low solubility of (NOON)$ZrCl_2$ in aromatic solvents (*vide infra*). This would make the separation of the desired zirconium complex from the salt byproduct tedious or impossible.

Since the acid-base reaction chemistry was successful with tetrabenzylzirconium and H_2(NOON), we returned to this strategy to produce (NOON)$ZrCl_2$. While many groups have successfully used a strategy of reacting a ligand with $Zr(NMe_2)_4$ followed by Me_3SiCl to produce a dichlorozirconium species, our own preference is to use $Zr[N(SiMe_3)_2]_2Cl_2$ and the protio ligand **1** to obtain (NOON)$ZrCl_2$ directly (Eq 15).[122] This reaction requires rugged conditions (110°C toluene, 2 days), but the product is very sparingly soluble in aromatic solvents, so it precipitates as a pale yellow powder from the reaction mixture and does not require further purification. While this low solubility could be a result of a dimeric or polymeric structure, this seems unlikely given that the

molecular ion is observed in the mass spectrum and the closely related [(3,5-$C_6H_3(CF_3)_2$)$NCH_2CH_2OCH_2$]$_2ZrCl_2$ is a monomer in the solid state.[121]

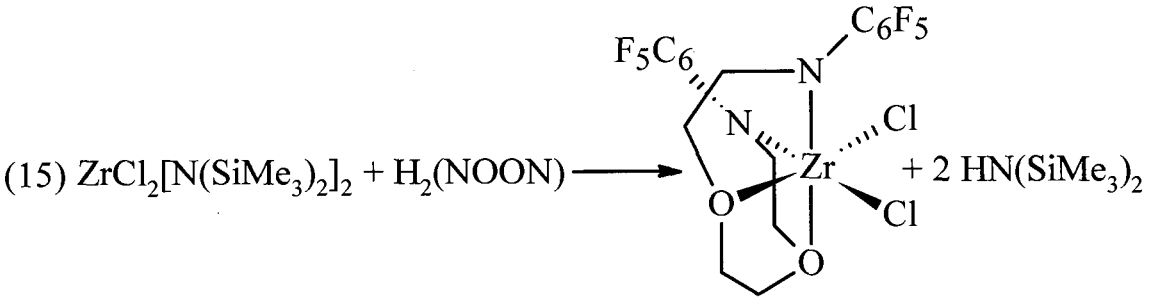

3

One drawback of this approach is that the $Zr[N(SiMe_3)_2]_2Cl_2$ is not commercially available. When it is prepared from $NaN(SiMe_3)_2$ and zirconium tetrachloride, there is often contamination with $Zr[N(SiMe_3)_2]_3Cl$. This led to the fortuitous discovery of $(NOON)ZrClN(SiMe_3)_2$ (**4**) (Eq 16). In contrast to the dichloro analogue **3**, **4** is soluble in aromatic solvents allowing it to be recrystallized from hot toluene to yield **4** as clear, colourless crystals suitable for X-ray crystallography (Section 2.3). To further confirm the identity of **4**, it was prepared from $Zr[N(SiMe_3)_2]_3Cl$ and $H_2(NOON)$ as well as by metathesis reaction of **3** and $NaN(SiMe_3)_2$ (Eq 17).

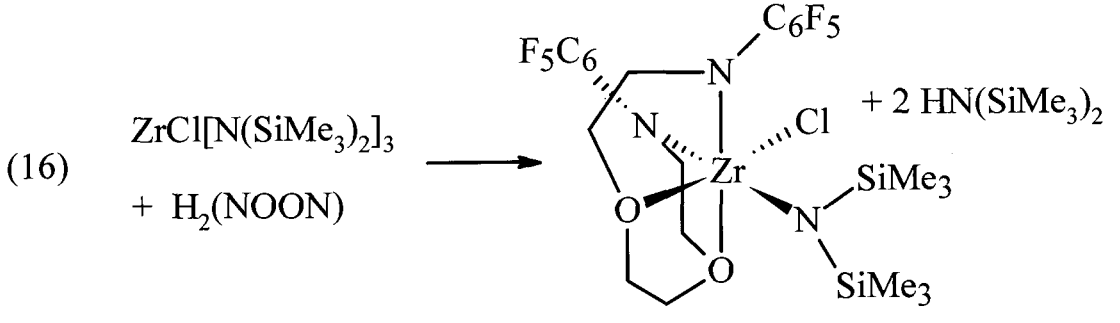

4

(17) $(NOON)ZrCl_2 + NaN(SiMe_3)_2$ → 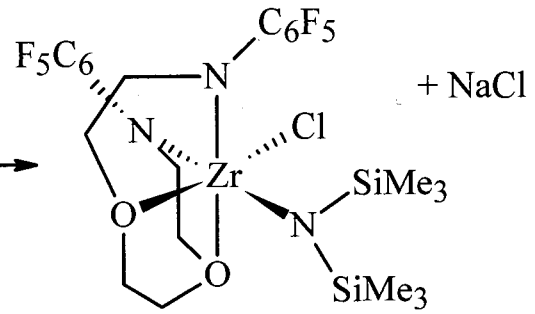 + NaCl

4

The purpose of preparing $(NOON)ZrCl_2$ was to derivatize it with suitable alkylating agents. Indeed, reaction of **3** with MeLi affords $(NOON)ZrMe_2$ (**5**) in modest yield (Eq 18). Recrystallizing this compound from toluene affords clear colourless crystals which are soluble in aromatic solvents and sparingly soluble in aliphatic ones. These crystals were analysed by X-ray crystallography (Section 2.3). The dimethyl species **5** is not as thermally robust as the dibenzyl compound **2**, showing 50% decomposition after heating overnight at 80°C, compared to 25h at 105°C for the latter. This is consistent with the smaller size of a methyl group and the stabilizing effect of the phenyl substituent. Other attempts at metathesis reactions will be discussed further in Section 2.5.

(18) $(NOON)ZrCl_2 + 2\ MeLi \longrightarrow$ 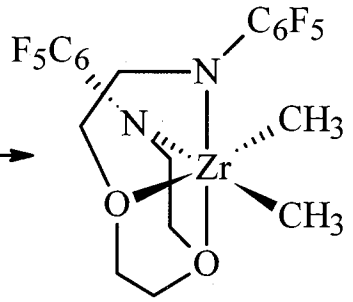 $+ 2LiCl$

5

2.2.1 Photochemistry

When a solution of the yellow dibenzyl compound **2** was left to recrystallize under ambient conditions red crystals were discovered on the wall of the flask after several weeks. These crystals were of sufficient quality for an X-ray crystallographic analysis to be performed (Section 2.3). The product proved to be the metallated complex $[(C_6F_4NCH_2CH_2OCH_2CH_2OCH_2CH_2NC_6F_5)ZrCH_2Ph]_2(C_7H_8)$, **6** (Fig 22). Initially, it was not evident if this was a result of a thermal or photochemical process; however, a solution of **2** that was protected from light remained unchanged after several months at room temperature. In contrast, a solution of **2** exposed to ambient light did react; moreover, the reaction showed a strong wavelength dependence. When a solution of **2** was irradiated with a 150 W incandescent bulb masked with a 435 nm filter, the reaction was complete after 14 h. In contrast, when a shorter wavelength filter (375 nm) was used, a complex mixture of products resulted and a longer wavelength filter (550 nm) resulted in no reaction, even after several days of irradiation.

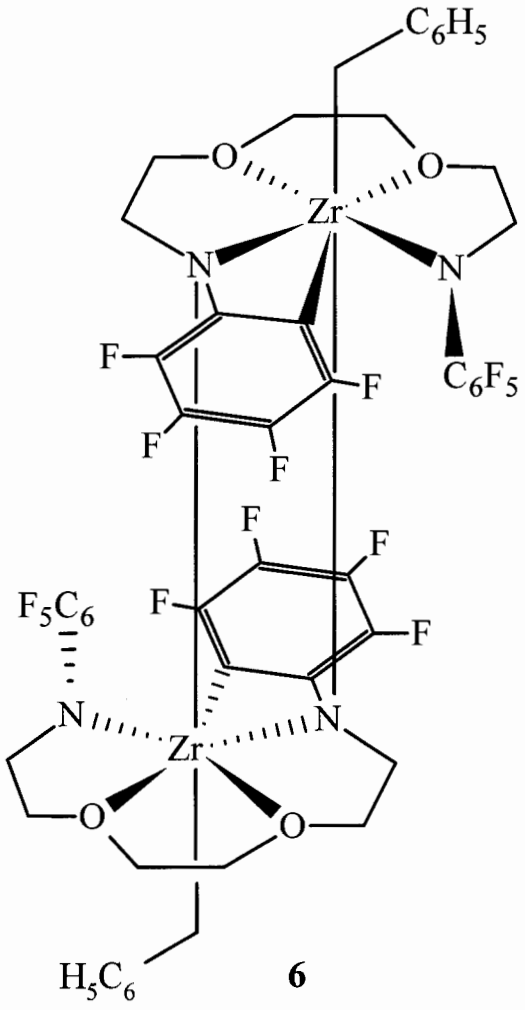

Figure 22. One Photoproduct.

When this reaction was followed by NMR spectroscopy (Fig 23), the metallated product **6** was insoluble in aromatic solvents and precipitated. However, bibenzyl was identified by its characteristic methylene ^{1}H (2.7 ppm) and ^{13}C resonances.[123] A second organometallic species was identified in the supernate.

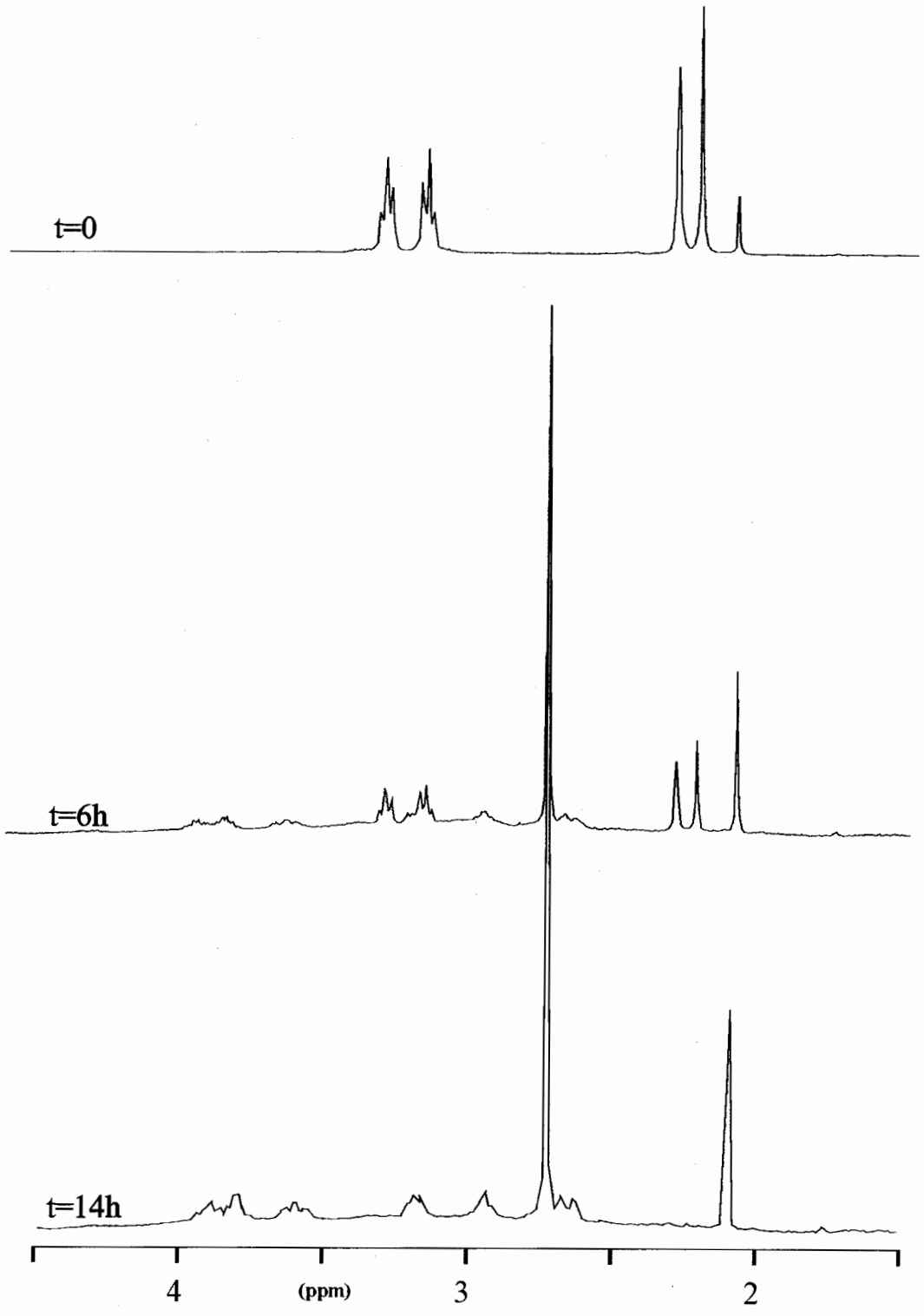

Figure 23. Photolysis of (NOON)Zr(CH_2Ph)$_2$ at 435nm (300 MHz ^{1}H NMR, C_6D_6 295 K).

The formation of bibenzyl accounts for the benzyl group that is lost in the formation of the metallated product **6**. The only other species that has not been accounted for in the formation of dimeric **6**, is two fluorine atoms. The ^{19}F NMR of the reaction mixture indicates that the other species in solution is $[(NOON)ZrF_2]_n$, **7**. The ^{19}F NMR spectrum contains not only the usual three Ar-F resonances (-150.1 to -166.6 ppm) of the C_6F_5 groups, but also two signals well outside this region. The downfield resonance at +109.2 ppm is consistent with a terminal Zr-F (terminal Zr-F groups range +20 to +110 ppm for cyclopentadienyl zirconium complexes),[124-130] while the signal at -51.4 is consistent with a bridging Zr-F-Zr (bridging Zr-F-Zr groups range from -19 to -112 ppm for cyclopentadienyl zirconium complexes).[126-129,131] Moreover, Fig 23 shows that **7** has six resonances for the ligand backbone. This is in contrast to the other complexes with the same substituents, including the dichloride **3**, which show three resonances for the ligand. This anomaly is a result of a bridging fluoride interaction between the zirconium centres. Based on this information, the structure could be dimeric or polymeric as shown in the equation below. Unfortunately, the low solubility of this species in aromatic solvents prevented characterization of this compound by ^{13}C NMR.

(19) 3 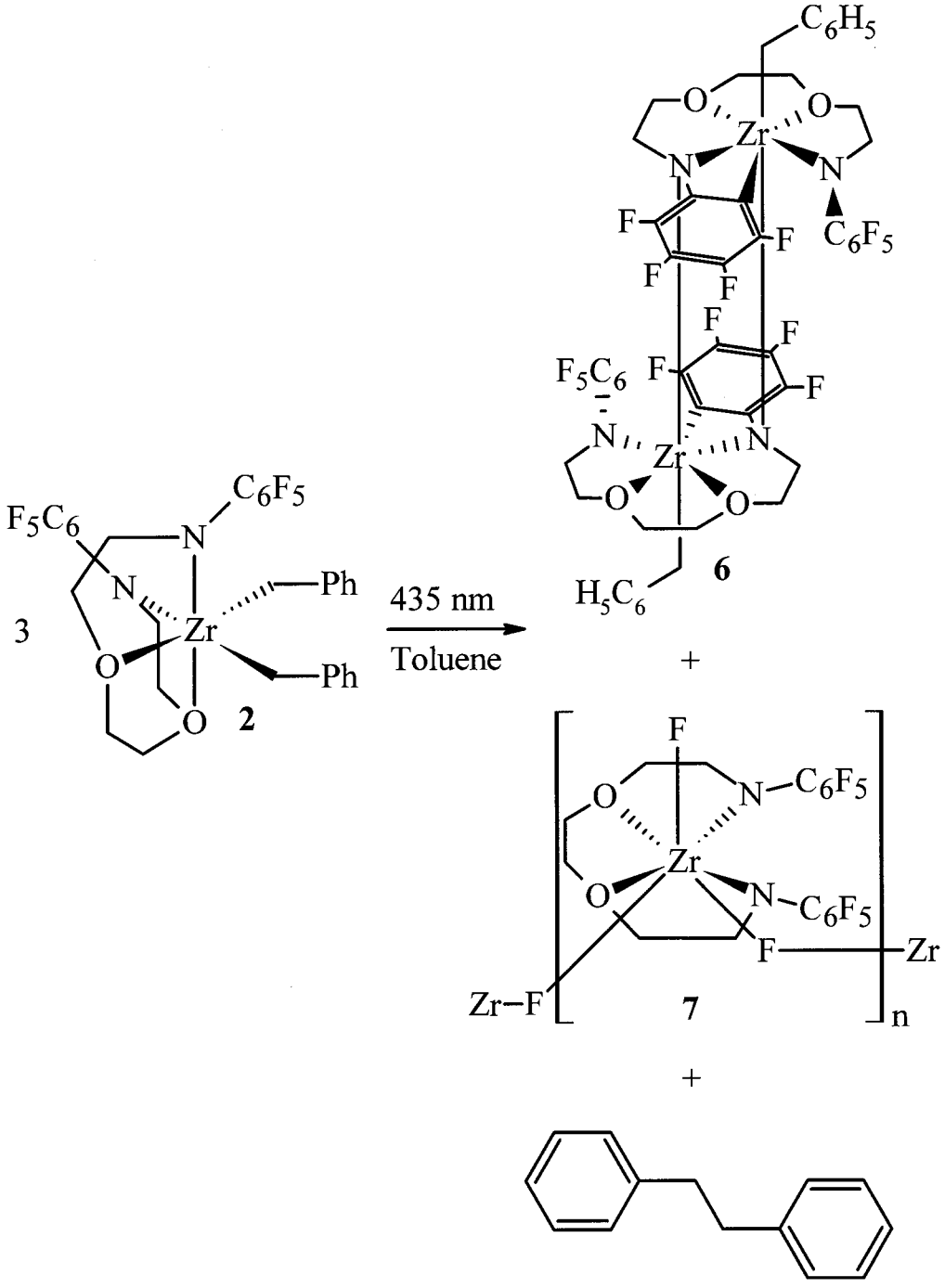

The discovery of the metallated dimer **6** was made during an attempt to recrystallize the dibenzyl compound; this was simply scaled up to furnish bulk amounts of **6**. The first two crops of **6** were pure; unfortunately, subsequent crops were

increasingly contaminated with the difluoride. To prepare **7** independently, the dibenzyl compound **2** was stirred overnight in toluene with two equivalents of solid Bu_3SnF. The characteristic ^1H and ^{19}F resonances due to the difluoride species were observed in the supernate in addition to Bu_3SnCH_2Ph – the major soluble product. The low solubility of both Bu_3SnF and $(NOON)ZrF_2$ prevented the isolation of pure **7** by this method.

(20)

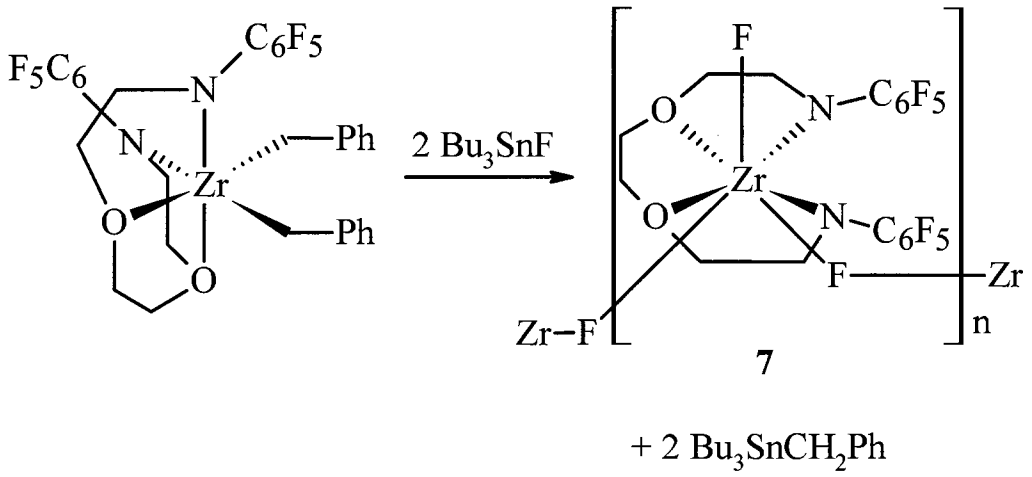

7

$+ 2\ Bu_3SnCH_2Ph$

Thus far the mechanism of this photochemical reaction has not been discussed. Gambarotta and coworkers have shown that photolysis of $(C_5H_4Me)_2Zr(i\text{-}Bu)I$ (Eq 21) results in the formation of isobutane and isobutene.[132] The organometallic product of this reaction is a zirconium (III) dimer, which was characterized in solid state. The other products from the reaction, isobutane and isobutene, are consistent with zirconium-carbon bond homolysis. When the corresponding chloride zirconium (III) dimer, $[(C_5H_4Me)_2ZrCl]_2$, was prepared, it showed a greater tendency to disproportionate into zirconium (II) and (IV) species.

(21) $2\ (C_5H_4Me)_2Zr(i\text{-}Bu)I \xrightarrow{h\upsilon}$ $(C_5H_4Me)_2Zr(\mu\text{-}I)_2Zr(C_5H_4Me)_2$ + isobutene + isobutane

These observations suggest a possible mechanism for the photochemistry of $(NOON)Zr(CH_2Ph)_2$. The likely first step is homolytic bond cleavage, as observed in the system studied by Gambarotta. This is also consistent with the wavelength dependence of the reaction. The reaction of **2** proceeds cleanly when a 435 nm filter is used; this corresponds to an energy of 276 kJ mol^{-1}, which is comparable to the Zr-C bond strength in tetrabenzyl zirconium (263 kJ mol^{-1}).[133] Also, the observation of a broad EPR signal (g = 2.001) during the photolysis is consistent with the formation of a zirconium (III) species. Given the long photolysis time to complete the reaction, the steady state concentration of benzyl radicals is likely to be quite low, making observation of this species difficult.

(22) 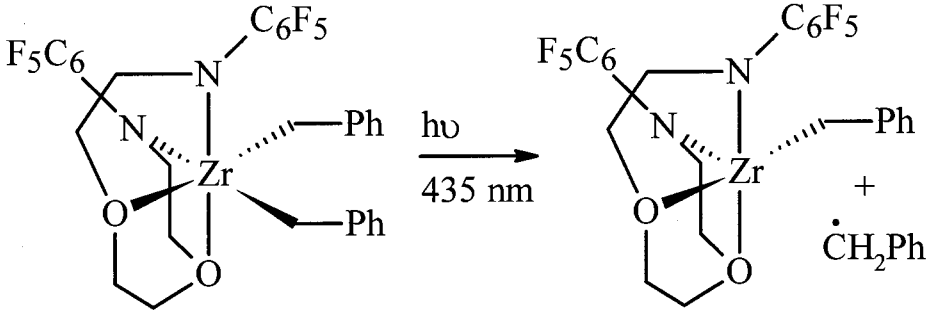

If this zirconium intermediate undergoes disproportionation to zirconium (II) and (IV) species, the low valent species can then undergo oxidative addition of the aryl C-F bond (Scheme 6). This oxidative addition of an aryl C-F bond to a zirconium has been proposed previously,[134] and there are many examples of this with late, electron rich,

transition metals.[135] This species would have the metallated ligand, but with a fluoride as the other ligand, rather than the observed benzyl group. Accordingly, ligand redistribution must occur in order to obtain the metallated producted **6** and the difluoride **7**.

Another possible mechanism that would account for the observed products again involves two zirconium (III) species, but rather than disproportionation to yield zirconium (II) and (IV) directly, intermolecular electron transfer from one metal to the electron deficient C_6F_5 ring of another Zr(III) complex could occur (Scheme 7). This would result in the formation of the zirconium carbon bond and elimination of fluoride to the cationic zirconium complex. Ligand redistribution would again lead to the observed products. This type of reaction pathway has been proposed in divalent lanthanide chemistry.[135,136]

Since the first mechanism involves a zirconium (II) intermediate, the reaction was carried out in the presence of alkynes and phosphines in attempt to trap these intermediates. The added reagents did not affect the outcome of the reaction. Likewise, the addition of perfluorobenzene to the reaction mixture did not result in any evidence of intermolecular C-F bond activation. Photolysis of (NOON)Zr($CH_2Ph)_2$ in d_8-THF did not result in the formation of the metallated product **6**, but rather a complex mixture of products. Since both mechanistic pathways could be affected by the presence of Lewis bases, this does not rule out either mechanism. It could indicate that dimerization of some of the intermediates may be important, since the THF would likely occupy any vacant coordination sites and might resist displacement by a second complex.

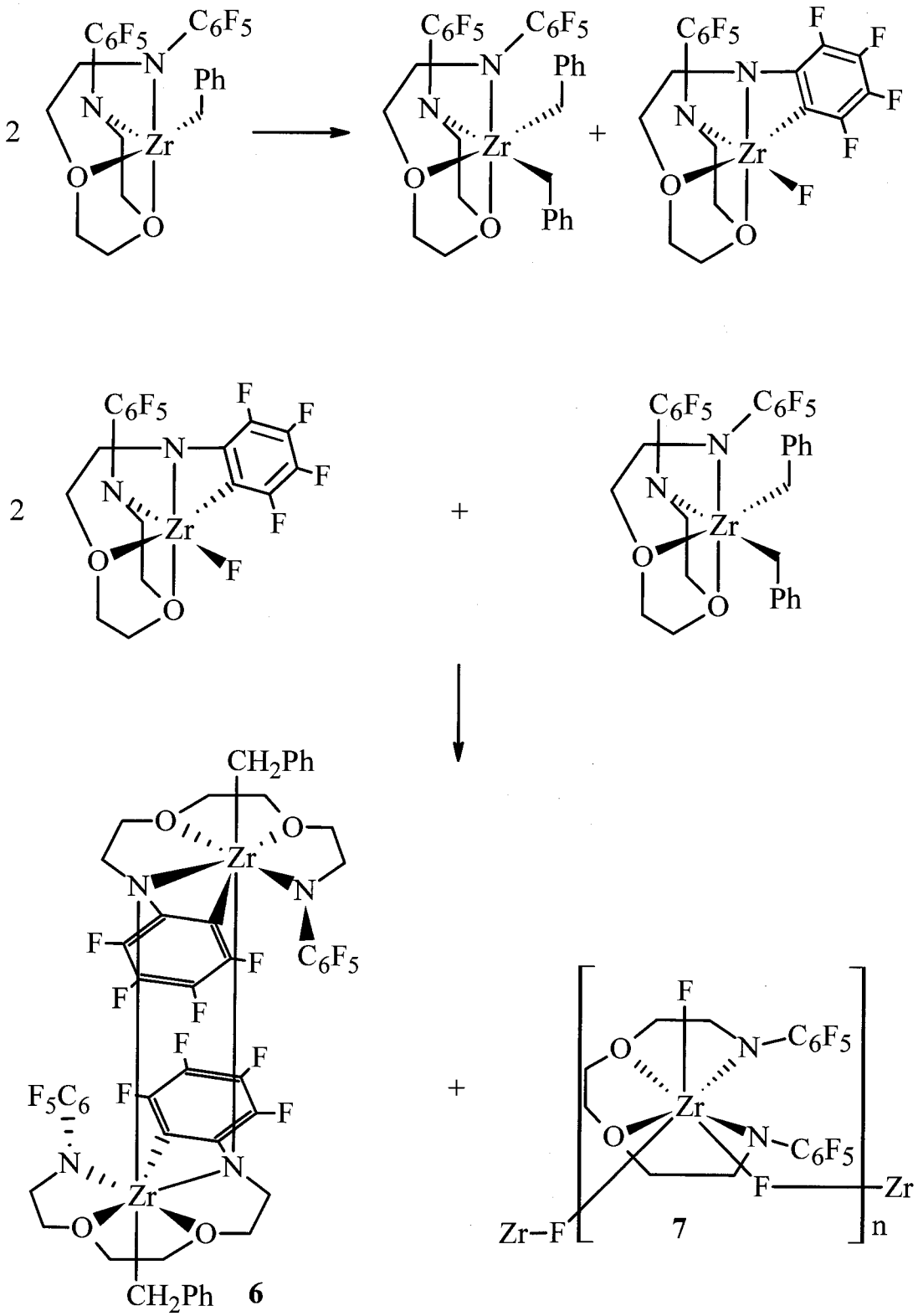

Scheme 6. Disproportionation and Redistribution Proposal.

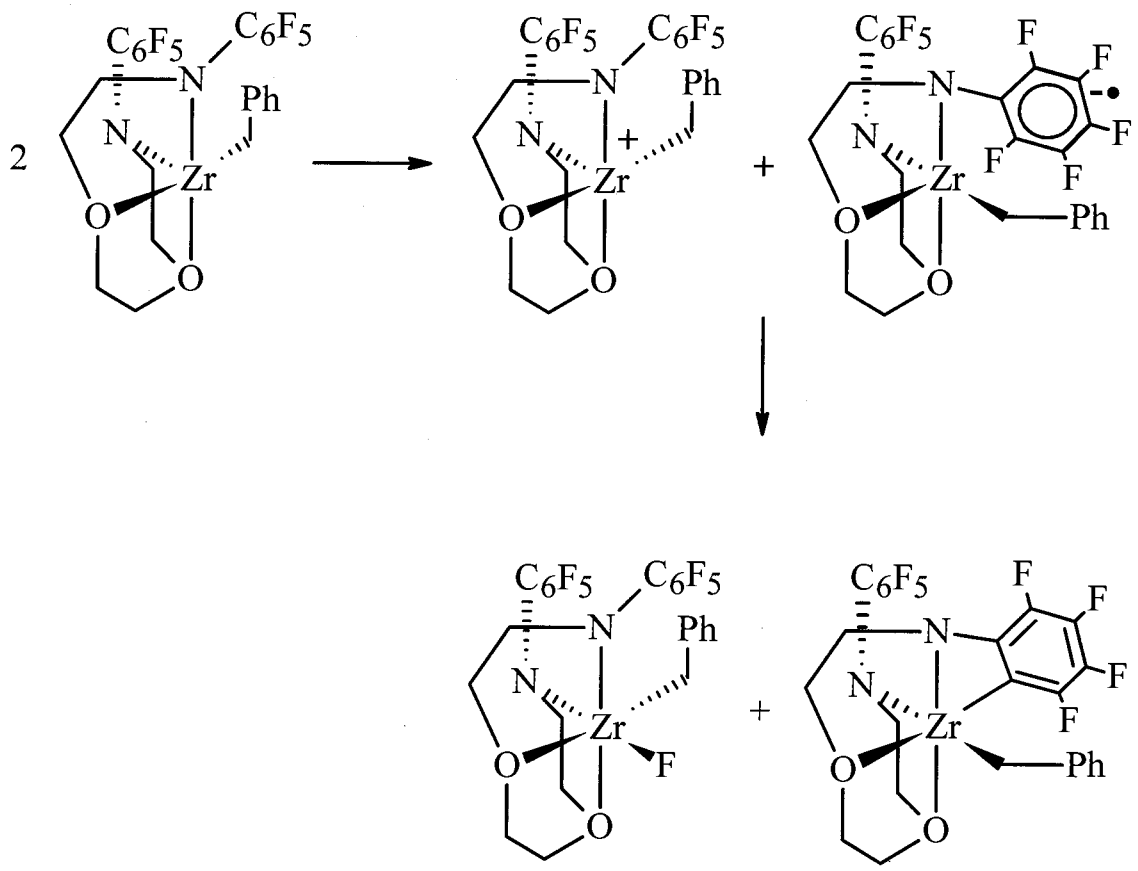

Scheme 7. Electron Transfer Proposal.

2.3 Solid State Structures

Several zirconium compounds bearing the (NOON) ligand (NOON)$ZrMe_2$ (**5**), (NOON)Zr(Cl)CH_2Ph,[121] (NOON)ZrCl[$N(SiMe_3)_2$] (**4**) and the closely related [$(C_6H_3(CF_3)_2)NCH_2CH_2OCH_2]_2ZrCl_2$[121] have been crystallographically characterized (Tables 1-4). The dimethyl species **5** (Fig 24) is typical of all the compounds but **4**, which has the sterically demanding $N(SiMe_3)_2$ amido group (Table 2).

(NOON)$ZrMe_2$ has a geometry that can best be described as distorted octahedral, with *cis* amido nitrogens, *cis* ether oxygens and *cis* methyl groups; one methyl group has

a *mer* relationship with the amido groups and the other has a *fac* relationship. Because each of the heteroatoms in the ligand is separated by two carbons, the ligand forms three five-membered chelate rings with the metal. The chelate rings also constrain the heteroatom-zirconium-heteroatom angle significantly, to an average of 69.9° for the rings with an amido nitrogen and an ether oxygen and to 68.88(10)° for the ring with both ether oxygens. Two of these rings lie in one plane and the third one lies roughly perpendicular to the first two. Thus, one oxygen atom forms a bridgehead between two rings that lie in a plane, and has a shorter Zr-O bond length (2.296(2)Å) than the oxygen that forms a bridgehead between the two chelate rings which are approximately perpendicular (2.411(2)Å). These bond lengths are shorter and longer than the normal range (2.302(2)-2.387(5)Å) found for zirconium-THF interactions in six-coordinate complexes and this is likely imposed by the geometry of the ligand.[112,137-142]

The zirconium-amido bond lengths (2.133(3), 2.103(3)Å) fall well within the normal range (2.063-2.192Å)[91,94,99,143,144] for polydentate ligands in a six coordinate environment. And, as is typical for amido ligands, the sum of the angles around the amido nitrogen is, on average, 357° indicating planarity. Perhaps due to the constraints of the ligand geometry, the amide-zirconium-amide angle is larger than might be expected – 116.66(10)°; however, the carbon-zirconium-carbon angle is closer to the ideal octahedral angle of 90° (91.03(13)°) and the zirconium-carbon bond lengths are well within the normal range.[112,139-141,145]

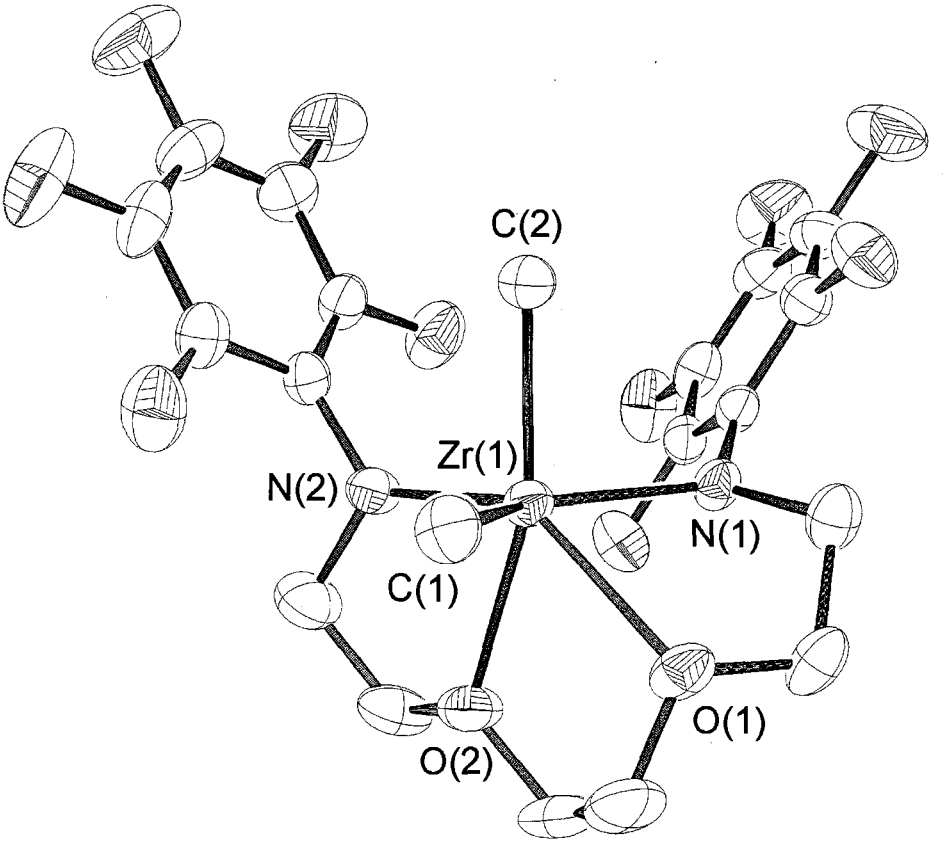

Figure 24. ORTEP3 drawing (thermal ellipsoids at 30% probability) of 5.

In contrast to the series (NOON)$ZrMe_2$, $[(C_6H_3(CF_3)_2)NCH_2CH_2OCH_2]_2ZrCl_2$ and (NOON)Zr(Cl)CH_2Ph, the steric influence of the $N(SiMe_3)_2$ group in **4** (Fig 25) causes further distortions to the geometry of the complex. The $N(SiMe_3)_2$ group occupies a site coplanar with the other amido groups and the chloride is located *trans* to an ether oxygen. Accordingly, the amido-zirconium-amido angle of the ligand is compressed to 104.8(2)° compared to 116.66(10) in **5**. The other significant difference between the two structures is the further compression of the angle between the *trans* amido nitrogen and the oxygen; in the dimethyl species **5**, this angle is 139.54(10) and in **4** it is 133.6(2). Obviously both these angles are significantly different than the ideal 180° and it could be argued that this

geometry could be described as a mono-capped trigonal bipyramid, but for convenience the complexes will be described as octahedral.

The ligand bond lengths in **4** are comparable to the rest of the compounds in the series (Table 2). The zirconium-chloride bond (2.431(3)Å) is comparable to those found in other six coordinate complexes (2.420-2.503Å).[94,105,108,137,138,140-142,146] The zirconium-amido bond (2.100(5)Å) of the *bis*(trimethylsilyl)amide is longer than all but one of the reported bond lengths for this group, (2.070-2.142Å)[147-150] reflecting the crowded six coordinate environment – it is usually found in complexes with lower coordination numbers.

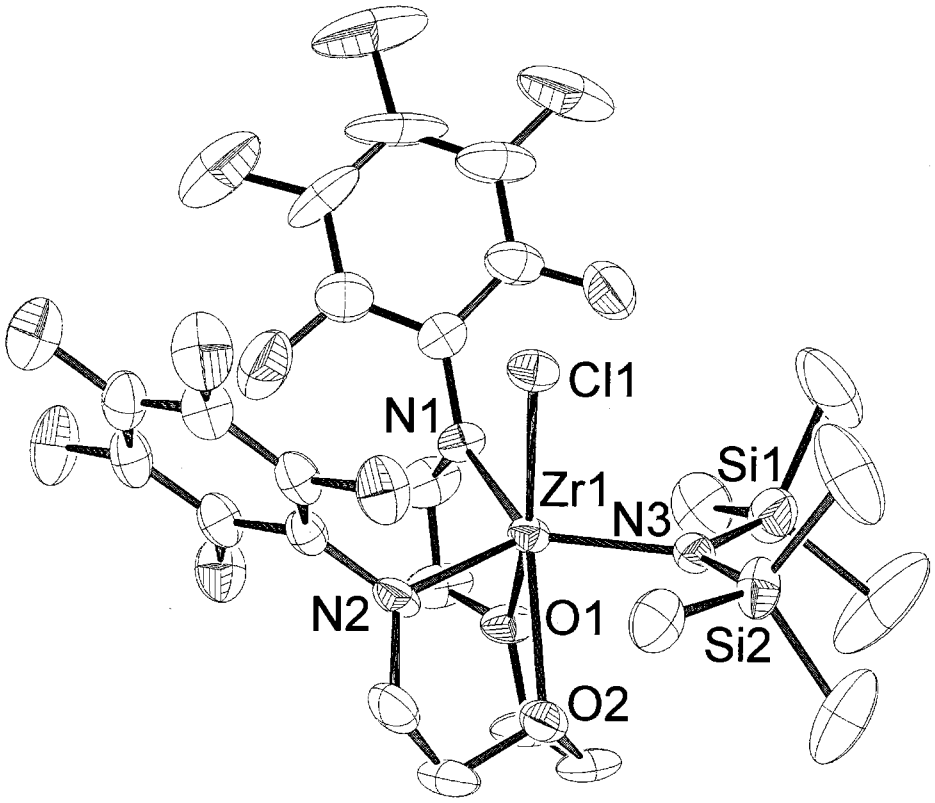

Figure 25. ORTEP3 drawing (thermal ellipsoid 30% probability) of 4. The toluene of solvation is omitted for clarity.

Table 1. Selected Bond Distances (Å) and Angles (deg) for 4 and 5.[a]

4		5	
		Bond Distances	
Zr(1) – Cl(1)	2.461(2)	Zr(1)—N(1)	2.133(3)
Zr(1) – O(1)	2.296(4)	Zr(1)—N(2)	2.103(3)
Zr(1) – O(2)	2.372(5)	Zr(1)—O(1)	2.411(2)
Zr(1) – N(1)	2.102(5)	Zr(1)—O(2)	2.296(2)
Zr(1) – N(2)	2.131(5)	Zr(1)—C(1)	2.256(3)
Zr(1) – N(3)	2.100(5)	Zr(1)—C(2)	2.251(3)
		Bond Angles	
Cl(1) – Zr(1) – O(1)	155.3(1)	N(1)—Zr(1)—N(2)	116.66(10)
Cl(1) – Zr(1) – O(2)	138.7(1)	N(1)—Zr(1)—O(1)	69.05(9)
Cl(1) – Zr(1) – N(1)	85.5(2)	N(1)—Zr(1)—O(2)	101.74(10)
Cl(1) – Zr(1) – N(2)	90.7(2)	N(1)—Zr(1)—C(1)	133.56(13)
Cl(1) – Zr(1) – N(3)	92.7(1)	N(1)—Zr(1)—C(2)	87.34(12)
O(1) – Zr(1) – O(2)	65.9(2)	N(2)—Zr(1)—O(1)	139.54(10)
O(1) – Zr(1) – N(1)	70.4(2)	N(2)—Zr(1)—O(2)	70.82(10)
O(1) – Zr(1) – N(2)	99.8(2)	N(2)—Zr(1)—C(1)	109.73(13)
O(1) – Zr(1) – N(3)	95.5(2)	N(2)—Zr(1)—C(2)	89.48(12)
O(2) – Zr(1) – N(1)	133.6(2)	O(1)—Zr(1)—O(2)	68.88(10)
O(2) – Zr(1) – N(2)	69.1(2)	O(1)—Zr(1)—C(1)	77.59(11)
O(2) – Zr(1) – N(3)	78.9(2)	O(1)—Zr(1)—C(2)	130.81(12)
N(1) – Zr(1) – N(2)	104.8(2)	O(2)—Zr(1)—C(1)	95.05(12)
N(1) – Zr(1) – N(3)	120.8(2)	O(2)—Zr(1)—C(2)	160.30(12)
N(2) – Zr(1) – N(3)	134.4(2)	C(1)—Zr(1)—C(2)	91.03(13)

[a] Estimated standard deviations in parentheses.

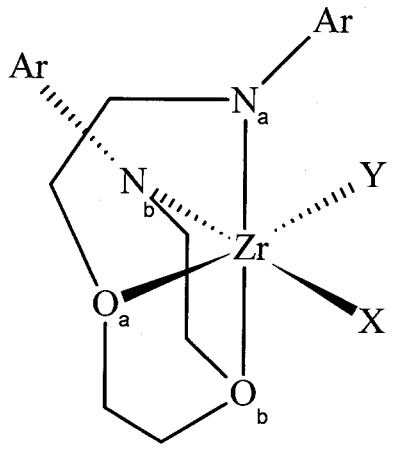

Figure 26. Key for Table 2.

Table 2. Comparison of Ligand Geometries.[a]

	5	$[(C_6H_3(CF_3)_2)NCH_2CH_2OCH_2]_2ZrCl_2$[121]	(NOON)ZrCl (CH_2Ph)[121]	**4**
		Bond Distances (Å)		
$Zr\text{-}N_a$	2.103(3)	2.101(5)	2.076(10)	2.102(5)
$Zr\text{-}N_b$	2.133(3)	2.120(5)	2.076(9)	2.131(5)
$Zr\text{-}O_a$	2.296(2)	2.263(4)	2.276(7)	2.296(4)
$Zr\text{-}O_b$	2.411(2)	2.294(4)	2.347(8)	2.372(5)
		Bond Angles (°)		
$N_a\text{-}Zr\text{-}N_b$	116.66(10)	110.2(2)	121.7(4)	104.8(2)
$N_a\text{-}Zr\text{-}O_a$	70.82(10)	71.8(2)	71.9(3)	70.4(2)
$N_b\text{-}Zr\text{-}O_b$	69.05(9)	72.4(2)	68.9(3)	69.1(2)
$O_a\text{-}Zr\text{-}O_b$	68.88(10)	67.0(2)	68.6(3)	65.9(2)

[a] Estimated standard deviations in parentheses.

Compound **6** is one of the photochemical decomposition products of **2**, having lost a benzyl group as well as a fluoride from one of the aromatic rings, resulting in an

ortho metallation of the aryl ring (Fig 27, Tables 3 and 4). The structure is dimeric in the solid state with one of the amido nitrogens from each of the ligands bridging between the zirconium centres, forming a four membered Zr_2N_2 ring. The geometry can be best described as a pentagonal bipyramid; the sum of the angles about the zirconium in the plane is 363.6° with all the ligand amido nitrogens, ether oxygens and the carbon of the metallated aryl ring lying approximately in a plane (maximum deviations N(1) +0.35 Å, O(1) -0.26Å). Accordingly, the benzyl group occupies one of the apical positions, while the amido group from the other unit in the dimer occupies the other. As with the dimethyl analogue **5**, the heteroatom-zirconium-heteroatom angles are constrained to approximately 70° due to the five membered chelate rings. Likewise, the N(1)-Zr(1)-C(1) angle of the metallated aryl ring is constrained to 61.51(8)°; all of this allows these five atoms to lie in a plane around the zirconium.

Because the metallation of the aryl ring results in it being almost coplanar with the pentagonal plane (dihedral angle 24°), the amido nitrogen can then bridge between the zirconium centres. In contrast, the C_6F_5 ring is nearly perpendicular to the pentagonal plane (dihedral angle 98°) which orients a fluoride towards the other unit in the dimer. The amido nitrogen that does not bridge show the typical trigonal planar geometry (sum of angles 360°) and an elongated bond length (Zr(1)-N(2) 2.163(2)Å) compared to other complexes in this class (average for the other three complexes with ligand **1**: 2.10Å). The bridging amido nitrogen shows distorted tetrahedral geometry and longer bond lengths (angles ranging from 90.8(2) to 116.3(2) and bond lengths Zr(1)-N(1) 2.308(2), Zr(1)-N(1)' 2.401(2)Å).

The zirconium-oxygen bond lengths in **6** (Zr(1)-O(1) 2.286(2), Zr(1)-O(2) 2.285(2)) are comparable to those in the other structures where the oxygen is between two chelate rings that are coplanar (the average for the other three complexes with ligand **1** is 2.29 Å). Likewise, the bond between the benzylic carbon in **6** and the zirconium (2.314(3) Å) is comparable to that found in (NOON)Zr(Cl)CH_2Ph (2.292(11) Å) as well as those reported for similar systems.[94,105,116,144,151] Furthermore, the bond angle (118.52(18)°) between the Zr-C(19)-C(20) indicates that the benzyl group is bonded η^1 to the metal.

The bond distance to the metallated aryl ring (2.326(3) Å) is comparable to the range found for zirconium-phenyl bonds;[116,152] however, it is longer than that found in the only other crystallographically characterized $ZrNC_2$ ring (2.260(2) Å)[153] and this is likely due to the constraints of the pentagonal bipyramidal geometry.

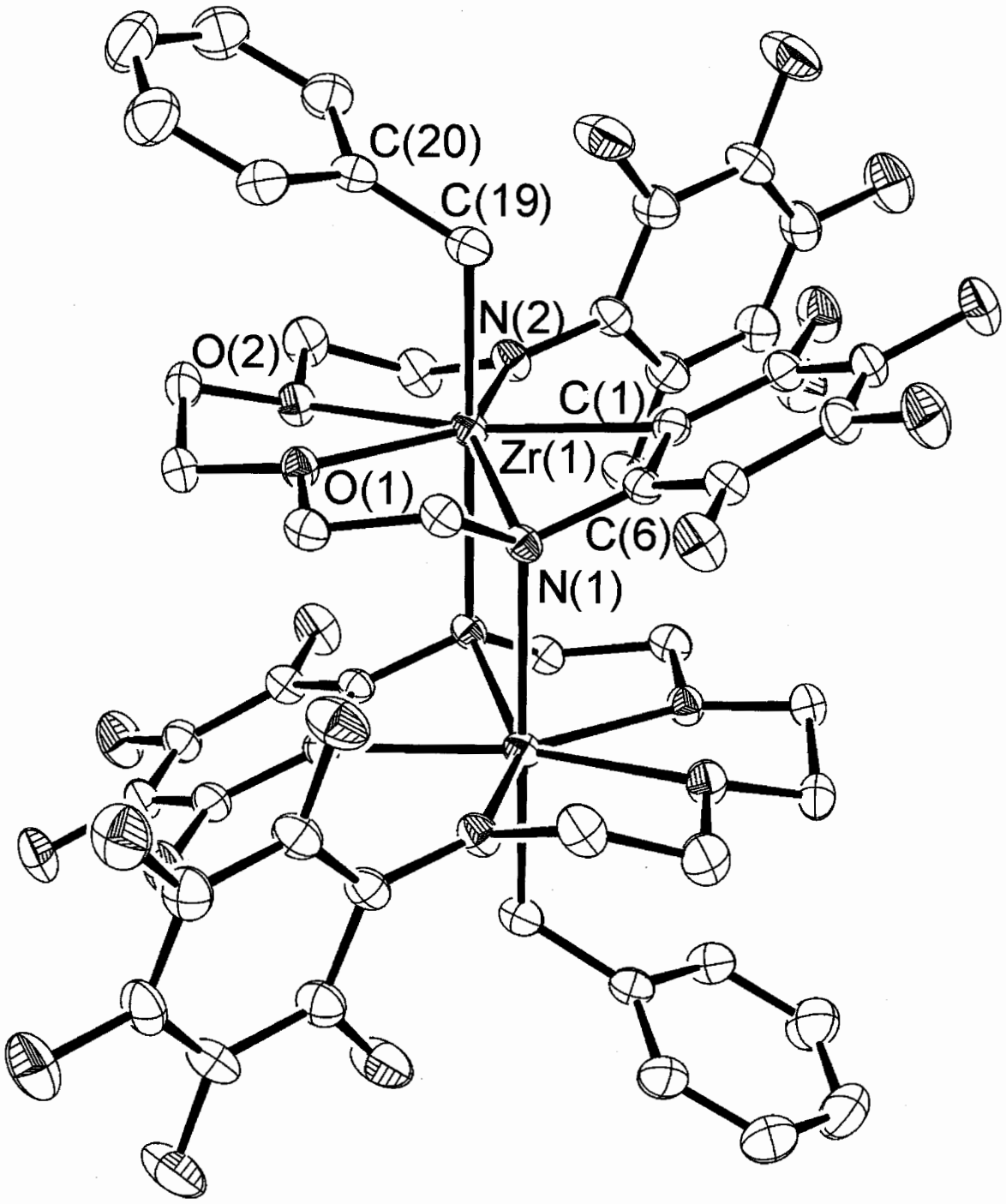

Figure 27. ORTEP3 drawing (thermal ellipsoids at 30% probability) of 6. The toluene of solvation is omitted for clarity.

Table 3. Selected Bond Distances (Å) and Angles (deg) for 6.[a]

	6		
Bond Lengths			
Zr(1)—N(1)	2.308(2)	Zr(1)—N(2)	2.163(2)
Zr(1)—N(1)'	2.401(2)	Zr(1)—O(1)	2.286(2)
Zr(1)—O(2)	2.285(2)	Zr(1)—C(1)	2.326(3)
Zr(1)—C(19)	2.314(3)		
Bond Angles			
N(1)—Zr(1)—N(2)	150.29(8)	N(1)—Zr(1)—N(1)'	74.85(7)
N(1)—Zr(1)—O(1)	69.70(7)	N(1)—Zr(1)—O(2)	133.18(7)
N(1)—Zr(1)—C(1)	61.51(8)	N(1)—Zr(1)—C(19)	91.93(9)
N(2)—Zr(1)—N(1)'	94.10(7)	N(2)—Zr(1)—O(1)	138.92(7)
N(2)—Zr(1)—O(2)	72.40(7)	N(2)—Zr(1)—C(1)	93.08(9)
N(2)—Zr(1)—C(19)	99.30(9)	O(1)—Zr(1)—N(1)'	90.02(6)
O(1)—Zr(1)—O(2)	66.89(6)	O(1)—Zr(1)—C(1)	127.20(8)
O(1)—Zr(1)—C(19)	81.81(8)	O(2)—Zr(1)—N(1)'	88.34(7)
O(2)—Zr(1)—C(1)	165.23(8)	O(2)—Zr(1)—C(19)	98.44(9)
C(1)—Zr(1)—N(1)'	95.56(8)	C(1)—Zr(1)—C(19)	80.89(9)
C(19)—Zr(1)—N(1)'	166.28(8)	Zr(1)—N(1)—Zr(1)'	105.15(7)
Zr(1)—N(1)—C(6)	90.8(2)	Zr(1)—N(1)—C(7)	111.2(2)
Zr(1)'—N(1)—C(6)	114.8(2)	Zr(1)'—N(1)—C(7)	116.3(2)
Zr(1)—N(2)—C(12)	115.5(2)	Zr(1)—N(2)—C(13)	134.1(2)
Zr(1)—C(1)—C(6)	90.5(2)	Zr(1)—C(19)—C(20)	118.5(2)
N(1)—C(6)—C(1)	113.8(2)	C(6)—N(1)—C(7)	115.0(2)
C(12)—N(2)—C(13)	110.1(2)		

[a] Estimated standard deviations in parentheses.

Table 4. Summary of Crystallographic Data for Compounds 4, 5 and 6.

	4	5	6
formula	$C_{27.5}H_{34}N_3O_2F_{10}ClSi_2Zr$	$C_{20}H_{18}N_2O_2F_{10}Zr$	$C_{64}H_{54}N_4O_4F_{18}Zr_2$
fw	811.40	599.58	1467.55
T (K)	ambient	ambient	ambient
λ (Å)	1.542	0.7107	0.7107
cryst syst	monoclinic	triclinic	triclinic
space group	*P2₁/n* (No. 14)	*P-1* (No. 2)	*P-1* (No. 2)
a (Å)	12.815(1)	8.8830(18)	8.9913(11)
b (Å)	18.883(2)	10.415(2)	11.0332(14)
c (Å)	14.915(2)	13.156(3)	15.2867(19)
α (deg)	90	83.147(4)	82.974(2)
β (deg)	103.226(9)	74.269(4)	79.912(2)
γ (deg)	90	82.043(4)	87.465(2)
V (Å^3)	3513.3(6)	1156.0(4)	1481.4(3)
Z	4	2	1
ρ (calcd) (g cm^{-3})	1.54	1.72	1.64
μ (mm^{-1})	4.769	0.58	0.46
F_{000}	1648	596	596
$2\theta_{max}$ (deg)	120	50	50
no. obsd reflns	5574	6268	6268
no. unique reflns	5351	4065	4065
absorption correction	Semi-empirical	Semi-empirical	Semi-empirical
R[a]	0.048	0.037	0.037
Rw[b]	0.039	0.072	0.072

[a] $R = \Sigma(|F_o|-|F_c|)/\Sigma|F_o|$. [b] $R_w = [\Sigma w(|F_o|-|F_c|^2)/\Sigma w(|F_o|)^2]^{1/2}$.

2.4 Behaviour of Complexes in Solution

The solid state structure of the dimethyl compound **5** has no internal symmetry elements; therefore, one would expect two methyl resonances and multiple resonances for the ligand. In solution, only one methyl resonance is observed and three signals for the ligand (Fig 29). This could be a result of a fluxional process occurring on the NMR timescale. The simplest explanation for this observation is something akin to a Berry pseudorotation. If one imagines N(1) in Fig 24 moving forward to a position *trans* to O(2) with a simultaneous movement of C(2) back between the amido nitrogens the result is a structure with the ligand in one plane and the methyl groups *trans* to one another. Since all the donors of the ligand can lie in one plane as observed in dimeric species **6**, it is reasonable that this geometry could arise for **5** as well. This species would have C_{2v} symmetry and this would account for the observed NMR spectrum. A static high symmetry structure different from the X-ray structure cannot be ruled out, but it seems more likely that a fluxional process is occurring in which the geometry changes from the low symmetry structure found in the solid state through a C_{2v} intermediate and back again. Schrock and coworkers have observed a similar phenomena with complexes of $\mathbf{L^{XXa}}$, which typically has a *fac* geometry in the solid state, but which shows higher symmetry in solution, consistent with a *mer* intermediate (Fig 13).[69] Alternatively, a fluxional process involving dissociation of one of the ethers in **5** results in a five coordinate complex that undergoes rapid Berry pseudorotation is also a possibility. As shown in Table 2, one Zr-O bond distance is much longer than the other, which may

suggest that the ether is weakly bound, lending credibility to a process involving oxygen dissociation.

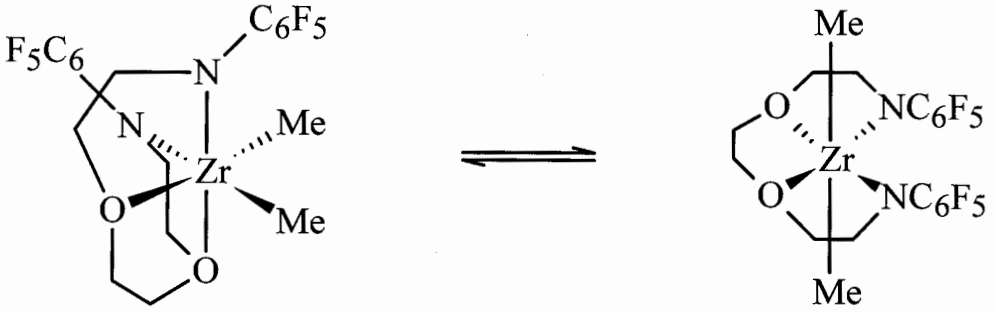

Figure 28. Fluxional Process.

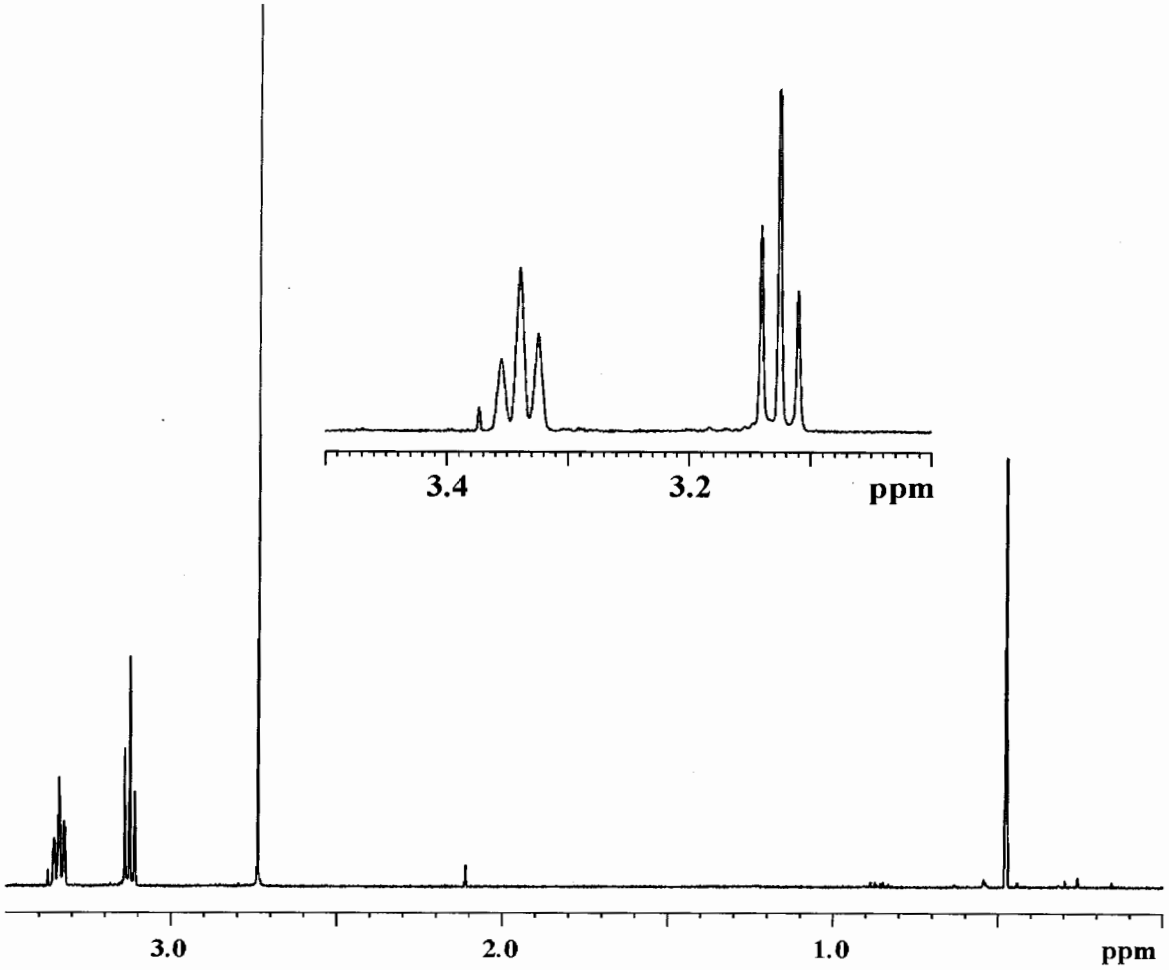

Figure 29. 360 MHz ^{1}H NMR of (NOON)ZrMe$_2$, C$_6$D$_6$, 295 K.

All complexes where zirconium bears two identical substituents show only three resonances for the ligand backbone, suggesting that fluxional processes are operative here as well. In compound **2**, the benzylic protons appear as a singlet and the compound does not display the features commonly associated with η^2-benzyl coordination: typically, the *ortho* protons are upfield of 6.7 ppm (6.92 ppm in **2**) and the benzylic $^1J_{CH}$ coupling constant is greater than 130Hz (124 Hz) in η^2-bound species.[79,154-157]

As in compound **5**, the observed symmetry in solution for (NOON)ZrCl[$N(SiMe_3)_2$], **4**, is higher than in the crystal structure. The observation of six ^1H resonances for the ligand in **4** is entirely consistent with the fluxional process proposed for **4**. In the highest symmetry intermediate, the chloride and $N(SiMe_3)_2$ groups would be *trans* to one another with the ligand occupying a plane giving effective C_s symmetry and thereby rendering all the methylene protons of the ligand diastereotopic. Furthermore, this is also consistent with the ^{13}C spectrum, since only three resonances are observed for the ligand backbone.

Consistent with the steric crowding in the solid state structure of **4**, the ^{19}F spectrum shows evidence of restricted rotation of the perfluorophenyl rings.[121] At room temperature, the *ortho* fluorine resonance is broad; lowering the temperature results in the signal decoalescing into two signals. The *meta* fluorine signal shows similar behavior. The *para* signal is a triplet over the entire temperature range studied. From the coalescence temperature shown in Fig 30, the activation energy for this process is calculated to be 49 ± 3 kJ/mol using the equal population two-site exchange equation.[121] The free energy of activation was calculated from the coalescence temperature (T_c in K) and the equation $\Delta G^{\ddagger} = (1.912 \times 10^{-2})(T_c)[9.972 + \log(T_c/\delta\upsilon)]$ in kJ mol^{-1} where $\delta\upsilon$ is the

separation of the resonances in Hz.[158] The error in $\Delta G^{\ddagger}$ was estimated assuming an error of 3 K in the estimate of T_c. Since the other complexes in this series do not show this hindered rotation, it is likely a result of the $N(SiMe_3)_2$ group and as outlined previously, this steric crowding is also reflected in the crystal structure of **4**. Schrock and coworkers have observed similar restricted rotation of the 2,6-$C_6H_3{}^iPr_2$ rings in complexes with $\mathbf{L}^{\mathbf{XXXIVf}}$, which has one less ether donor than the (NOON) ligand.[85,86]

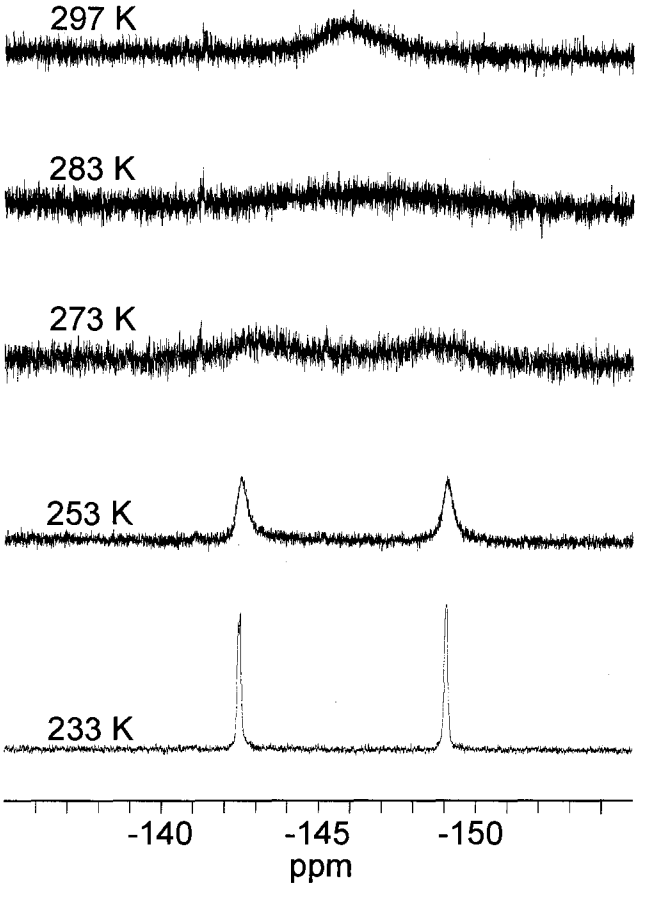

Figure 30. VT 339MHz ^{19}F NMR of (NOON)ZrCl[$N(SiMe_3)_2$], (4), C_6D_6.

While complex **6** is not soluble in aromatic solvents, it is suffiently soluble in deuterated THF to obtain NMR spectra. As expected, the ^{1}H NMR spectrum shows 12 overlapping signals for the ligand and the benzylic protons are diastereotopic and appear

as doublets consistent with a low symmetry environment. Likewise, the ^{13}C NMR spectrum shows six resonances for the ligand backbone. The ^{19}F NMR spectrum shows seven signals for the two aryl rings. Six of these signals are between -147 and -170 ppm, typical for these complexes, while one appears at -115 ppm, outside the usual range for these complexes. This resonance has been assigned to the fluorine *ortho* to the metallated position. In the crystal structure, this fluorine is located over the face of the other aryl ring of the same ligand (F(1)-C(aryl) distances from 2.819(4) to 3.782(4)Å). The unusual chemical shift may suggest that the same relative positions are maintained in solution. This could also indicate that the dimeric structure is maintained in solution, but the possibility that the geometry of a monomer is such that the relative positions remain the same, for example, with THF occupying an apical position rather than the bridging amido group, cannot be discounted.

2.5 Reactivity

2.5.1 Polymerization

As outlined in the introduction, one potential application of diamido zirconium complexes is as catalysts for olefin polymerization. Accordingly, the dichloride **3** was tested with 500 equivalents of MAO at 50°C in toluene and it showed modest activity for the polymerization of ethylene (3.2 kg mol^{-1} Zr h^{-1} atm^{-1}).

Treatment of the dibenzyl compound **2** with one equivalent of $B(C_6F_5)_3$ in dichloromethane resulted in an orange solution which showed no activity for ethylene or 1-hexene polymerization. The NMR data strongly support the formation of $[(C_6F_5NCH_2CH_2OCH_2)_2ZrCH_2Ph]^+[PhCH_2B(C_6F_5)_3]^-$, **8**, which decomposes over a

period of 24 hours in solution. The ^{1}H NMR spectrum of the starting material shows three resonances for the ligand and one for the benzylic protons in dichloromethane. Addition of $B(C_6F_5)_3$ results in six resonances for the ligand and two resonances for the benzylic protons. The ^{19}F resonances of the ligand are largely unchanged after abstraction of the benzyl group, the *ortho* fluorines in particular (-150.8 in **2**, -150.4 ppm in **8**), making it unlikely that there is an interaction between the fluorinated rings of the ligand and the metal. The $^{1}J_{CH}$ coupling constant for the benzyl methylene group increases from 124 Hz in **2** to 138 Hz in **8**, consistent with η^2-benzyl coordination; however, none of the aryl protons are as far upfield as one might expect.[79,154-157] Addition of d_8-THF does cause considerable changes to the spectrum, the $^{1}J_{CH}$ constant decreases from 138 Hz to 126 Hz and the ^{1}H resonance for the Zr-CH_2 shifts from 2.81 to 2.41 ppm. We take this as further evidence of η^2-benzyl coordination in the cation prior to the addition of a Lewis base.

The other factor to be considered in **8** is the role of the anion; the observation of the large upfield shift of the ^{11}B resonance on addition of $B(C_6F_5)_3$ is evidence of anion formation. It has been suggested that a $\Delta\delta_{m,p}$ value greater than 3.0 ppm in the borate anion is evidence of strong anion binding to the metal.[79] Thus the $\Delta\delta_{m,p}$ value of 3.0 ppm in **8** is somewhat ambiguous. However, addition of d_8-THF has very little impact on the NMR spectra of the $[PhCH_2B(C_6F_5)_3]^-$ unit. This suggests that the anion is only weakly coordinated to the cation in noncoordinating solvents.

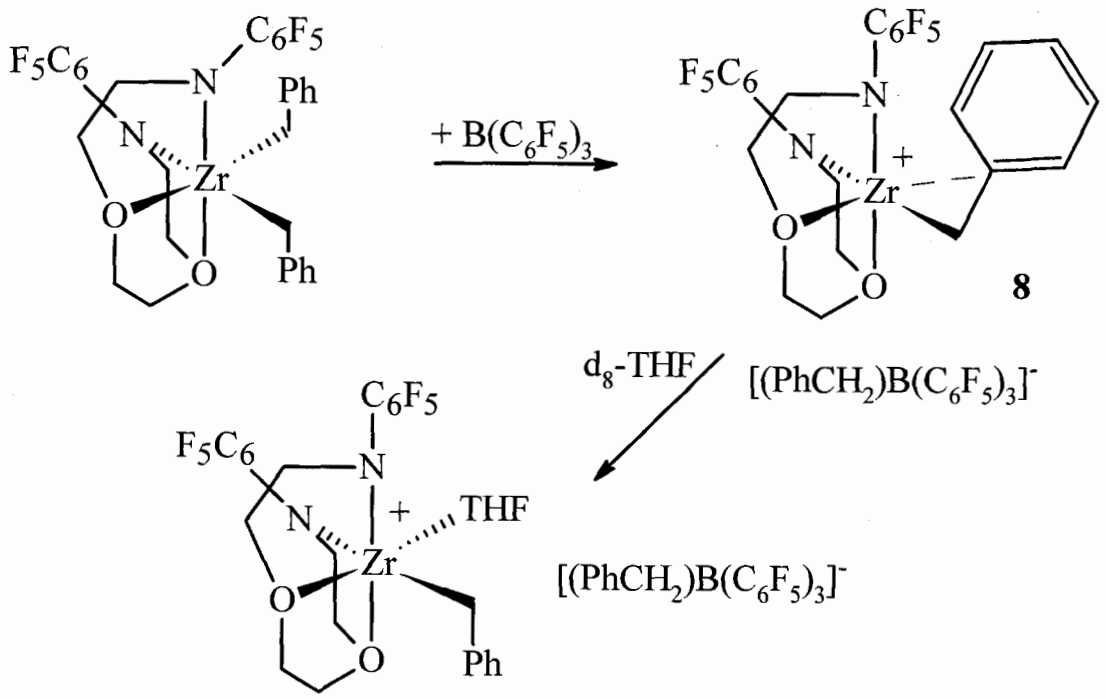

Scheme 8. Cation Formation.

This η^2-benzyl coordination in **8** likely accounts for the lack of ethylene or 1-hexene polymerization activity. Accordingly, the dimethyl complex **5** was treated with $B(C_6F_5)_3$ in attempt to generate a catalytically active species. Unfortunately, this species was not stable in solution and decomposed before it could be characterized by ^1H NMR spectroscopy. Thus, it appears that the η^2-benzyl coordination in **8** is essential to stabilize the cationic centre. This may also play a part in the relatively low activity when the dichloride **3** is treated with MAO. The resulting alkyl cation is likely decomposing over the course of the one hour polymerization run.

It is also worth noting that Schrock and coworkers have developed several diamido ligands with ether and pyridine donors that are effective ethylene and 1-hexene polymerization catalysts. They have shown repeatedly that addition of diethyl ether to a

cationic zirconium catalyst prevents polymerization.[60,69,82,83,85] In the case of the (NOON) system, the extra ether is essentially built into the ligand system. Thus, this ligand system is not likely to be effective in olefin polymerization chemistry.

2.5.2 Hydrides and Alkyls

As outlined in the conceptual cycle in the introduction, there are several classes of compounds that would be desirable in order to compare their reactivity with the metallocene and other diamido ligands. One class of compound is the hydrides, especially since Schwartz's reagent, $[Cp_2ZrHCl]_n$, has seen such widespread use. In practice there are two routes to make zirconium hydrides: the first is to treat $(NOON)ZrCl_2$ with a hydride source such as NaH, $LiBH_4$ or $LiAlH_4$; the second is to treat $(NOON)Zr(CH_2Ph)_2$ or $(NOON)ZrMe_2$ with hydrogen. Both routes were attempted without success. The reaction resulted in a complex mixture of products when hydride sources were employed and the starting material was recovered when hydrogen was used. This is disappointing, but not surprising in light of work with zirconocene hydrides; these compounds have been shown to be efficient at C-F bond activation.[134]

$$(23)\quad 3.5\ [Cp_2ZrH_2]_2 + C_6F_6\ (\text{excess}) \xrightarrow[\text{r.t.}]{\text{THF}} \begin{array}{l} 6\ Cp_2Zr(C_6F_5)F + 13\ H_2 \\ +\ 2\ C_6F_5H + Cp_2ZrF_2 \end{array}$$

Subsequent to our own work on the (NOON) system, Tilley and Turculet were successful in isolating such a product from the C-F bond activation of a triamido ligand.[139] Not only was C-F bond activation found with the perfluorophenyl ring, but also with 3,5-$C_6H_3(CF_3)_2$ aryl groups on the amido nitrogens, suggesting that intermolecular

processes might be involved. Thus, it seems likely that the failure to isolate a (NOON)ZrH_2 species can likely be attributed to the formation of a multitude of products due to the C-F bond activation of the ligand.

(24)

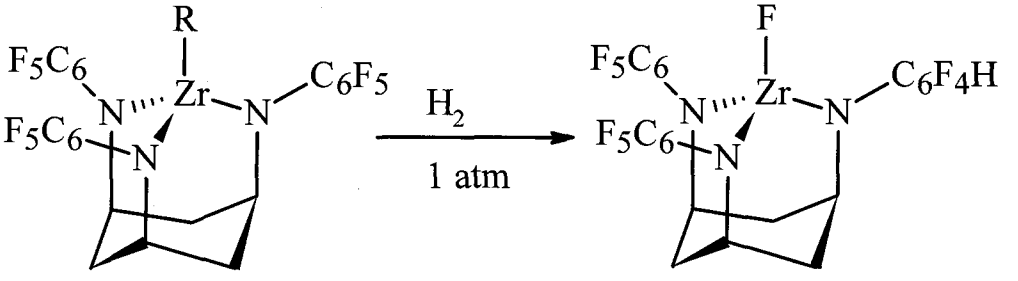

R = $Me(OEt_2)$,

CH_2SiMe_3, CH_2Ph

Another class of zirconium compounds of interest is zirconacyclopropanes and zirconacyclopentadienes (Section 1.2.1). Schrock and coworkers were able to isolate the trimethylphosphine adducts of several zirconacyclopropanes supported by $(RNC_6H_4)_2O$ ligands ($\mathbf{L}^{XXa}$ and $\mathbf{L}^{XXb}$ in Fig 12).[63,69] It was hoped the extra ether donor in the (NOON) ligand might allow for the preparation of these compounds without the need for phosphines, however, repeated attempts prepare similar compounds proved to be unsuccessful (Scheme 9).

In hindsight, this again may be due to the C_6F_5 rings in the ligand. In the same report as the zirconium hydrides are reported to react with perfluorobenzene (Eq 23), the authors report testing the zirconacyclopropanes with perfluorobenzene and obtaining a mixture of products rather than the formation of $Cp_2Zr(C_6F_5)F$.[134] This is consistent with our experimental observations; for example, the crude NMR of the reaction with EtMgBr was consistent with the formation of (NOON)$ZrEt_2$. All attempts to purify this compound

resulted in further decomposition, presumable due to transient formation of the zirconacyclopropane and subsequent decomposition by C-F bond activation. It is not obvious if the zirconacyclopropanes, which are often treated as zirconium (II) synthons, are in fact undergoing loss of alkene and oxidative addition, or rather acting as nucleophiles. Subsequent work from Schrock's group has shown that nucleophilic attack is possible with hafnium amides (Eq 25).[90]

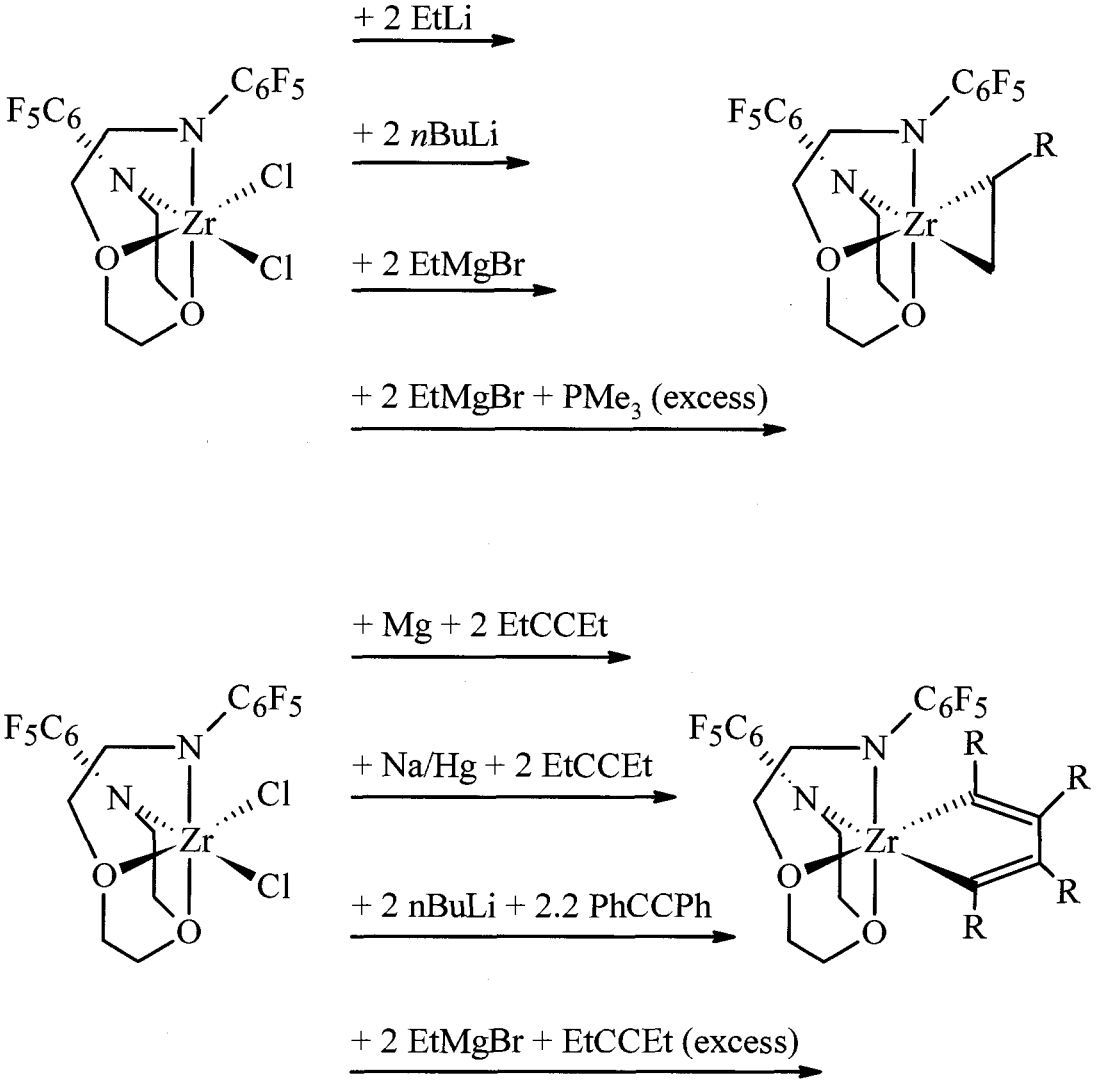

Scheme 9. Unsuccessful Attempts to Generate Zirconacycles.

(25)

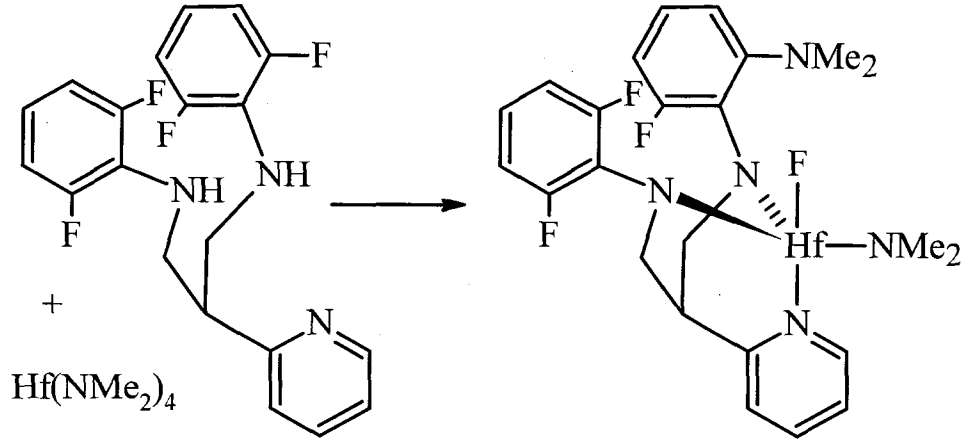

There is another general decomposition route that must be considered for alkyl complexes. As outlined in the introduction, Buchwald and coworkers have shown that complexes of the type $Cp_2ZrMeAr$ react to lose methane and produce a benzyne complex (Scheme 2). They have extended this chemistry to amides (Scheme 10).[159] While this has proved to be a useful route to a number of substituted pyrroles, it must also be considered as a decomposition pathway for amido ligands with β-hydrogens.

In the NOON system, the ligand is flexible and there is a fluxional process occurring in solution, this likely means that some of the β-hydrogens are sterically accessible for reaction with an alkyl group. When the decomposition of $(NOON)Zr(CH_2Ph)_2$ is followed by NMR at 105°C, toluene is observed as a product in addition to multiple resonances in the region of the ligand backbone. This suggests that decomposition of this compound involves hydrogen abstraction from the ligand.

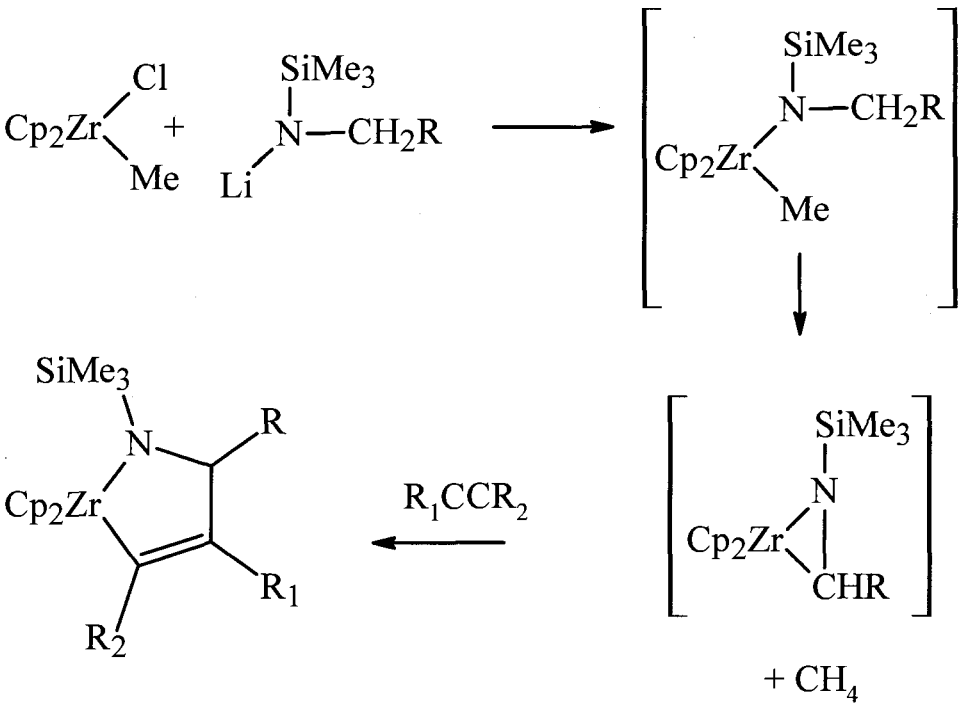

R = H, Ph, nC$_5$H$_{11}$, furan, thiophene

R$_1$ = H, Ph, Me, nC$_8$H$_{17}$

R$_2$ = H, Ph, nC$_3$H$_7$, SiMe$_3$, (CH$_2$)$_3$CN

Scheme 10. Generation of Azazirconacyclopropanes.

This type of decomposition pathway may account for the lack of success in isolating other dialkyl complexes. In addition to the attempts to isolate the dialkyl precursors to zirconacyclopropanes outlined already, all attempts to make allyl, methylallyl, zirconacyclobutanes and zirconacyclopentanes complexes from (NOON)ZrCl$_2$ and suitable Gringard, lithium and potassium reagents were unsuccessful. These reactions typically resulted in numerous products and attempts to selectively crystallize any reaction products were unsuccessful. These compounds may simply be more prone to decomposition either by reaction with the C$_6$F$_5$ ring or the ligand

backbone. There is a third possibility, namely that "ate" complexes are formed under the reaction conditions and rather than the lithium or magnesium halide being eliminated from the coordination sphere of the metal, it is retained. This has been observed by Schrock and coworkers using $\mathbf{L}^{\mathbf{XIX}}$, which has a pendant amino donor. Since the (NOON) ligand is flexible, it is possible that it could adopt a conformation in which the ethers or amides bind to the lithium or magnesium cations. Typically these complexes have lower solubility in aromatic solvents than the neutral complexes, so they would likely be discarded along with any salts produced during the reaction.

2.5.3 Insertion Chemistry

The final area of interest was the reaction of unsaturated species with the dialkyl compounds. As outlined in Chapter 1, bent metallocene dialkyls typically react reversibly with one equivalent carbon monoxide to produce an η^2-acyl complex. Contrasting this behaviour, treatment of a toluene solution of dibenzyl compound **2** with carbon monoxide resulted in complex mixture of products. It is not clear at this point if this due to the formation of multiple products (insertion of two equivalents of CO, migration of the second alkyl to the acyl, rearrangements of the initial insertion product) or decomposition of the insertion products via the routes already outlined. Unfortunately, a similar problem occurred when the dialkyl complexes were treated with alkynes (terminal, internal and 1,7-octadiyne). Typically, no reaction occurred at room temperature and the starting material was recovered, while heating again resulted in a complex mixture of products.

2.6 Summary

The ligand development cycle in Fig 19 outlines the five steps in ligand development that are typical of this research program. The (NOON) ligand system has been studied in this context. Several complexes have been prepared and fully characterized, including the dialkyl complexes. These compounds are thermally robust in solution in the absence of ambient light. The solid state structures show distorted octahedral geometry and increasing the steric bulk of the substituents causes further distortions to the geometry, indicating that the ligand can adopt different conformations. The observed symmetry in solution suggests a fluxional process is occurring. This also is consistent with a decomposition pathway in which the flexibility of the ligand backbone allows for the metallation of the ligand and loss of toluene in the decomposition of (NOON)$ZrBz_2$. The alkyl complexes do react with unsaturated substrates and hydrogen, but the result is multiple uncharacterizable products. This is in contrast to the macrocyclic DAC zirconium dialkyl complexes, which were too crowded to react with unsaturated substrates.[120]

Chapter 3. Organozirconium Complexes Supported by Cross-Bridged Cyclam

3.1 Introduction

The start of this research effort into diamido supporting ligands began with the macrocyclic DAC system, diaza-18-crown-6. This led to the use of the linear H_2(NOON), which supported a number of zirconium complexes. However, it did suffer from both photochemical and thermal decomposition pathways. In hindsight, the drawbacks of adding perfluorophenyl rings far outweigh the benefits of incorporating them into the ligand since they are potentially reactive not only under reducing conditions, but also with nucleophiles. One possible step in the evolution of this ligand system would be to retain the two central ethers and simply use other amido substituents; however, this does not address the second decomposition pathway that the (NOON) system was prone to – metallation of the ligand backbone. This process requires that the Zr-C and C-H units form a four membered transition state and the flexibility of the (NOON) ligand accommodated this geometry. Thus, the desired next generation of ligand should be rigid, thereby precluding, or at least reducing this decomposition pathway. While other macrocyclic ligands used to support group 4 chemistry thus far are certainly rigid, they are unsaturated and prone to alkyl migration from the metal to the macrocycle framework (Eq 9, Section 1.3.4).[102-105]

Cross-bridged cyclam, (CBC), is a 14-membered macrocycle with two amido donors and two amino donors. As the name indicates, the amido groups are located *trans*

to one another with an ethylene cross-bridge between the amino groups. This bridge should effectively restrict the geometry of the ligand, so that the metallation of the ligand is reduced.

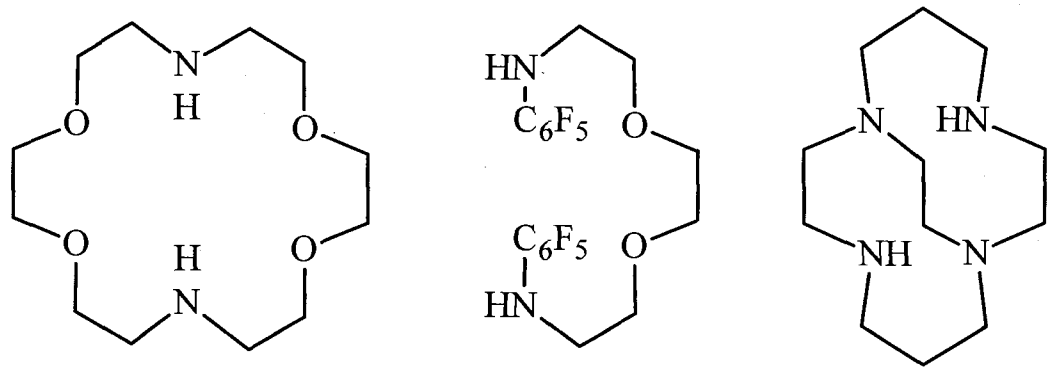

H_2(DAC) H_2(NOON) H_2(CBC)

Figure 31. Continued Ligand Evolution

3.2 Synthesis of Complexes

The synthesis of cross-bridged cyclam has been reported,[160] as has the chemistry of either protio[160] or N-alkylated[161-163] coordination compounds with lithium,[160] copper,[160,163] manganese,[162] iron,[162] gallium[164] and indium.[164] However, to the best of our knowledge, neither its use as a diamido ligand nor its use with early transition metals has been reported previously.

The synthesis of H_2(CBC) is considerably longer than that of H_2(NOON), but it is routinely carried out on large scale to produce 10-15 g in 7% overall yield (Scheme 11). The ligand must be dried by sublimation from potassium hydroxide prior to storage in a toluene solution over activated 4Å molecular sieves.

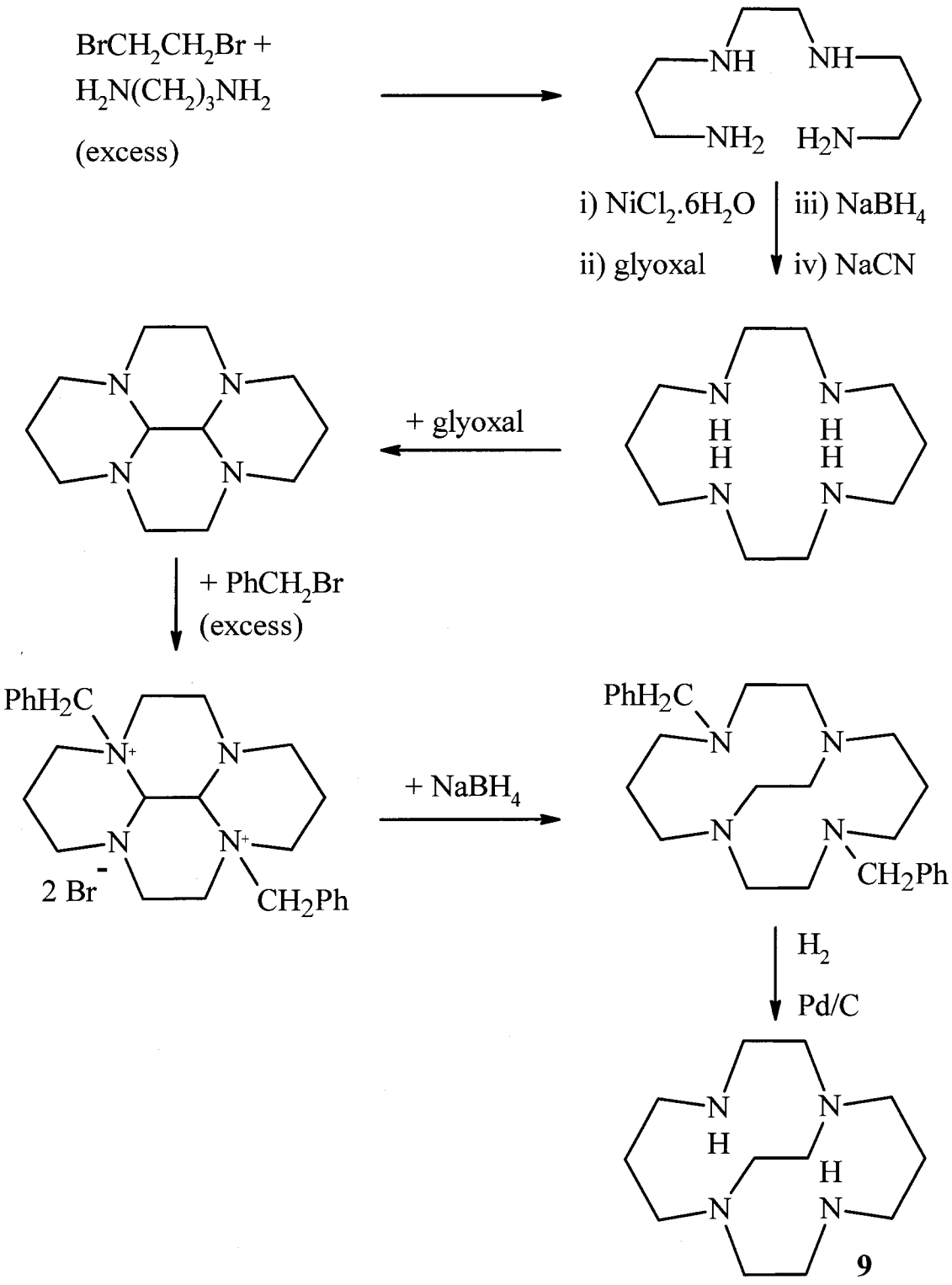

Scheme 11. Synthesis of H_2(CBC)

An efficient route into organozirconium chemistry is the acid-base reaction chemistry with homoleptic alkyl complexes (Eq 26). The reaction of tetrabenzylzirconium with H_2(CBC) yields **10** in excellent yield. This yellow compound is soluble in aromatic solvents and only sparingly soluble in aliphatic ones. Compound **10** is thermally robust in solution: heating at 105°C for 26 hours causes 50% decomposition (compared to an internal standard by ^{1}H NMR); the process does not follow first order kinetics and ultimately results in disappearance of ligand resonances into the baseline.

(26) H_2(CBC) + $Zr(CH_2Ph)_4$ ⟶ 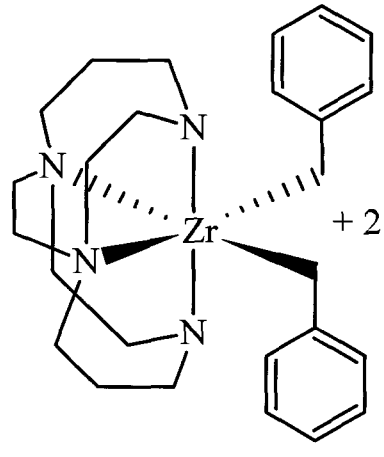 + 2 C_7H_8

10

Given the previous observations of photolytic benzyl-Zr bond cleavage in (NOON)$Zr(CH_2Ph)_2$ due to ambient light, we were concerned that this might again be a possibility. Irradiation of **2** for 14h at 435nm led to complete transformation of the compound; in contrast, **10** showed minor degradation when irradiated at 375nm for 24h and bibenzyl was not produced. This suggests that **10** is not significantly degraded by ambient light.

To further understand the reactivity of **10**, it was treated with *t*-butyl-isonitrile. This resulted not in the expected η^2-iminoacyl (Eq 10), but rather the formation of a vinylamide complex, **11** (Eq 27); The vinyl amido group in **11** has ^{1}H resonances at 8.40 and 6.15 ppm with a coupling constant of $^3J_{HH}$ = 14.0 Hz. This is consistent with the *trans* configuration of the double bond observed in the solid state (Section 3.3) and is similar to other vinyl amide complexes.[165] Prolonged heating of **11** (90h, 80°C) results in the formation of multiple products when followed by ^{1}H NMR and no attempt was made to isolate these products.

The formation of vinylamide complexes by this route is rare, but not without precedent.[120,165] Similar transformations have been observed by Rothwell and coworkers (Scheme 12); deuterium labelling experiments confirmed that both vinyl protons come from the benzylic methylene group. As shown in Scheme 12, the *bis*(alkyl) complex reacts with two equivalents of the isonitrile to yield the *bis*(vinylamide) complex. In contrast, treating **10** with two equivalents of *t*-BuNC only produces **11**; the steric bulk of the t-butyl group on the amine of **11** likely prevents a second insertion.

(27) $(CBC)Zr(CH_2Ph)_2$ + *t*-BuNC ⟶

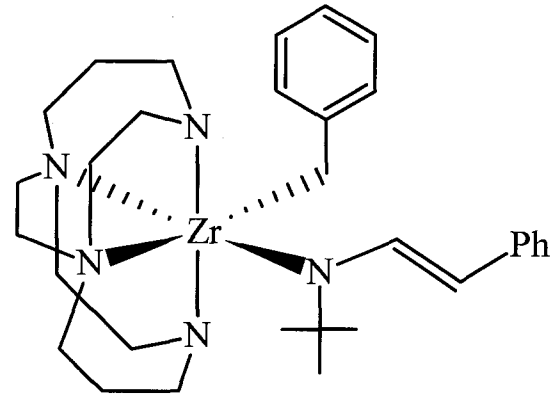

11

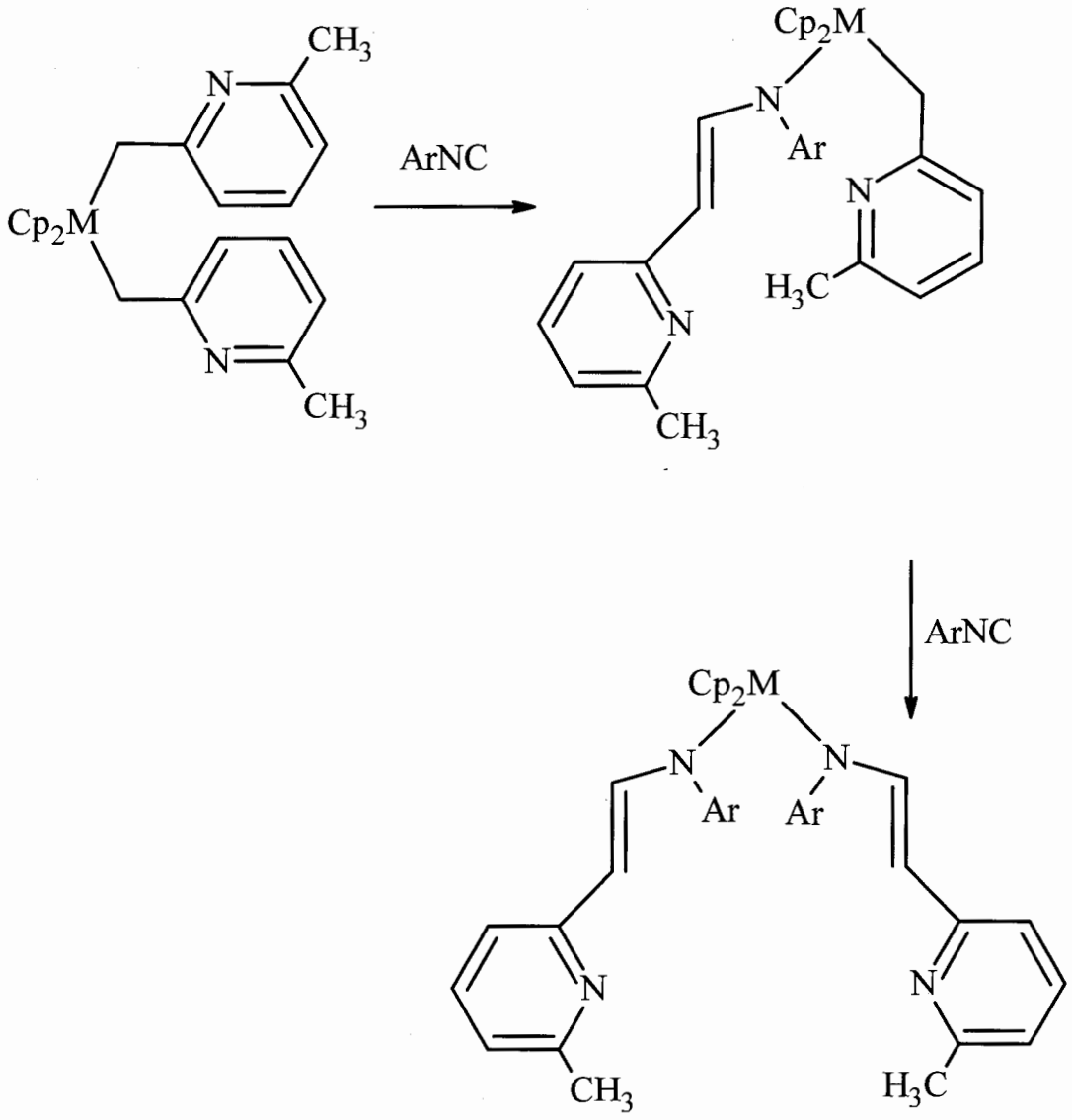

Scheme 12. Isonitrile Insertion.

We initially encountered difficulties preparing $(CBC)ZrCl_2$ as a general precursor (*vide infra*), so as an alternative, we explored protonolysis of **10** with phenols, since the resulting phenoxides can be used in metathesis reactions as an alternative to halides with group 3 metals.[166] Reaction of **10** with two equivalents of 2,6-di-*t*-butylphenol produces the monosubstituted product $(CBC)Zr(CH_2Ph)(O\text{-}2,6\text{-}C_6H_3Bu^t)$ **12** as a pale yellow

powder (Eq 28). When the reaction of **10** with two equivalents of 2,6-di-*t*-butylphenol is followed by NMR, there is no evidence for either reaction of the benzyl group or the amido groups of the ligand with the second equivalent of phenol. Given the acidity of the phenol, it is surprising that the amido groups do not react, but this may be attributable to the strong chelate effect of the macrocycle and the steric congestion at the metal centre. The NMR spectra of **12** are further discussed in Section 3.4.

(28)

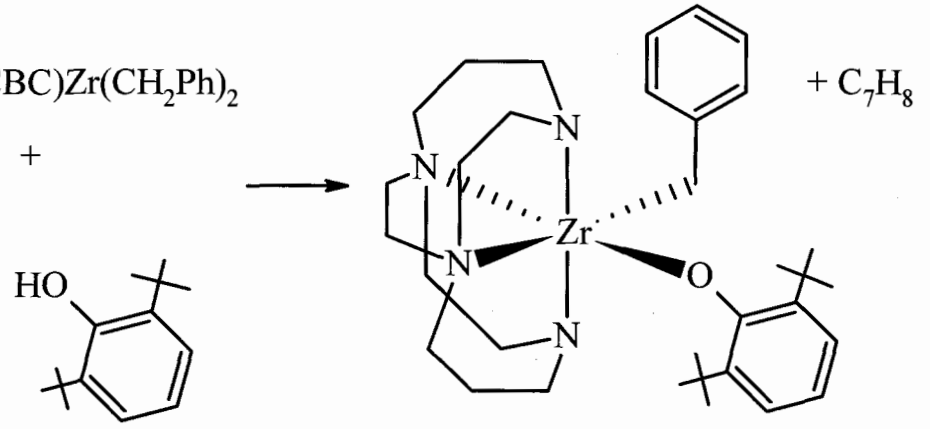

12

Prolonged heating of **12** in aromatic solvents leads to loss of toluene and the formation of a six-membered metallacycle **13** (CBC)Zr[κ^2(C,O)-OC_6H_3(6-Bu^t)(2-CMe_2CH_2)] (Eq 29). The formation of **13** is clearly indicated by the loss of a *t*-butyl group and the formation of two CH_3 groups and a CH_2 group that has a ^{13}C chemical shift of 75.4, typical of alkyl groups bound to zirconium. This type of elimination has been observed previously with a related aniline species.[147] Presumably the methyl group of the phenoxide can more readily adopt the correct orientation for the metallation to occur than any of the methylene groups of the cross-bridged cyclam ligand.

(29)

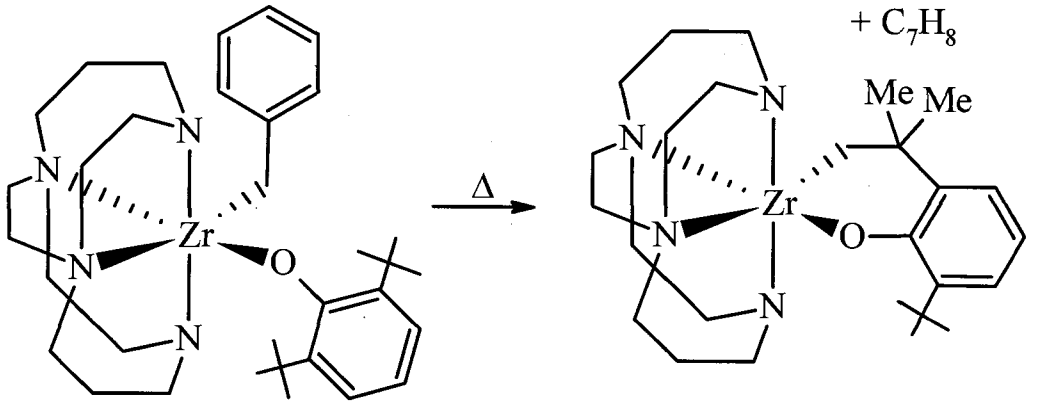

13

We wondered if other zirconacycles could be generated in a similar manner to **13** by reacting (CBC)Zr(CH_2Ph)$_2$ with one equivalent of an alcohol, followed by elimination of toluene. An interesting possibility was to use a silanol with a β-hydrogen. If this hydrogen were to be eliminated, a novel zirconacycle would be generated (Scheme 13). However, when **10** was treated with one equivalent of HOSi(Bu^t)$_2$H the mixed alkyl-siloxide compound was not recovered, instead the *bis*(siloxide) **14** was isolated (Eq 30). This compound has been crystallographically characterized (Section 3.3) and the NMR spectra lack any benzylic or aromatic resonances. This is in contrast to the reaction with 2,6-di-*t*-butylphenol, where only one equivalent reacts, even under forcing conditions. This difference likely results from the different orientations of the *t*-butyl groups. In the phenoxide, the *t*-butyl groups are oriented towards the metal centre providing more steric protection of the metal centre than the *t*-butyl groups of the silanol, which are oriented away from the metal centre (*vide infra*).

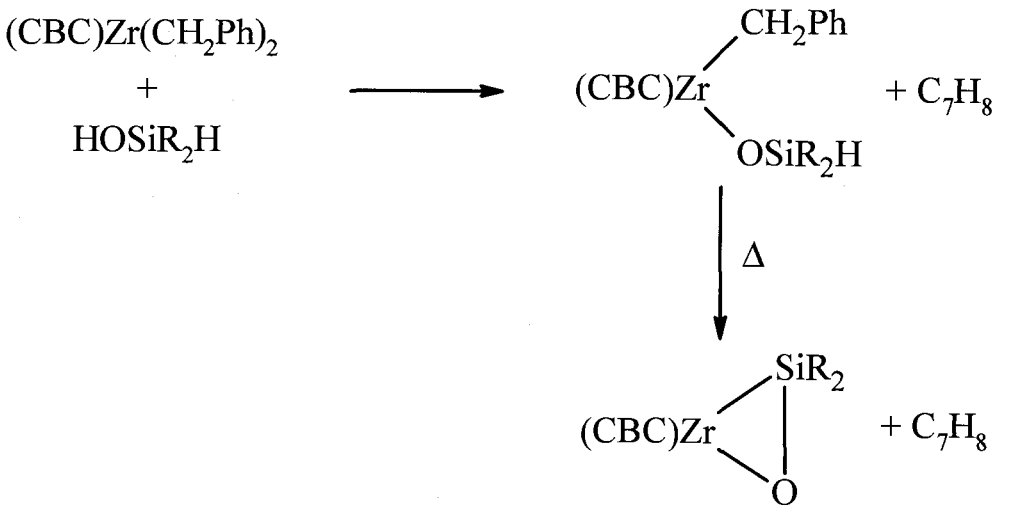

Scheme 13. A Potential Route to an Oxasilazirconacyclopropane.

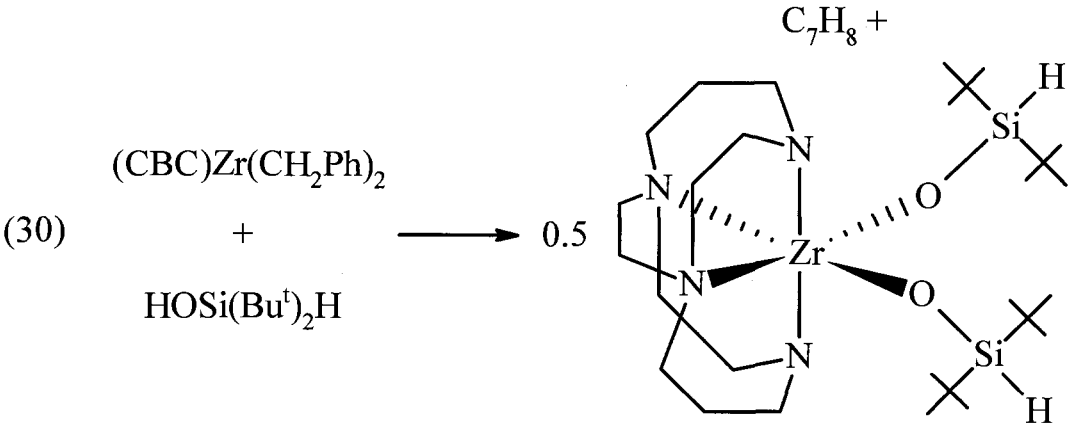

14

Since steric effects likely prevent the reaction of the second equivalent of 2,6-di-*t*-butylphenol with $(CBC)Zr(CH_2Ph)_2$ we turned to the less hindered 2,6-dimethylphenol. The reaction of $(CBC)Zr(CH_2Ph)_2$ with two equivalents of 2,6-dimethylphenol produces diphenoxide **15** in good yield (Eq 31), and this compound has been crystallographically characterized (Section 3.3) and its ^1H NMR spectrum is discussed in Section 3.4.

(31) 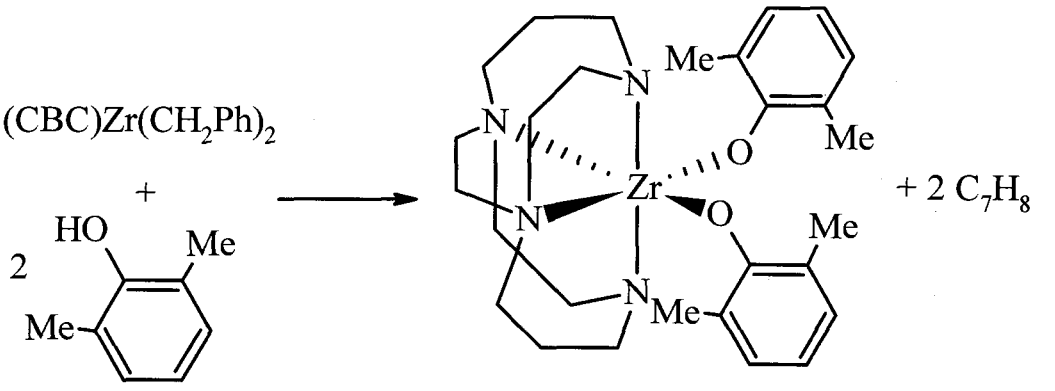

15

Attempts to carry out metathesis reactions with MeLi or $LiCH_2SiMe_3$ and **15** were unsuccessful; as a result, we turned our attention back to the synthesis of $(CBC)ZrCl_2$ **16**, as a potential precursor to a range of organometallic compounds. Unfortunately, to date, the clean isolation of the Li, Na, or K salts of cross-bridged cyclam itself has not been accomplished. These salts would be desirable for metathesis reactions with zirconium tetrachloride. Likewise, we initially experienced low yields in the direct protonolysis of $ZrCl_2[N(SiMe_3)_2]_2$ with $H_2(CBC)$. Given the previous problems with the $H_2(NOON)$ reaction resulting from contamination of the $ZrCl_2[N(SiMe_3)_2]_2$ with $ZrCl[N(SiMe_3)_2]_3$, we suspected that this problem was occurring here. Fortunately, $(CBC)ZrCl_2$, **16** precipitates directly from the reaction mixture as a yellow powder. Investigation of the supernate also led to the isolation of the mixed amide-chloride $(CBC)Zr(Cl)[N(SiMe_3)_2]$ **17** as a second product (Eq 32-33). The identity of **17** was confirmed by the synthesis of **17** from **16** and $NaN(SiMe_3)_2$ (Eq 34) and its NMR features are discussed in Section 3.4. The preparation of $ZrCl_2[N(SiMe_3)_2]_2$ from $NaN(SiMe_3)_2$ and zirconium tetrachloride results in contamination with $ZrCl[N(SiMe_3)_2]_3$.[122] If $LiN(SiMe_3)_2$ is used, $ZrCl[N(SiMe_3)_2]_3$ can be avoided and the subsequent yield of **16** is 90%.

(32) $ZrCl_2[N(SiMe_3)_2]_2 + H_2CBC$ → 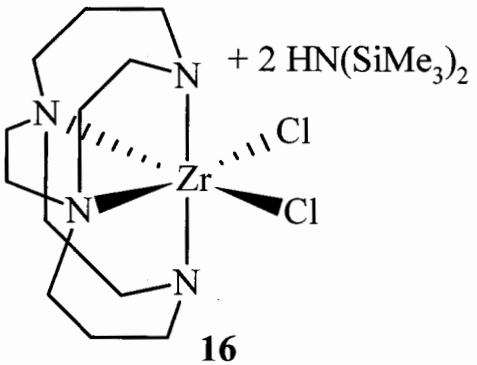 + 2 $HN(SiMe_3)_2$

16

(33) $ZrCl[N(SiMe_3)_2]_3 + H_2(CBC)$ → 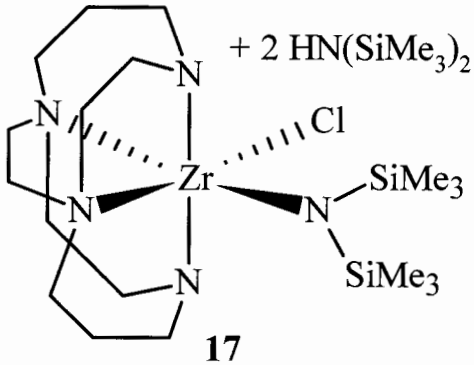 + 2 $HN(SiMe_3)_2$

17

(34) $(CBC)ZrCl_2 + NaN(SiMe_3)_2$ → 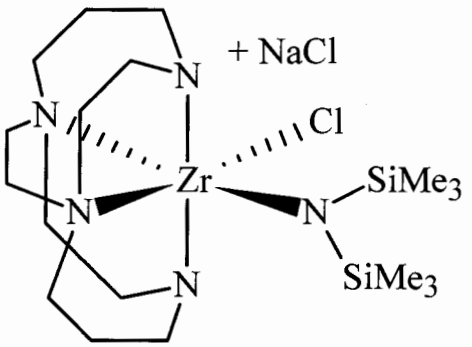 + NaCl

17

The dimethyl compound **18** was prepared by reaction of dichloride **16** with 2 equivalents of MeLi in poor yield (24%) (Eq 35). The methyl resonance in the ^1H NMR of **18** integrates for 6 protons, ruling out a mixed chloro-alkyl species and the downfield

^{13}C chemical shift of the methyl groups in **18** (39.3 ppm) are consistent with zirconium bound alkyl groups. Attempts to use MeMgBr in the production of **18** resulted in even lower yields and contamination with the starting dichloride.

(35) $(CBC)ZrCl_2 + 2\ MeLi \longrightarrow$ 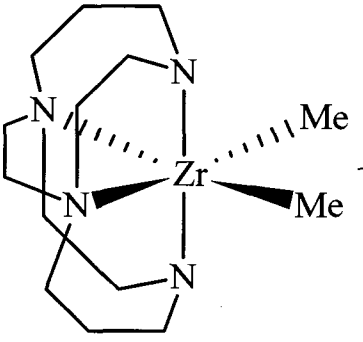 $+ 2\ LiCl$

18

As outlined in the introduction, zirconacycles are a class of compounds of general interest, especially those with two carbons attached to zirconium. One possible route to these compounds is the hydrocarbon elimination, as had been observed for the mixed benzyl phenoxide **12** (Eq 29). To test the generality of this route, $(CBC)Zr(CH_2SiMe_3)_2$, **19**, was prepared via metathesis of the dichloride **16** and $LiCH_2SiMe_3$ (Scheme 14). Compound **14** was crystallographically characterized (Section 3.3) and the key features of its NMR spectra are discussed in Section 3.4. Unfortunately, thermolysis of **19** did not lead to the formation of a zirconacycle nor to the isolation of any organometallic products.

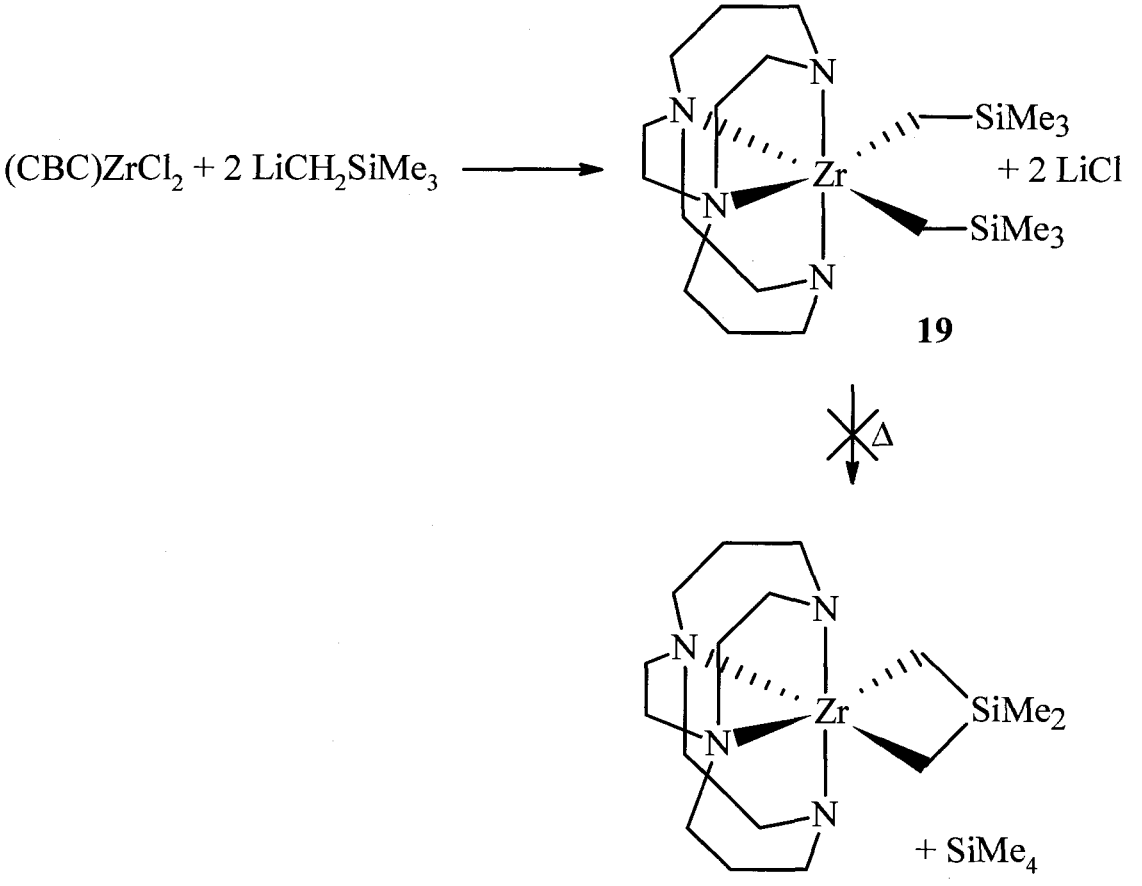

Scheme 14. Production of (CBC)Zr(CH_2SiMe_3)$_2$ and its Thermal Decomposition.

Negishi developed a general route to zirconacycles that involves treating Cp_2ZrCl_2 with two equivalents of n-BuLi in the presence of an alkyne (Scheme 3).[167] In the present case, treatment of a dichloro complex **16** with two equivalents of n-BuLi and two equivalents of diphenylacetylene generates metallacyclopentadiene **20** in modest yield. This compound has poor solubility in aromatic solvents, and is a yellow powder. Despite obtaining a crystal structure of **20** (Section 3.3), the ^{1}H NMR of **20** in d_6-benzene was ambiguous as several resonances were obscured by the solvent. Thus, we were concerned that the bulk of the sample might have been a zirconacyclopropene, rather than

the zirconacyclopentadiene. However, when the NMR spectra were obtained in d_8-THF all of the expected aromatic resonances for **20** were observed.

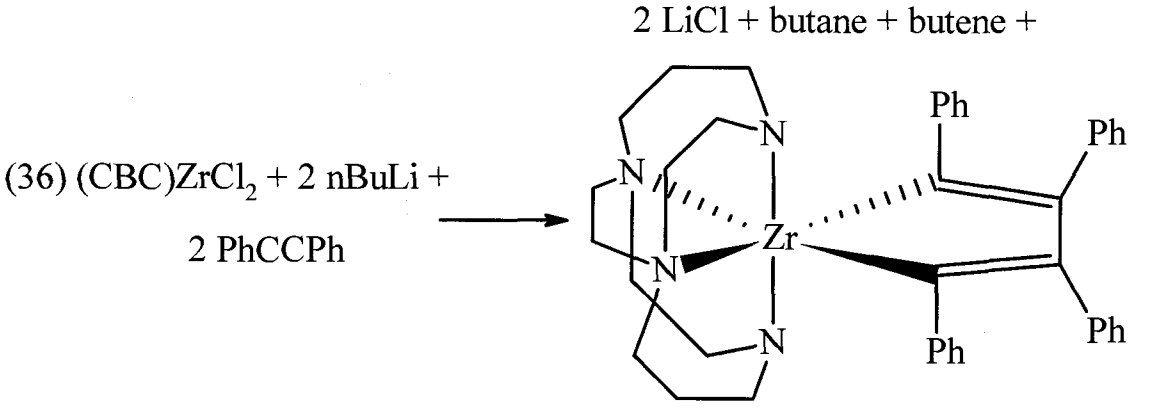

20

3.3 Solid State Structures

Several of the compounds presented in the previous section have been structurally characterized: the *bis*(phenoxide) **15**, the bis(siloxide) **14**, the *bis*(alkyl) **19** and the zirconacyclopentadiene **20** and the mixed benzyl-vinyl amide **11**.

The solid state structure of the bis(phenoxide) (CBC)Zr(O-2,6-$C_6H_3Me_2$)$_2$ was determined by X-ray crystallography (Tables 5 and 6). The structure is depicted in Fig 32 and important bond distances and angles are given in Table 6. The zirconium centre is six-coordinate and best described as distorted octahedral. The ligand can be thought of as saddle shaped, with the amido nitrogens *trans* to one another and the amino nitrogens adopting a *cis* geometry, constrained by the cross-bridge to the points where the saddle is at its narrowest. The oxygen atoms are *trans* to the amino nitrogens and *cis* to one

another. This is in contrast to the saddle shape of the tetraaza[14]annulenes (Fig 18) where the four nitrogens are equivalent and coplanar.

The largest distortion from octahedral is the average amide-Zr-amide angle of 145.2° (the asymmetric unit contains two half molecules). Zirconium (IV) is typically too large to fit in the pocket of 14-membered tetraazaannulene rings, so this is consistent with previous reports. This may also account for the lack of planarity at the amido nitrogens: the sum of the angles about the amido nitrogens is on average 353.0°. Also, the average amine-Zr-amine angle is constrained by the ethyl cross-bridge to 76.5°; accordingly, the O-Zr-O angle expands to an average 99.5°.

The amido-Zr bond lengths (2.094(4), 2.125(4)Å) in **15** are within the normal range (2.063-2.192Å)[91,94,99,121,143,144] for polydentate ligands with amido donors in a six coordinate environment. On the other hand, the amino-Zr bonds (2.377(4), 2.394(4)Å) are short compared to the normal range (2.414-2.604Å)[74,99,144] for polydentate ligands with mixed amino and amido donors in a six coordinate environment – this appears to be a peculiarity of **15**, as the rest of the compounds have longer bond distances (Tables 6 and 8) The oxygen bond lengths (1.997(3), 1.994(4)Å) and Zr-O-C angles (163.8(3) and 164.2(3)°) are consistent with the range found for 2,6-dimethylphenoxide in other systems containing tris(pyrazolylborate), Cp, Cp* and PNP supporting ligands (1.948-2.020Å).[168-171] The Zr-O-C angles in these systems span a very large range from 145.8-176.8° which has been attributed to steric factors so this angle is not a good indication of the extent of M-O π interactions.[170]

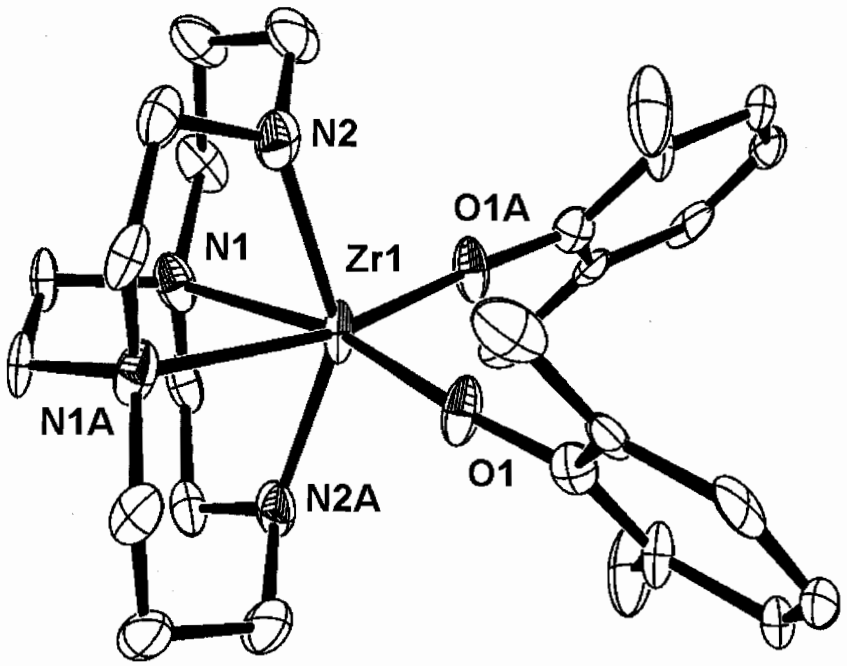

Figure 32. ORTEP3 drawing (thermal ellipsoids at 30% probablity) of 15. Only one molecule is shown, and hydrogen atoms have been removed for clarity.

Compound **14** has been crystallographically characterized (Table 5, Fig 33) and significant bond distances and angles are given in Table 6. The ligand geometry is very similar to that of **15**, but it shows greater distortion from the ideal octahedral geometry. The amide-zirconium amide angle (142.42(10)°) is compressed compared to the ideal of 180° and smaller than that of **15** (avg. 145.2°). Likewise, the oxygen-zirconium-oxygen angle in **14** (106.27(8)°) is greater than in **15** (avg. 99.5°). This is likely due to the orientation of the substituents on the different alkoxides: in **14** the *t*-butyl groups point away from the metal, in **15** the methyl groups are directed towards the metal. Thus, the steric bulk of the siloxide ligands in **14** is further from the metal, allowing for the slightly larger angle between the oxygen atoms and zirconium. The zirconium-oxygen bond length in **14** is longer than other reported zirconium-siloxide interactions in a six

coordinate environment (1.928Å)[172] but it is comparable to the zirconium-oxygen bonds found in **15**. The long distance between the hydrogen on silicon in **14** and the zirconium centre (4.108 Å) indicates that an agostic interaction is not present, since the distance for an agostic interaction is typically much shorter (2.16-2.28 Å)[173] than that seen in **14**.

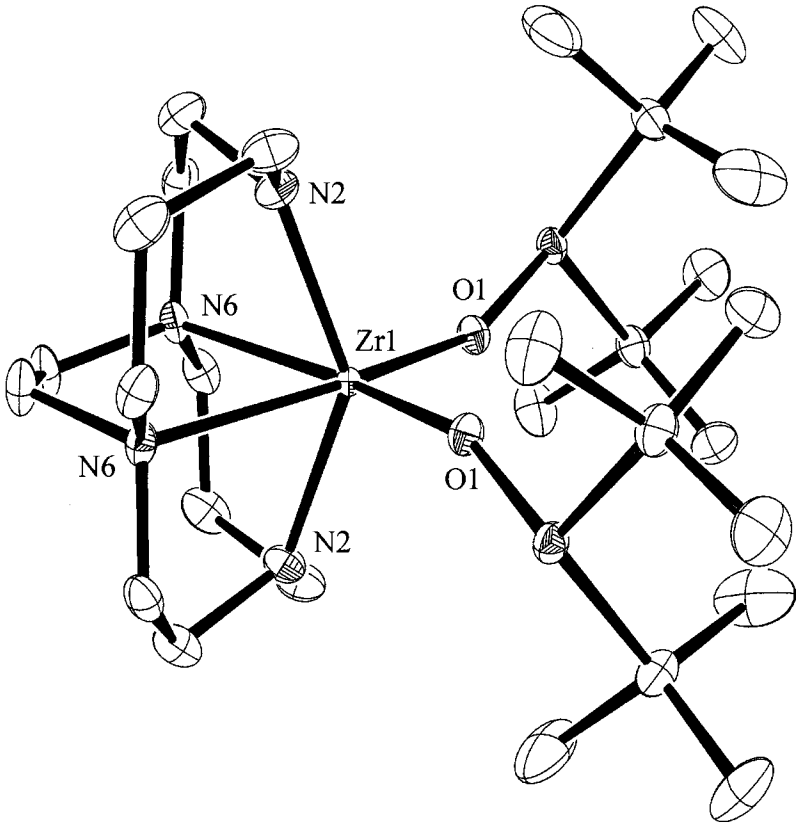

Figure 33. ORTEP3 drawing (thermal ellipsoids at 30% probablity) of 14. Hydrogen atoms have been removed for clarity.

Table 5. Summary of Crystallographic Data for Compounds 14 and 15.

	15	**14**
formula	$C_{28}H_{42}N_4O_2Zr$	$C_{28}H_{62}N_4O_2Si_2Zr$
fw	557.88	634.22
T (K)	83(2)	85(2)
wavelength (Å)	0.71073	0.71073
cryst syst	orthorhombic	monoclinic
space group	*Pcc2*	*C2/c*
a (Å)	11.9203(10)	13.759(3)
b (Å)	11.9130(10)	18.667(4)
c (Å)	19.4240(16)	13.335(3)
β (deg)	90	99.40(3)
V ($Å^3$)	2758.3(4)	3379.0(13)
Z	4	4
density (cald) (Mg/m^3)	1.343	1.247
absorption coefficient (mm^{-1})	0.429	0.425
F(000)	1176	1368
θ range for data collection	1.05 to 28.33	1.85 to 27.50
no. obsd reflns	32772	24228
no. of unique reflns	6859	3873
	[R(int)=0.0424]	[R(int)=0.0402]
completeness to theta	28.33°, 99.7%	27.50°, 99.8%
absorption correction	Semi-empirical	Semi-empirical
final R indices [I>sigma (I)]	R1=0.0329,	R1=0.0359
	wR2=0.0720	wR2=0.0783
R indices (all data)	R1=0.0402,	R1=0.0434
	wR2=0.0757	wR2=0.0783

[a] Refinement method was full-matrix least-squares on F^2 for all compounds.

Table 6. Selected Bond Distances (Å) and Angles (deg) for Complexes 15 and 14.

	15[a]	**14**
	Bond Distances	
Zr-amide	2.125(4) (Zr1-N2)	2.1108(18) (Zr1-N2)
	2.094(4) (Zr2-N4)	
Zr-amine	2.377(4) (Zr1-N1)	2.4113(17) (Zr1-N6)
	2.394(4) (Zr2-N3)	
Zr-O	1.997(3) (Zr1-O1)	2.0039(14) (Zr1-O1)
	1.994(4) (Zr2- O2)	
	Bond Angles	
amide- Zr-amide	145.1(3) (N2-Zr1-N2)	142.42(10) (N2-Zr1-N2)
	145.3(3) (N4-Zr2-N4)	
amine- Zr-amine	76.6(2) (N1-Zr1-N1)	76.33(8) (N6-Zr1-N6)
	76.4(2) (N3-Zr-N3)	
O-Zr-O	98.4(2) (O1-Zr1-O1)	106.27(8) (O1-Zr1-O1)
	100.6(2) (O2-Zr2-O2)	
sum of angles	352.8 (N2)	354.7 (N2)
at amido N	353.3 (N4)	

[a] The asymmetric unit contains two half molecules

Compound **19** has also been characterized by X-ray crystallography (Table 7) and the structure is depicted in Fig 34. The significant bond lengths and angles are given in Table 8. The gross features of the ligand are comparable to **15** with the exception that the Zr-amine distance in **19** (2.452(2)Å) is longer and more typical of the usual range. The Zr-C bond length and C-Zr-C angle are within the typical range for the CH_2SiMe_3 moeity.[106,174-179] The Zr-C bond length (2.290(2)Å), Zr-C-Si bond angle (120.69(12)°)

and the Zr-H9a and Zr-H9b bond distance (both 2.750Å, some reported agostic interactions range from 2.16-2.28 Å)[173] do not suggest that an agostic interaction is present.[175]

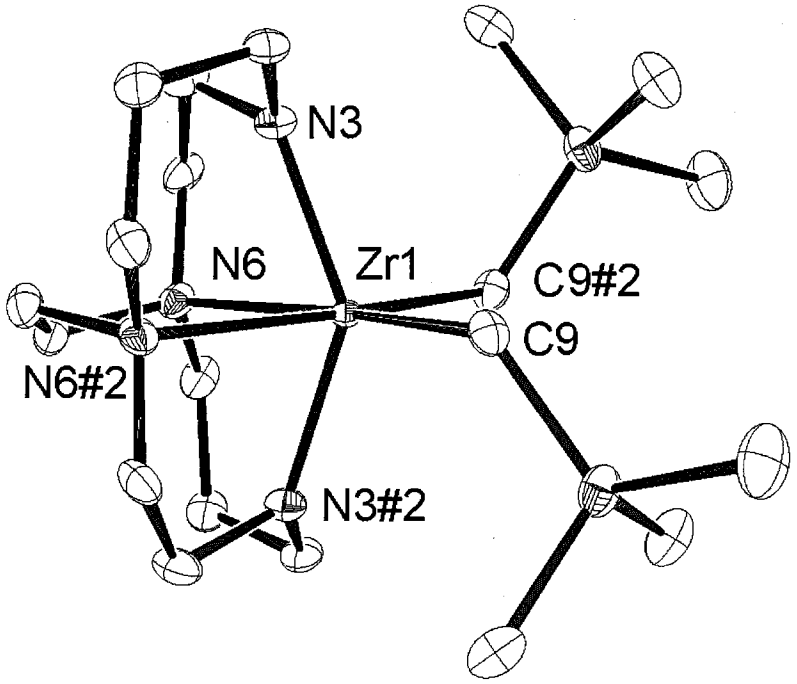

Figure 34. ORTEP3 drawing (thermal ellipsoid 30% probability) of complex 19. The hydrogen atoms have been omitted for clarity.

Of the over 30 zirconacyclopentadiene structures in the Cambridge Crystallographic Database, all contain at least one cyclopentadienyl ligand, albeit one is a phosphacyclopentadienyl ligand[180] (a metallacycle supported by benzamidinate ligands has been reported, but its solid state structure has not been determined).[181] Thus, compound **20** is the first zirconacyclopentadiene without a cyclopentadienyl ligand characterized by X-ray crystallography (Table 7) and it is depicted in Fig 35 with relevant bond lengths and angles found in Table 8. The Zr-C bond lengths typically range from 2.172-2.324Å for zirconacyclopentadienes; thus, at 2.313(2)Å **20** falls at the long end of

this range.[182-186] Accordingly, the C-Zr-C angle is reduced to 77.19(11)°, falling at the short end of the range 76.4 to 98.5°. The geometry of the cross-bridged cyclam moiety in **20** is remarkably similar to that of the *bis*(alkyl) **19**, especially given the large difference in the C-Zr-C angles - 99.61(12)° in **19** and 77.19(11)° in **20**. This suggests that the geometry of the ligand about the metal is constrained by the cross-bridge and largely invariant, regardless of the other substituents on the metal center.

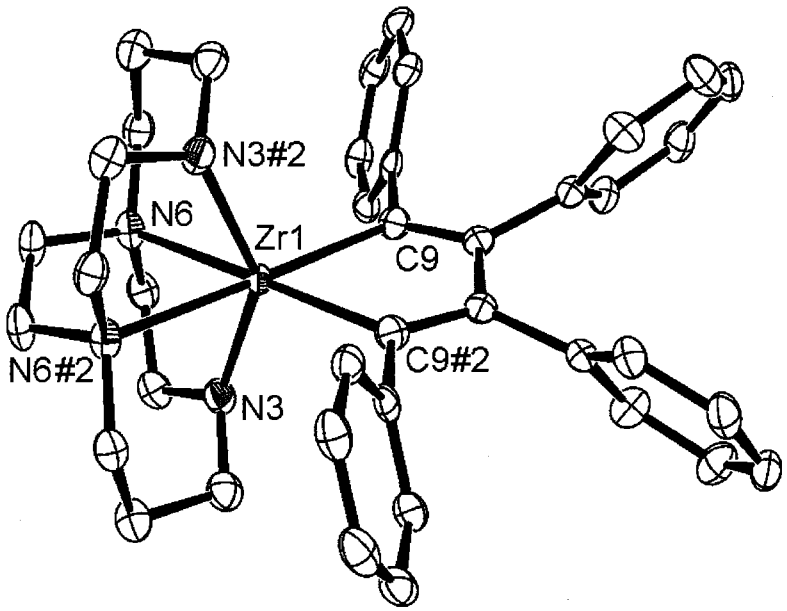

Figure 35. ORTEP3 drawing (thermal ellipsoid 30% probability) of complex 20. The hydrogen atoms and toluene of solvation have been omitted for clarity.

Compound **11** has been crystallographically characterized (Table 7, Fig 36) and significant bond distances and angles are given in Table 8. The ligand features are typical of this class of compounds. The zirconium-vinyl amide distance is comparable to those found in other zirconium and hafnium vinyl amides[165,187] and other zirconium-amide bonds in six coordinate complexes.[91,94,99,121,143,144] Likewise, the N24-C29A (1.3977(14)Å) and C29A-C30A (1.329(4)Å) bonds of the vinyl amides are comparable to

the other reported group 4 vinyl amide bond lengths.[165,187] The Zr1-C17-C18 angle is 133.86°, which indicates that the benzyl group is η^1 bound to the metal. Given the very different steric and electronic properties of the benzyl and vinyl amide groups, it is surprising that the zirconium-amine bond distances are so similar (2.419(2) and 2.426(2)Å) given the range for these compounds (2.377(4) to 2.452(2)Å). We take this as further support for the proposition that the substituents on the metal centre have only a small influence on the geometry of the ligand.

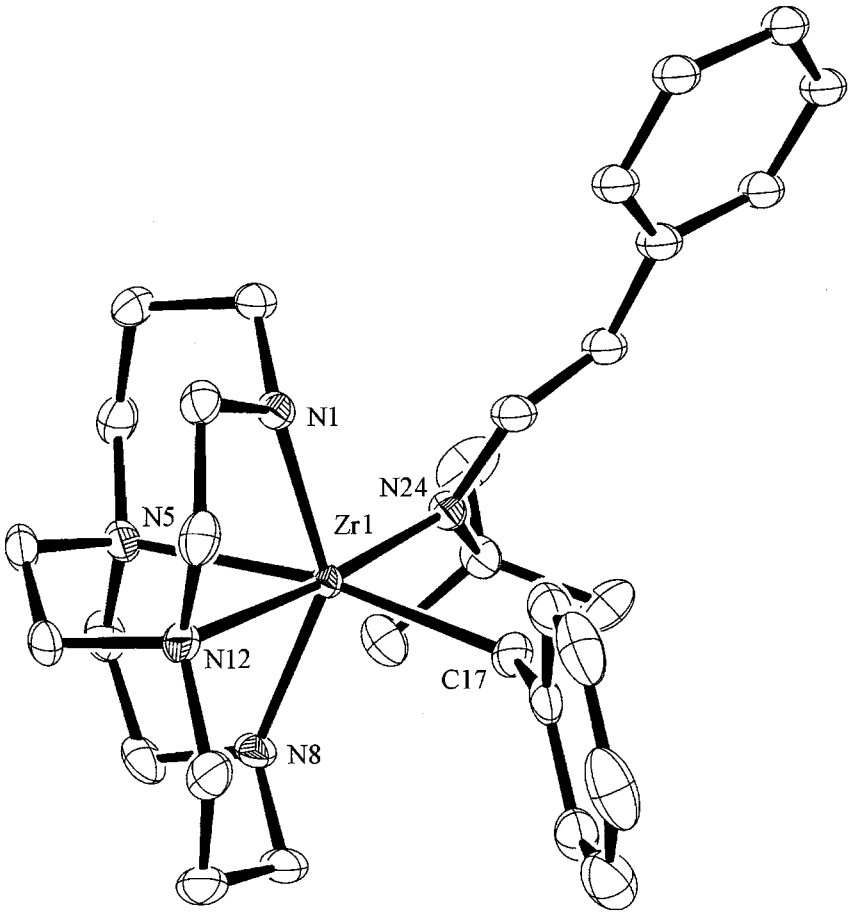

Figure 36. ORTEP3 drawing (thermal ellipsoid 30% probability) of complex 11. The hydrogen atoms and toluene of solvation have been omitted for clarity.

Table 7. Summary of Crystallographic Data for Compounds 11, 19 and 20.

	19	**20**	**11**
formula	$C_{20}H_{46}N_4Si_2Zr$	$C_{47}H_{52}N_4Zr$	$C_{34.5}H_{51}N_5Zr$
fw	490.01	764.15	627.02
T (K)	83(2)	83(2)	84(2)
wavelength (Å)	0.71073	0.71073	0.71073
cryst syst	monoclinic	monoclinic	monoclinic
space group	*C2/c*	*C2/c*	*P2(1)/n*
a (Å)	14.891(3)	16.770(3)	13.039(3)
b (Å)	18.461(4)	12.417(3)	17.875(4)
c (Å)	9.4278(19)	18.247(4)	14.140(3)
β (deg)	101.26(3)	91.34(3)	103.79(3)
V ($Å^3$)	2541.8(9)	3798.6(14)	3200.7(13)
Z	4	4	4
density (cald) (Mg/m^3)	1.280	1.336	1.301
absorption coefficient (mm^{-1})	0.539	0.329	0.375
F(000)	1048	1608	1332
θ range for data collection	1.78 to 27.49	2.04 to 27.50	1.87 to 27.50
no. obsd reflns	31721	24631	41217
no. of unique reflns	2916	4368	7337
	[R(int)=0.0628]	[R(int)=0.0477]	[R(int)=0.0674]
completeness to theta	27.49°, 99.5%	27.5°, 99.8%	27.50°, 99.9%
absorption correction	None	Semi-empirical	Semi-empirical
final R indices [I>sigma (I)]	R1=0.0386,	R1=0.0395,	R1=0.0444
	wR2=0.0773	wR2=0.0884	wR2=0.0914
R indices (all data)	R1=0.0431,	R1=0.0534,	R1=0.0681
	wR2=0.0785	wR2=0.0949	wR2=0.1000

[a] Refinement method was full-matrix least-squares on F^2 for all compounds.

Table 8. Selected Bond Distances (Å) and Angles (deg) for Complexes 19, 20 and 11.

	19	20	11
		Bond Distances	
Zr-amide	2.103(2) (N3)	2.0820(19) (N3)	2.105(2) (N1)
			2.092(2) (N8)
Zr-amine	2.452(2) (N6)	2.4269(19) (N6)	2.419(2) (N5)
			2.426(2) (N12)
Zr-X	2.290(2) (C9)	2.313(2) (C9)	2.349(3) (C17)
			2.193(2) (N24)
		Bond Angles	
amide- Zr-amide	142.29(11) (N3)	142.43(10) (N3)	142.35(9) (N1-Zr1-N8)
amine- Zr-amine	74.78(10) (N6)	76.81(9) (N6)	75.66(8) (N5-Zr1-N12)
X-Zr-X	99.61(12) (C9)	77.19(11) (C9)	87.66(9) (C17-Zr-N24)
sum of angles	353.8 (N3)	354.4 (N3)	353.9 (N1)
at amido N			354.7 (N8)
			359.1 (N24)

Overall, the similarities between the solid state structures of $(CBC)ZrX_2$ and Cp_2ZrX_2[169,174,183] are striking as illustrated in Table 9. The CBC system shows slightly longer bond lengths on average (0.02Å). The average difference in bond angle between the substituents in the two systems is slightly more than 1°, remarkable given that, for example, the C-Zr-C angle for the $L_2Zr(CH_2Si(CH_3)_3)_2$ compounds varies by 25°. This leads us to postulate that CBC and two Cp groups are sterically very similar.

Table 9. Comparison of (CBC)ZrX_2 and Cp_2ZrX_2.

X		CBC	Cp_2
O-2,6-$C_6H_3Me_2$	Zr-O (Å)	1.994(4)	1.996(5)[169]
		1.997(3)	1.997(5)
	O-Zr-O (°)	98.4(2)	98.6(2)
		100.6(2)	
CH_2SiMe_3	Zr-C (Å)	2.290(2)	2.278(4)[174]
			2.281(4)
	C-Zr-C (°)	99.61(12)	97.8(1)
PhCCPh	Zr-C (Å)	2.313(2)	2.250(5)[183]
			2.265(6)
	C-Zr-C (°)	77.19(11)	77.5(2)

3.4 Behavior of Complexes in Solution

Consistent with the solid state structures, the ^1H and ^{13}C NMR of the cross-bridged cyclam ligand in complexes which have two identical substituents (**10**, **14**, **15**, **16**, **18**, **19**, **20**) show effective C_2 symmetry. Accordingly, these complexes have a complicated pattern of twelve diastereotopic protons and six carbon resonances and Fig 37 has a representative example. In contrast, the C_2 axis is lost in complexes in which the substituents are different (**11**, **12**, **13**, **17**) resulting in twenty-four proton resonances and twelve carbon resonances.

The benzylic protons in **10** appear as AB doublets, due to the C_2 symmetry of the complex. Compound **10** displays features typically associated with η^1 benzyl coordination: the *ortho* protons are downfield of 6.7 ppm (7.14 ppm in **10**) and the $^1J_{CH}$

coupling constant for the benzylic groups are less than 130 Hz (113 Hz in **10**).[154-157] Likewise, the geminal coupling constant of the CH_2SiMe_3 group in **19** (12Hz) is slightly larger than in similar species and does not indicate any agostic interactions. [176] [177]

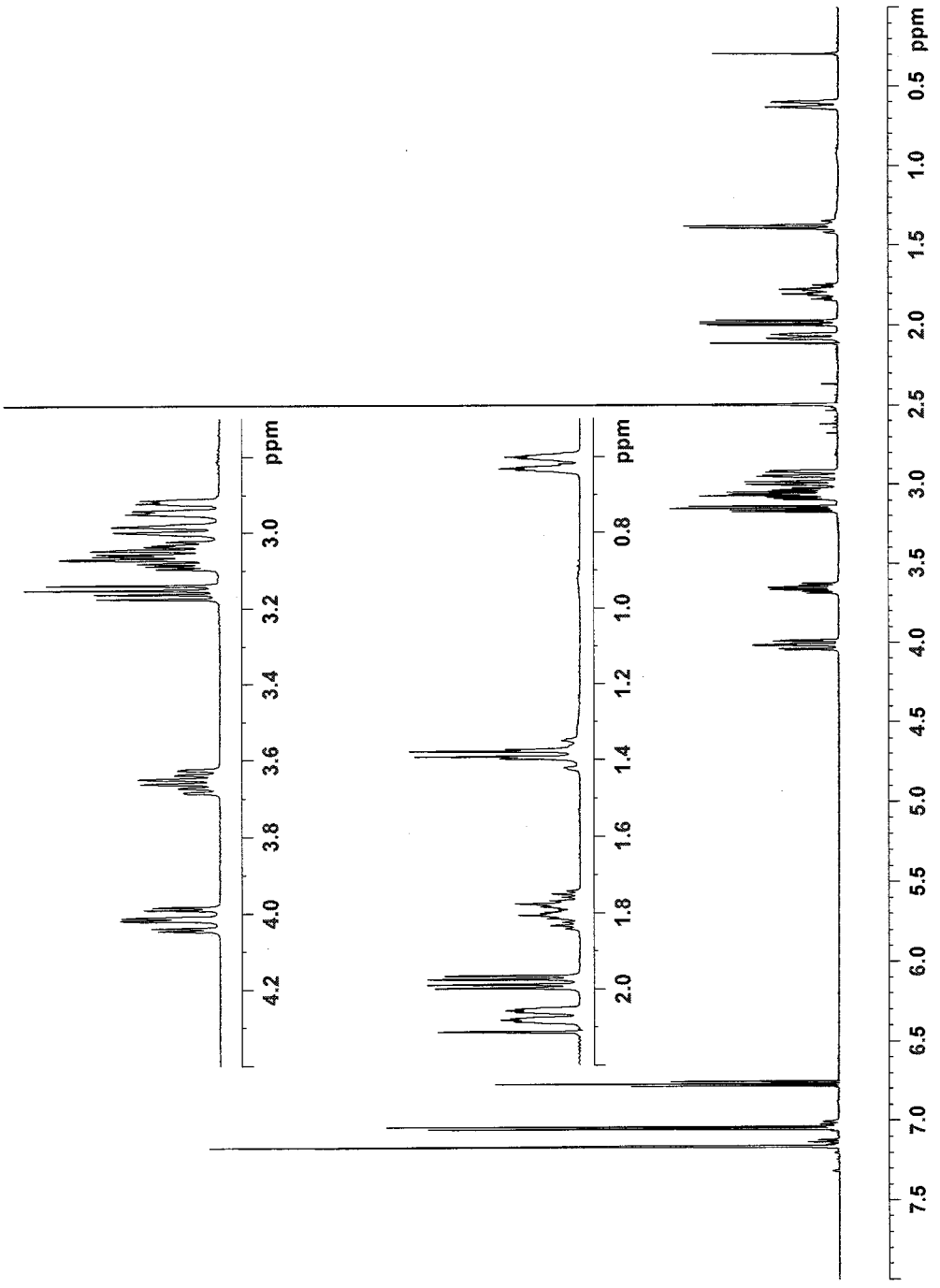

Figure 37. 500 MHz ^{1}H NMR of (CBC)Zr(O-2,6-$C_6H_3Me_2$)$_2$, C_6D_6, 295 K.

As shown in Fig 37, the methyl groups of (CBC)Zr(O-2,6-$C_6H_3Me_2$)$_2$ only have one resonance. This is consistent with rapid rotation about the O-C linkage. In contrast, for (CBC)Zr(CH_2Ph)(O-2,6-$C_6H_3Bu^t_2$) two resonances are observed for the ^{t}Bu groups and *meta* protons at room temperature. This suggests that the steric bulk of the ^{t}Bu groups hinder rotation about the O-C linkage. Increasing the temperature of **12** results in coalescence of both the ^{t}Bu groups and and the *meta* protons (Fig 38). From the coalescence temperature of the ^{t}Bu groups, the activation energy for this process was calculated to be 69 ± 1 kJ/mol using the equal population two-site exchange equation. The free energy of activation was calculated from the coalescence temperature (T_c in K) and the equation $\Delta G^{\ddagger} = (1.912 \times 10^{-2})(T_c)[9.972 + \log(T_c/\delta\upsilon)]$ in kJ mol^{-1} where $\delta\upsilon$ is the separation of the resonances in Hz.[158] The error in $\Delta G^{\ddagger}$ was estimated assuming an error of 3 K in the estimate of Tc.

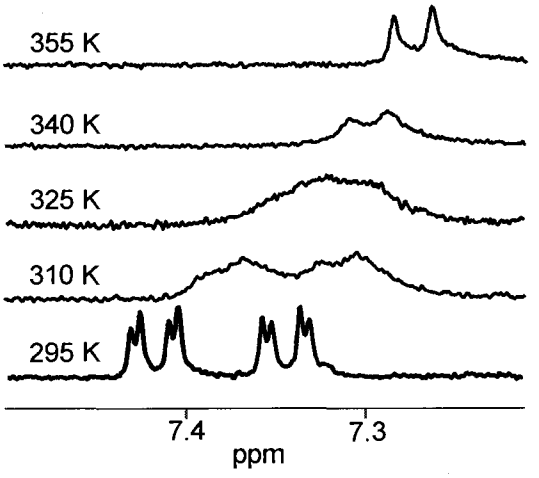

Figure 38. Variable temperature 360 MHz ^{1}H NMR of the *meta* protons in (CBC)Zr(CH_2Ph)(O-2,6-$C_6H_3Bu^t_2$), d_8-toluene

A similar phenomenon was observed in (CBC)ZrClN($SiMe_3$)$_2$; two resonances are observed for the $SiMe_3$ groups at room temperature. Since N($SiMe_3$)$_2$ groups are usually trigonal planar,[147,149,150] this is consistent with hindered rotation about the Zr-N bond. Heating a sample in d_8-toluene did result in significant broadening of these signals, but the coalescence temperature was greater than the boiling point of the solvent. From this information, the free energy of activation must be greater than 77 kJ mol^{-1}.[158] Since the $SiMe_3$ groups are likely to be closer to the metal centre than the ^{t}Bu groups in **12**, this too is consistent with steric crowding causing the hindered rotation.

3.5 Reactivity

3.5.1 Hydrides

We were interested in the possible insertion chemistry of zirconium hydrides with unsaturated species. However, attempts to prepare hydrides by metathesis reactions of the pale yellow (CBC)$ZrCl_2$ with potassium hydride, lithium aluminium hydride, or Red-Al (sodium bis-(2-methoxyethoxy)-aluminum hydride) resulted in colourless, intractable materials. This likely indicates the formation of insoluble "ate" complexes or coordination polymers.

When (CBC)Zr(CH_2Ph)$_2$ was treated with either hydrogen or phenylsilane, no reaction was observed by NMR at room temperature. Increasing the temperature resulted in decomposition of the organometallic species. This lack of reactivity is similar to that of the zirconium DAC alkyl complexes.[120] Indeed, the reactivity of organozirconium complexes supported by diamido ligands with hydrogen has only rarely been reported. One exception is the porphyrin complex ($\mathbf{L}^{\mathbf{XXXVIa}}$)$ZrR_2$, which is an active hydrogenation

catalyst when treated with both hydrogen and ethylene or propylene; however, treatment with hydrogen alone results in a deep green paramagnetic complex that has not been characterized.[106]

3.5.2 Reduction Chemistry

Zirconocene (II) species are well known and have a variety of interesting chemistry associated with them including the formation of complexes with CO, N_2 and unsaturated hydrocarbons.[7] Thus, we attempted to make zirconium (II) complexes supported by cross-bridged cyclam. Treatment of the pale yellow THF solutions of $(CBC)ZrCl_2$ with either magnesium or sodium amalgam and carbon monoxide did result in the formation of coloured products, consistent with zirconium (II) or (III), but the coloured species were insoluble (Eq 37). Likewise, reduction of dichloride **16** with sodium amalgam in the prescence of N_2 resulted in insoluble materials. Even treatment of **16** with sodium amalgam in prescence of diphenylacetylene did not result in the formation of known compound **20** (Eq 38).

(37) $(CBC)ZrCl_2 + CO$ + Mg or Na/Hg → (CBC)Zr(CO)(CO)

(38) $(CBC)ZrCl_2$ + Na/Hg + 2 PhCCPh → (CBC)Zr(Ph)(Ph)(Ph)(Ph)

20

3.5.3 Insertion Chemistry

(CBC)$ZrCl_2$ was tested for ethylene polymerization activity under our standard conditions (toluene, 50°C, 500 equivalents MAO, 1 atm ethylene); however, it proved to be too insoluble to act as a catalyst. Accordingly, the dimethyl analogue **18** was prepared and tested under the same conditions. There was no evidence for production of polyethylene.

As previously discussed in Sections 2.5.1 and 1.3.2, Schrock and coworkers have done extensive research on olefin polymerization with diamido-donor ligands. They have noted that coordination of an additional Lewis base inhibits or quenches the catalytic activity of these complexes. For example, the cation shown in Fig 39 is an active 1-hexene polymerization catalyst; however, addition of stoichiometric amounts of diethyl ether or THF completely quenches the polymerization.[60] Thus, the lack of activity in the CBC system fits with these observations, since it has two neutral donors incorporated into the ligand.

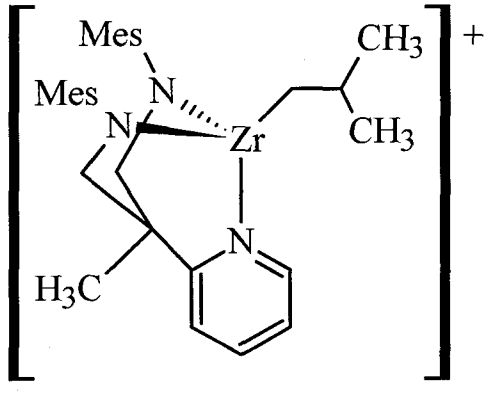

Figure 39. Cationic Olefin Polymerization catalyst.

(CBC)Zr(CH_2Ph)$_2$ was also tested with stoichiometric quantities of unsaturated species to understand the insertion chemistry of this complex. Compound **10** did not react with 2-butyne, even at elevated temperatures. As outlined in Section 3.2, **10** does react with a single equivalent of *t*-butyl isonitrile to produce the vinyl amide **11**. As one would expect, **10** also reacts with CO. In this case the reaction is not clean and all attempts to purify the product were unsuccessful.

3.5.4 Metallacycle Chemistry

Heating a yellow solution of **20** at 50°C for 7 days resulted in a deep red solution. Attempts to grow a crystal suitable for X-ray diffraction have been unsuccessful, but a deep red powder (**21**) has been isolated that gives clean NMR spectra. One notable feature of this compound is that there is a ligand ^{13}C resonance at 77.9 ppm which correlates with a proton resonance at 1.36 ppm. In the DEPT experiment this ^{13}C signal is antiphase to the others, indicating that it is a methine unit rather than a methylene one. Table 10 compares the ^{1}H and ^{13}C chemical shifts of (CBC)Zr(CH_2SiMe_3)$_2$ and (CBC)Zr(CH_2Ph)$_2$ and contrasts them with the chemical shift of tetramethylsilane and toluene respectively. The trend is clear; replacing the C-H bond with a C-Zr bond has very little effect on the α protons, but causes a 50 ppm downfield shift in the ^{13}C resonances. Accordingly, the methine unit is consistent with ligand metallation since subtracting 50 ppm from the ^{13}C chemical shift of 77.9 ppm results in a chemical shift of *ca* 28 ppm prior to metallation. This is more consistent with the chemical shift of the $CH_2CH_2CH_2$ in the starting material (22.4 ppm) rather than any of the NCH_2 units (61.9-

50.6 ppm). Moreover, hydrolysis (D_2O) of **21** results in a decrease in intensity of one of the $CH_2CH_2CH_2$ resonances in the resulting free ligand.

Table 10. Effect of Replacing a C-H Bond with a Zr-C bond on ^1H and ^{13}C Spectra.

	19	$Si(CH_3)_4$	**10**	$C_6H_5CH_3$[123]
^1H	0.03, 0.42 ppm	0	2.47, 2.56 ppm	2.32
^{13}C	53.1 ppm	0	70.3 ppm	21.8

The other notable feature of the **21** is a singlet at 5.67 ppm which is tentatively assigned as an alkene proton. This could be the result of one of the carbons of the metallacycle deprotonating the ligand to yield a butadieneyl fragment as shown in Eq 39. However, this proton signal correlates with a carbon signal at 67.7 ppm – far upfield of where one would expect an alkene ^{13}C resonance, even if coordinated to zirconium. Unfortunately, the hydrolysis of **21** with D_2O was complicated by the formation of insoluble materials and the amount of the hydrocarbon material obtained was not sufficient for NMR analysis. The mass spectrum showed a molecular ion with an isotope pattern that suggested both C_4Ph_4HD and $C_4Ph_4H_2$ were present. This seems inconsistent with either coupling of two metallacycles to form a dimer, or coupling of the butadienyl fragment with the ligand. However, we cannot rule out the possibility that the hydrocarbon portion of **21** is an isomer of that shown in Eq 39.

(39) 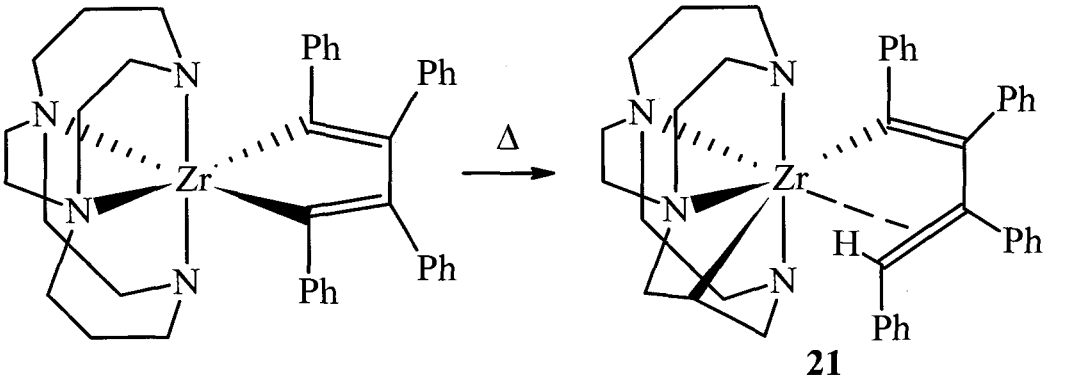

21

Attempts to isolate the tetramethyl analogue of **20** by reaction of $(CBC)ZrCl_2$ with 2-butyne have been unsuccessful thus far. Since the tetraphenyl zirconacyclopentadiene decomposes under relatively mild conditions, and it seems likely that both steric and electronic factors in the tetramethyl analogue would make it more prone to decomposition; it is unsurprising that this compound has not been isolated.

The insertion chemistry of **20** with *t*-butyl-isonitrile and carbon monoxide was examined. In both cases reaction occurred; however, the reactions were not clean and recrystallization did not afford identifiable organometallic species.

One of the uses of zirconacycles is to transfer the ring to a main group element in a metallacycle transfer reaction (Scheme 3). We wondered if this type of reaction would be possible with **20**. Jordan and coworkers have reported secondary amides acting as nucleophiles,[102] (Eq 40) as have Schrock and coworkers – even in the presence of zirconium alkyls (Eq 41).[82] Therefore, it was not obvious if the metallacycle transfer reaction would be possible, or if the amides of the cross-bridged cyclam would also react.

(40) $(L^{\mathbf{XXXVIIIa}})Zr(NMe_2)_2$ + CD_2Cl_2 ⟶ $(L^{\mathbf{XXXVIIIa}})ZrCl_2$ + $CD_2(NMe_2)_2$

(41) 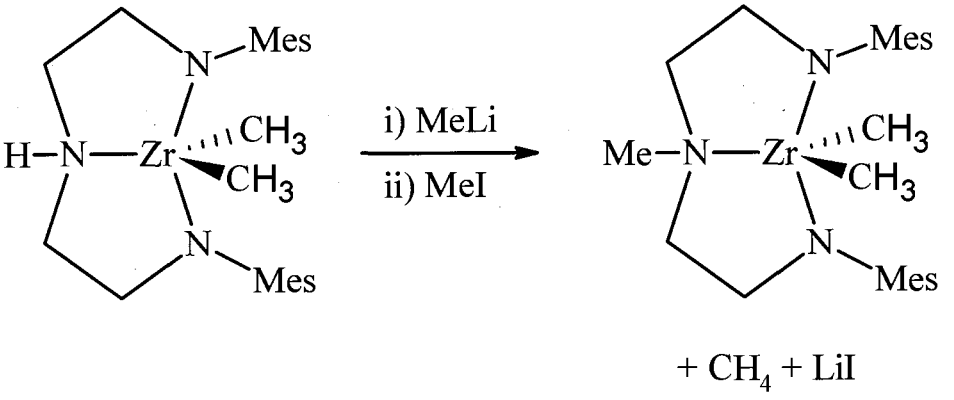

$+ CH_4 + LiI$

Three different substrates were chosen to try the metallacycle transfer reaction: thionyl chloride, dichlorophenylborane and dichlorophenylphosphine. These were selected not only because the resulting heterocycles were known compounds, but also because they were on hand. The reaction with thionyl chloride was successful and resulted in the production of the bright yellow tetraphenylthiopheneoxide (**22**) in a 49 % yield (Eq 42), slightly less than that reported when $Cp_2ZrC_4Ph_4$ was used (59 %).[188] This clearly demonstrates that the metallacycle transfer is possible despite the presence of the cross-bridged cyclam.

(42) 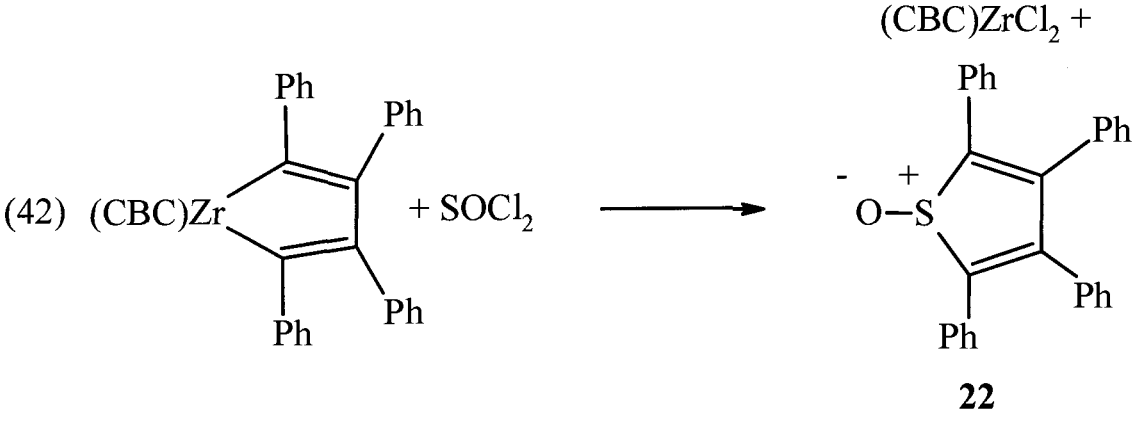

22

In contrast, the reaction with dichlorophenylborane was not successful (Eq 43). During the course of the reaction, the yellow colour of $(CBC)ZrC_4Ph_4$ gradually

deepened to an orange colour. Since the base free pentaphenylborole is reported to be a *blue*, it seems likely that this species was not formed.[189] The pentaphenylborole is reported to form stable *yellow* complexes with diethyl ether and even benzonitrile. With this in mind, it was possible that pentaphenylborole had indeed formed, but was coordinated to the nitrogens of the cross-bridged cyclam. Thus, we attempted to extract the borole with ethereal solvents, but this proved unsuccessful. Given the Lewis acidity of dichlorophenylborane, it is also possible that it coordinated to the amido nitrogens of (CBC)ZrC_4Ph_4 prior to reaction with amido groups and that pentaphenylborole was not formed.

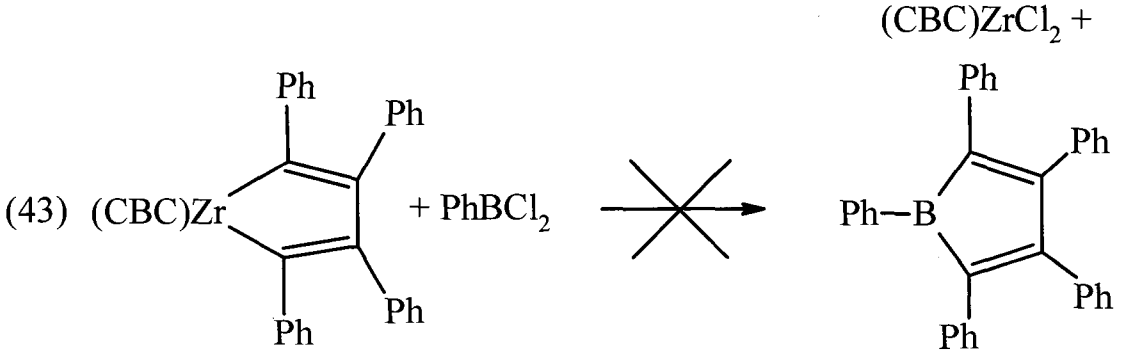

The third attempt at the metallacycle transfer reaction transferred the metallacycle to phosphorus, albeit in a modest 34 % yield (Eq 44). Pentaphenylphosphole fluoresces blue when irradiated with short wave ultraviolet light, which aids in its purification.[190,191] While the metallacycle transfer reactions are limited to Lewis bases, we consider this a proof of concept – metallacycle transfer reactions can occur despite the presence of amido ligands.

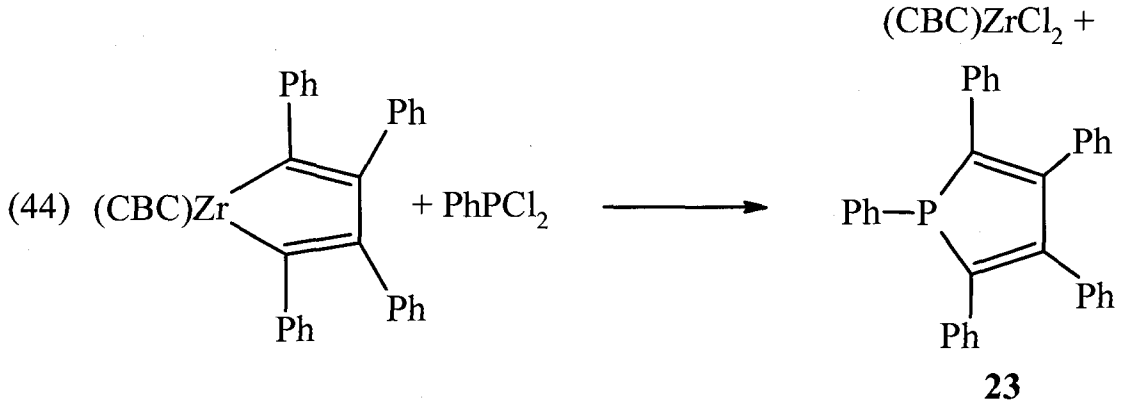

23

3.6 Summary

The ligand development cycle outlined in the introduction outlines the studies that have been undertaken with cross-bridged cyclam. Several organozirconium compounds have been prepared and their solid and solution state behaviour examined. The solid state structures suggest that this ligand has fixed coordination geometry, regardless of the other substituents on the zirconium centre and the NMR spectra support this. The reactivity studies indicate that the ligand can tolerate reactions with relatively acidic substrates such as phenols and silanols without being displaced. Furthermore, the organometallic complexes do react with polar small molecules, although only the reaction with *t*-butyl isonitrile resulted in identifiable products. Also, we have shown that it is possible to carry out metallacycle transfer reactions supported by a diamido ligand.

Chapter 4. Organolanthanide Complexes supported by Cross-Bridged Cyclam

4.1 Introduction

The use of diamido ligands in organolanthanide chemistry has received much less attention than the corresponding organozirconium chemistry and this work has been recently reviewed.[192-194] As briefly outlined in the introduction, the genesis of the current effort to develop new ligands for organolanthanide chemistry (in this context lanthanides are considered to include Y, La-Lu) began with the use of diaza-18-crown-6 (DAC). Several complexes were prepared of the type (DAC)LnN(SiMe$_3$)$_2$ (Ln = Y, Ce, Sm)[195] as well as (DAC)YCH$_2$SiMe$_3$[196] and divalent ytterbium dimers and trimers.[195] Unfortunately, the organoyttrium species proved to be unreactive with CO, H_2 and ethylene,[120] but it did react with phenylacetylene to produce an equilibrium mixture of the alkynide-bridged dimer and a coupled butatrienediyl complex with bridging ligands (Eq 45).[197]

The next development in lanthanide chemistry was the use of the *mono* aza-18-crown-6 (MAC). Since this ligand is monoanionic, it could support the potentially more interesting dialkyl complexes. However, the geometry of this ligand proved to be one with the alkyl ligands *trans* to one another and the MAC ligand in a belt around the yttrium. A notable feature of the solid state structure was that two of the ethers were only weakly coordinated to the metal (Y-O = 3.033(3) Å). Furthermore, (MAC)Y(CH$_2$SiMe$_3$)$_2$ proved to be reactive with carbon monoxide, unlike the DAC complex (Eq 46). However,

the MAC complex still proved to be unreactive with hydrogen and ethylene. Accordingly, a logical development in ligand design seemed to be to simple remove two of the ether donors, since they were not coordinating to the metal, at least in the solid state. Thus the (NOON) system, $(C_6F_5NHCH_2CH_2OCH_2)_2$, was developed; the reduced number of donors opens the coordination sphere of the metal, hopefully resulting in more reactive metal complexes.

(45)

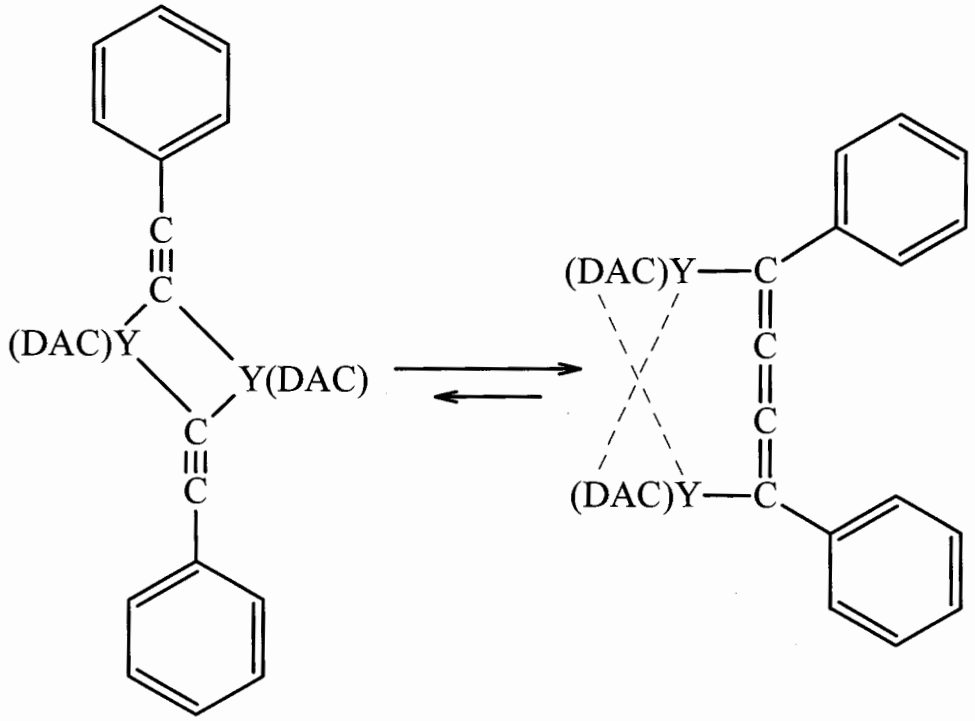

(46)

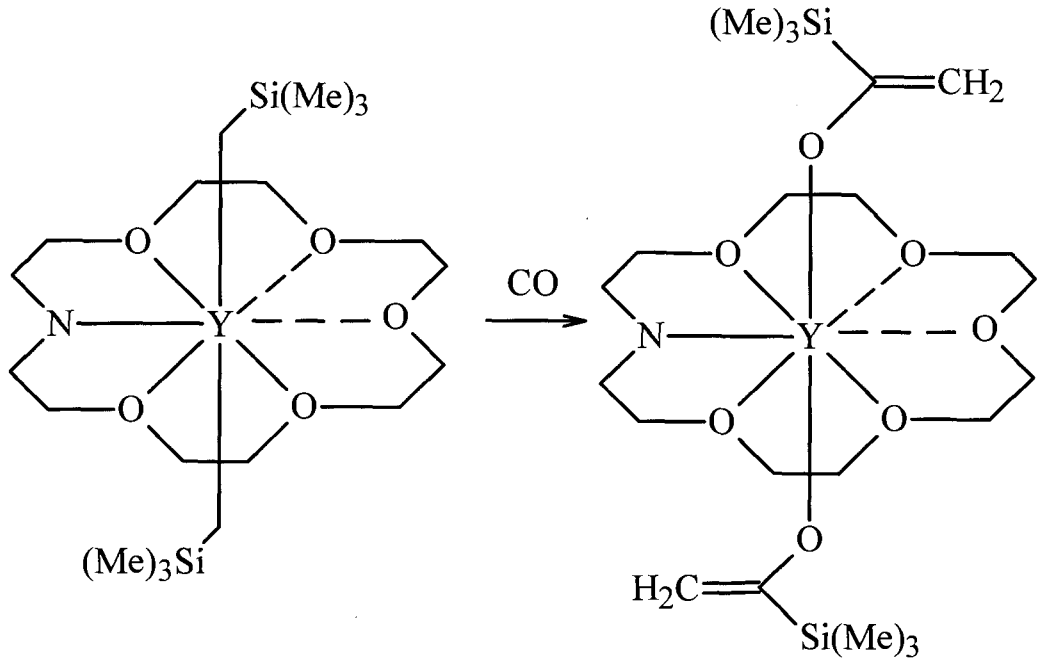

All attempts to make (NOON)LnN(SiMe$_3$)$_2$ and (NOON)Ln(O-2,6-C$_6$H$_3$Bu$^t_2$) complexes by acid-base reactions with Ln[N(SiMe$_3$)$_2$]$_3$ or by salt metathesis with Ln(O-2,6-C$_6$H$_3$Bu$^t_2$)$_3$ resulted in multiple or insoluble products. There are several possible reasons for this result: 1) C-F bond activation, 2) metallation of the ligand backbone or 3) formation of coordination polymers. C-F bond activation seems unlikely with trivalent lanthanides and lanthanide complexes with HNC$_6$F$_5$ and Me$_3$SiNC$_6$F$_5$ have been prepared using Sm[N(SiMe$_3$)$_2$]$_3$(THF)$_2$.[198] Also, metallation of the ligand was found to be a problem with the DAC and MAC systems, but only with much more reactive alkyl substituents – not amido or phenoxide ligands. Thus, it seems most likely that the formation of coordination polymers is the problem.

In the DAC system, bridging was often observed in di- and trimetallic systems but the complexes generally remained soluble (Fig 40). Our attempts to use the (NOON) ligand system in lanthanide chemistry resulted in insoluble products most likely because

the acyclic (NOON) can adopt an even broader range of bridging modes than the cyclic DAC and MAC systems. The rigidity of the (CBC) ligand should limit its ability to bridge between lanthanide centres and hopefully provide soluble products. In addition, the rigidity of the ligand should make it difficult for ligand backbone metallation to occur, avoiding the major limitation encountered with the DAC and MAC lanthanide alkyls.

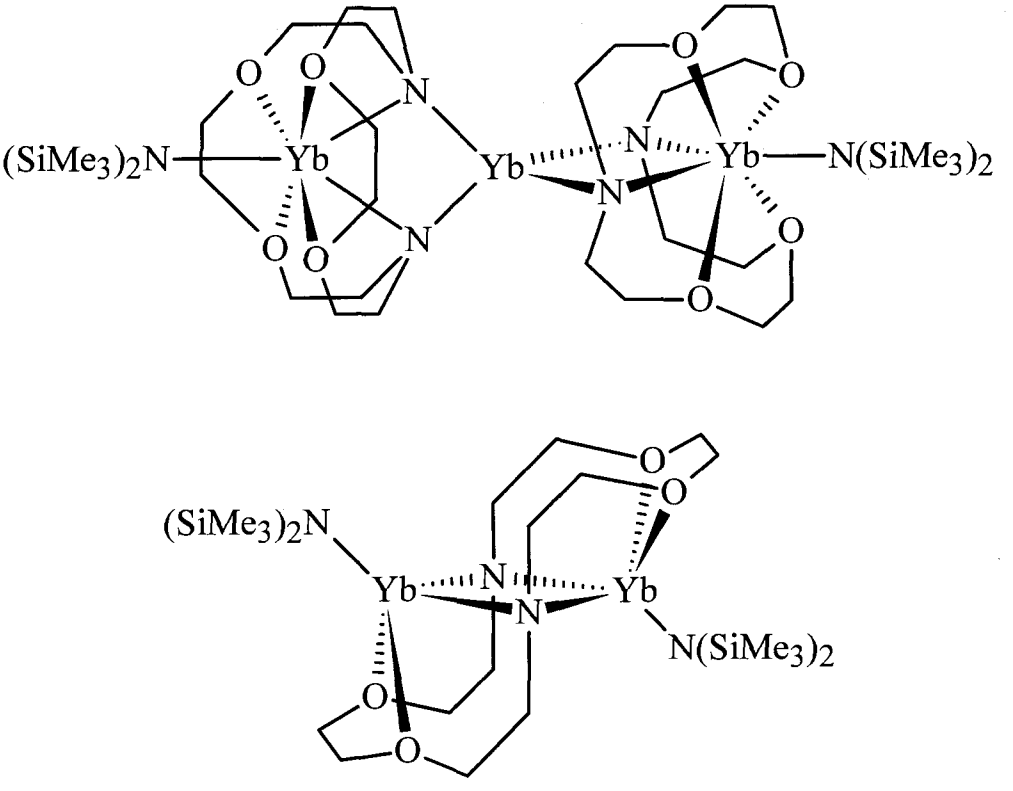

Figure 40. Bridging DAC structures.

4.2 Divalent Chemistry

An initial NMR scale reaction between orange $Yb[N(SiMe_3)_2]_2THF_2$ and colourless $H_2(CBC)$ resulted in a small number of dark green crystals precipitating in the NMR tube. Subsequent X-ray analysis of these crystals revealed them to be {[(μ-

CBC)Yb]$_3$(μ^3-O)}$^+${Yb[N(SiMe$_3$)$_2$]$_3$}$^-$ (Tables 11 and 13, Fig 42). The cation is a cyclic trimer with three ytterbium (III) centres, three (CBC) ligands in which one of the amido nitrogens bridged between metals and an *oxygen* atom bridging between the three metal centres (Figs 41). The counterion in **24** is the *tris*(*bis*(trimethylsilyl)amido) ytterbium (II) anion.

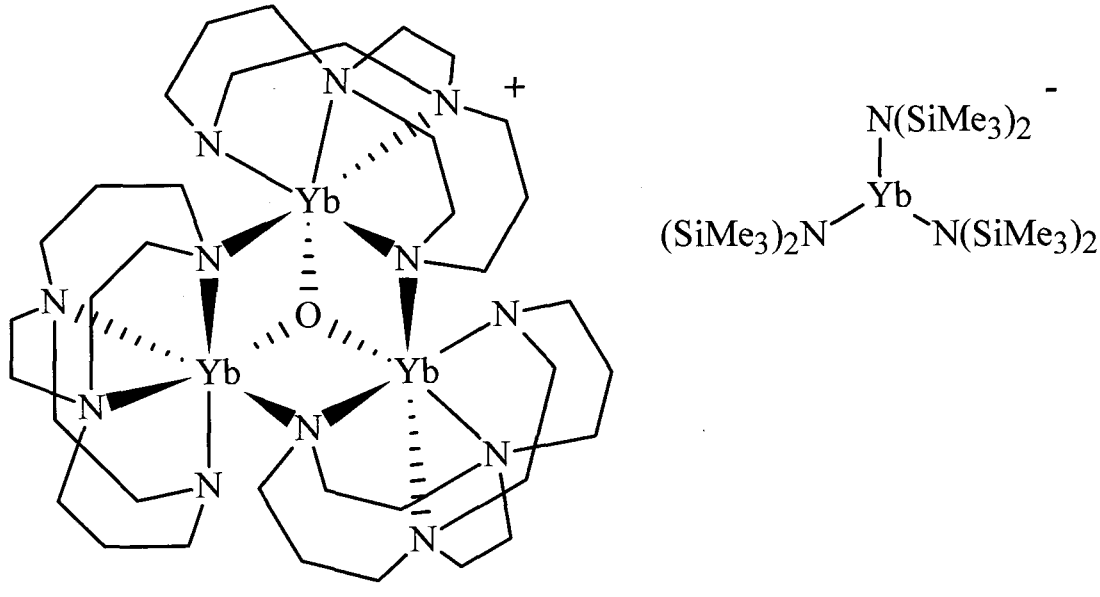

Figure 41. {[(μ-CBC)Yb]$_3$(μ^3-O)}$^+${Yb[N(SiMe$_3$)$_2$]$_3$}$^-$ (24).

Since the reaction was carried out in a glovebox, the oxygen present in **24** is likely a result of water or oxygen being introduced either during the synthesis of YbI_2 from ytterbium metal, or in the subsequent preparation of Yb[N(SiMe$_3$)$_2$]$_2$THF$_2$. Since ligand redistribution chemistry is quite common in lanthanide chemistry, it is not clear if the anion is also a contaminant in the starting material, or if it formed during the course of the reaction. Scaling up the reaction using the same batch of Yb[N(SiMe$_3$)$_2$]$_2$THF$_2$ resulted in the formation of **24**; however, when a freshly prepared batch was used, **24** was

not produced (*vide infra*) lending weight to the argument that the oxygen was present in the starting material.

When a green d_8-THF solution of **24** was allowed to stand, yellow crystals precipitated from solution. These yellow crystals of **25** were also analysed by X-ray crystallography (Tables 12 and 13, Fig 43) and proved to be closely related to **24.** The same $\{[(\mu\text{-CBC})Yb]_3(\mu^3\text{-O})\}^+$ cation was present, but the anion in **25** is iodide rather than $\{Yb[N(SiMe_3)_2]_3\}^-$. Since the $Yb[N(SiMe_3)_2]THF_2$ was prepared from YbI_2, contamination with iodide is quite possible.

The oxygen in **24** sits above the plane of the ytterbium centres, while the bridging amido groups sit on the opposite side of this plane. The Yb_3O unit has been reported previously, and the bond lengths in **24** and **25** fall within the reported range, although the Yb-O-Yb angles in **24** and **25** are more acute (average 100.2°) than the other reported structures (104.7 to120°).[199-201] The other structures have bridging chloride or bromide groups, which have longer bond distances to the metals than the amido bridges in **24** and **25**, which results in the more obtuse angle in these structures.

The geometries about the three metal centres are very similar, so Yb(3) in **24** will be explicitly discussed as a representative example of **24** and **25**. The geometry at Yb(3) is distorted octahedral, with the largest distortion being the amide-ytterbium-amide angle (142.80(11)°), far from the ideal (180°). Likewise, the amine-ytterbium-amine angle is constrained to 76.53(11)° by the cross-bridge and the oxygen-ytterbium-bridging amide angle is 82.83(10)°, presumably due to the constraints of forming the trimer.

The terminal amide has roughly a trigonal planar geometry (sum of angles about N(11) = 355.6°) and the Yb(3)-N(11) bond distance (2.181(3)Å) is within the normal range for six coordinate ytterbium (III) complexes.[199,201] In contrast, the bridging amide is roughly tetrahedral (angles ranging from 92.33(10), Yb(3)-N(9)-Yb(2) to 118.9(2), C(25)-N(9)-Yb(2)) The distance from Yb(3) to N(9) (2.376(3)Å) is much longer than the terminal amide and similar to that of the N(9)-Yb(2) distance (2.421(3)Å). A similar pattern is observed in $[(C_5H_4CH_3)_2YbNH_2]_2$ where the Yb-N-Yb angle is 99.9(4)° and the bond distances are only slightly different (Yb-N 2.29(1), Yb-N' 2.32(1) Å).[202]

The only significant difference between the geometries around Yb(1) and Yb(2) with that of Yb(3) is disorder in one of the propyl bridges in the ligand. In Yb(1) and Yb(2) the propyl bridge from the terminal amide to an amine has two configurations: one with the centre methylene oriented towards the metal in a pseudo-boat configuration and one with the centre methylene oriented towards the rest of the ligand in a pseudo-chair configuration. For the (CBC) ligand attached to Yb(3), only the pseudo-boat configuration is observed.

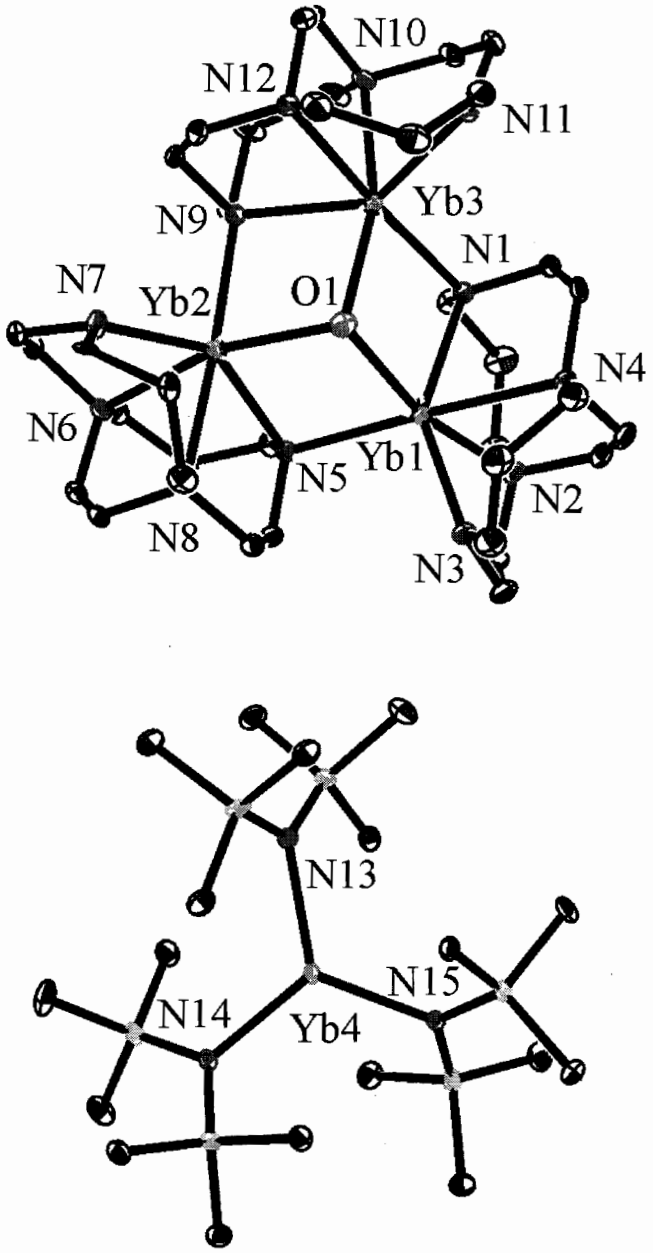

Figure 42. ORTEP3 drawing (thermal ellipsoid 30% probability) of complex 24. The hydrogen atoms have been omitted for clarity.

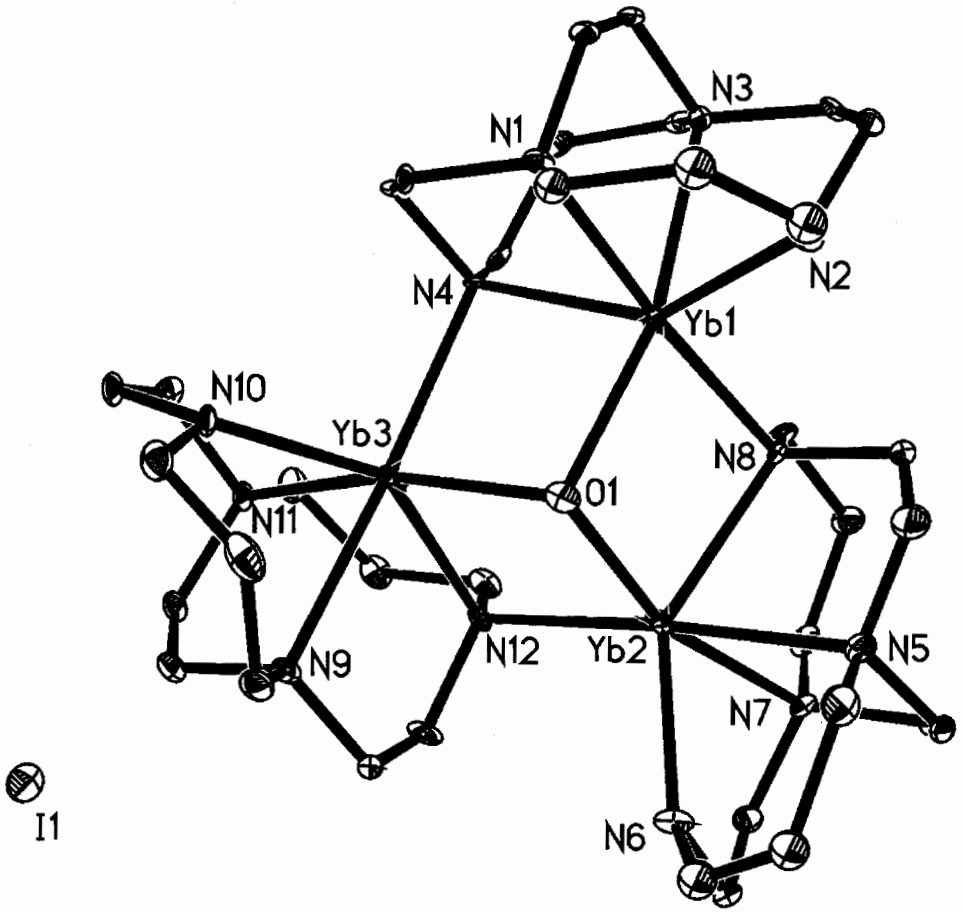

Figure 43. ORTEP3 drawing (thermal ellipsoid 30% probability) of complex 25. The hydrogen atoms and THF of solvation have been omitted for clarity.

Table 11. Selected Bond Distances (Å) and Angles (deg) for 24.[a]

	Yb(1)	Yb(2)	Yb(3)
	Bond Distances		
Yb-amine	2.442(3) N(2)	2.443(3) N(6)	2.449(3) N(10)
Yb-amine	2.473(3) N(4)	2.457(3) N(8)	2.439(3) N(12)
Yb- terminal amide	2.181(3) N(3)	2.194(3) N(7)	2.181(3) N(11)
Yb-bridging amide	2.367(3) N(1)	2.367(3) N(5)	2.376(3) N(9)
Yb-bridging amide	2.439(3) N(5)	2.421(3) N(9)	2.416(3) N(1)
Yb-oxygen	2.255(3) O(1)	2.266(3) O(1)	2.266(3) O(1)
	Bond Angles		
amine-Yb-amine	74.92(10)	75.41(10)	76.53(11)
	N(2)-Yb-N(4)	N(6)-Yb-N(8)	N(10)-Yb-N(12)
amide-Yb-amide	144.52(10)	143.90(11)	142.80(11)
	N(3)-Yb-N(1)	N(5)-Yb-N(7)	N(9)-Yb-N(11)
oxygen-Yb-amide	82.04(10)	83.30(10)	82.83(10)
	O(1)-Yb-(N5)	O(1)-Yb-N(9)	O(1)-Yb-N(1)
Yb-amide-Yb	92.81(9)	93.03(10)	92.33(10)
	Yb(1)-N(1)-Yb(3)	Yb(2)-N(5)-Yb(1)	Yb(3)-N(9)-Yb(2)
Yb-oxygen-Yb	101.15(11)	99.75(11)	100.01(11)
	Yb(1)-O(1)-Yb(2)	Yb(2)-O(1)-Yb(3)	Yb(3)-O(1)-Yb(1)

[a] Estimated standard deviations in parentheses.

Table 12. Selected Bond Distances (Å) and Angles (deg) for 25.[a]

	Yb(1)	Yb(2)	Yb(3)
	Bond Distances		
Yb-amine	2.453(5) N(1)	2.460(6) N(5)	2.457(6) N(9)
Yb-amine	2.461(5) N(3)	2.459(6) N(7)	2.427(5) N(11)
Yb- terminal amide	2.186(6) N(2)	2.194(6) N(6)	2.187(5) N(10)
Yb-bridging amide	2.349(5) N(4)	2.382(5) N(8)	2.383(5) N(12)
Yb-bridging amide	2.435(5) N(8)	2.400(5) N(12)	2.406(5) N(4)
Yb-oxygen	2.255(5) O(1)	2.257(5) O(1)	2.279(5) O(1)
	Bond Angles		
amine-Yb-amine	74.24(18)	74.3(2)	76.8(2)
	N(1)-Yb-N(3)	N(5)-Yb-N(7)	N(9)-Yb-N(11)
amide-Yb-amide	145.4(2)	144.1(2)	142.89(19)
	N(2)-Yb-N(4)	N(6)-Yb-N(8)	N(10)-Yb-N(12)
oxygen-Yb-amide	82.59(18)	83.27(18)	82.48(17)
	O(1)-Yb-(N8)	O(1)-Yb-N(12)	O(1)-Yb-N(4)
Yb-amide-Yb	92.46(19)	93.20(18)	93.47(17)
	Yb(1)-N(8)-Yb(2)	Yb(2)-N(12)-Yb(3)	Yb(3)-N(4)-Yb(1)
Yb-oxygen-Yb	100.9(2)	100.0(2)	99.6(2)
	Yb(1)-O(1)-Yb(2)	Yb(2)-O(1)-Yb(3)	Yb(3)-O(1)-Yb(1)

[a] Estimated standard deviations in parentheses.

Table 13. Summary of Crystallographic Data for Compounds 24 and 25.

	24	**25**
formula	$C_{54}H_{126}N_{15}OSi_6Yb_4$	$C_{44}H_{88}IN_{12}O_3Yb_3$
fw	1862.40	1479.28
T (K)	83(2)	83(2)
wavelength (Å)	0.71073	0.71073
cryst syst	monoclinic	monoclinic
space group	*P2(1)/n*	*P2(1)/c*
a (Å)	17.625(4)	11.879(2)
b (Å)	19.305(4)	13.385(3)
c (Å)	23.440(5)	31.948(6)
β (deg)	109.93(3)	92.97(3)
V ($Å^3$)	7498(3)	5073.1(18)
Z	4	4
density (cald) (Mg/m^3)	1.650	1.937
absorption coefficient (mm^{-1})	5.083	6.144
F(000)	3708	2892
θ range for data collection	1.40 to 30.07	1.65 to 27.50
no. obsd reflns	98901	61429
no. of unique reflns	21461 [R(int)=0.0516]	11637 [R(int)=0.0691]
completeness to theta	30.07°, 97.4%	27.50°, 99.8%
absorption correction	semi-empirical	Semi-empirical
final R indices [I>sigma (I)]	R1=0.0327, wR2=0.0710	R1=0.0444, wR2=0.0779
R indices (all data)	R1=0.0458, wR2=0.0755	R1=0.0606, wR2=0.0822

[a] Refinement method was full-matrix least-squares on F^2 for all compounds.

Since ytterbium (III) is paramagnetic, the ^{1}H NMR of **24** showed an extremely wide chemical shift range (225 ppm) and broad signals for the ligand (the average width at half height was 334 Hz at room temperature). Consequently, not all of the ligand resonances were located. Nevertheless, a plot of chemical shift vs 1/T yields a straight line for the observable resonances, consistent with Curie-Weiss behaviour (ytterbium does not show Curie-Weiss behaviour over the whole temperature range, but does in this region). A plot of chemical shift vs 1/T for the furthest downfield and furthest upfield resonances is shown in Fig 44. The observation of linear behaviour for both resonances suggests that a single species is present in solution over this temperature range (295 to 335 K).

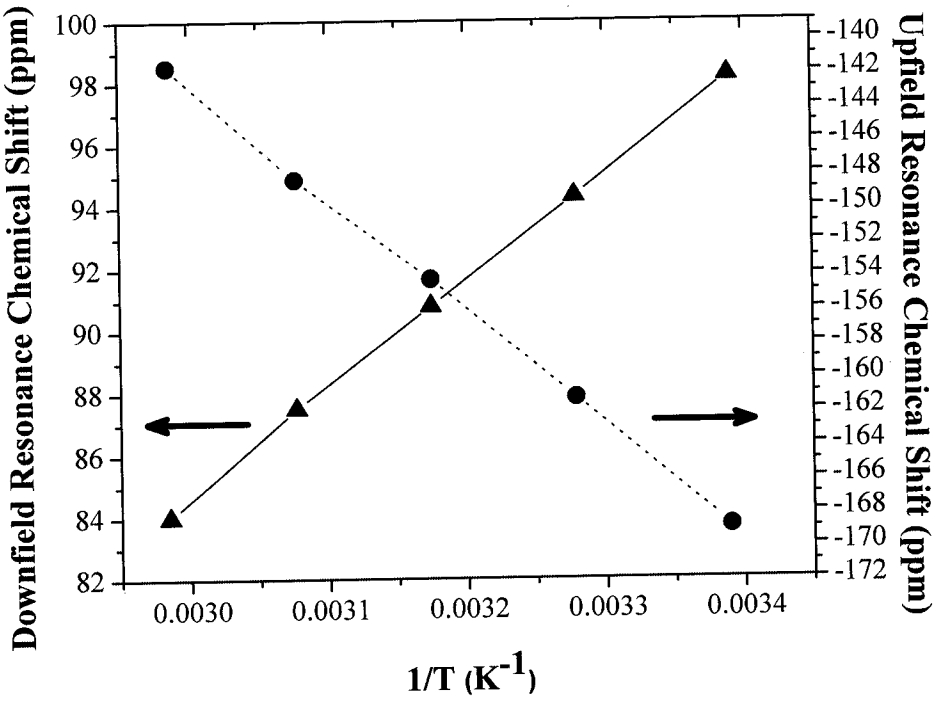

Figure 44. Furthest Downfield and Upfield Resonances of 24 (360 MHz ^{1}H NMR, d_8-THF).

When freshly prepared $Yb[N(SiMe_3)_2]_2(OEt_2)_2$ was allowed to react with one equivalent of $H_2(CBC)$ the result was a deep purple product **26** (Eq 47). This product proved to be insoluble in aromatic and aliphatic solvents. Even if the reaction was carried out in THF, **26** still precipitated as a purple powder. This result is consistent with the formation of an insoluble coordination polymer, $[(CBC)Yb]_n$, in which one or both of the amido groups is bridging between metal centres. Since ytterbium (II) centre in **26** is larger than the ytterbium (III) centres in **24** and **25**, it seems likely that additional bridging interactions would be required to satisfy this larger metal centre. Attempts to oxidize **26** with 0.5 equivalents of *p*-tolyl disulfide did result in a noticeable colour change, but the product of this reaction remained sparingly soluble and could not be isolated in pure form.

(47) $H_2(CBC)$ + $Yb[N(SiMe_3)_2]_2(OEt_2)_2$ ⟶ **26**

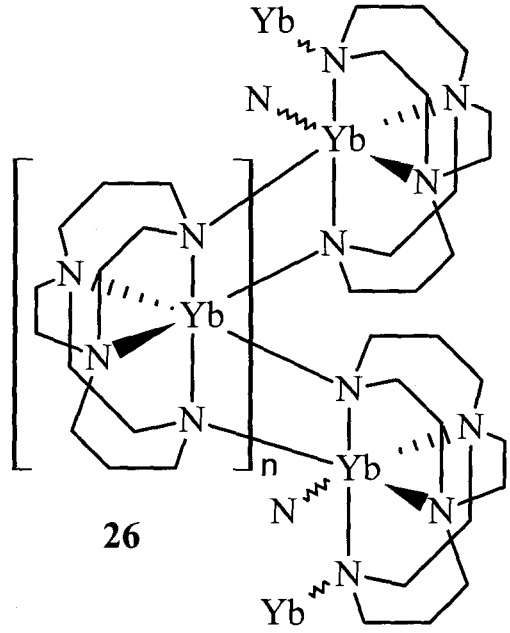

4.3 Trivalent chemistry

Thus far, attempts to isolate $Li_2(CBC)$ or similar species for use in metathesis reactions have been unsuccessful. Accordingly, several attempts were made to generate lanthanide complexes with cross-bridged cyclam by way of an *in situ* metathesis reactions. It was hoped that by allowing the ligand to coordinate to the lanthanide trichloride species prior to addition of a base, complexes might be generated (Eq 48). However, these reactions proved unsuccessful, possibly due to formation of insoluble $Li(CBC)LnCl_2$ "ate" complexes.

$$\begin{array}{ll} & LnCl_3THF_n + H_2(CBC) + 2\ n\text{BuLi} \\ (48) & (Ln = Y,\ n = 3.5, \\ & Ln = La,\ Ce,\ Er,\ Nd,\ n = 0) \end{array} \quad \not\longrightarrow$$

Since amine and hydrocarbon elimination reactions were successful in zirconium chemistry, we again turned to this route in an attempt to produce lanthanide complexes with cross-bridged cyclam. When the reaction of $H_2(CBC)$ with the various yttrium compounds was followed by NMR, there was evidence of reaction. However, the new ligand signals were often broad indicating a multitude of products (Eq 49-51). In all cases, attempts to scale up the reactions and isolate lanthanide complexes were unsuccessful. The reaction of $H_2(CBC)$ with $La[N(SiMe_3)_2]_3THF_2$ was investigated and resulted in different products depending on the specific batch of $La[N(SiMe_3)_2]_3THF_2$ that was used (Eq 52). In some cases the $N(SiMe_3)_2$ group had two resonances in the ^1H NMR, suggesting a dimeric structure and in other cases the integration of the $N(SiMe_3)_2$ resonances integrated to ca 3 equivalents per (CBC) ligand – not consistent with the

formation of a mononuclear lanthanide species. The variability in the reactions between $La[N(SiMe_3)_2]_3THF_2$ and $H_2(CBC)$ prevented the isolation of these species. Finally, the reaction of $CeCl[N(SiMe_3)_2]_2THF_2$ with $H_2(CBC)$ resulted in over 50 paramagnetic ligand resonances, indicating that a number of species were present in solution and all attempts to isolate a single species were unsuccessful (Eq 53).

(49) $Y[N(SiMe_3)_2]_3THF_2 + H_2(CBC)$ 

(50) $Y[N(SiHMe_2)_2]_3THF_2 + H_2(CBC)$ 

(51) $Y(CH_2SiMe_3)_3(OEt_2)_3 + H_2(CBC)$ 

(52) $Ln[N(SiMe_3)_2]_3THF_2 + H_2(CBC)$ 

(Ln = La, Ce)

(53) $LnCl[N(SiMe_3)_2]_2 + H_2(CBC)$ 

(Ln = Ce, Nd)

4.4 Summary and Future Directions

It was hoped that by moving from the relatively flexible DAC, MAC and (NOON) systems to cross-bridged cyclam we could avoid or reduce both bridging amido interactions and ligand metallation reactions. Clearly, the isolation of **24** and **25** show that there is enough flexibility in the cross-bridged cyclam to adopt a geometry with bridging amido groups. Also, an unappreciated consequence of moving from the ethyl bridges of

DAC and MAC to the propyl bridges in the macrocycle framework of cyclam is the ability to form pseudo-boat conformations, which brings a hydrogen towards the metal and may promote metallation of this position.

Attempts to isolate monomeric complexes of the type (CBC)LnX (X is a monoanion) have been unsuccessful thus far. This is not unexpected since the metal would only be five coordinate and not sterically saturated. Thus, there are several issues that could result in multiple products in solution: formation of dimers or oligomers, monomers or oligomers with a variable number of THF, ligands that have been metallated in different positions or fluxional processes interconverting some of the aforementioned species.

One way to solve some of these problems would be to convert H_2(CBC) into a monoanion. Not only would this reduce the number of amido groups in the ligand, but it would also result in six coordinate complexes and the steric protection afforded by the other two anions should help to prevent bridging interactions between metal centres. One way to derivatize H_2(CBC) is to use a palladium catalyzed C-N bond forming reaction to introduce an aryl group onto the ligand.[203] The latter is particularly appealing since a range of groups could potentially be introduced.

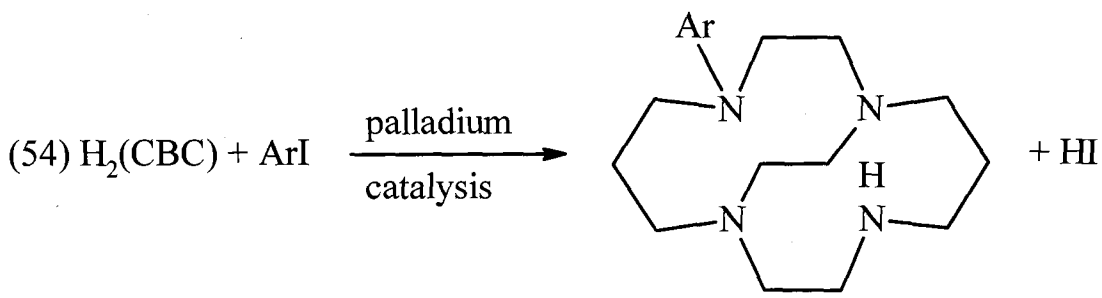

If these types of ligands were successful, then a longer term goal would be to link two cross-bridged cyclam units together. This might allow for the formation of dinuclear lanthanide complexes, especially desirable for ytterbium and samarium (II), since dinuclear species would be two electron reducing agents and the potential exists for novel chemistry.

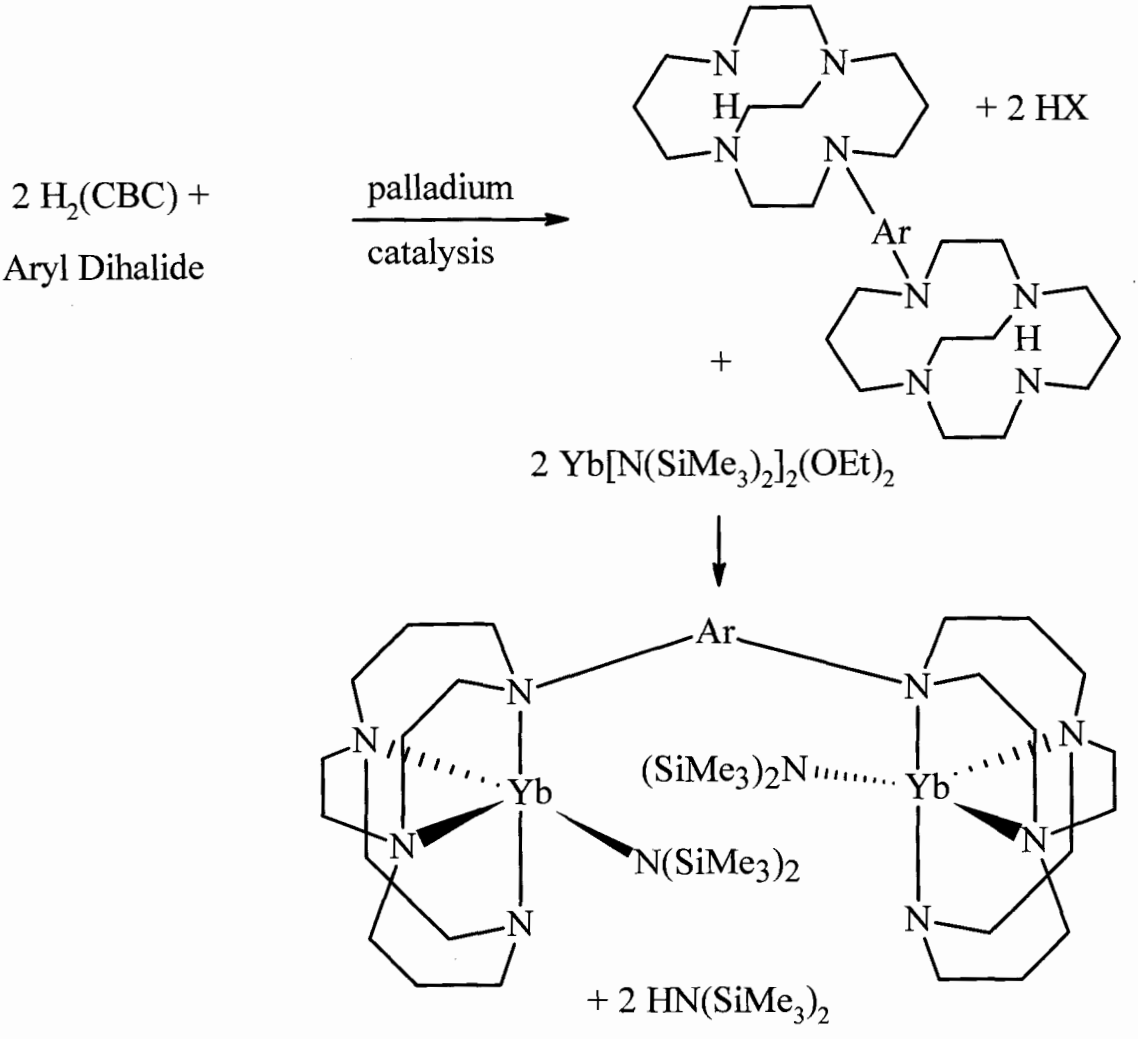

Scheme 15. Proposed Divalent Lanthanide Chemistry

Chapter 5. Experimental Details

General Procedures.

All manipulations were carried out under a nitrogen or argon atmosphere, with the rigorous exclusion of oxygen and water, using standard glovebox (Braun MB150-GII) or Schlenk techniques. Tetrahydrofuran (THF), diethyl ether, hexane and toluene were dried by distillation from sodium benzophenone ketyl under argon immediately prior to use. 1,2-*Bis*(2-iodoethoxy)ethane,[204] tetrabenzylzirconium,[205] $Zr[N(SiMe_3)_2]_3Cl$ and $Zr[N(SiMe_3)_2]_2Cl_2$[206] were prepared according to literature procedures. Tributyltin fluoride, n-butyllithium and MAO were obtained commercially (Aldrich) and were used as received. $B(C_6F_5)_3$ was a generous gift from Boulder Scientific and was purified by stirring with Me_2SiCl_2 followed by vacuum sublimation.

NMR spectra were recorded using a Bruker AMX-360 MHz spectrometer: ^1H (360 MHz), ^{11}B (115.54 MHz), ^{13}C (90.55 MHz), ^{19}F (338.86 MHz), ^{29}Si (71.54 MHz), ^{31}P (90.57 MHz) or a Bruker AV-500 MHz spectrometer: ^1H (500.13 MHz), ^{13}C (125.77 MHz). All deuterated solvents were dried over activated 4Å molecular sieves except for tetrahydrofuran (THF), which was dried by distillation from sodium benzophenone ketyl under argon and stored over activated 4Å molecular sieves. Spectra were recorded using 5 mm tubes fitted with a teflon valve (Brunfeldt) at room temperature unless otherwise specified. ^1H and ^{13}C NMR spectra were referenced to residual solvent resonances. ^{11}B NMR spectra were referenced to external BF_3OEt_2 (0.1 M in $CDCl_3$), ^{19}F NMR spectra were referenced to external CCl_3F, ^{29}Si NMR spectra were referenced to external TMS, and ^{31}P NMR spectra were referenced to external H_3PO_4 (aqueous 85%). Melting points were

recorded using a Büchi melting point apparatus in sealed capillary tubes and are not corrected. Elemental analyses were performed by Canadian Microanalytical, Delta, BC. Despite the use of co-oxidants such as V_2O_5 and PbO_2, the analytical data for most complexes were consistently 2 to 4 % low in carbon, likely due to metal carbide formation. Despite repeated attempts satisfactory elemental anayses of **2**, **4**, **6**, **7**, **10**, **12**, **13**, **14**, **19**, **20** and **21** were not obtained. This may be a result of decomposition of the compounds during shipping and handling of the samples or metal carbide formation. Mass spectra were recorded on a Kratos Concept H spectrometer using electron impact ionization (70 eV).

H_2(NOON), (1)

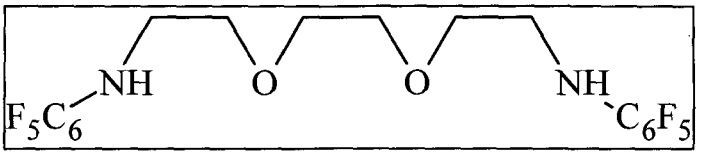

Pentafluoroaniline (5.82 g, 31.8 mmol) was weighed into a large Schlenk flask and dissolved with stirring in 100 mL dry THF under argon. The solution was cooled to -78 °C with an acetone-dry ice bath and 20 mL of 1.6 M n-BuLi (32 mmol) was added via syringe. The dark red solution was stirred for 10 minutes and *bis*(2-iodoethoxy)ethane (2.96 g, 8.00 mmol) was added by dropping funnel over a 30 minute period. The solution was allowed to warm to room temperature over a 1 h period and was refluxed overnight. The THF solvent was removed under reduced pressure and the residue was redissolved in diethyl ether. Water was carefully added and the dark red organic phase was separated and dried over anhydrous $MgSO_4$. After filtration, the ether solution was reduced in volume to *ca.* 2 mL and transferred to a short-path distillation apparatus. The remaining ether was removed and the residue was heated at 120 °C (10^{-1} mm Hg) to distill off all remaining pentafluoroaniline. The black tarry residue was extracted with diethyl ether and taken to dryness. Repeated

recrystallization from hot hexane yielded very pale yellow crystals. Yield: 2.42g, 63 %. Mp. 62-4 °C. NMR (d_6-benzene): ^{1}H δ 3.81 (br s, 2H, N*H*), 3.13 (m, 4H, CH_2O), 3.08 (m, 4H, CH_2N), 3.07 (m, 4H, CH_2O); ^{13}C{^{1}H} (d_6-benzene) δ 138.4 (d, *m*-aryl*C*, $^1J_{CF}$ = 249 Hz), 133.7 (d, *p*-arylC, $^1J_{CF}$ = 244 Hz), 127.3 (*quat*-aryl*C*), 125.8 (d, *o*-aryl*C*, $^1J_{CF}$ = 255 Hz), 70.3 (NCH$_2$*C*H$_2$O), 69.7 (O*C*H$_2$CH$_2$O), 45.8 (OCH$_2$*C*H$_2$N); ^{19}F{^{1}H} (*d*-chloroform) δ -160.3 (dd, *o*-aryl*F*, $^3J_{FF}$ = 22.5 Hz, $^4J_{FF}$ = 7.5 Hz), -166.0 (br t, *m*-aryl*F*, $^3J_{FF}$ = 22.5 Hz), -175.2 (tt, *p*-aryl*F*, $^3J_{FF}$ = 22.5 Hz, $^4J_{FF}$ = 7.5 Hz). High Res. MS (EI) Found (Calcd): M^+ 480.0883 (480.0896).

(C$_6$F$_5$NCH$_2$CH$_2$OCH$_2$)$_2$Zr(CH$_2$Ph)$_2$, (2)

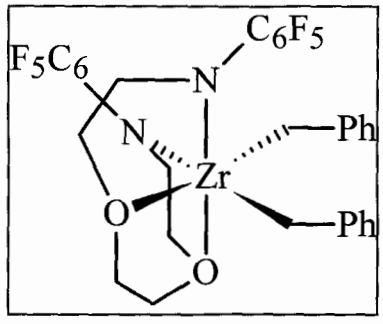

A solution of **1** (2.00 g, 4.17 mmol) in 30 mL toluene was added to a solution of Zr(CH$_2$Ph)$_4$ (1.898 g, 4.128 mmol) in 12 mL toluene and the reaction mixture was stirred at room temperature for 30 minutes and cooled to -30 °C. Complex **2** precipitated (two crops) on cooling and was obtained as a yellow powder after drying under vacuum. Yield: 2.66g, 85 %. Mp. 167-9 °C. NMR (d_5-bromobenzene): ^{1}H δ 7.14 (t, 4H, *m*-aryl*H*, $^3J_{HH}$ = 7.7 Hz), 6.92 (d, 4H, *o*-aryl*H*, $^3J_{HH}$ = 8.1 Hz), 6.80 (t, 2H, *p*-aryl*H*, $^3J_{HH}$ = 7.0 Hz), 3.56 (m, 4H, NCH$_2$C*H*$_2$O), 3.53 (m, 4H, NC*H*$_2$CH$_2$O), 2.82 (s, 4H, OC*H*$_2$C*H*$_2$O), 2.18 (s, 4H, C*H*$_2$Ph); ^{13}C{^{1}H} δ 147.6 (*quat*-aryl*C*), 142.3 (d, aryl*C*F, $^1J_{CF}$ = 246 Hz), 138.0 (d, aryl*C*F, $^1J_{CF}$ = 251 Hz), 135.5 (d, aryl*C*F, $^1J_{CF}$ = 280 Hz), 128.2 (*quat*-aryl*C*), 127.6 (*o*- or *m*-benzyl*C*), 127.0 (*o*- or *m*-benzyl*C*), 120.6 (*p*-benzyl*C*), 72.7 (*C*H$_2$Ph, t (gated ^{13}C), $^1J_{CH}$ = 124 Hz), 72.0 (NCH$_2$*C*H$_2$O), 68.7 (O*C*H$_2$CH$_2$O), 52.0

(NCH_2CH_2O). Assignments confirmed by ^1H-^{13}C COSY. ^{19}F (d_6-benzene): δ -150.8 (d, *o*-aryl*F*, $^3J_{FF}$ = 21.2 Hz), -164.9 (*m*-aryl*F*, $^3J_{FF}$ = 21.0 Hz), -166.6 (br t, *p*-aryl*F*). ^1H (d_6-benzene): δ 7.16 (t, 4H, *m*-aryl*H*, $^3J_{HH}$ = 7.7 Hz), 7.00 (d, 4H, *o*-aryl*H*, $^3J_{HH}$ = 8.1 Hz), 6.83 (t, 2H, *p*-aryl*H*, $^3J_{HH}$ = 7.0 Hz), 3.26 (m, 4H, NCH_2CH_2O), 3.18 (m, 4H, NCH_2CH_2O), 2.28 (s, 4H, OCH_2CH_2O), 2.22 (s, 4H, CH_2Ph). UV (CH_2Cl_2): λ_{max} 259 nm (ε 70 700 M^{-1} cm^{-1}) Anal. Calcd for $C_{32}H_{26}N_2O_2F_{10}Zr$: C, 51.13; H, 3.49; N, 3.72 %. Found: C, 47.89; H, 3.40; N, 3.69 %.

$(C_6F_5NCH_2CH_2OCH_2)_2ZrCl_2$, (3)

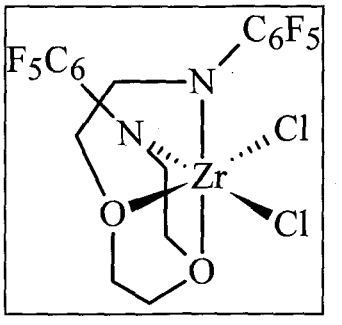

A solution of **1** (0.100 g, 0.208 mmol) in 4 mL toluene was added to a suspension of $Zr[N(SiMe_3)_2]_2Cl_2$ (0.100 g, 0.208 mmol) in 16 mL toluene and the reaction mixture was heated at 110 °C for 2 days. Complex **3** precipitated directly from the reaction mixture on cooling and was obtained as an analytically pure powder after washing with hexane and drying under vacuum. Yield: 0.12g, 90 %. Mp. 231-2 °C. NMR (d_5-bromobenzene): ^1H δ 4.04 (br s, 4H, NCH_2CH_2O), 3.84 (s, 4H, OCH_2CH_2O), 3.80 (br s, 4H, NCH_2CH_2O); $^{13}C\{^1H\}$ δ 71.5 (NCH_2CH_2O), 69.9 (OCH_2CH_2O), 53.2 (NCH_2CH_2O); $^{19}F\{^1H\}$ δ -148.4 (d, *o*-aryl*F*, $^3J_{FF}$ = 22.4 Hz), -164.1 (t, *p*-aryl*F* , $^3J_{FF}$ = 22.4 Hz), -170.2 (br s, *m*-aryl*F*). ^1H NMR (d_6-benzene): δ 3.58 (br s, 4H, NCH_2CH_2O), 3.48 (br s, 4H, NCH_2CH_2O), 3.07 (s, 4H, OCH_2CH_2O). Anal. Calcd for $C_{18}H_{12}N_2O_2F_{10}Cl_2Zr$: C, 33.76; H, 1.89; N, 4.37 %. Found: C, 33.86; H, 1.96; N, 4.14 %. High Res. MS (EI) Found (Calcd): M^+ 637.9185 (637.9159). The quaternary aryl ^{13}C

resonances were not located due to the extremely low solubility of this compound and the presence of solvent aryl resonances.

$(C_6F_5NCH_2CH_2OCH_2)_2ZrCl[N(SiMe_3)_2](C_7H_8)_{0.5}$, (4)

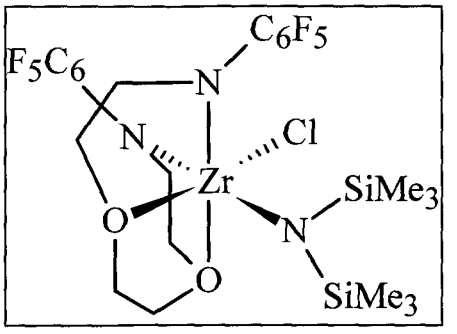

Method 1: A solution of **1** (0.100 g, 0.208 mmol) and $Zr[N(SiMe_3)_2]_3Cl$ (0.126 g, 0.208 mmol) in toluene (20 mL) was placed in a Schlenk flask sealed with a Kontes valve. The mixture was heated at 110 °C for 3 days with stirring. After cooling, the solvent was removed under vacuum leaving **4** as a powder. Recrystallization from hot toluene gave white crystals. Yield: 0.10g, 61 %. *Method 2:* A toluene solution of $NaN(SiMe_3)_2$ (0.028 g, 0.156 mmol) was added to a suspension of **3** (0.100 g, 0.156 mmol) in toluene with stirring. The cloudy reaction mixture was stirred overnight and filtered through Celite on a sintered glass frit. The filtrate was concentrated and cooled to yield **4** as a white crystalline solid. Yield: 0.11g, 90%. Mp. 230-2 °C. NMR (d_6-benzene): ^{1}H δ 3.74 (m, 2H, C*H*$_2$), 3.57 (m, 2H, C*H*$_2$), 3.23 (m, 2H, C*H*$_2$), 3.09 (m, 2H, C*H*$_2$), 2.72 (m, 4H, C*H*$_2$), 0.32 (s, 18H, Si*Me*$_3$); ^{13}C{^{1}H} δ 143.8 (d, aryl*C*F, $^1J_{CF}$ = 237 Hz), 137.9 (d, aryl*C*F, $^1J_{CF}$ = 244 Hz), 134.5 (d, aryl*C*F, $^1J_{CF}$ = 272 Hz), 128.9 (*quat*-aryl*C*), 72.5 (NCH_2CH_2O), 68.1 (OCH_2CH_2O), 54.0 (OCH_2CH_2N)), 4.2 (Si*Me*$_3$). ^{19}F{^{1}H} δ -146.0 (br s, *o*-aryl*F*), -164.4 (t, *p*-aryl*F* , $^3J_{FF}$ = 22.2 Hz), -166.6 (br t, *m*-aryl*F*, $^3J_{FF}$ = 22.2 Hz). ^{29}Si{^{1}H} (d_8-toluene): δ -4.21 ppm. Anal. Calcd for the hemi-toluene solvate $C_{27.5}H_{34}N_3O_2F_{10}ClSi_2Zr$: C, 40.71; H, 4.22; N, 5.18 %. Found: C, 38.55; H, 4.13; N, 5.15 %.

$(C_6F_5NCH_2CH_2OCH_2)_2ZrMe_2$, (5)

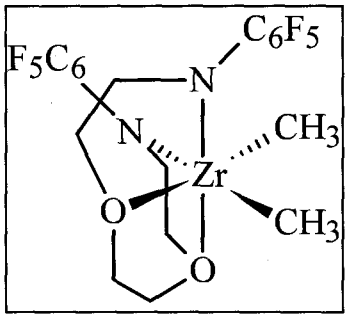

A stirred suspension of $Zr[CH_2OCH_2CH_2N(C_6F_5)]_2Cl_2$ (0.485 g 0.76 mmol) in dry diethyl ether (60 mL) was cooled in a dry ice-acetone bath. MeLi (1.4 M, 1.1 mL, 1.5 mmol) was added via syringe and the mixture was allowed to stir for 75 minutes. The Schlenk flask was transferred to an ice bath and the solvent removed under vacuum. Toluene (2 x 10 mL) was added to the residue and the resulting suspension was filtered through Celite. The filtrate was concentrated to *ca.* 4 mL and cooled at -30°C to afford **5** as colorless crystals. Repeated recrystallization from toluene afforded crystals suitable for X-ray diffraction. Yield: 0.219g, (48 %). Mp. 153 °C dec. NMR (d_6-benzene): ^{1}H δ 3.33 (t, 4H, NC*H*$_2$ or OC*H*$_2$CH$_2$N, $^3J_{HH}$ = 5.5Hz), 3.11 (t, 4H, NC*H*$_2$ or OC*H*$_2$CH$_2$N, $^3J_{HH}$ = 5.5Hz), 2.73 (s, 4H, OC*H*$_2$CH$_2$O), 0.47 (s, 6H, C*H*$_3$); ^{13}C δ 143.1 (d, *o*- or *m*-aryl *C*F, $^1J_{CF}$ = 234 Hz), 138.5 (d, *o*- or *m*-aryl *C*F, $^1J_{CF}$ = 250 Hz), 133.3 (d, *p*-aryl *C*F, $^1J_{CF}$ = 271 Hz), 73.5 (t, OCH$_2$CH$_2$N, $^1J_{CH}$ = 143 Hz), 68.9 (t, OCH$_2$CH$_2$O, $^1J_{CH}$ = 148 Hz), 52.5 (t, NCH$_2$, $^1J_{CH}$ = 136 Hz), 45.2 (q, *C*H$_3$, $^1J_{CH}$ = 114 Hz); ^{19}F{^{1}H} δ -152.0 (d, *o*-aryl*F*, $^3J_{FF}$ = 22 Hz), -165.5 (t, *m*-aryl*F*, $^3J_{FF}$ = 22 Hz), -167.3 (t, *p*-aryl*F*, $^3J_{FF}$ = 22 Hz). UV (CH_2Cl_2): λ_{max} = 277 nm (ε = 10,000 M^{-1} cm^{-1}). Anal. Calcd for $C_{20}H_{18}N_2O_2F_{10}Zr$: C, 40.06; H, 3.03; N, 4.67 %. Found: C, 39.71; H, 3.04; N, 4.59 %.

$[(C_6F_4NCH_2CH_2OCH_2CH_2OCH_2CH_2NC_6F_5)ZrCH_2Ph]_2(C_7H_8)_2$, (6)

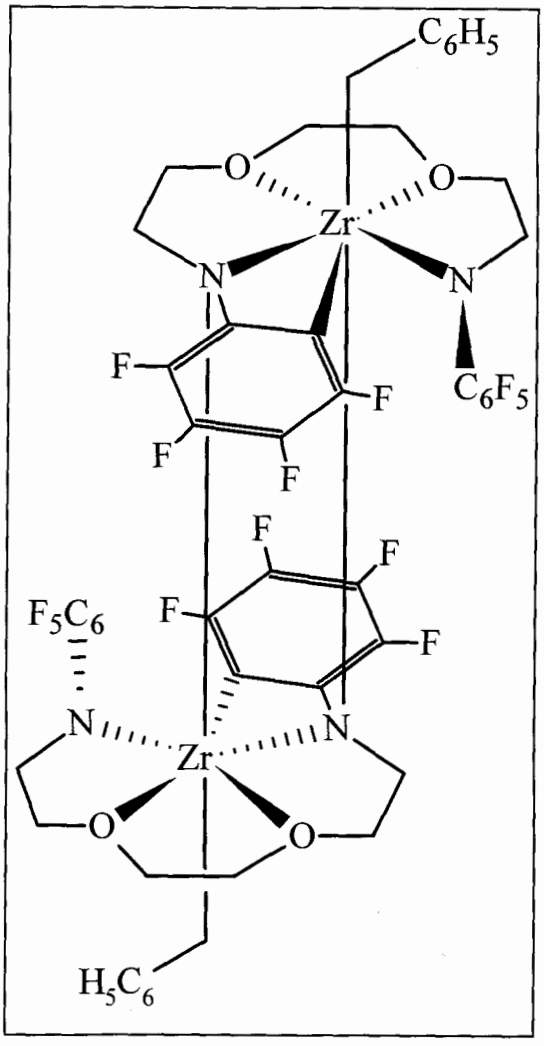

$(C_6F_5NCH_2CH_2OCH_2)_2Zr(CH_2Ph)_2$ (1.00 g, 1.33 mmol) was weighed into an Erlenmyer flask in the glovebox and dissolved in 120 mL of toluene. The solution was allowed to stand exposed to ambient light for 11 days during which time red crystals of **6** deposited from solution. The supernate was decanted off and allowed to stand for a further 7 days producing a second crop of **6**. The crystals were washed with toluene and dried under reduced pressure. Total yield: 0.098g, (17 %). Further crops of **6** can be obtained but these are invariably contaminated with increasing amounts of **7**. Mp. 193 °C (dec). NMR (d_8-THF): ^{1}H δ 6.91 (t, 2H, *m*-aryl*H*, $^3J_{HH}$ = 7.7 Hz), 6.53 (t, 1H, *p*-aryl*H*, $^3J_{HH}$ = 7.3 Hz), 6.43 (d, 2H, *o*-aryl*H*, $^3J_{HH}$ = 8.2 Hz), 4.38 (m, 1H), 4.31 (m, 2H), 4.24 (m, 1H), 4.12 (m, 2H), 4.05 (m, 1H), 4.00 (m, 2H), 3.77 (m, 2H), 3.11 (m, 1H), 1.85 (d, 1H, CH_aPh, $^2J_{HH}$ = 10.4 Hz), 1.72 (d, 1H, CH_bPh, $^2J_{HH}$ = 10.4 Hz); ^{13}C{^{1}H} and DEPT δ 151.2 (*quat*-aryl*C*), 146.2 (aryl*C*F, $^1J_{CF}$ = 228), 145.0 (aryl*C*F, $^1J_{CF}$ = 238), 139.4 (aryl*C*F, $^1J_{CF}$ = 256), 136.6 (aryl*C*F, $^1J_{CF}$ = 233), 134.2 (aryl*C*F, $^1J_{CF}$ = 252), 130.0 (*quat*-aryl*C*), 129.3 (aryl*C*F, $^1J_{CF}$ = 228), 129.2 (*quat*-aryl*C*), 128.1 (*m*-aryl*C*), 126.3 (*o*-aryl*C*), 120.3 (*p*-aryl*C*), 77.4 (NCH_2CH_2O), 76.9 (NCH_2CH_2O), 73.1

(OCH_2CH_2O), 71.6 (OCH_2CH_2O), 68.0 (CH_2Ph), 56.4 (NCH_2CH_2O), 50.2 (NCH_2CH_2O); $^{19}F\{^1H\}$ δ -114. 9 (dd, Zr-CC*F*), -147.1 (d, *o*-aryl*F*, $^3J_{FF}$ = 21 Hz), -156.2 (t, NCC*F*), -163.8 (t, *m*-arylC*F*, $^3J_{FF}$ = 21 Hz), -165.7 (dd, NCCC*F*), -167.0 (t, *p*-aryl*F* , $^3J_{FF}$ = 22 Hz), -170.1 (m, ZrCCC*F*). Anal. Calcd for $C_{57}H_{46}N_4O_4F_{18}Zr_2$ (one molecule of toluene per dimer, prolonged exposure of this compound to vacuum results in the loss of one toluene of solvation as shown by ^1H NMR and elemental analysis): C, 49.77; H, 3.37; N, 4.07 %. Found: C, 48.50; H, 3.36; N, 4.09 %.

$[(C_6F_5NCH_2CH_2OCH_2)_2ZrF_2]_n$, (7)

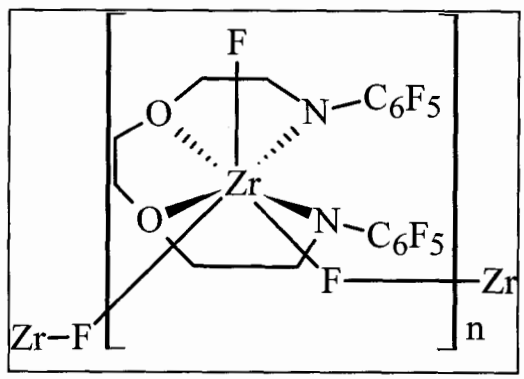

Method 1: (*in situ* generation during photolysis) A sample of $Zr(C_6F_5NCH_2CH_2OCH_2)_2(CH_2Ph)_2$ (0.010 g, 13 μmol) dissolved in d_6-benzene was placed in a sealable NMR tube under argon. The NMR tube was placed in glass cooling jacket and irradiated with filtered light (435 nm cutoff) from a 150 W incandescent light bulb for 14 h. At the end of this period no trace of starting material was detectable by ^1H NMR spectroscopy and red crystals of **6** were seen coating the wall of the tube. Compound **7** was characterized *in situ* by NMR spectroscopy. Larger scale photolysis resulted in precipitation of **7** as a white solid that was very difficult to redissolve. *Method 2:* (using n-Bu_3SnF) Solid n-Bu_3SnF (2 equiv) was added to a vigorously stirred solution of $Zr(C_6F_5NCH_2CH_2OCH_2)_2(CH_2Ph)_2$ in toluene. After 24 h, solid **7** was filtered away from the toluene supernate containing n-$Bu_3Sn(CH_2Ph)$. The NMR spectrum of **7** generated in this manner was identical to that observed by Method 1. Unfortunately, **7** produced by this

method was contaminated with unreacted n-Bu_3SnF. NMR (d_6-benzene): ^1H δ 3.90 (m, 2H), 3.80 (m, 2H), 3.60 (m, 2H), 3.18 (m, 2H), 2.94 (m, 2H), 2.65 (m, 2H); $^{19}F\{^1H\}$ δ +109.2 (s, Zr-F_{term}), -51.4 (s, Zr-μ-*F*-Zr), -150.1 (br s, *o*-aryl*F*), -165.8 (t, *p*-aryl*CF*, $^3J_{FF}$ = 20 Hz), -166.6 (t, *m*-aryl*F*, $^3J_{FF}$ = 21 Hz). Anal. Calcd for $C_{36}H_{24}N_4O_4F_{24}Zr_2$: C, 35.59; H, 1.99; N, 4.61 %. Found: C, 35.05; H, 1.74; N, 4.55 %.

Photolysis experiments.

Toluene or d_6-benzene solutions of the samples were irradiated with a 150 W incandescent light bulb. Samples were cooled during irradiation by means of a water jacket. The light was filtered through coloured filters with low wavelength cutoffs of 375, 435 and 550 nm. Initial experiments showed that only the 435 nm filter afforded clean photoproducts with $(C_6F_5NCH_2CH_2OCH_2)_2Zr(CH_2Ph)_2$. Irradiation using the 375 nm filter resulted in very complex ^1H NMR spectra consistent with formation of several products. Irradiation at 550 nm did not result in any significant reaction over a period of 28 hours. As a control experiment, a solution of $(C_6F_5NCH_2CH_2OCH_2)_2Zr(CH_2Ph)_2$ in toluene was wrapped in foil and kept at room temperature for several months; no detectable formation of **6** or **7** was observed and the starting zirconium complex was recovered unchanged. Irradiation of $(C_6F_5NCH_2CH_2OCH_2)_2Zr(CH_2Ph)_2$ in d_8-THF at 435 nm resulted in the formation of bibenzyl and a complex mixture of products that did not contain **6**.

$[(C_6F_5NCH_2CH_2OCH_2)_2ZrCH_2Ph][PhCH_2B(C_6F_5)_3]$, (8)

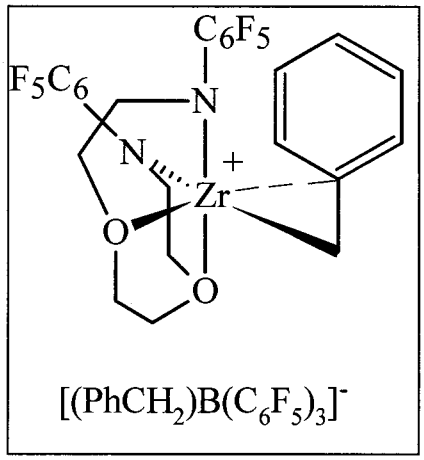

A solution of $B(C_6F_5)_3$ (0.011 g, 0.020 mmol) in 0.1 mL CD_2Cl_2 was added to a pre-cooled (-30 °C) solution of **2** (0.015 g, 0.021 mmol) in 0.4 mL CD_2Cl_2 in the glovebox. The deep orange solution was thoroughly mixed and allowed to stand at room temperature for 1 h. The product was characterized *in situ* by NMR spectroscopy; slow degradation of the sample was observed over 24 h. ^{1}H NMR: δ 7.52 (t, 2H, *m*-aryl*H*), 7.32 (t, 1H, *p*-arylH), 6.98 (d, 2H, *o*-aryl*H*), 6.87 (t, 2H, *m*-aryl*H*), 6.79 (t, 1H, *p*-aryl*H*), 6.73 (d, 2H, *o*-aryl*H*), 4.54 (dt, 2H, C*H*$_2$, J = 9.5, 4.8 Hz), 4.27 (dt, 2H, C*H*$_2$, J = 9.5, 5.0 Hz), 4.17 (m, 2H, C*H*$_2$), 4.04 (br t, 4H, C*H*$_2$, J = 5.0Hz), 3.90 (m, 2H, C*H*$_2$), 2.81 (s, 2H, ZrC*H*$_2$), 2.77 (br s, 2H, BC*H*$_2$). ^{13}C{^{1}H} NMR: 132.7, 130.0, 129.0, 128.7, 127.3, 122.9 (aryl*C*H), 79.3 (NCH$_2$*C*H$_2$O), 75.2 (Zr*C*H$_2$Ph, t (gated ^{13}C), $^1J_{CH}$ = 138 Hz), 73.2 (OCH$_2$*C*H$_2$O), 60.8 (B*C*H$_2$Ph), 52.9 (N*C*H$_2$CH$_2$O). The quaternary aryl carbon resonances were not observable. ^{19}F{^{1}H} NMR: δ-132.0 (d, 6F, borate *o*-aryl*F*, $^3J_{FF}$ = 23.4 Hz), -150.4 (d, 4F, ligand *o*-aryl*F*, $^3J_{FF}$ = 23.2 Hz), -162.4 (dt, 4F, ligand *m*-aryl*F*, J_{FF} = 22.5, 3.5 Hz), -165.0 (t, 3F, borate *p*-aryl*F*, $^3J_{FF}$ = 20.4 Hz), -165.4 (t, 2F, ligand *p*-aryl*F*, $^3J_{FF}$ = 21.6 Hz), -168.1 (t, 6F, borate *m*-aryl*F*, $^3J_{FF}$ = 19.6 Hz). ^{11}B{^{1}H} NMR: δ-10.9 (s).

Olefin polymerization tests.

A solution of **3** (0.040 g, 0.062 mmol) in toluene (30 mL) was placed in a Schlenk flask equipped with a Kontes valve and degassed by three freeze-pump-thaw cycles. The solution was placed under 1 atm of ethylene, MAO (20 mL of a 10% by wt. solution in toluene, ca. 500 equiv) was added and the sealed flask was immersed in a 50 °C oil bath for 1 h with rapid stirring. At the end of this period, methanol (12 mL) was added to the flask and the precipitated solids were collected by filtration. The solids were stirred in aqueous HCl (20%) overnight, collected by filtration and washed with water, methanol and hexanes. The remaining solid was dried under vacuum to yield polyethylene (0.199 g; rate = 3.2 kg mol^{-1} Zr h^{-1}). A blank experiment run with only MAO produced no polyethylene under these conditions.

H_2(CBC), (9)

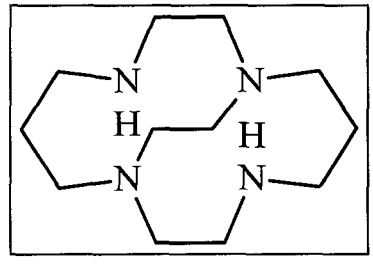

Cyclam was prepared via a nickel templated reaction, which does not require the use of perchlorate salts.[207] The free base was obtained without isolating the nickel cyclam complex.[208] The synthesis of cross-bridged cyclam has been described previously;[160] however, we found it necessary to sublime the oil obtained after benzene extraction from KOH and to store a toluene solution of the title compound over freshly activated molecular sieves for several days to thoroughly dry the product.

(CBC)Zr(CH_2Ph)$_2$, (10)

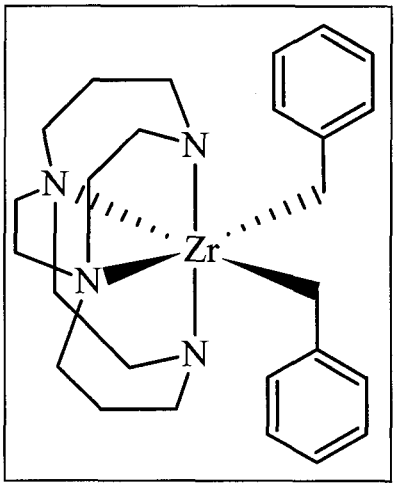

H_2(CBC) (0.500g, 2.21mmol) was added to a solution of tetrabenzylzirconium (1.00g, 2.19 mmol) in 20 mL toluene. The solution was protected from light and stirred at room temperature overnight. Cooling to -30°C afforded a yellow powder after decanting the mother liquor and drying under vacuum. Yield: 0.935g, 85 %. Mp. 171°C (dec) NMR (d_6-benzene): ^{1}H δ 7.20 (m, 4H, *m*-aryl*H*), 7.14 (m, 4H, *o*-aryl*H*), 6.84 (tt, 2H, *p*-aryl*H*), 4.30 (m, 2H), 3.11 (dd, 2H), 2.90-2.84 (m, 4H), 2.78 (td, 2H), 2.56(d, 2H, C*H*HPh, $^2J_{HH}$ = 10.2 Hz), 2.51 (td, 2H), 2.47 (d, 2H, C*H*HPh, $^2J_{HH}$ = 10.2 Hz), 2.41-2.36 (m, 2H), 1.80 (m, 2H), 1.64-1.54 (dd and m, 4H), 1.37 (m, 2H), 0.72 (m, 2H); ^{13}C{^{1}H} δ 151.9 (*quat*-aryl*C*), 128.7 (*m*-aryl*C*), 126.3 (*o*-aryl*C*), 120.3 (*p*-aryl*C*), 70.3 (*C*H_2Ph, t in the gated ^{13}C, $^1J_{CH}$ = 113 Hz), 60.4, 58.60, 54.2, 54.0, 50.8 (N*C*H_2), 22.2 (CH_2*C*H_2*C*H_2); Anal. Calcd for $C_{26}H_{38}N_4Zr$: C, 62.73; H, 7.69; N, 11.25 %. Found: C, 57.97; H, 7.19; N, 11.45 %.

[(CBC)Zr(CH_2Ph)N(Bu^t)C(H)=CHPh](C_7H_8)$_{0.5}$, (11)

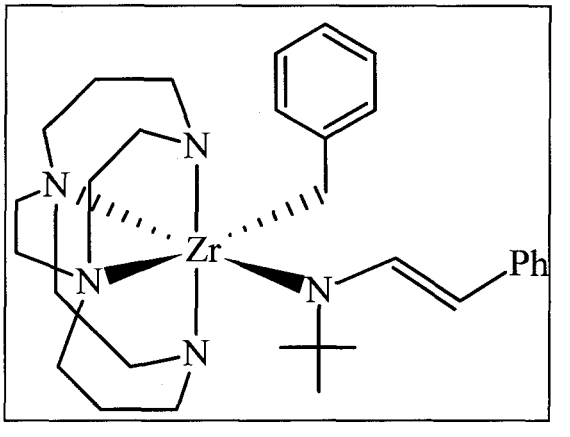

A solution of ^{t}BuNC in toluene (0.136 M, 5.9 mL, 0.80 mmol) was added to a solution of (CBC)Zr(CH_2Ph)$_2$ (0.2g, 0.40 mmol) in 20 mL toluene. This was allowed to stir at room temperature for 3 days. The solvent was

removed under reduced pressure and the product obtained by recrystallizing the bright yellow powder from hot toluene. Yield: 0.72 g (3 crops), 29 %. Mp. 158°C (dec) NMR (d_6-benzene): ^{1}H δ 8.40 (d, 1H, PhC=C*H*, $^3J_{HH}$ = 14.0 Hz), 7.51 (d, 2H, o-arylH), 7.30 (m, 6H, aryl*H*), 7.02 (m, 1H, *p*-aryl-H), 6.89 (t, 1H, *p*-aryl*H*), 6.15 (d, 1H, C=C*H*Ph, $^3J_{HH}$ = 14.0 Hz), 4.27 (t, 1H, NC*H*), 4.02 (t, 1H, NC*H*), 3.25 (m, 1H), 3.11 (m, 3H), 2.91 (m, 3H), 2.70 (m, 4H), 2.55 (br s, 2H), 2.44 (t, 1H), 1.93 (br d, 2H), 1.71 (m, 3H), 1.57 (s, 9H, CH_3), 1.51-1.22 (m, 3H), 0.85 (d, 1H), 0.54 (d, 1H); ^{13}C{^{1}H} δ 153.3 (benzyl *quat-C*), 142.4 (phenyl *quat-C*), 136.9 (*C*=CPh), 129.7 (aryl*C*H), 126.8 (aryl*C*H), 126.0 (aryl*C*H), 124.5 (aryl*C*H), 123.6 (aryl*C*H), 120.3 (aryl*C*H), 106.0 (C=*C*Ph), 62.5, 61.3, 60.5, 60.0, 58.7 (4 NCH_2 and ZrCH_2), 56.8 (N*C*$(CH_3)_3$) 55.1, 54.7, 54.4, 52.6, 52.4, 49.5 (NCH_2), 31.6 (*C*H_3), 22.0, 21.8 ($CH_2CH_2CH_2$). Anal. Calcd for the hemi-toluene solvate $C_{34.5}H_{51}N_5Zr$: C, 66.08; H, 8.20; N, 11.17 %. Found: C, 61.15; H, 7.99; N 12.05 %.Calcd for $C_{31}H_{47}N_5Zr$: C, 64.09; H, 8.15; N, 12.05 %.

(CBC)Zr(CH_2Ph)(O-2,6-$C_6H_3Bu^t_2$), (12)

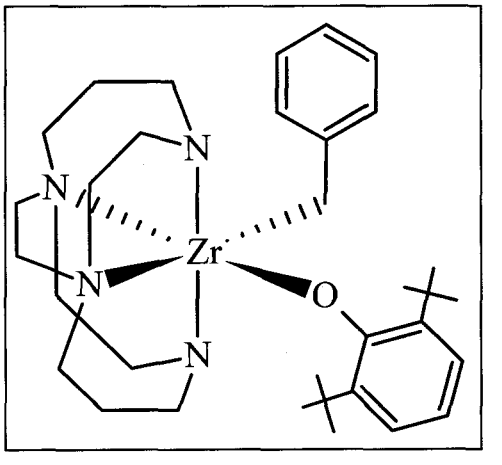

Toluene (5 mL), was added to an intimate mixture of (CBC)Zr(CH_2Ph)$_2$ (0.050g, 0.10 mmol) and 2,6-di-t-butylphenol (0.021g, 0.10 mmol). The mixture was stirred at room temperature overnight and the solvent removed under reduced pressure. The powder was recrystallized by cooling a hot toluene solution to -30°C to produce pale yellow microcrystals. Yield: 0.026g, 43 %. Mp. 220-4°C. NMR (d_6-benzene): ^{1}H δ 7.50 (dd, 1H, *m*-phenoxide*H*), 7.42 (dd, 1H, *m*-

phenoxide*H*), 7.12 (1H obscured by d_6-benzene, *p*-benzyl or p-phenoxide) 6.97 (t, 1H, *p*-benzyl or *p*-phenoxide*H*) 6.88-6.82 (m, 4H, *o*- and *m*-benzyl*H*), 4.64 (m, 1H), 4.03 (m, 1H), 3.13-2.96 (m, 10H), 2.79-2.71 (m, 2H), 2.61-2.54 (m, 3H), 2.54 (d, 1H, C*H*HPh, $^2J_{HH}$ = 10.7 Hz), 2.34 (d, 1H, C*H*HPh, $^2J_{HH}$ = 10.7 Hz), 2.00 (m, 2H), 1.88-1.67 (m, 1H), 1.85 (s, 9H, ^{t}Bu), 1.78 (s, 9H, ^{t}Bu), 1.38-1.22 (m, 2H), 0.88 (m, 2H); $^{13}C\{^1H\}$ δ 164.5 (O*C*), 153.0 (*quat*-benzyl*C*), 140.5 (*C*C(CH$_3$)$_3$), 139.4 (*C*C(CH$_3$)$_3$), 128.7 (*o*- or *m*-aryl obscured by d_6-benzene), 126.6 (*o*- or *m*-aryl*C*), 126.4 (*o*- or *m*-aryl*C*), 125.8 (*o*- or *m*-aryl*C*), 120.2 (*p*-aryl*C*), 118.9 (*p*-aryl*C*) 64.8 (*C*H$_2$Ph), 61.6, 60.7, 59.4, 58.1, 55.2, 54.7, 54.6, 52.5, 51.7, 49.7 (N*C*H$_2$), 36.7, 36.4 (*C*(CH$_3$)$_3$), 32.9, 32.1 (*C*H$_3$), 21.9, 21.5(CH$_2$*C*H$_2$*C*H$_2$); Anal. Calcd for $C_{33}H_{52}N_4OZr$: C, 64.76; H, 8.56; N, 9.15 %. Found: C, 63.80; H, 8.25; N, 9.03 %.

(CBC)Zr[κ^2(C,O)-OC$_6$H$_3$(6-Bu^t)(2-CMe$_2$CH$_2$)], (13)

A solution of (CBC)Zr(CH$_2$Ph)(O-2,6-C$_6$H$_3$Bu$^t_2$)] (0.140g, 0.229 mmol) in 30 mL toluene was sealed in a Kontes bomb and heated at 100°C for 7 days. The solvent was removed and the product was recrystallized from a minimum volume of hot toluene.

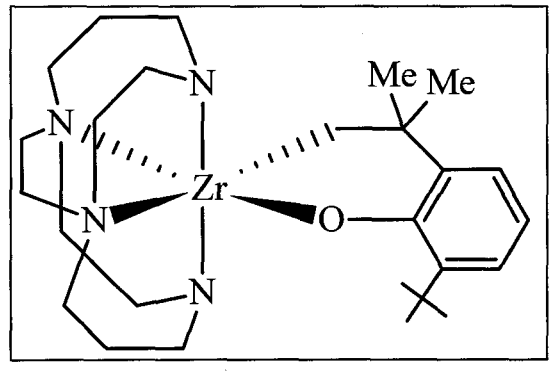

Cooling to -30°C yielded the product as a pure colourless powder. Yield: 0.054g, 39 %. Mp. 224-229°C (dec) NMR (d_6-benzene): ^1H δ 7.65 (dd, 1H, *m*-aryl*H*), 7.39 (dd, 1H, *m*-aryl*H*), 7.05 (t, 1H, *p*-aryl*H*), 4.25 (m 1H), 3.98 (m, 1H), 3.32 (m, 1H), 3.11-2.97 (m, 7H), 2.92-2.73 (m, 4H), 2.17 (m, 1H), 2.00-1.96 (m, 2H), 1.93 (m, 1H), 1.90-1.68 (m,

2H), 1.88 (s, 3H, CH_3), 1.81 (s, 3H, CH_3), 1.73 (s, 9H, C(CH_3)$_3$), 1.40 (dd, 1H), 1.29 (dd, 1H), 1.16 (d, 1H, ZrC*H*H, $^2J_{HH}$ = 13.3 Hz), 0.87 (d, 1H, ZrC*H*H, $^2J_{HH}$ = 13.3 Hz), 0.85 (m, 1H), 0.70 (m, 1H); $^{13}C\{^1H\}$ and DEPT δ 162.1 (O*C*), 143.7 (*o*-aryl*C*), 136.4 (*o*-aryl*C*), 125.8 (*m*-aryl*C*), 124.5 (*m*-aryl*C*), 118.8 (*p*-aryl*C*), 75.4 (Zr*C*H$_2$) 62.3,62.0, 58.8, 58.3, 54.4, 53.2, 53.0, 51.4, 51.2, 51.2 (N*C*H$_2$), 42.9 (*quat-C*), 39.8 (*quat-C*), 35.8 (*C*H$_3$), 33.4 (*C*H$_3$), 31.3 (C(*C*H$_3$)$_3$), 22.0 (overlapping CH$_2$*C*H$_2$*C*H$_2$); Anal. Calcd for the toluene solvate $C_{33}H_{52}N_4OZr$: C, 64.76; H, 8.56; N, 9.15 %. Found: C, 63.80; H, 8.25; N, 9.03 %.

(CBC)Zr(OSi(Bu^t)$_2$H)$_2$, (14)

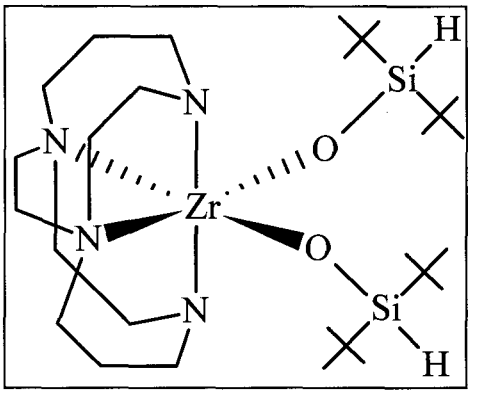

A yellow solution of (CBC)Zr(CH$_2$Ph)$_2$ (0.093g 0.19 mmol) in toluene (6 mL) was slowly added to solid HOSi(Bu^t)$_2$H (0.030g, 0.19 mmol). After approximately half the volume of the yellow solution was added, the reaction mixture was colourless. The remainder of the (CBC)Zr(CH$_2$Ph)$_2$ was added and the solution was allowed to stir at room temperature for 2.5 hours and cooled to -30°C. The yellow precipitate was (CBC)Zr(CH$_2$Ph)$_2$. Removal of the solvent from the supernate and recrystallization from hexanes afforded (CBC)Zr(OSi(Bu^t)$_2$H)$_2$ as colourless crystals. Yield: 0.21g, 35 % (based on HOSi(Bu^t)$_2$H). Mp. 196-8°C. NMR (d$_6$-benzene): ^{1}H δ 4.67 (s, 2H, Si*H*, $^1J_{HSi}$ = 186 Hz), 4.32 (td, 2H), 3.34 (td, 2H), 3.26 (td, 2H), 3.08 (m, 2H), 2.97 (m, 4H), 2.74 (m, 2H), 2.19 (m, 2H), 1.95 (dd, 2H), 1.85 (m, 2H), 1.54(m, 2H), 1.34 (s, 18 H, C*H*$_3$), 1.32 (s, 18 H, C*H*$_3$), 0.94 (m, 2H); ^{13}C $\{^1H\}$ δ 62.1, 60.0, 52.9, 52.8, 52.7 (N*C*H$_2$), 28.9, 28.7 (*C*H$_3$),

22.2 ($CH_2CH_2CH_2$), 21.1, 21.0 ($C(CH_3)_3$); ^{29}Si (DEPT) 2.9. Anal. Calcd for $C_{28}H_{62}N_4O_2Si_2Zr$: C, 53.87; H, 9.85; N, 8.84 %. Found: C, 53.26; H, 9.51; N, 8.80.

(CBC)Zr(O-2,6-$C_6H_3Me_2$)$_2$, (15)

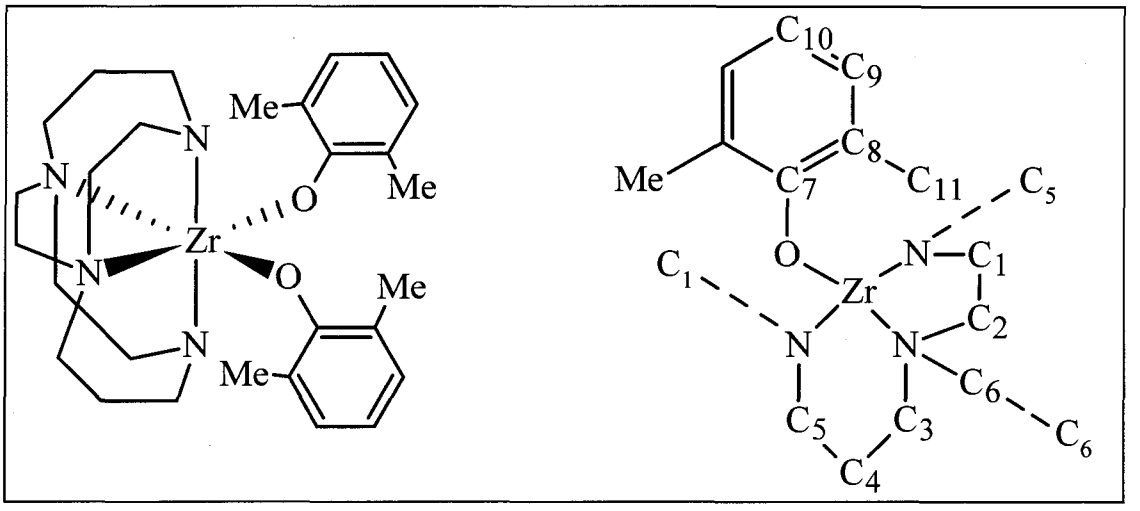

Figure 45. Numbering scheme for NMR assignments of 15. Each carbon bears hydrogens of the same number. For the ligand, H_a's have coupling constants consistent with pseudoaxial sites and H_b's with pseudoequatorial sites.

(CBC)Zr(CH_2Ph)$_2$ (0.930g, 1.87 mmol) was dissolved in 50 mL of warm toluene and 2,6-dimethylphenol (0.456g, 3.73 mmol) was added. The solution was stirred at room temperature for 2h and stored at -30°C resulting in clear colourless crystals of **5** (two crops). Yield: 0.89g, 85 %. Mp. 270°C (dec) NMR (d_6-benzene): ^1H δ 7.04 (d, 4H, H_9), 6.77 (t, 2H, H_{10}), 4.01 (m, 2H, H_{5a}), 3.65 (m, 2H, H_{2a}), 3.15 (m, 2H, H_{1b}), 3.10-3.02(m, 4H, H_{1a}, and H_{3a}), 2.99 (m, 2H, H_{6b}), 2.93(m, 2H, H_{5b}), 2.50 (s, 12H, H_{11}), 2.06 (m, 2H, H_{3b}), 1.98 (m, 2H, H_{2b}), 1.79 (m, 2H, H_{4a}), 1.38 (m, 2H, H_{6a}), 0.62 (m, 2H, H_{4b});

$^{13}C\{^1H\}$ δ 161.0 (C_7), 129.2 (C_9), 127.3 (C_8), 119.3 (C_{10}), 62.7 (C_2), 59.7 (C_3), 53.3 (C_1), 52.9 (C_5), 52.3 (C_6), 21.7 (C_4), 18.6 (C_{11}). Assignments are based on ^1H-^1H and ^1H-^{13}C COSY. Anal. Calcd for $C_{28}H_{42}N_4O_2Zr$: C, 60.28; H, 7.59; N, 10.04 %. Found: C, 60.24; H, 7.45; N, 10.05 %. MS (EI) M^+ 556.

(CBC)$ZrCl_2$, (16)

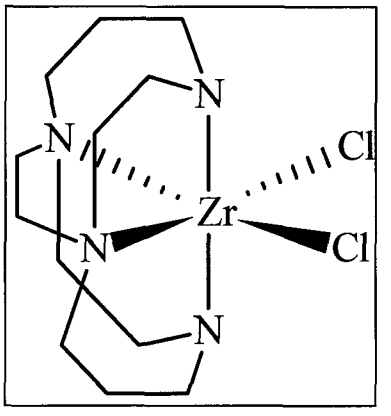

H_2(CBC) (1.50g, 6.63 mmol) and $ZrCl_2[N(Si(CH_3)_3)_2]_2$ (3.30g, 6.62 mmol) were sealed in a Kontes bomb with 20 mL toluene and heated at 100°C for 2 days. The product precipitated from solution as a yellow powder and was washed twice with 5mL of hexanes and dried at reduced pressure. Yield: 2.64g, 90 %. Mp. 271-5°C (dec) NMR (d_6-benzene): ^1H δ 4.73 (m, 2H), 3.30 (m, 4H), 2.95 (m, 2H), 2.87 (m, 2H), 2.76 (dd 2H), 2.64 (m 2H), 1.91 (dd 2H), 1.71 (dd 2H), 1.56 (m 2H), 1.34 (m, 2H), 0.80 (m, 2H); $^{13}C\{^1H\}$ δ 61.8, 60.3, 54.0, 53.3, 52.8, 30.6 (CH_2N), 21.7 ($CH_2CH_2CH_2$); Anal. Calcd for $C_{12}H_{24}N_4Cl_2Zr$: C, 37.29; H, 6.26; N, 14.50 %. Found: C, 37.33; H, 6.54; N, 13.78 %.

(CBC)Zr(Cl)[$N(Si(CH_3)_3)_2$], (17)

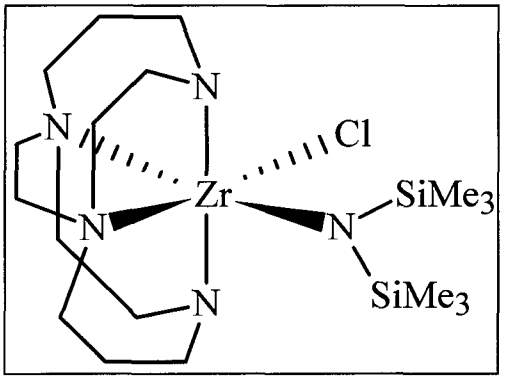

Method A: Complex **17** was isolated as a byproduct in the synthesis of (CBC)$ZrCl_2$ from $ZrCl_2[N(Si(CH_3)_3)_2]_2$, possibly due to the presence of $ZrCl[N(Si(CH_3)_3)_2]_3$ as a contaminant

in the *bis*(trimethylsilylamide) complex. *Method B:* THF (15 mL) was added to a mixture of (CBC)$ZrCl_2$ (0.200g, 0.518 mmol) and $NaN(Si(CH_3)_3)_2$ (0.095g, 0.518 mmol) and the resulting solution was stirred at room temperature overnight. The solvent was removed under reduced pressure and the solid residue was extracted with toluene (15 mL) then filtered through Celite to afford a clear solution. The product was isolated as clear colourless crystals by layering a saturated toluene solution with hexamethyldisiloxane and storing at -30°C. The crystals become opaque when removed from the solvent. Yield: 0.037g, 14 %. Mp. 173-6°C (dec) NMR (d_6-benzene): ^1H δ 4.89 (m, 1H), 4.09 (m, 1H), 3.75 (m, 1H), 3.50 (m, 1H), 3.25-2.70 (m, 10H), 1.98 (m, 1H), 1.88 (m, 1H), 1.80-1.55 (m, 4H), 1.30 (m, 1H), 1.16 (m, 1H), 0.99 (m, 1H), 0.88 (m, 1H), 0.79 (s, 9H, CH_3), 0.54 (s, 9H, CH_3); $^{13}C\{^1H\}$ δ 61.9, 61.0, 60.0, 58.5, 54.8, 54.6, 54.5, 53.3, 53.0, 52.7 (CH_2N), 22.3, 21.5 ($CH_2CH_2CH_2$), 7.4 (CH_3), 7.2 (CH_3); Anal. Calcd for $C_{18}H_{42}N_5ClSi_2Zr$: C, 42.27; H, 8.28; N, 13.69 %. Found: C, 41.88; H, 7.87; N, 13.69 %.

(CBC)$Zr(CH_3)_2$, (18)

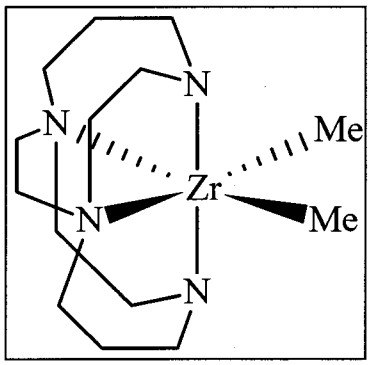

MeLi (1.4M, 1.85 mL, 2.6 mmol) was added to a suspension of (CBC)$ZrCl_2$ (0.500g, 1.29 mmol) in 20 mL THF and stirred at room temperature overnight. The solvent was removed under reduced pressure and the solids extracted twice with 50 mL toluene. The extract was filtered (Celite), and the solvent removed under reduced pressure. The product was repeatedly recrystalized from warm toluene to yield colourless or pale yellow microcrystals. Yield: 0.107g, 24 %. Mp. 175°C (dec) NMR (d_6-benzene): ^1H δ 4.50 (m, 2H), 3.25 (dd, 2H), 3.13-2.96 (m, 6H), 2.80 (m,

2H), 2.47 (m, 2H), 1.99 (m, 2H) 1.83 (dd, 2H), 1.81 (m, 2H), 1.75 (m, 2H), 0.80 (m 2H), 0.60 (s, 6H); $^{13}C\{^{1}H\}$ and DEPT δ 60.9, 59.8, 53.9, 53.8, 51.6 (CH_2N), 39.3 (CH_3, t in the gated ^{13}C, $^{1}J_{CH}$ = 109 Hz), 22.1 ($CH_2CH_2CH_2$); Anal. Calcd for $C_{14}H_{30}N_4Zr$: C, 48.65; H, 8.75; N, 16.21 %. Found: C, 48.38; H, 8.54; N, 16.13%.

(CBC)Zr[$CH_2Si(CH_3)_3$]$_2$, (19)

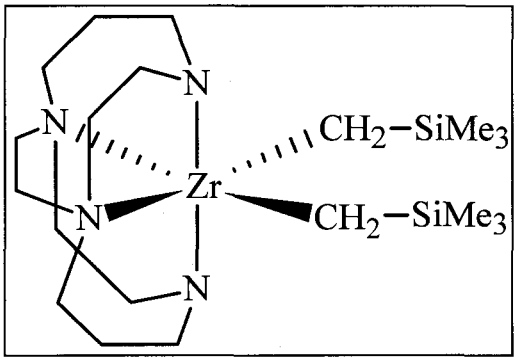

(CBC)$ZrCl_2$ (0.500g, 1.29 mmol) was suspended in 50 mL toluene and $LiCH_2Si(CH_3)_3$ (0.244g, 2.59 mmol) was added; the mixture was stirred at room temperature overnight. Filtration (Celite) of the reaction mixture and removal of the solvent at reduced pressure afforded a white powder. The product was dissolved in 14 mL of 5:2 toluene: hexanes and cooled to -30°C to yield clear, colourless, rod-shaped crystals. Yield: 0.399g, 63 %. Mp. 127-8°C. NMR (d_6-benzene): ^{1}H δ 4.30 (m, 2H), 3.22 (m, 2H), 3.02 (m, 4H), 2.95 (m, 2H), 2.75 (m, 2H), 2.50 (m, 2H) 1.97 (m, 2H), 1.81 (m, 2H), 1.78-1.67 (m, 2H), 1.51 (m, 2H), 0.76 (m, 2H) 0.47 (s, 18H, $Si(CH_3)_3$), 0.42 (d, 2H, $ZrCHH$, $^{2}J_{HH}$ = 12.1 Hz), 0.03 (d, 2H, $ZrCHH$, $^{2}J_{HH}$ = 12.1 Hz); $^{13}C\{^{1}H\}$ δ 60.7, 60.2, 54.0, 54.0 (CH_2N), 53.1 (CH_2Si, t in the gated ^{13}C, $^{1}J_{CH}$ = 102 Hz), 51.4 (CH_2N), 22.1 ($CH_2CH_2CH_2$), 4.3 ($Si(CH_3)_3$); Anal. Calcd for $C_{20}H_{46}N_4Si_2Zr$: C, 49.02; H, 9.46; N, 11.43 %. Found: C, 48.08; H, 8.75; N, 11.67%.

(CBC)Zr(C_4Ph_4), (20)

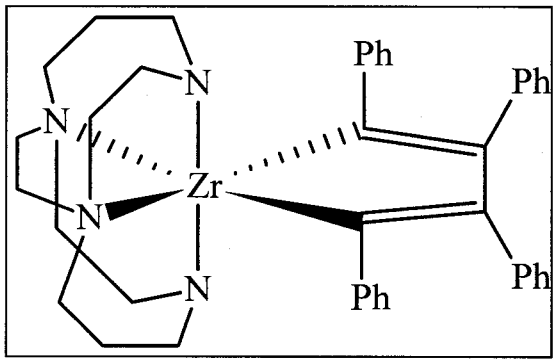

Diphenylacetylene (0.507 g, 2.84 mmol), (CBC)$ZrCl_2$ (0.500g, 1.29 mmol) and 50 mL of THF were cooled in a dry ice – acetone (-78°C) bath prior to the addition of n-BuLi (1.6M, 1.62 mL, 2.6 mmol). The mixture was stirred at low temperature for 20 minutes and transferred to an ice bath for 2 h. The solvent was removed under reduced pressure to yield a brown oil. Toluene (40 mL) was added and the suspension was filtered through Celite. The volume of the filtrate was reduced to 10 mL and the solution cooled to -30°C. The resulting yellow powder was washed twice with 4 mL hexanes and dried under reduced pressure. Yield: 0.307g, 33 %. Mp. turns red at 135-40°C, melts 169-73°C (dec) NMR (d_6-benzene): ^{1}H δ 7.22 (d, 4H, *o*-aryl*H*, $^3J_{HH}$ = 6.9 Hz), 7.15 (8H, aryl, obscured by solvent) 6.83 (m, 6H, *o*- and/or *m*-aryl*H*), 6.62 (t, 2H, *p*-aryl*H*, $^3J_{HH}$ = 7.4 Hz), 4.94 (m, 2H), 3.23-3.09 (m, 8H) 2.73 (m, 2H), 2.23 (m, 2H), 1.76-1.62 (m, 6H), 1.11 (m, 2H), 0.7 (m, 2H); ^{13}C{^{1}H} δ 203.1 (Zr*C*), 151.2 (*quat-C*), 150.0 (*quat-C*), 143.8 (*quat-C*), 128.4 (signals obscured by solvent), 127.1 (*o*- or *m*-aryl*C*), 126.7 (*o*- or *m*-aryl*C*), 124.9 (*p*-aryl*C*), 122.4 (*p*-aryl*C*), 61.3, 57.2, 53.9, 52.9, 50.3 (CH_2N), 21.8 ($CH_2CH_2CH_2$). NMR (d_8-THF): ^{1}H δ 6.96 (t, 4H, *o*- or *m*-aryl*H*, $^3J_{HH}$ = 7.7 Hz), 6.74 (m, 8H, *o*- and/or *m*-aryl*H*), 6.63 (m, 6H, *o*- and/or *m*-aryl*H* and *p*-aryl*H*), 6.53 (t, 2H, *p*-aryl*H*, $^3J_{HH}$ = 7.3 Hz), 4.80 (m, 2H), 3.62 (m, 2H) 3.52 (m, 2H), 3.24 (dd, 2H), 3.15 (m, 2H), 3.04 (m, 2H), 2.27-2.17 (m, 8H), 2.09 (m, 2H), 0.95 (m, 2H); ^{13}C{^{1}H} δ 203.5 (Zr*C*), 152.1 (*quat-C*), 149.5 (*quat-C*), 144.1 (*quat-C*), 131.0 (*o*- or *m*-aryl*C*), 128.0 (*o*- or

m-aryl*C*), 126.8 (*o*- or *m*-aryl*C*), 126.7 (*o*- or *m*-aryl*C*), 124.4 (*p*-aryl*C*), 122.1 (*p*-aryl*C*),61.9, 57.7, 54.3, 53.7, 50.6 (CH_2N), 22.4 ($CH_2CH_2CH_2$); Anal. Calcd for the toluene solvate $C_{47}H_{52}N_4Zr$: C, 73.87; H, 6.86; N, 7.33 %. Found: C, 71.09; H, 6.82; N, 7.33%. The yield improves slightly if the reaction is carried out in toluene (41%).

(CBC')Zr(C_4Ph_4H), (21)

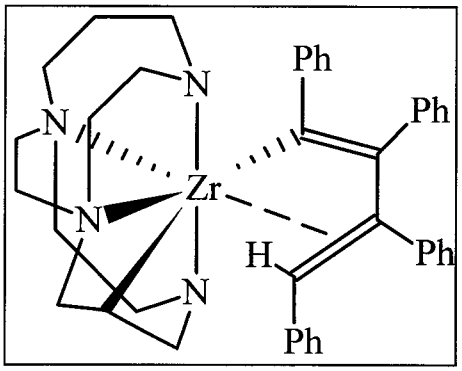

(CBC)Zr(C_4Ph_4) (0.250 g, 0.372 mmol) and 20 mL of toluene were sealed in a bomb. The solution was stirred at 50°C for 7 days and the solvent was removed under reduced pressure to yield a brown oil. This was dissolved in 3 mL toluene and layered with 1 mL hexanes and stored at low temperature. The first crop of tan solids was discarded and the solvent removed to yield a deep red material which was recrystalized from 1:1 toluene/hexanes to afford a dark red solid that displayed a clean NMR spectrum (two crops). Yield: 0.103 g, 41.0 %. Mp. 224-229°C (dec) NMR (d_6-benzene): ^{1}H δ 7.46 (br s, 1H, aryl*H*), 7.26 (br s, 5H, aryl*H*), 7.14 (br s, 2H, aryl*H*), 7.10-6.98 (m, 7H, aryl*H*), 6.78 (m, 3H, aryl*H*), 6.46 (br s, 1H, aryl*H*), 6.26 (t, 1H, *p*-aryl*H*, $^3J_{HH}$ = 7.2 Hz), 5.67 (s, 1H, C=C*H*Ph), 3.72 (dt, 1H), 3.46 (dd, 1H), 3.14 (td, 1H), 3.02-2.95 (m, 2H), 2.59 (td, 1H), 2.47 (td, 1H), 2.27 (td, 1H), 2.23-2.09 (m, 7H), 1.87 (dd, 1H), 1.75 (m, 2H), 1.65 (m, 1H), 1.4-1.3 (m, 4H); $^{13}C\{^1H\}$ δ 155.2, 145.1, 144.5, 144.4, 142.1, 138.6 (*quat*-C), 130.7, 128.6, 128.4, 128.2, 127.7, 127.1, 126.4, 125.6, 124.5 (aryl*C*H), 115.4 (*p*-aryl*C*), 77.9 (Zr*C*H, correlates with a ^{1}H resonance at 1.4-1.3 ppm)), 75.0 (quat-C), 69.4 67.7 (C=*C*HPh, correlates with a ^{1}H resonance at 5.67 ppm), 60.7, 60.4. 60.4, 59.5, 55.8, 51.5, 51.4, 51.2, 31.9, 30.7. Assignments are based on

DEPT, ^{1}H-^{1}H and ^{1}H-^{13}C COSY. Anal. Calcd for $C_{40}H_{44}N_4Zr$: C, 71.48; H, 6.60; N, 8.34 %. Found: C, 66.76; H, 6.65; N, 6.61%. A small sample of **21** in d_6-benzene was hydrolyzed with D_2O and the organic and aqueous phases separated. The ^{1}H NMR of the aqueous phase showed pure (CBC) ligand, but the integration of one resonance due to the central CH_2 of the 3-carbon bridge (0.80 ppm) was decreased substantially. The organic phase contained $C_4Ph_4H_2$ and C_4Ph_4HD by mass spectroscopy (M^+ = 358 and 359 amu, respectively).

Tetraphenylthiophene oxide, (22)

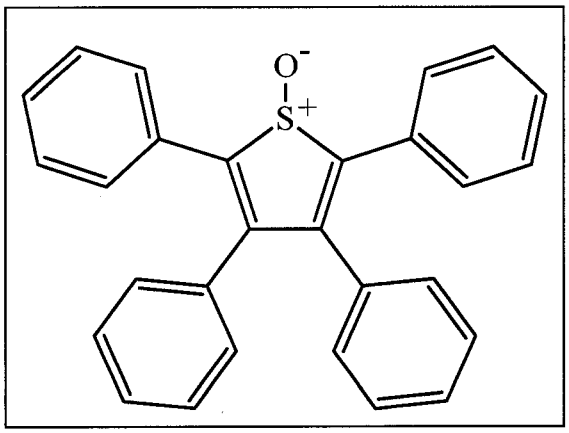

Thionyl chloride was freshly distilled from triphenylphosphite under argon and a 0.125 M solution in toluene was prepared. The solution of thionyl chloride (2.4 mL, 0.30 mmol) was added to a solution of (CBC)ZrC_4Ph_4 (0.200g, 0.298 mmol) in toluene (40 mL) which had been cooled to 0°C. The solution was stirred at low temperature for 1 hour and then at room temperature overnight. The precipitate was removed via filtration (Celite) and the solvent removed at reduced pressure to afford the crude product as a bright yellow hygroscopic oil. This was purified via column chromatography (silica gel, 1:10 THF: toluene eluant). Some fractions required further purification via preprative TLC (silica gel, 1:10 THF: toluene eluant). Yield: 0.059g, 49 %. The identity of the product was confirmed by NMR[188] ($CDCl_3$): ^{1}H δ 7.36 (m, 4H), 7.25 (m, 6H), 7.21-7.08 (m, 6H), 6.92 (m, 4H); $^{13}C\{^{1}H\}$ δ 146.2, 141.2, 133.4, 130.7,

129.9, 129.9, 128.8, 128.7, 128.4, 128.3; and high resolution MS Calcd for $C_{28}H_{20}OS$: 404.1235. Found 404.1231.

Pentaphenylphosphole, (23)

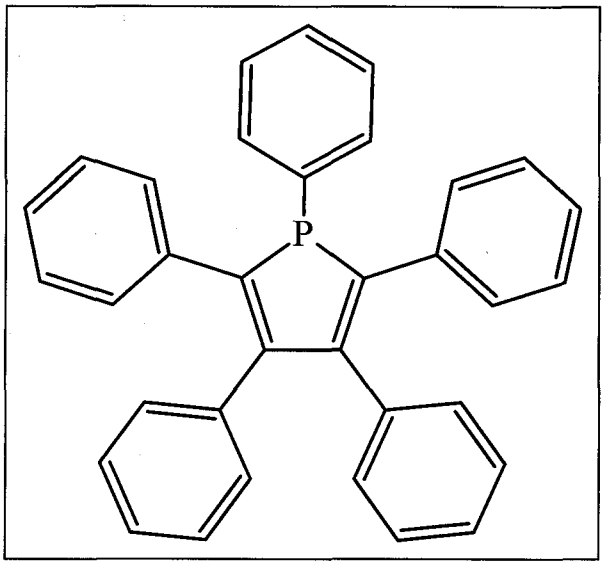

Dichlorophenylphosphine was freshly distilled under argon and a 0.125 M solution prepared in toluene. The solution of dichlorophenylphosphine (2.4 mL, 0.30 mmol) was added to a solution of $(CBC)ZrC_4Ph_4$ (0.200g, 0.298 mmol) in toluene (30 mL) at room temperature and an orange colour developed immediately. The solution was allowed to stir at room temperature overnight and the solvent was removed under reduced pressure. The product was extracted with toluene (60 mL), filtered (Celite) and the solvent removed from the filtrate to yield the crude product as a yellow powder. This was purified via column chromatography (neutral alumina, 1:3 benzene: hexanes eluant); the compound fluoresces when irradiated with short wave UV light. Yield 0.051g 34%. Mp. 238-242°C NMR ($CDCl_3$): ^1H δ 7.31 (m, 1H), 7.11 (m, 4H), 6.97-6.90 (m, 15H), 6.85 (m, 5H); $^{13}C\{^1H\}$ δ 148.4 (d, J_{CP} = 11Hz), 136.9 (d, J_{CP} = 17 Hz), 134.3, 134.0, 130.6 (d, J_{CP} = 3 Hz), 129.8, 129.7, 129.6, 128.9 (d, J_{CP} = 8Hz), 128.6, 128.1, 127.8, 126.8, 126.6; $^{31}P\{^1H\}$ δ 16.5. High resolution MS Calcd for $C_{34}H_{25}P$: 464.1694. Found 464.1694.

$\{[(\mu\text{-CBC})Yb]_3(\mu^3\text{-O})\}^+\{Yb[N(SiMe_3)_2]_3\}^-$, (24)

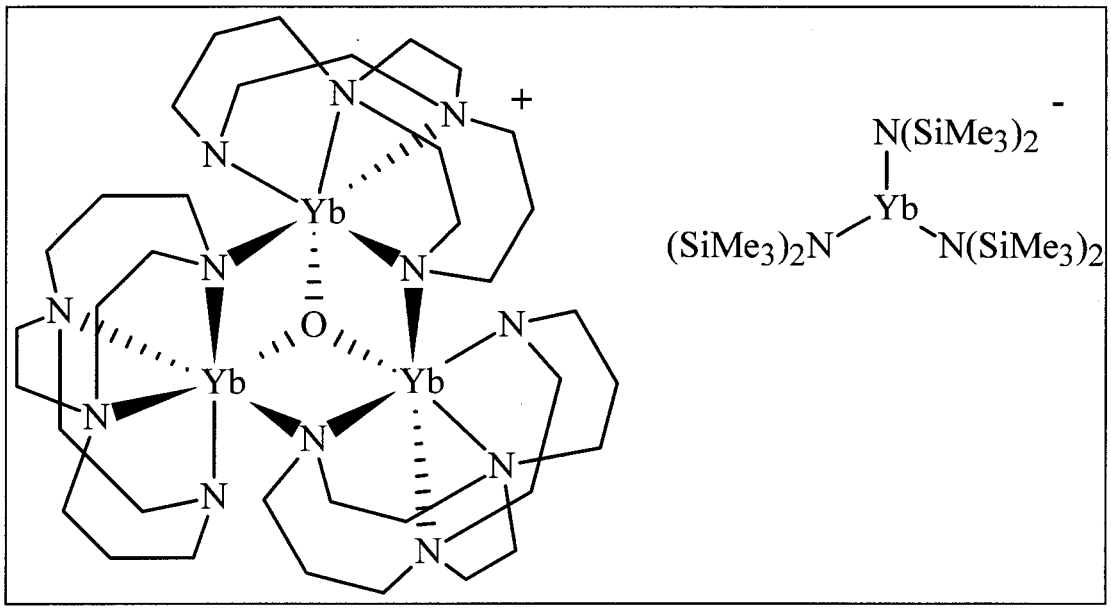

A solution of $Yb[N(SiMe_3)_2]_2THF_2$ (0.172 mmol) in toluene (2.5 mL) was added to $H_2(CBC)$ (0.050g, 0.221 mmol). After two days at room temperature a dark green crystals and a dark red powder had precipitated. The solvent was decanted and the solids washed with toluene (6mL) and hexanes (2mL). THF (3mL) was added and the resulting green solution was decanted from the red powder. The solvent was removed under reduced pressure to afford the product as a green powder. Yield 0.015 g, 4.7 % NMR (d_8-THF): (not all resonances were located, widths at half height are given) ^1H δ 98 (3H, 202 Hz), 67 (3H, 450 Hz), 65 (3H, 371 Hz), 57 (3H, 666 Hz) 13 (3H, 176 Hz), 1 (56H, $Si(CH_3)_3$, 12 Hz) -8 (3H, 205 Hz), -31 (3H, 360 Hz), -45 (3H, 166 Hz), -85 (3H, 281 Hz), -91 (3H, 133 Hz), -96 (3H, 274 Hz), -99 (3H, 220 Hz), -131 (6H, 500 Hz), -143 (3H, 137 Hz), -168 (3H, 871 Hz). Anal. Calcd for $C_{54}H_{126}N_{15}OSi_6Yb_4$: C, 34.79; H, 6.92; N, 11.27 %. Found: C, 32.81; H, 6.45; N, 11.12.

{[(μ-CBC)Yb]$_3$(μ^3-O}$^+$I$^-$, (25)

A green d_8-THF solution of [(μ-CBC)Yb]$_3$O]$^+$[N(SiMe$_3$)$_2$]$_3^-$ was stored in a sealed J. Young NMR tube, the colour gradually changed to yellow and crystals of **25** suitable for X-ray diffraction precipitated on the wall of the NMR tube.

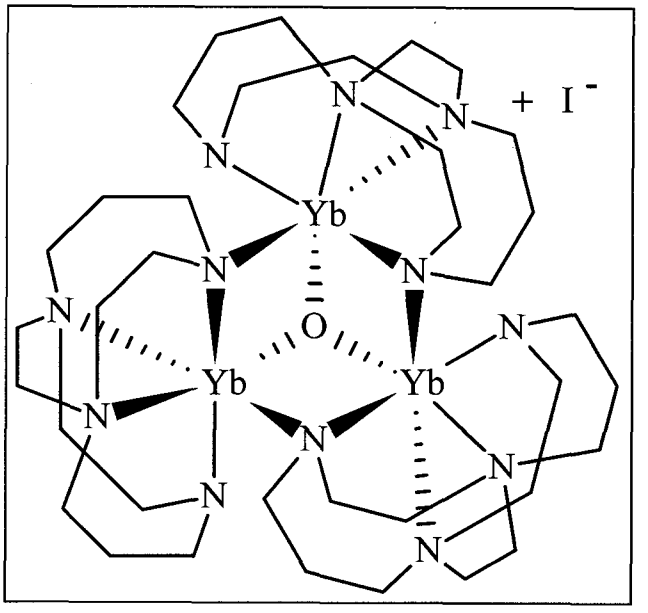

[(CBC)Yb]$_n$, (26)

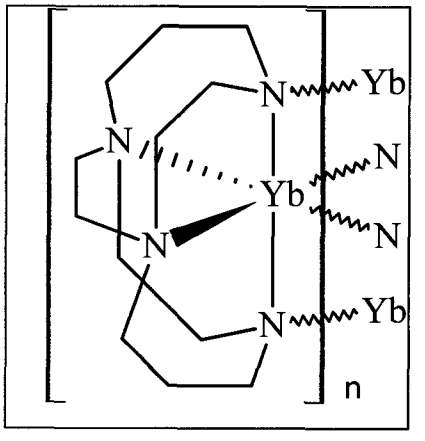

H_2CBC (0.100g, 0.442 mmol) in 2.5 mL toluene was added to a solution of freshly prepared Yb[N(SiMe$_3$)$_2$]$_2$OEt$_2$ (0.286 g, 0.435 mmol) in 2.5 mL toluene. Immediate precipitation of a purple powder occurred. The solvent was decanted and the purple precipitate was dried under reduced pressure. Yield 0.074 g, 43%. Mp > 275°C. Anal. Calcd for $C_{12}H_{24}N_4Yb$: C, 36.27; H, 6.09; N, 14.10 %. Found: C, 30.64; H, 6.10; N, 8.36%.

References

1 Kealy, T. J.; Pauson, P. L. *Nature* **1951**, *168*, 1039.

2 Pauson, P. L.; Kealy, T. J. *Journal of the Chemical Society* **1952**, 632.

3 Schumann, H.; Janiak, C. *Advances in Organometallic Chemistry* **1991**, *33*, 291.

4 Wilkinson, G.; Pauson, P. L.; Birmingham, J. M.; Cotton, F. A. *Journal of the American Chemical Society* **1953**, *75*, 1011.

5 Cardin, D. J.; Lappert, M. F.; Raston, C. L.; Riley, P. I. In *Comprehensive Organometallic Chemistry*; Pergamon: Toronto, 1982; Vol. 3.

6 Cloke, F. G. N. In *Comprehensive Organometallic Chemistry II*; Lappert, M. F., Ed.; Elsevier: Oxford, 1995; Vol. 4.

7 Binger, P.; Podubrin, S. In *Comprehensive Organometallic Chemistry II*; Lappert, M. F., Ed.; Elsevier: Oxford, 1995; Vol. 4.

8 Ryan, E. J. In *Comprehensive Organometallic Chemistry II*; Lappert, M. F., Ed.; Elsevier: Oxford, 1995; Vol. 4.

9 Ryan, E. J. In *Comprehensive Organometallic Chemistry II*; Lappert, M. F., Ed.; Elsevier: Oxford, 1995; Vol. 4.

10 Hey-Hawkins, E. In *Comprehensive Organometallic Chemistry II*; Lappert, M. F., Ed.; Elsevier: Oxford, 1995; Vol. 4.

11 Gambarotta, S.; Jubb, J.; Song, J.; Richeson, D. In *Comprehensive Organometallic Chemistry II*; Lappert, M. F., Ed.; Elsevier: Oxford, 1995; Vol. 4.

12 Guram, A. S.; Jordan, R. F. In *Comprehensive Organometallic Chemistry II*; Lappert, M. F., Ed.; Elsevier: Oxford, 1995; Vol. 4.

13 Lappert, M. F.; Power, P. P.; Sanger, A. R.; Srivastava, R. C. *Metal and Metalloid Amides*; Ellis Horwood: Toronto, 1980.

14 Cotton, F. A.; Wilkinson, G. *Advanced Inorganic Chemistry*; 4 ed.; Wiley: Toronto, 1980.

15 Shannon, R. D. *Acta Crystallographica. Section A.* **1976**, *32*, 751.

16 Kobayashi, S.; Mori, Y.; Yamashita, Y. In *Comprehensive Coordination Chemistry II*; Elsevier: San Francisco, 2004; Vol. 9.

17 Negishi, E. In *Organometallics in Synthesis*; Wiley: Etobicoke, 2002.

18 Buchwald, S. L.; Lum, R. T.; Dewan, J. C. *Journal of the American Chemical Society* **1986**, *108*, 7441.

19 Peat, A. J.; Buchwald, S. L. *Journal of the American Chemical Society* **1996**, *118*, 1028.

20 Negishi, E.; Takahashi, T. *Accounts of Chemical Reserch* **1994**, *27*, 124.

21 Nugent, W. A. *Journal of the American Chemical Society* **1994**, *116*, 1880.

22 Scollard, J. D.; McConville, D. H.; Vittal, J. *Organometallics* **1995**, *14*, 5478.

23 Tullo, A. H. *Chem. Eng. News* **2003**, *81*, 26.

24 Tullo, A. H. *Chemical and Engineering News* **2004**, *82*, 21.

25 Gavens, P. D.; Bottrill, M.; Kelland, J. W.; McMeeking In *Comprehensive Organometallic Chemistry*; Pergamon: Toronto, 1982; Vol. 3.

26 McKnight, A. L.; Waymouth, R. M. *Chemical Reviews* **1998**, *98*, 2587.

27 Rudin, A. *Polymer Science and Engineering*; 2 ed.; Academic Press: Toronto, 1999.

28 Bochmann, M. *Journal of the Chemical Society, Dalton Transactions* **1996**, 255.

29 Britovsek, G. J. P.; Gibson, V. C.; Wass, D. F. *Angewandte Chemie International Edition* **1999**, *38*, 428.

30 Coates, G. W.; Hustad, P. D.; Reinartz, S. *Angewandte Chemie International Edition* **2002**, *41*, 2236.

31 Odian, G. *Principles of Polymerization*; 3 ed.; Wiley-Interscience: Toronto, 1991.

32 Andersen, R. A. *Inorganic Chemistry* **1979**, *18*, 1724.

33 Brauer, D. J.; Burger, H.; Essig, E.; Gesschwandtner, W. *Journal of Organometallic Chemistry* **1980**, *190*, 343.

34 Horton, A. D.; de With, J. *Organometallics* **1997**, *16*, 5424.

35 Burger, H.; Gesschwandtner, W.; Liewald, G. R. *Journal of Organometallic Chemistry* **1983**, *259*, 145.

36 Gibson, V. C.; Kimberley, B. S.; White, A. J. P.; Williams, D. J.; Howard, P. *Chemical Communications* **1998**, 313.

37 Aoyagi, K.; Gantzel, P. K.; Kalai, K.; Tilley, T. D. *Organometallics* **1996**, *15*, 923.

38 Mack, H.; Eisen, M. S. *Journal of Organometallic Chemistry* **1996**, *525*, 81.

39 Male, N. A. H.; Thornton-Pett, M.; Bochmann, M. *Journal of the Chemical Society, Dalton Transactions* **1997**, 2487.

40 Lee, C. H.; La, Y.; Park, J. W. *Organometallics* **2000**, *19*, 344.

41 Scollard, J. D.; McConville, D. H. *Journal of the American Chemical Society* **1996**, *118*, 10008.

42 Scollard, J. D.; McConville, D. H.; Rettig, S. J. *Organometallics* **1997**, *16*, 1810.

43 Warren, T. H.; Schrock, R. R.; Davis, W. M. *Organometallics* **1996**, *15*, 562.

44 Warren, T. H.; Schrock, R. R.; Davis, W. M. *Organometallics* **1998**, *17*, 308.

45 Patton, J. T.; Feng, S. G.; Abboud, K. A. *Organometallics* **2001**, *20*, 3399.

46 Jager, F.; Roesky, H.; Dorn, H.; Shah, S.; Noltemeyer, M.; Schmidt, H. *Chemische Berichte / Recueil* **1997**, *130*, 399.

47 Daniele, S.; Hitchcock, P. B.; Lappert, M. F.; Merle, P. G. *Journal of the Chemical Society, Dalton Transactions* **2001**, 13.

48 Bol, J. E.; Hessen, B.; Teuben, J. H.; Smeets, W. J. J.; Spek, A. L. *Organometallics* **1992**, *11*, 1981.

49 Herrmann, W. A.; Denk, M.; Scherer, W.; Klingan, F. *Journal of Organometallic Chemistry* **1993**, *444*, C21.

50 Scollard, J. D.; McConville, D. H.; Vittal, J. *Organometallics* **1997**, *16*, 4415.

51 Ziniuk, Z.; Goldberg, I.; Kol, M. *Inorganic Chemical Communications* **1999**, *2*, 549.

52 Friedrich, S.; Gade, L. H.; Scowen, I. J.; McPartlin, M. *Organometallics* **1995**, *14*, 5344.

53 Friedrich, S.; Gade, L. H.; Scowen, I. J.; McPartlin, M. *Angewandte Chemie International Edition* **1996**, *35*, 1338.

54 Lorber, C.; Donnadieu, B.; Choukroun, R. *Organometallics* **2000**, *19*, 1963.

55 Lee, C. H.; La, Y.; Park, J. W.; Park, S. J. *Organometallics* **1998**, *17*, 3648.

56 Jeon, Y.; Heo, J.; Lee, W. M.; Chang, T.; Kim, K. *Organometallics* **1999**, *18*, 4107.

57 Shafir, A.; Power, M. P.; Whitener, G. D.; Arnold, J. *Organometallics* **2001**, *20*, 1365.

58 Gibson, V. C.; Long, N. J.; Marshall, E. L.; Oxford, P. J.; White, A. J. P.; Williams, D. J. *Journal of the Chemical Society, Dalton Transactions* **2001**, 1162.

59 Siemeling, U.; Kuhnert, O.; Neumann, B.; Stammler, A.; Stammler, H.; Bildstein, B.; Malaun, M.; Zanello, P. *European Journal of Inorganic Chemistry* **2001**, 913.

60 Mehrkhodavandi, P.; Schrock, R. R.; Pryor, L. L. *Organometallics* **2003**, *22*, 4569.

61 Guerin, F.; McConville, D. H.; Vittal, J. *Organometallics* **1997**, *16*, 1491.

62 Gade, L. H. *Chemical Communications* **2000**, 173.

63 Baumann, R.; Stumpf, R.; Davis, W. M.; Liang, L.; Schrock, R. R. *Journal of the American Chemical Society* **1999**, *121*, 7822.

64 Cloke, F. G. N.; Geldbach, T. J.; Hitchcock, P. B.; Love, J. B. *Journal of Organometallic Chemistry* **1996**, *506*, 343.

65 Jeon, Y.; Park, S. J.; Heo, J.; Kim, K. *Organometallics* **1998**, *17*, 3161.

66 Schattenmann, F. J.; Schrock, R. R.; Davis, W. M. *Organometallics* **1998**, *17*, 989.

67 Baumann, R.; Davis, W. M.; Schrock, R. R. *Journal of the American Chemical Society* **1997**, *119*, 3830.

68 Goodman, J. T.; Schrock, R. R. *Organometallics* **2001**, *20*, 5205.

69 Schrock, R. R.; Baumann, R.; Reid, S. M.; Goodman, J. T.; Stumpf, R.; Davis, W. M. *Organometallics* **1999**, *18*, 3649.

70 Baumann, R.; Schrock, R. R. *Journal of Organometallic Chemistry* **1998**, *557*, 69.

71 Schrock, R. R.; Liang, L.; Baumann, R.; Davies, W. M. *Journal of Organometallic Chemistry* **1999**, *591*, 163.

72 Liang, L.; Schrock, R. R.; Davies, W. M. *Organometallics* **2000**, *19*, 2526.

73 Graf, D. D.; Schrock, R. R.; Davis, W. M.; Stumpf, R. *Organometallics* **1999**, *18*, 843.

74 Li, Y.; Turnas, A.; Ciszewski, J. T.; Odom, A. L. *Inorganic Chemistry* **2002**, *41*, 6298.

75 Guerin, F.; McConville, D. H.; Vittal, J. *Organometallics* **1996**, *15*, 5586.

76 Guerin, F.; McConville, D. H.; Vittal, J.; Yap, G. A. P. *Organometallics* **1998**, *17*, 5172.

77 Guerin, F.; Del Vecchio, O.; McConville, D. H. *Polyhedron* **1998**, *17*, 917.

78 Schrock, R. R.; Bonitatebus Jr., P. J.; Schrodi, Y. *Organometallics* **2001**, *20*, 1056.

79 Horton, A. D.; de With, J.; van der Linden, A. J.; van de Weg, H. *Organometallics* **1996**, *15*, 2672.

80 Skinner, M. E. G.; Cowhig, D. A.; Mountford, P. *Chemical Communications* **2000**, 1167.

81 Liang, L.; Schrock, R. R.; Davis, W. M.; McConville, D. H. *Journal of the American Chemical Society* **1999**, *121*, 5797.

82 Schrock, R. R.; Casado, A. L.; Goodman, J. T.; Liang, L.; Bonitatebus Jr., P. J.; Davis, W. M. *Organometallics* **2000**, *19*, 5325.

83 Schrodi, Y.; Schrock, R. R.; Bonitatebus Jr., P. J. *Organometallics* **2001**, *20*, 3560.

84 Cloke, F. G. N.; Hitchcock, P. B.; Love, J. *Journal of the Chemical Society, Dalton Transactions* **1995**, 25.

85 Aizenberg, M.; Turculet, L.; Davis, W. M.; Schattenmann, F. J.; Schrock, R. R. *Organometallics* **1998**, *17*, 4795.

86 Schrock, R. R.; Schattenmann, F. J.; Aizenberg, M.; Davis, W. M. *Chemical Communications* **1998**, 199.

87 Schrock, R. R.; Seidel, S. W.; Schrodi, Y.; Davis, W. M. *Organometallics* **1999**, *18*, 428.

88 Flores, M. A.; Manzoni, M. R.; Baumann, R.; Davis, W. M.; Schrock, R. R. *Organometallics* **1999**, *18*, 32220.

89 Mehrkhodavandi, P.; Bonitatebus Jr., P. J.; Schrock, R. R. *Journal of the American Chemical Society* **2000**, *122*, 7841.

90 Schrock, R. R.; Adamchuk, J.; Ruhland, K.; Lopez, L. P. H. *Organometallics* **2003**, *22*, 5079.

91 Mehrkhodavandi, P.; Schrock, R. R.; Bonitatebus Jr., P. J. *Organometallics* **2002**, *21*, 5785.

92 Friedrich, S.; Schubart, M.; Gade, L. H.; Scowen, I. J.; Edwards, A. J.; McPartlin, M. *Chemische Berichte / Recueil* **1997**, *130*, 1751.

93 Fryzuk, M. D.; Love, J. B.; Rettig, S. J.; Young, V. G. *Science* **1997**, *275*, 1445.

94 Fryzuk, M. D.; Love, J.; Rettig, S. J. *Organometallics* **1998**, *17*, 846.

95 Fryzuk, M. D.; Kozak, C. M.; Mehrkhodavandi, P.; Morello, L.; Patrick, B. O.; Rettig, S. J. *Journal of the American Chemical Society* **2002**, *124*, 516.

96 Grocholl, L.; Stahl, L.; Staples, R. J. *Chemical Communications* **1997**, 1465.

97 Bai, G.; Roesky, H.; Schmidt, H.; Noltemeyer, M. *Organometallics* **2001**, *20*, 2962.

98 Grocholl, L.; Huch, V.; Stahl, L.; Staples, R. J.; Steinhart, P.; Johnson, A. *Inorganic Chemistry* **1997**, *36*, 4451.

99 Skinner, M. E. G.; Li, Y.; Mountford, P. *Inorganic Chemistry* **2002**, *41*, 1110.

100 Uhrhammer, R.; Black, D. G.; Gardner, T. G.; Olsen, J. D.; Jordon, R. F. *Journal of the American Chemical Society* **1993**, *115*, 8493.

101 Scott, M. J.; Lippard, S. J. *Organometallics* **1998**, *17*, 1769.

102 Martin, A.; Uhrhammer, R.; Gardner, T. G.; Jordan, R. F. *Organometallics* **1998**, *17*, 382.

103 Bonomo, L.; Toraman, G.; Solari, E.; Scopelliti, R.; Floriani, C. *Organometallics* **1999**, *18*, 5198.

104 Giannini, L.; Solari, E.; De Angelis, S.; Ward, T. R.; Floriani, C.; Chiesi-Villa, A.; Rizzoli, C. *Journal of the American Chemical Society* **1995**, *117*, 5801.

105 Black, D. G.; Swenson, D. C.; Jordan, R. F.; Rogers, R. D. *Organometallics* **1995**, *14*, 3539.

106 Brand, H.; Arnold, J. *Journal of the American Chemical Society* **1992**, *114*, 2266.

107 Kim, H.; Jung, S.; Jeon, Y.; Whang, D.; Kim, K. *Chemical Communications* **1999**, 1033.

108 Brand, H.; Arnold, J. *Organometallics* **1993**, *12*, 3655.

109 Kim, H.; Jung, S.; Jeon, Y.; Whang, D.; Kim, K. *Chemical Communications* **1997**, 2201.

110 Thorman, J. L.; Guzei, I. A.; Young, V. G.; Woo, L. K. *Inorganic Chemistry* **1999**, *38*, 3814.

111 Blake, A. J.; Mountford, P.; Nikonov, G. I.; Swallow, D. *Chemical Communications* **1996**, 1835.

112 Floriani, C.; Ciurli, S.; Chiesi-Villa, A.; Guastini *Angewandte Chemie International Edition* **1987**, *26*, 70.

113 De Angelis, S.; Solari, E.; Gallo, E.; Floriani, C.; Chiesi-Villa, A.; Rizzoli, C. *Inorganic Chemistry* **1992**, *31*, 2520.

114 Giannini, L.; Solari, E.; Floriani, C.; Chiesi-Villa, A.; Rizzoli, C. *Angewandte Chemie International Edition* **1994**, *33*, 2204.

115 Black, D. G.; Jordon, R. F.; Rogers, R. D. *Inorganic Chemistry* **1997**, *36*, 103.

116 Scott, M. J.; Lippard, S. J. *Organometallics* **1997**, *16*, 5857.

117 Scott, M. J.; Lippard, S. J. *Journal of the American Chemical Society* **1997**, *119*, 3411.

118 Durfee, l. D.; Rothwell, I. P. *Chemical Reviews* **1988**, *88*, 1059.

119 Scott, M. J.; Lippard, S. J. *Organometallics* **1998**, *17*, 466.

120 Lee, L. W. M. *Deprotonated Aza-Crown Ligands as Simple and Effective Alternatives to Pentamethylcyclopentadienyl in Group 3, 4, and Lanthanide Chemistry (Ph.D. Thesis)*; University of Victoria: Victoria, 1997.

121 O'Connor, P. E.; Morrison, D. J.; Steeves, S.; Burrage, K.; Berg, D. J. *Organometallics* **2001**, *20*, 1153.

122 Andersen, R. A. *Inorganic Chemistry* **1979**, *18*, 2928.

123 Pouchert, C. J.; Behnke, J. *The Aldrich Library of ^{13}C and ^{1}H FT NMR Spectra, Edition 1*; Aldrich Chemical Co., 1993.

124 Shah, S.; Dorn, H.; Voight, A.; Roesky, H.; Parisini, E.; Schmidt, H.; Noltemeyer, M. *Organometallics* **1996**, *15*, 3176.

125 Shah, S.; Dorn, H.; Roesky, H.; Parisini, E.; Schmidt, H.; Noltemeyer, M. *Journal of the Chemical Society, Dalton Transactions* **1996**, 4143.

126 Shah, S.; Dorn, H.; Gindl, J.; Noltemeyer, M.; Schmidt, H.; Roesky, H. *Journal of Organometallic Chemistry* **1998**, *550*, 1.

127 Herzog, A.; Liu, F.; Roesky, H.; Demsar, A.; Keller, K.; Noltemeyer, M.; Pauer, F. *Organometallics* **1994**, *13*, 1251.

128 Herzog, A.; Roesky, H.; Jager, F.; Steiner, A. *Chemical Communications* **1996**, 29.

129 Murphy, E. F.; Lubben, T.; Herzog, A.; Roesky, H.; Demsar, A.; Noltemeyer, M.; Schmidt, H. *Inorganic Chemistry* **1996**, *35*, 23.

130 Kraft, B. M.; Lachilotte, R. J.; Jones, W. D. *Organometallics* **2002**, *21*, 727.

131 Chen, Y.; Mertz, M. V.; Li, L.; Stern, C. L.; Marks, T. J. *Journal of the American Chemical Society* **1998**, *120*, 6287.

132 Wieistra, Y.; Gambarotta, S.; Meetsma, A.; Spek, A. L. *Organometallics* **1989**, *8*, 2948.

133 Simoes, J. A. M.; Beauchamp, J. L. *Chemical Reviews* **1990**, *90*, 629.

134 Edelbach, B. L.; Rahman, A. K. F.; Lachilotte, R. J.; Jones, W. D. *Organometallics* **1999**, *18*, 3170.

135 Kiplinger, J. L.; Richmond, T. G.; Osterburg, C. E. *Chemical Reviews* **1994**, *94*, 373.

136 Burns, C. J.; Andersen, R. A. *Chemical Communications* **1989**, 136.

137 Brenner, S.; Kempe, R.; Arndt, P. *Zeitschrift für Anorganische und Allgemeine Chemie* **1995**, *621*, 2021.

138 Hill, M. S.; Hitchcock, P. B. *Organometallics* **2002**, *21*, 3258.

139 Turculet, L.; Tilley, T. D. *Organometallics* **2002**, *21*, 3961.

140 Zhang, X.; Zhu, Q.; Guzei, I. A.; Jordon, R. F. *Journal of the American Chemical Society* **2000**, *122*, 8093.

141 Gade, L. H.; Friedrich, S.; Trosch, D. J. M.; Scowen, I. J.; McPartlin, M. *Inorganic Chemistry* **1999**, *38*, 5295.

142 Renner, P.; Galka, C.; Memmler, H.; Kauper, U.; Gade, L. H. *Journal of Organometallic Chemistry* **1999**, *591*, 71.

143 Rogers, A. J.; Solari, E.; Floriani, C.; Chiesi-Villa, A.; Corrado, R. *Journal of the Chemical Society, Dalton Transactions* **1997**, 2385.

144 Giesbrecht, G. R.; Shafir, A.; Arnold, J. *Chemical Communications* **2000**, 2135.

145 Kobriger, L. M.; McMullen, A. K.; Fanwick, P. E.; Rothwell, I. P. *Polyhedron* **1989**, *8*, 77.

146 Toupance, T.; Dubberley, S. R.; Rees, N. H.; Tyrrell, B. R.; Mountford, P. *Organometallics* **2002**, *21*, 1367.

147 Zuckerman, R. L.; Bergman, R. G. *Organometallics* **2000**, *19*, 4795.

148 Chen, C.; Rees, L. H.; Cowley, A. R.; Green, M. L. H. *Journal of the Chemical Society, Dalton Transactions* **2001**, 1761.

149 Airoldi, C.; Bradley, D. C.; Chudzynska, H.; Hursthouse, M. B.; Malik, K. M. A.; Raithby, P. R. *Journal of the Chemical Society, Dalton Transactions* **1980**, 2010.

150 Bradley, D. C.; Chudzynska, H.; Backer-Dirks, J. D. J.; Hursthouse, M. B.; Ibrahim, A. A.; Motevalli, M.; Sullivan, A. C. *Polyhedron* **1990**, *9*, 1423.

151 Tshuva, E. Y.; Goldberg, I.; Kol, M.; Weitman, H.; Goldschmidt, Z. *Chemical Communications* **2000**, 379.

152 Bouwkamp, M.; van Leusen, D.; Meetsma, A.; Hessen, B. *Organometallics* **1998**, *17*, 3645.

153 Qian, B.; Scanlon IV, W. J.; Smith III, M. R. *Organometallics* **1999**, *18*, 1693.

154 Latesky, S. L.; McMullen, A. K.; Niccolai, G. P.; Rothwell, I. P.; Huffman, J. C. *Organometallics* **1985**, *4*, 902.

155 Bochmann, M.; Lancaster, S. J. *Organometallics* **1993**, *12*, 633.

156 Bochmann, M.; Lancaster, S. J.; Hursthouse, M. B.; Malik, K. M. A. *Organometallics* **1994**, *13*, 2235.

157 Jordan, R. F.; LaPointe, R. E.; Bajgur, C. S.; Echolls, S. F.; Willet, R. *Journal of the American Chemical Society* **1987**, *109*, 4111.

158 Sandstrom, J. *Dynamic NMR Spectroscopy*; Pergamon: London, 1982.

159 Buchwald, S. L.; Wannamaker, M. W.; Watson, B. T. *Journal of the American Chemical Society* **1989**, *111*, 776.

160 Wong, E. H.; Weisman, G. R.; Hill, D. C.; Reed, D. P.; Rogers, M. E.; Condon, J. S.; Fagan, M. A.; Calabrese, J. C.; Lam, K.-C.; Guzei, I. A.; Rheingold, A. L. *Journal of the American Chemical Society* **2000**, *122*, 10561.

161 Weisman, G. R.; Rogers, M. E.; Wong, E. H.; Jasinski, J. P.; Paight, E. S. *Journal of the American Chemical Society* **1990**, *112*, 8604.

162 Hubin, T. J.; McCormick, J. M.; Collinson, S. R.; Buchalova, M.; Perkins, C. M.; Alcock, N. W.; Kahol, P. W.; Raghunathan, A.; Busch, D. H. *Journal of the American Chemical Society* **2000**, *122*, 2512.

163 Sun, X.; Wuest, M.; Weisman, G. R.; Wong, E. H.; Reed, D. P.; Boswell, C. A.; Motekaitis, R.; Martell, A. E.; Welch, M. J.; Andersen, C. J. *Journal of Medicinal Chemistry* **2002**, *45*, 469.

164 Niu, W.; Wong, E. H.; Weisman, G. R.; Sommer, R. D.; Rheingold, A. L. *Inorganic Chemical Communications* **2002**, *5*, 1.

165 Beshouri, S. M.; Chebi, D. E.; Fanwick, P. E.; Rothwell, I. P. *Organometallics* **1990**, *9*, 2375.

166 Schaverien, C. J.; Orpen, A. G. *Inorganic Chemistry* **1991**, *30*, 4968.

167 Negishi, E.; Cederbaum, F. E.; Takahashi, T. *Tetrahedron Letters* **1986**, *27*, 2829.

168 Kresinski, R. A.; Isam, L.; Hamor, T. A.; Jones, C. J.; McCleverty, J. A. *Journal of the Chemical Society, Dalton Transactions* **1991**, 1835.

169 Benetollo, F.; Cavinato, G.; Crosara, L.; Milani, F.; Rossetto, G.; Scelza, C.; Zanella, P. *Journal of Organometallic Chemistry* **1998**, *555*, 177.

170 Antinolo, A.; Carrillo-Hermosilla, F.; Corrochano, A.; Fernandez-Baeza, J.; Lara-Sanchez, A.; Ribeiro, M. R.; Lanfranchi, M.; Otero, A.; Pellinghelli, M. A.; Portela, M. F.; Santos, J. V. *Organometallics* **2000**, *19*, 2837.

171 Cohen, J. D.; Fryzuk, M. D.; Loehr, T. M.; Mylvaganam, M.; Rettig, S. J. *Inorganic Chemistry* **1998**, *37*, 112.

172 Schweder, B.; Gorls, H.; Walther, D. *Inorganica Chimica Acta* **1999**, *286*, 14.

173 Ciruelo, G.; Cuenca, T.; Gomez, R.; Gomez-Sal, P.; Martin, A. *Journal of the Chemical Society, Dalton Transactions* **2001**, 1657.

174 Jeffery, J.; Lappert, M. F.; Luong-Thi, N. T.; Webb, M.; Atwood, J. L.; Hunter, W. E. *Journal of the Chemical Society, Dalton Transactions* **1981**, 1593.

175 Cayias, J. Z.; Babaian, E. A.; Hrncir, D. C.; Bott, S. G.; Atwood, J. L. *Journal of the Chemical Society, Dalton Transactions* **1986**, 2743.

176 Okuda, J.; Schattenmann, F. J.; Wocadlo, S.; Massa, W. *Organometallics* **1995**, *14*, 789.

177 Dias, H. V. R.; Wang, Z. *Journal of Organometallic Chemistry* **1997**, *539*, 77.

178 Scott, M. J.; Lippard, S. J. *Inorganica Chimica Acta* **1997**, *263*, 287.

179 Gentil, S.; Pirio, N.; Meunier, P.; Gallucci, J. C.; Schloss, J. D.; Paquette, L. A. *Organometallics* **2000**, *19*, 4169.

180 Buzin, F.; Nief, F.; Ricard, L.; Mathey, F. *Organometallics* **2002**, *21*, 259.

181 Hagadorn, J. R.; Arnold, J. *Organometallics* **1994**, *13*, 4670.

182 Hay, C.; Hissler, M.; Fischmeister, C.; Rault-Berthelot, J.; Toupet, L.; Nyulaszi, L.; Reau, R. *Chemistry - A European Journal* **2001**, *7*, 4222.

183 Hunter, W. E.; Atwood, J. L. *Journal of Organometallic Chemistry* **1981**, *204*, 67.

184 Metzler, N.; Noth, H.; Thomann, M. *Organometallics* **1993**, *12*, 2423.

185 Erker, G.; Zwettler, R.; Kruger, C.; Hyla-Kryspin, I.; Gleiter, R. *Organometallics* **1990**, *9*, 524.

186 Wieistra, Y.; Gambarotta, S.; Meetama, A.; de Boer, J. L. *Organometallics* **1989**, *8*, 2696.

187 Scholtz, J.; Nolte, M.; Kruger, C. *Chemische Berichte / Recueil* **1993**, *126*, 803.

188 Meier-Brocks, F.; Weiss, E. *Journal of Organometallic Chemistry* **1993**, *453*, 33.

189 Eisch, J. J.; Galle, J. E.; Kozima, S. *Journal of the American Chemical Society* **1986**, *108*, 379.

190 Leavitt, F. C.; Johnson, M. F.; Matternas, L. U.; Lehman, D. S. *Journal of the American Chemical Society* **1960**, *82*, 5099.

191 Charrier, C.; Guilhem, J.; Mathey, F. *Journal of Organic Chemistry* **1981**, *46*, 3.

192 Piers, W. E. *Coordination Chemistry Reviews* **2002**, *233-234*, 131.

193 Brand, H.; Arnold, J. *Coordination Chemistry Reviews* **1995**, *140*, 137.

194 Edelmann, F. T.; Freckmann, D. M. M.; Schumann, H. *Chemical Reviews* **2002**, *102*, 1851.

195 Lee, L. W. M.; Berg, D. J.; Bushnell, G. W. *Inorganic Chemistry* **1994**, *33*, 5302.

196 Lee, L. W. M.; Berg, D. J.; Bushnell, G. W. *Organometallics* **1995**, *14*, 8.

197 Lee, L. W. M.; Berg, D. J.; Bushnell, G. W. *Organometallics* **1995**, *14*, 5021.

198 Click, D. R.; Scott, B. L.; Watkin, J. G. *Chemical Communications* **1999**, 633.

199 Niemeyer, M. *Zeitschrift für Anorganische und Allgemeine Chemie* **2002**, *628*, 647.

200 Schumann, H.; Lee, P. R.; Loebel, J. *Angewandte Chemie International Edition* **1989**, *28*, 1033.

201 Karl, M.; Neumuller, B.; Seybert, G.; Massa, W.; Dehnicke, K. *Zeitschrift für Anorganische und Allgemeine Chemie* **1997**, *623*, 1203.

202 Hammel, A.; Weidlein, J. *Journal of Organometallic Chemistry* **1990**, *388*, 75.

203 Hartwig, J. F. *Angewandte Chemie International Edition* **1998**, *37*, 2047.

204 Kulstad, S.; Malmsten, L. A. *Acta Chemica Scandinavica. Series B.* **1979**, *33B*, 469.

205 Zucchini, U.; Albizatti, E.; Giannini, U. *Journal of Organometallic Chemistry* **1971**, *26*, 357.

206 Andersen, R. A. *Journal of the Chemical Society, Dalton Transactions* **1980**, 2010.

207 Berry, D. E.; Girard, S.; McAuley, A. *Journal of Chemical Education* **1996**, *73*, 551.

208 Barefield, E. K.; Wagner, F.; Herlinger, A. W.; Dahl, A. R.; Holt, S. *Inorganic Synthesis* **1976**, *16*, 223.

Appendix: X-Ray Crystallographic Data

List of Figures in Appendix.

List of Tables in Appendix.

The crystal structures presented in this thesis were solved by Dr. David Berg (**4**) Dr.Tosha Barclay (**5, 6**) and Dr. Bendan Twamley (**11, 14, 15, 19, 20, 24, 25**).

Crystals of **4** were loaded into glass capillaries in the glovebox and transferred to a Nonius CAD4F diffractometer equipped with Cu Kα radiation. The unit cell was refined using 25 reflections int the 2θ range 59-64°. Experimental densities were not determined. The standard reflections for 4 decayed to 59.9% of their original intensity so a decay correction was applied. Intensity measurements were collected for one-fourth of the sphere. Following data reduction (NRCVAX), the structures were solved using the Patterson or direct methods (SIR97) options in teXsan98. The toluene of solvation in **4** lies on a special position, so that the methyl group is disordered about the 2_1 screw axis. The methyl group was successfully modeled with half occupancy over both sites.

Crystals of **5** and **6** were placed under mineral oil and sealed in a glass capillary under argon. Data was collected on a Siemens Smart 1000 CCD diffractometer equipped with graphite-monochromated Mo Kα radiation (λ = 0.71073 Å) at 293 K. Structure solutions were carried out using SHELXS-97, and refinement was done on F^2. An absorption correction was applied in both cases (abs range: **5** 0.74-1.00; **6** 0.72-1.00). The final Fourier difference maps showed maximum and minimum peaks of -0.50/+0.29 (**5**) and -0.33/+0.33 (**6**) e Å-3. Thermal ellipsoid plots were drawn with ORTEP3.

For compounds **11, 14, 15, 19, 20, 24** and **25** the crystals were removed from the flask and covered with a layer of hydrocarbon oil. A suitable crystal was selected, attached to a glass fiber and placed in a low-temperature nitrogen stream. Data was collected using a Bruker/Siemens SMART APEX instrument (Mo Kα radiation, λ = 0.71073 Å) equipped with a Cryocool NeverIce low temperature device. Data were

measured using omega scans of 0.3° per frame for 30 seconds, and a full sphere of data was collected. A total of 2132 frames were collected with a final resolution of 0.75 Å for **13**, 0.77 Å for **11**, **14**, **19**, **20, 25** and 0.71 Å for **24**. The first 50 frames were recollected at the end of data collection to monitor for decay. Cell parameters were retrieved using SMART software and refined using SAINTPlus on all observed reflections. Data reduction and correction for Lp and decay were performed using the SAINTPlus software. Absorption corrections were applied using SADABS. The structures were solved by direct methods and refined by the least squares method on F^2 using the SHELXTL program package.

For compound **11**, the structure was solved solved in the space group P2(1)/n (#14) by analysis of systematic absences. All atoms were refined anisotropically. The toluene of solvation was refined as a rigid group at half occupancy using coordinates abtained from the Cambridge Database. The $(CH_3)_3CNC(H)C(H)Ph$ group was disordered and modeled with occupancies of 76 and 24% for the major and minor component. The thermal parameters were held equal for each individual moiety and bond lengths were loosely restrained. The $(CH_3)_3C$ group also displayed disorder in one of the methyl positions and this was modeled at half occupancy and the thermal parameters loosely constrained to be approximately equal and isotropic. No decomposition was observed during data collection.

For compound **14**, the structure The structure was solved in the space group C2/c (# 15) by analysis of systematic absences. All atoms were refined anisotropically. Hydrogen atom bonded to Si1 and Si2 were located on the difference map and freely refined. No decomposition was observed during data collection.

For compound **15**, the structure was solved in the space group *Pcc2* (# 116) by analysis of systematic absences. The compound was refined as a pseudo-merohedral twin using the twin law 0 1 0 1 0 0 0 0 -1. Although the absences suggest a higher symmetry, i.e. the tetragonal space group *P-4c2*, refinement using this solution clearly leads to a twinned structure with a higher R value. All atoms were refined anisotropically. No decomposition was observed during data collection.

For compound **19**, the structure was solved in the space group *C2/c* (#15) by analysis of systematic absences. All atoms were refined anisotropically. No decomposition was observed during data collection.

For compound **20**, the structure was solved in the space group *C2/c* (# 15) by analysis of systematic absences. There is a half occupied toluene molecule in the asymmetric unit that is disordered over the inversion center. All atoms were refined anisotropically. No decomposition was observed during data collection.

For compound **24**, the structure was solved in the space group P2(1)/n (# 14) by analysis of systematic absences. There is disorder in two of the cyclam rings at C7 and C19. C18 was also disordered. The counter ion also shows disorder in one $SiMe_3$ group (Si2 C40-C42) as well as the central Yb position. The occupancies of all these disordered sites were refined and then set at 50%. There are large residuals of ca. 3 e/Å^3 near Yb4/Yb4'. All atoms were refined anisotropically. No decomposition was observed during data collection.

For compound **25**, The structure was solved in the space group P2(1)/c (# 14) by analysis of systematic absences. There is disorder present in two of the cyclam rings around the central Yb trimer. The occupancy of the disordered atoms in these rings was

refined as 60% for the major fraction. One of the THF molecules is also completely disordered. This was modeled with occupancies of 60%, also for the major fraction. Disordered atoms were held isotropic and all other atoms were refined anisotropically. The thermal parameters of each disordered moiety were constrained to be approximately equal. Large residuals of ca. 2.2 e.Å^{-3}are located ca. 1 Å from the Yb centers. These are due to absorption effects and could not be modeled or eliminated. No decomposition was observed during data collection. All structural plots were drawn with ORTEP3.

Figure I. ORTEP3 Drawing of 4.

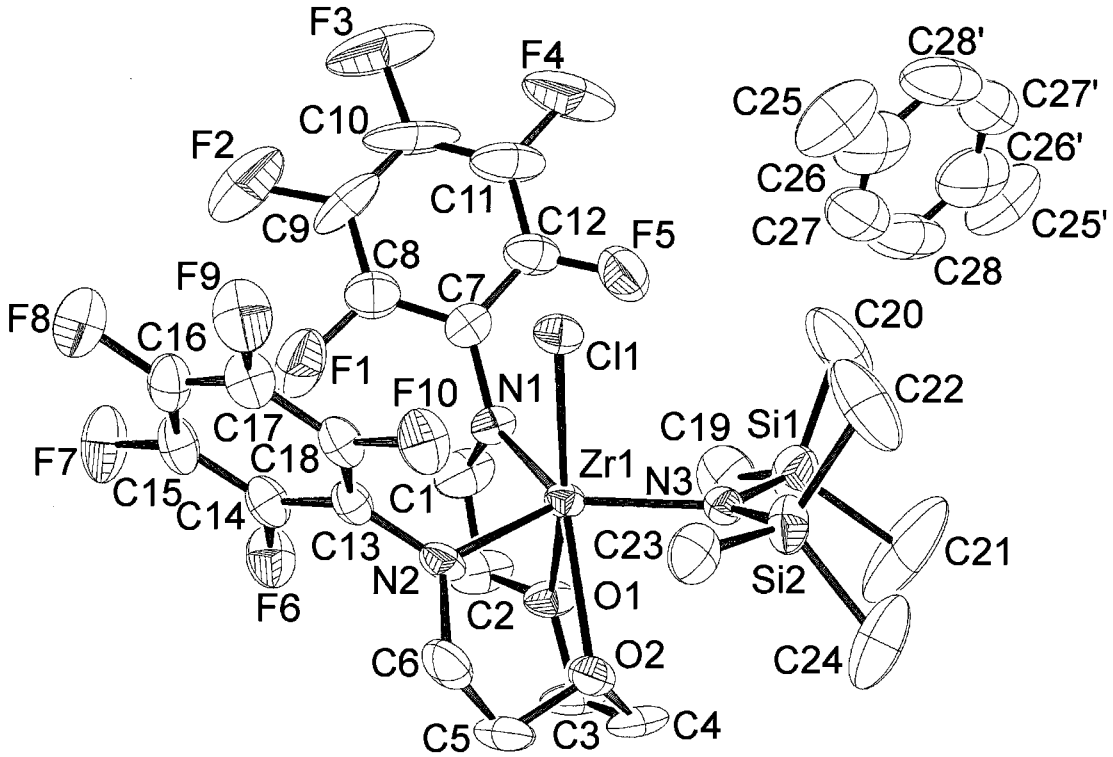

Table I. Atomic Coordinates and Biso/Beq for 4.

atom	x	y	z	Beq	occ
Zr(1)	0.03877(2)	0.20001(1)	0.30251(2)	3.489(7)	
Cl(1)	-0.08467(6)	0.16453(4)	0.15758(5)	4.51(2)	
Si(1)	0.25741(10)	0.22739(6)	0.21352(10)	7.16(4)	
Si(2)	0.08269(9)	0.33439(6)	0.17689(8)	5.99(3)	
F(1)	-0.0922(2)	0.00094(12)	0.3641(2)	9.87(9)	
F(2)	-0.1715(2)	-0.1088(2)	0.2637(3)	15.14(13)	
F(3)	-0.1020(3)	-0.1407(1)	0.1113(2)	17.49(13)	
F(4)	0.0521(3)	-0.0601(2)	0.0627(2)	15.11(13)	
F(5)	0.1300(2)	0.05188(13)	0.1654(2)	9.07(9)	
F(6)	-0.1154(2)	0.11636(11)	0.4818(1)	6.96(7)	
F(7)	-0.2895(2)	0.03316(11)	0.4550(2)	8.25(7)	
F(8)	-0.4557(2)	0.05598(11)	0.3122(2)	7.85(7)	
F(9)	-0.4489(2)	0.16391(12)	0.1929(1)	7.64(7)	
F(10)	-0.2766(1)	0.24739(10)	0.21846(13)	6.19(6)	
O(1)	0.1696(2)	0.18252(11)	0.4342(1)	5.16(7)	
O(2)	0.0766(2)	0.30134(12)	0.3984(1)	4.76(6)	
N(1)	0.0639(2)	0.09088(13)	0.3256(2)	4.10(7)	
N(2)	-0.0931(2)	0.22505(13)	0.3617(2)	4.28(7)	
N(3)	0.1357(2)	0.25862(12)	0.2335(2)	3.89(7)	
C(1)	0.1313(3)	0.0623(2)	0.4102(3)	7.73(13)	
C(2)	0.1725(4)	0.1154(2)	0.4762(3)	8.09(13)	
C(3)	0.2169(3)	0.2381(2)	0.4952(3)	7.82(13)	
C(4)	0.1862(3)	0.3060(2)	0.4446(3)	6.59(12)	
C(5)	0.0085(4)	0.3124(2)	0.4605(3)	7.38(13)	
C(6)	-0.1014(3)	0.2916(2)	0.4074(3)	6.53(12)	
C(7)	0.0207(3)	0.0337(2)	0.2661(3)	4.71(11)	
C(8)	-0.0564(4)	-0.0113(3)	0.2859(3)	6.8(2)	
C(9)	-0.0950(4)	-0.0674(3)	0.2335(5)	10.0(2)	
C(10)	-0.0598(7)	-0.0837(3)	0.1599(5)	12.2(3)	
C(11)	0.0167(5)	-0.0409(3)	0.1357(4)	9.5(2)	
C(12)	0.0567(4)	0.0137(2)	0.1909(3)	6.5(1)	
C(13)	-0.1874(3)	0.1830(2)	0.3483(2)	4.01(10)	
C(14)	-0.1963(3)	0.1293(2)	0.4083(3)	4.89(11)	
C(15)	-0.2847(3)	0.0864(2)	0.3977(3)	5.41(12)	
C(16)	-0.3700(3)	0.0985(2)	0.3236(3)	5.66(12)	
C(17)	-0.3658(3)	0.1511(2)	0.2643(3)	5.28(12)	
C(18)	-0.2762(3)	0.1935(2)	0.2776(2)	4.41(10)	
C(19)	0.3171(3)	0.1562(2)	0.2919(3)	9.4(2)	
C(20)	0.2386(4)	0.1900(3)	0.0974(3)	14.3(2)	
C(21)	0.3586(3)	0.2985(3)	0.2214(6)	21.6(3)	
C(22)	0.0596(4)	0.3264(3)	0.0490(3)	12.9(2)	

C(23)	-0.0520(3)	0.3570(2)	0.1981(3)	6.36(11)	
C(24)	0.1648(3)	0.4160(2)	0.2146(4)	11.8(2)	
C(25)	0.3079(10)	0.0081(9)	-0.026(3)	14.5(7)	1/2
C(26)	0.396(2)	0.0034(6)	-0.007(2)	15.6(5)	
C(27)	0.436(3)	-0.0061(10)	-0.087(2)	19.5(9)	
C(28)	0.538(3)	-0.0065(9)	-0.074(2)	16.8(8)	
H(1)	0.1898	0.0379	0.3951	9.276	
H(2)	0.0899	0.0301	0.4366	9.276	
H(3)	0.2446	0.1042	0.5053	9.708	
H(4)	0.1306	0.1168	0.5211	9.708	
H(5)	0.2927	0.2331	0.5110	9.380	
H(6)	0.1902	0.2370	0.5496	9.380	
H(7)	0.2290	0.3130	0.4011	7.903	
H(8)	0.1964	0.3444	0.4869	7.903	
H(9)	0.0096	0.3608	0.4784	8.851	
H(10)	0.0303	0.2836	0.5137	8.851	
H(11)	-0.1289	0.3270	0.3629	7.835	
H(12)	-0.1479	0.2865	0.4483	7.835	
H(13)	0.2833	0.1125	0.2708	11.301	
H(14)	0.3915	0.1530	0.2936	11.301	
H(15)	0.3074	0.1660	0.3520	11.301	
H(16)	0.2158	0.1422	0.0978	17.146	
H(17)	0.3044	0.1919	0.0784	17.146	
H(18)	0.1858	0.2166	0.0558	17.146	
H(19)	0.4183	0.2811	0.2003	25.920	
H(20)	0.3279	0.3374	0.1843	25.920	
H(21)	0.3816	0.3134	0.2836	25.920	
H(22)	-0.0076	0.3043	0.0253	15.436	
H(23)	0.1150	0.2988	0.0339	15.436	
H(24)	0.0595	0.3723	0.0227	15.436	
H(25)	-0.1031	0.3227	0.1692	7.635	
H(26)	-0.0481	0.3572	0.2625	7.635	
H(27)	-0.0733	0.4025	0.1734	7.635	
H(28)	0.1729	0.4226	0.2790	14.106	
H(29)	0.1297	0.4560	0.1826	14.106	
H(30)	0.2334	0.4108	0.2012	14.106	
H(31)	0.2784	-0.0112	0.0219	17.389	1/2
H(32)	0.2884	0.0566	-0.0342	17.389	1/2
H(33)	0.2809	-0.0171	-0.0813	17.389	1/2
H(34)	0.3670	-0.0083	-0.1424	14.1(15)	
H(35)	0.5487	-0.0197	-0.1444	20.6(14)	

$B_{eq} = 8/3\ \pi^2(U_{11}(aa^*)^2 + U_{22}(bb^*)^2 + U_{33}(cc^*)^2 + 2U_{12}(aa^*bb^*)\cos\gamma +$

$2U_{13}(aa^*cc^*)\cos\beta + 2U_{23}(bb^*cc^*)\cos\alpha)$

Table II. Non-Hydrogen Bond Lengths (Å) for 4.

atom	atom	distance	atom	atom	distance
ZR1	CL1	2.461(2)	ZR1	O1	2.296(4)
ZR1	O2	2.372(5)	ZR1	N1	2.102(5)
ZR1	N2	2.131(5)	ZR1	N3	2.100(5)
SI1	N3	1.755(5)	SI1	C19	1.831(9)
SI1	C20	1.834(10)	SI1	C21	1.852(9)
SI2	N3	1.720(5)	SI2	C22	1.869(9)
SI2	C23	1.874(7)	SI2	C24	1.879(8)
F1	C8	1.367(9)	F2	C9	1.405(12)
F3	C10	1.340(12)	F4	C11	1.321(13)
F5	C12	1.308(9)	F6	C14	1.347(7)
F7	C15	1.331(7)	F8	C16	1.340(8)
F9	C17	1.345(7)	F10	C18	1.346(7)
O1	C2	1.411(8)	O1	C3	1.430(7)
O2	C4	1.419(8)	O2	C5	1.425(8)
N1	C1	1.459(8)	N1	C7	1.427(8)
N2	C6	1.445(8)	N2	C13	1.421(8)
C1	C2	1.420(9)	C3	C4	1.494(10)
C5	C6	1.502(10)	C7	C8	1.387(10)
C7	C12	1.359(10)	C8	C9	1.342(12)
C9	C10	1.32(2)	C10	C11	1.38(2)
C11	C12	1.347(12)	C13	C14	1.373(8)
C13	C18	1.378(8)	C14	C15	1.372(9)
C15	C16	1.385(9)	C16	C17	1.339(9)
C17	C18	1.377(9)	C25	C26	1.10(4)
C26	C27	1.42(5)	C26	C28	1.30(5)
C27	C28	1.28(6)			

Table III. Bond Angles (deg) for the Non-Hydrogen Atoms of 4.

atom	atom	atom	angle	atom	atom	atom	angle
CL1	ZR1	O1	155.34(12)	CL1	ZR1	O2	138.67(12)
CL1	ZR1	N1	85.5(2)	CL1	ZR1	N2	90.7(2)
CL1	ZR1	N3	92.7(1)	O1	ZR1	O2	65.9(2)
O1	ZR1	N1	70.4(2)	O1	ZR1	N2	99.8(2)
O1	ZR1	N3	95.5(2)	O2	ZR1	N1	133.6(2)
O2	ZR1	N2	69.1(2)	O2	ZR1	N3	78.9(2)
N1	ZR1	N2	104.8(2)	N1	ZR1	N3	120.8(2)
N2	ZR1	N3	134.4(2)	N3	SI1	C19	113.3(3)
N3	SI1	C20	111.1(4)	N3	SI1	C21	112.5(4)
C19	SI1	C20	105.4(4)	C19	SI1	C21	107.9(5)
C20	SI1	C21	106.1(6)	N3	SI2	C22	112.8(4)
N3	SI2	C23	112.5(3)	N3	SI2	C24	113.8(3)
C22	SI2	C23	104.7(4)	C22	SI2	C24	108.6(5)
C23	SI2	C24	103.7(4)	ZR1	O1	C2	116.7(4)
ZR1	O1	C3	124.0(4)	C2	O1	C3	114.3(6)
ZR1	O2	C4	112.7(4)	ZR1	O2	C5	116.1(4)
C4	O2	C5	111.2(6)	ZR1	N1	C1	122.9(5)
ZR1	N1	C7	128.0(4)	C1	N1	C7	109.1(6)
ZR1	N2	C6	122.6(5)	ZR1	N2	C13	123.1(4)
C6	N2	C13	113.6(6)	ZR1	N3	SI1	123.7(3)
ZR1	N3	SI2	117.9(3)	SI1	N3	SI2	117.5(3)
N1	C1	C2	113.0(7)	O1	C2	C1	111.0(7)
O1	C3	C4	106.5(6)	O2	C4	C3	108.0(7)
O2	C5	C6	105.0(6)	N2	C6	C5	108.3(7)
N1	C7	C8	121.7(8)	N1	C7	C12	124.6(8)
C8	C7	C12	113.5(9)	F1	C8	C7	118.2(9)
F1	C8	C9	118.7(12)	C7	C8	C9	123.1(11)
F2	C9	C8	116.3(14)	F2	C9	C10	122.4(13)
C8	C9	C10	121.3(13)	F3	C10	C9	117.7(18)
F3	C10	C11	123.4(16)	C9	C10	C11	118.9(13)
F4	C11	C10	117.0(12)	F4	C11	C12	124.0(14)
C10	C11	C12	118.7(13)	F5	C12	C7	119.3(9)
F5	C12	C11	116.2(11)	C7	C12	C11	124.4(11)
N2	C13	C14	121.1(7)	N2	C13	C18	123.6(7)
C14	C13	C18	115.3(7)	F6	C14	C13	120.0(8)
F6	C14	C15	116.6(7)	C13	C14	C15	123.4(8)
F7	C15	C14	122.1(8)	F7	C15	C16	119.6(8)
C14	C15	C16	118.4(8)	F8	C16	C15	118.5(8)
F8	C16	C17	121.1(9)	C15	C16	C17	120.4(8)
F9	C17	C16	120.8(8)	F9	C17	C18	119.5(8)
C16	C17	C18	119.6(8)	F10	C18	C13	119.3(7)

F10	C18	C17	117.9(7)	C13	C18	C17	122.8(7)
C25	C26	C27	109.5(81)	C25	C26	C28	130.5(88)
C27	C26	C28	119.9(30)	C26	C27	C28	115.1(58)
C26	C28	C27	124.8(60)				

Table IV. Anisotropic Displacement Parameters ($Å^2$ x 10^3) for 4.

	U_{11}	U_{22}	U_{33}	U_{12}	U_{13}	U_{23}
Zr(1)	0.0539(2)	0.0385(2)	0.0395(2)	0.0048(2)	0.00951(13)	-0.0015(2)
Cl(1)	0.0628(6)	0.0561(5)	0.0475(6)	0.0074(4)	0.0026(5)	-0.0036(5)
Si(1)	0.0798(9)	0.0765(9)	0.1313(12)	-0.0049(7)	0.0562(9)	-0.0128(8)
Si(2)	0.0722(8)	0.0826(8)	0.0744(9)	-0.0085(7)	0.0200(7)	0.0246(7)
F(1)	0.121(2)	0.086(2)	0.180(3)	-0.018(2)	0.058(2)	0.015(2)
F(2)	0.162(3)	0.108(2)	0.292(5)	-0.057(2)	0.024(3)	-0.015(3)
F(3)	0.280(4)	0.084(2)	0.229(4)	-0.013(2)	-0.091(3)	-0.057(2)
F(4)	0.337(5)	0.133(3)	0.095(2)	0.059(3)	0.030(3)	-0.043(2)
F(5)	0.166(3)	0.098(2)	0.101(2)	-0.002(2)	0.073(2)	-0.006(2)
F(6)	0.083(2)	0.108(2)	0.071(2)	0.0064(13)	0.0130(13)	0.034(1)
F(7)	0.094(2)	0.100(2)	0.125(2)	0.006(1)	0.036(2)	0.069(2)
F(8)	0.074(2)	0.099(2)	0.127(2)	-0.006(1)	0.026(1)	0.019(2)
F(9)	0.067(2)	0.128(2)	0.091(2)	0.017(1)	0.0103(13)	0.034(2)
F(10)	0.082(2)	0.080(2)	0.076(2)	0.0212(12)	0.0232(12)	0.0327(12)
O(1)	0.085(2)	0.053(2)	0.045(2)	0.0068(13)	-0.0105(13)	-0.0009(13)
O(2)	0.076(2)	0.058(1)	0.048(2)	0.002(2)	0.0155(13)	-0.006(1)
N(1)	0.056(2)	0.041(2)	0.053(2)	0.006(1)	-0.002(2)	0.004(2)
N(2)	0.074(2)	0.047(2)	0.047(2)	0.014(2)	0.025(2)	-0.008(2)
N(3)	0.053(2)	0.051(2)	0.043(2)	-0.001(1)	0.010(1)	-0.001(1)
C(1)	0.116(4)	0.072(3)	0.084(4)	-0.001(3)	-0.022(3)	0.016(3)
C(2)	0.166(4)	0.052(3)	0.065(3)	-0.001(3)	-0.025(3)	0.013(2)
C(3)	0.138(4)	0.070(3)	0.062(3)	0.009(3)	-0.033(3)	-0.027(3)
C(4)	0.100(3)	0.065(3)	0.071(3)	-0.014(3)	-0.010(3)	-0.034(3)
C(5)	0.136(4)	0.080(3)	0.067(3)	-0.013(3)	0.030(3)	-0.039(3)
C(6)	0.120(4)	0.064(3)	0.082(3)	0.012(3)	0.062(3)	-0.010(3)
C(7)	0.053(3)	0.053(3)	0.067(3)	0.008(2)	0.000(2)	0.007(2)
C(8)	0.095(4)	0.073(3)	0.090(4)	0.007(3)	0.016(3)	-0.009(3)
C(9)	0.097(4)	0.053(4)	0.209(8)	-0.036(3)	-0.005(5)	-0.008(4)
C(10)	0.243(10)	0.054(4)	0.116(6)	0.035(5)	-0.060(6)	-0.052(4)
C(11)	0.204(7)	0.053(4)	0.080(4)	0.017(4)	-0.014(4)	-0.016(3)
C(12)	0.119(4)	0.056(3)	0.067(4)	0.012(3)	0.012(3)	-0.007(3)
C(13)	0.061(2)	0.046(2)	0.051(2)	0.013(2)	0.025(2)	0.005(2)
C(14)	0.063(3)	0.076(3)	0.050(3)	0.018(2)	0.018(2)	0.017(2)
C(15)	0.074(3)	0.069(3)	0.072(3)	0.018(2)	0.036(3)	0.027(3)

C(16)	0.061(3)	0.072(3)	0.091(4)	0.004(2)	0.036(3)	0.007(3)
C(17)	0.060(3)	0.074(3)	0.067(3)	0.018(2)	0.015(2)	0.018(2)
C(18)	0.064(2)	0.054(2)	0.056(3)	0.023(2)	0.026(2)	0.012(2)
C(19)	0.072(3)	0.145(4)	0.149(5)	0.031(3)	0.042(3)	-0.002(4)
C(20)	0.283(7)	0.168(5)	0.141(5)	0.063(5)	0.151(5)	0.007(4)
C(21)	0.079(3)	0.131(5)	0.649(13)	-0.039(4)	0.164(6)	-0.056(7)
C(22)	0.148(4)	0.273(7)	0.075(4)	0.069(4)	0.041(3)	0.074(4)
C(23)	0.086(3)	0.071(3)	0.079(3)	0.001(2)	0.007(2)	0.026(3)
C(24)	0.094(3)	0.090(4)	0.254(6)	-0.008(3)	0.020(4)	0.076(4)
C(25)	0.135(12)	0.075(8)	0.30(3)	0.019(10)	-0.03(2)	0.025(11)
C(26)	0.30(2)	0.087(5)	0.180(13)	-0.006(10)	-0.01(2)	0.018(8)
C(27)	0.52(5)	0.087(6)	0.100(12)	-0.05(2)	0.00(2)	-0.004(6)
C(28)	0.45(4)	0.070(5)	0.13(2)	-0.05(2)	0.10(3)	-0.010(8)

The general temperature factor expression: $\exp(-2\pi^2(a^{*2}U_{11}h^2 + b^{*2}U_{22}k^2 + c^{*2}U_{33}l^2 + 2a^*b^*U_{12}hk + 2a^*c^*U_{13}hl + 2b^*c^*U_{23}kl))$

Figure II. ORTEP3 Drawing of 5.

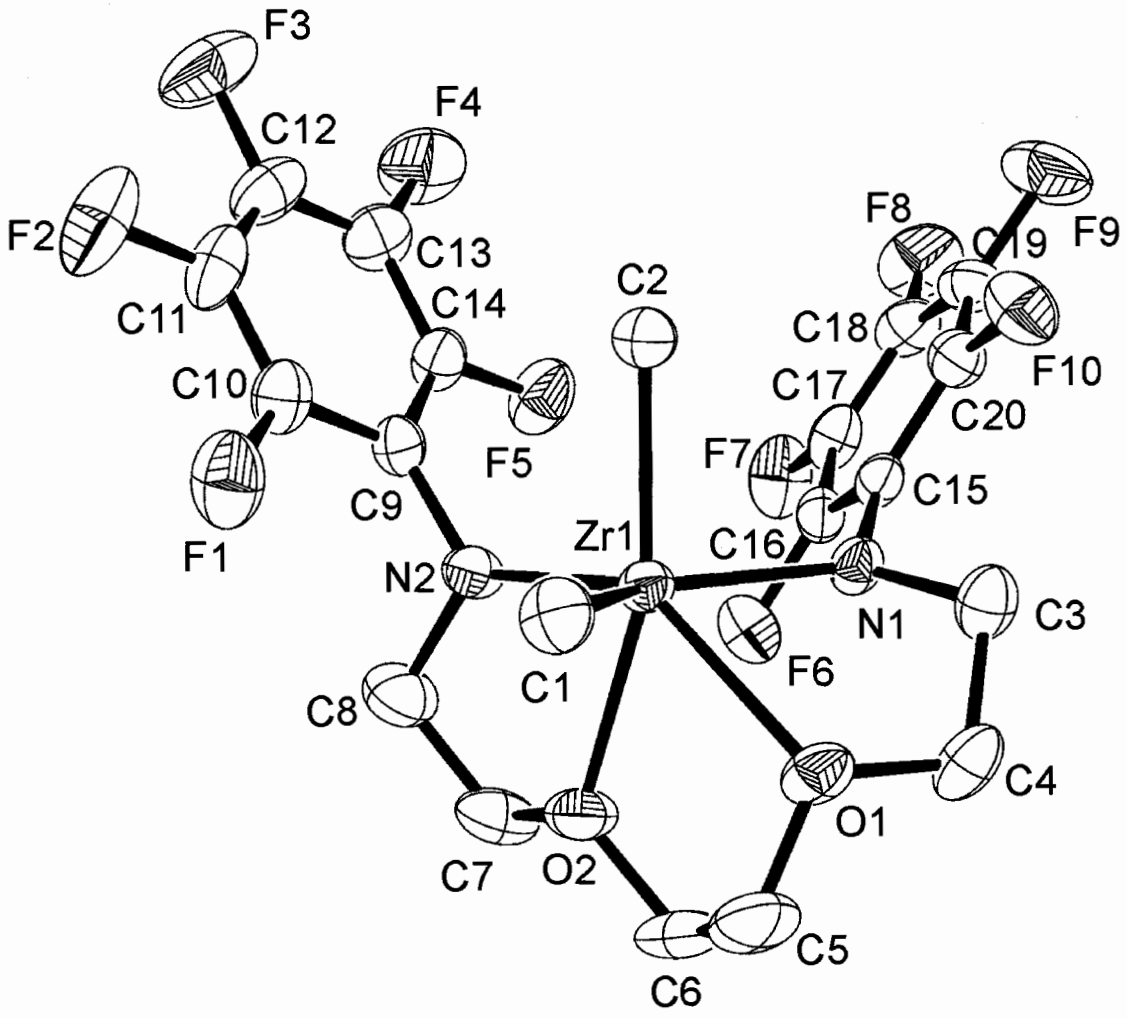

Table V. Atomic Coordinates (x 10^4) and Equivalent Isotropic Displacement Parameters ($Å^2$ x 10^3) for 5.

	x	y	z	U_{eq}
Zr(1)	7392(1)	8122(1)	6557(1)	44(1)
O(1)	9443(3)	6374(2)	6032(2)	62(1)
O(2)	9591(3)	8368(3)	7081(2)	68(1)
N(1)	6744(3)	6321(3)	7407(2)	48(1)
N(2)	6925(3)	9752(3)	7441(2)	53(1)
F(1)	6694(3)	11860(2)	5947(2)	97(1)
F(2)	4021(4)	13421(3)	6002(2)	119(1)
F(3)	1422(3)	13060(3)	7600(2)	126(1)
F(4)	1548(3)	11131(3)	9158(2)	116(1)
F(5)	4206(3)	9562(2)	9107(2)	89(1)
F(6)	6677(2)	7196(2)	9317(2)	72(1)
F(7)	4174(3)	7168(2)	10972(2)	88(1)
F(8)	1581(3)	6136(3)	10887(2)	107(1)
F(9)	1541(3)	5137(3)	9082(2)	108(1)
F(10)	3984(3)	5258(2)	7380(2)	80(1)
C(1)	8426(4)	8728(4)	4829(3)	68(1)
C(2)	4939(4)	8502(4)	6335(3)	63(1)
C(3)	7335(4)	5156(4)	6821(3)	65(1)
C(4)	9091(4)	5099(4)	6538(3)	70(1)
C(5)	10953(4)	6688(5)	6051(4)	94(2)
C(6)	10814(4)	7312(5)	7037(4)	96(2)
C(7)	9372(4)	9177(5)	7912(4)	85(1)
C(8)	8123(5)	10258(5)	7809(4)	87(1)
C(9)	5559(4)	10641(3)	7512(3)	51(1)
C(10)	5438(5)	11664(4)	6755(3)	64(1)
C(11)	4066(6)	12469(4)	6777(3)	78(1)
C(12)	2773(6)	12287(5)	7583(4)	82(1)
C(13)	2828(5)	11317(4)	8363(3)	73(1)
C(14)	4200(4)	10520(4)	8328(3)	60(1)
C(15)	5442(4)	6230(3)	8265(3)	45(1)
C(16)	5404(4)	6708(3)	9219(3)	50(1)
C(17)	4117(5)	6692(4)	10075(3)	58(1)
C(18)	2823(4)	6169(4)	10046(3)	66(1)
C(19)	2807(4)	5662(4)	9143(3)	66(1)
C(20)	4076(4)	5715(4)	8273(3)	56(1)

U_{eq} is defined as one third of the trace of the orthogonalized U_{ij} tensor.

Table VI. Bond Lengths (Å) and Angles (deg) for 5.

Bond Lengths

Zr(1)-N(2)	2.103(3)
Zr(1)-N(1)	2.133(3)
Zr(1)-C(2)	2.251(3)
Zr(1)-C(1)	2.256(3)
Zr(1)-O(2)	2.296(2)
Zr(1)-O(1)	2.411(2)
O(1)-C(5)	1.432(5)
O(1)-C(4)	1.448(4)
O(2)-C(7)	1.415(5)
O(2)-C(6)	1.430(4)
N(1)-C(15)	1.385(4)
N(1)-C(3)	1.473(4)
N(2)-C(9)	1.409(4)
N(2)-C(8)	1.463(5)
F(1)-C(10)	1.336(4)
F(2)-C(11)	1.339(4)
F(3)-C(12)	1.346(4)
F(4)-C(13)	1.339(4)
F(5)-C(14)	1.343(4)
F(6)-C(16)	1.344(4)
F(7)-C(17)	1.349(4)
F(8)-C(18)	1.335(4)
F(9)-C(19)	1.342(4)
F(10)-C(20)	1.346(4)
C(3)-C(4)	1.496(5)
C(5)-C(6)	1.486(6)
C(7)-C(8)	1.489(5)
C(9)-C(10)	1.383(5)
C(9)-C(14)	1.390(5)
C(10)-C(11)	1.376(5)
C(11)-C(12)	1.353(6)
C(12)-C(13)	1.357(6)
C(13)-C(14)	1.370(5)
C(15)-C(20)	1.390(5)
C(15)-C(16)	1.394(4)
C(16)-C(17)	1.371(5)
C(17)-C(18)	1.350(5)
C(18)-C(19)	1.360(5)
C(19)-C(20)	1.374(5)

C(5)-O(1)-C(4)	113.8(3)
C(5)-O(1)-Zr(1)	112.2(2)
C(4)-O(1)-Zr(1)	115.16(18)
C(7)-O(2)-C(6)	115.5(3)
C(7)-O(2)-Zr(1)	116.6(2)
C(6)-O(2)-Zr(1)	119.6(3)
C(15)-N(1)-C(3)	117.0(3)
C(15)-N(1)-Zr(1)	123.3(2)
C(3)-N(1)-Zr(1)	115.7(2)
C(9)-N(2)-C(8)	112.3(3)
C(9)-N(2)-Zr(1)	122.7(2)
C(8)-N(2)-Zr(1)	123.3(2)
N(1)-C(3)-C(4)	105.6(3)
O(1)-C(4)-C(3)	105.3(3)
O(1)-C(5)-C(6)	109.8(3)
O(2)-C(6)-C(5)	106.4(3)
O(2)-C(7)-C(8)	108.5(3)
N(2)-C(8)-C(7)	108.6(4)
C(10)-C(9)-C(14)	114.7(3)
C(10)-C(9)-N(2)	122.9(3)
C(14)-C(9)-N(2)	122.4(3)
F(1)-C(10)-C(11)	18.2(4)
F(1)-C(10)-C(9)	18.7(3)
C(11)-C(10)-C(9)	23.0(4)
F(2)-C(11)-C(12)	120.7(4)
F(2)-C(11)-C(10)	119.8(4)
C(12)-C(11)-C(10)	119.5(4)
F(3)-C(12)-C(11)	119.7(4)
F(3)-C(12)-C(13)	120.0(5)
C(11)-C(12)-C(13)	20.3(4)
F(4)-C(13)-C(12)	20.4(4)
F(4)-C(13)-C(14)	20.1(4)
C(12)-C(13)-C(14)	19.5(4)
F(5)-C(14)-C(13)	17.9(3)
F(5)-C(14)-C(9)	119.1(3)
C(13)-C(14)-C(9)	23.0(4)
N(1)-C(15)-C(20)	25.5(3)
N(1)-C(15)-C(16)	20.5(3)
C(20)-C(15)-C(16)	14.0(3)
F(6)-C(16)-C(17)	18.0(3)
F(6)-C(16)-C(15)	119.4(3)
C(17)-C(16)-C(15)	22.6(3)

Bond Angles			
		F(7)-C(17)-C(18)	119.7(4)
		F(7)-C(17)-C(16)	19.1(4)
N(2)-Zr(1)-N(1)	116.66(10)	C(18)-C(17)-C(16)	121.1(4)
N(2)-Zr(1)-C(2)	89.48(12)	F(8)-C(18)-C(17)	21.0(4)
N(1)-Zr(1)-C(2)	87.34(12)	F(8)-C(18)-C(19)	0.2(4)
N(2)-Zr(1)-C(1)	09.73(13)	C(17)-C(18)-C(19)	18.8(3)
N(1)-Zr(1)-C(1)	33.56(13)	F(9)-C(19)-C(18)	120.6(4)
C(2)-Zr(1)-C(1)	91.03(13)	F(9)-C(19)-C(20)	19.3(4)
N(2)-Zr(1)-O(2)	70.82(10)	C(18)-C(19)-C(20)	20.1(4)
N(1)-Zr(1)-O(2)	01.74(10)	F(10)-C(20)-C(19)	18.3(4)
C(2)-Zr(1)-O(2)	60.30(12)	F(10)-C(20)-C(15)	8.4(3)
C(1)-Zr(1)-O(2)	95.05(12)	C(19)-C(20)-C(15)	3.3(4)
N(2)-Zr(1)-O(1)	139.54(10)	C(1)-Zr(1)-O(1)	77.59(11)
N(1)-Zr(1)-O(1)	69.05(9)	O(2)-Zr(1)-O(1)	68.88(10)
C(2)-Zr(1)-O(1)	130.81(12)		

Table VII. Anisotropic Displacement Parameters ($Å^2$ x 10^3) for 5.

	U11	U22	U33	U23	U13	U12
Zr(1)	39(1)	46(1)	46(1)	-2(1)	-9(1)	-3(1)
O(1)	48(2)	67(2)	57(2)	0(1)	2(1)	8(1)
O(2)	43(2)	81(2)	83(2)	-11(2)	-22(1)	-3(1)
N(1)	46(2)	41(2)	49(2)	-5(1)	-1(1)	0(1)
N(2)	43(2)	59(2)	58(2)	-10(2)	-14(1)	-7(1)
F(1)	120(2)	81(2)	72(2)	10(1)	-1(2)	-19(2)
F(2)	198(3)	69(2)	88(2)	-3(2)	-57(2)	29(2)
F(3)	120(2)	118(2)	139(2)	-46(2)	-58(2)	64(2)
F(4)	71(2)	127(3)	124(2)	-26(2)	11(2)	13(2)
F(5)	85(2)	72(2)	83(2)	14(1)	7(1)	4(1)
F(6)	79(2)	74(2)	67(1)	-8(1)	-18(1)	-26(1)
F(7)	120(2)	76(2)	57(1)	-16(1)	1(1)	-8(1)
F(8)	73(2)	129(2)	86(2)	12(2)	22(1)	-1(2)
F(9)	66(2)	143(3)	118(2)	26(2)	-24(1)	-49(2)
F(10)	88(2)	90(2)	74(2)	-6(1)	-28(1)	-30(1)
C(1)	73(3)	71(3)	56(2)	6(2)	-14(2)	-10(2)
C(2)	57(2)	59(3)	78(3)	-11(2)	-25(2)	-3(2)
C(3)	75(3)	54(3)	58(2)	-10(2)	-3(2)	0(2)
C(4)	76(3)	59(3)	57(2)	-7(2)	0(2)	20(2)
C(5)	42(3)	108(4)	113(4)	-12(3)	3(2)	14(2)
C(6)	41(2)	114(4)	138(4)	-16(3)	-37(3)	11(2)
C(7)	58(3)	115(4)	95(3)	-20(3)	-34(2)	-19(3)
C(8)	71(3)	90(4)	114(4)	-33(3)	-34(3)	-14(3)

C(9)	57(2)	44(2)	54(2)	-9(2)	-14(2)	-8(2)
C(10)	80(3)	53(3)	54(2)	-9(2)	-9(2)	-5(2)
C(11)	125(4)	48(3)	64(3)	-10(2)	-37(3)	10(3)
C(12)	88(3)	74(3)	86(3)	-28(3)	-35(3)	29(3)
C(13)	64(3)	72(3)	74(3)	-21(2)	-2(2)	6(2)
C(14)	64(3)	48(2)	64(2)	-4(2)	-11(2)	-1(2)
C(15)	46(2)	36(2)	48(2)	1(2)	-10(2)	0(2)
C(16)	52(2)	39(2)	55(2)	-2(2)	-12(2)	-6(2)
C(17)	75(3)	47(2)	41(2)	-5(2)	-3(2)	6(2)
C(18)	48(2)	71(3)	60(3)	9(2)	6(2)	1(2)
C(19)	45(2)	74(3)	73(3)	14(2)	-13(2)	-12(2)
C(20)	59(2)	54(2)	55(2)	1(2)	-17(2)	-8(2)

The anisotropic displacement factor exponent takes the form:

$-2\pi^2[h^2 a^{*2} U_{11} + \ldots + 2 h k a^* U_{12}]$

Table VIII. Hydrogen Coordinates (x 10^4) and Isotropic Displacement Parameters ($Å^2$ x 10^3) for 5.

	x	y	z	U(eq)
H(1A)	7875	9538	4633	102
H(1B)	8326	8073	4404	102
H(1C)	9519	8830	4716	102
H(2A)	4783	7857	5921	95
H(2B)	4799	9350	5975	95
H(2C)	4188	8461	7015	95
H(3A)	6960	5228	6186	78
H(3B)	6988	4381	7259	78
H(4A)	9477	4910	7169	84
H(4B)	9570	4431	6058	84
H(5A)	11355	7277	5438	113
H(5B)	11686	5903	6023	113
H(6A)	10548	6693	7652	116
H(6B)	11799	7629	7017	116
H(7A)	10347	9525	7870	101
H(7B)	9062	8678	8592	101
H(8A)	7652	10609	8488	105
H(8B)	8574	10951	7306	105

Figure III. ORTEP3 Drawing of 6.

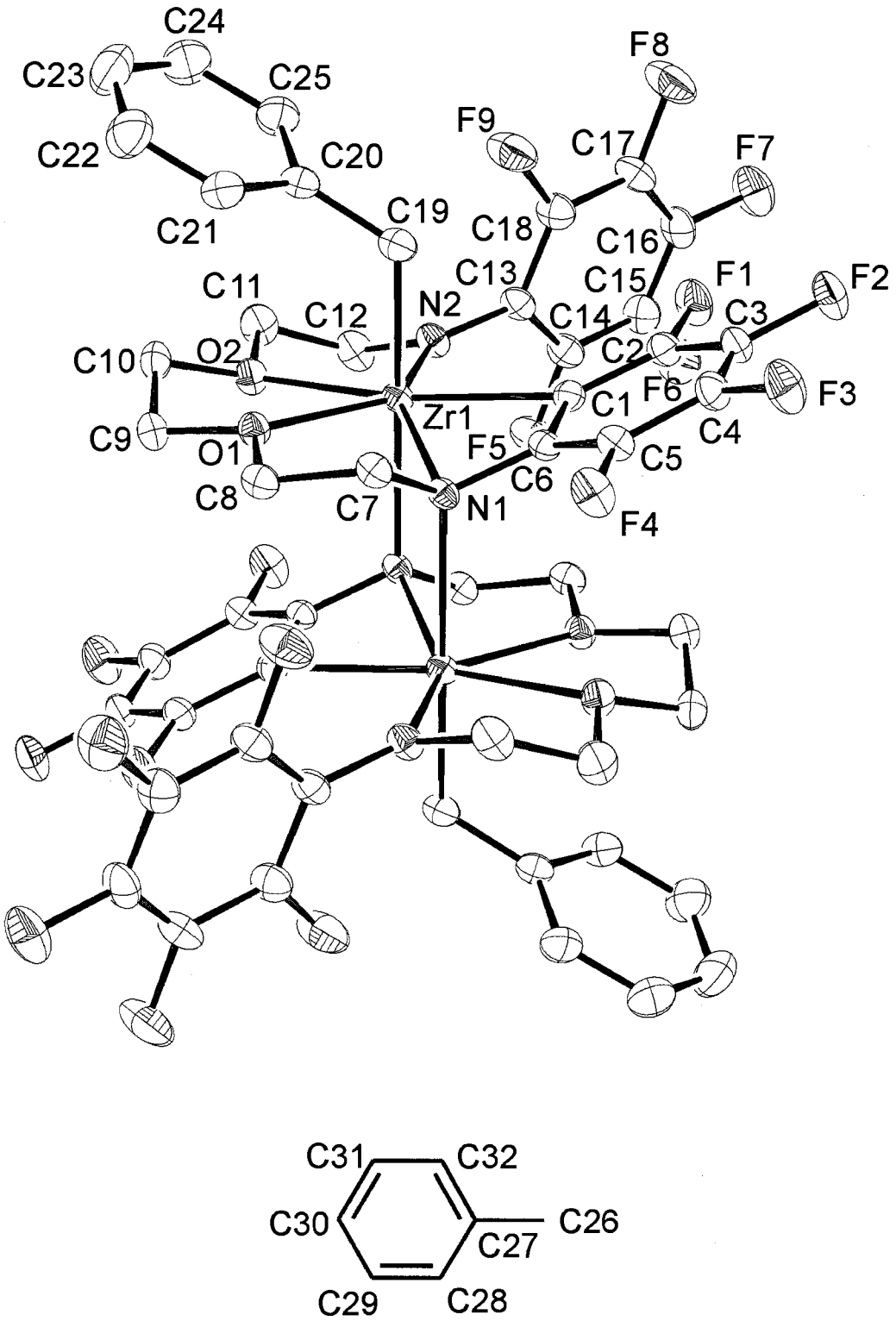

Table IX. Atomic Coordinates (x 10^4) and Equivalent Isotropic Displacement Parameters (Å x 10^3) for 6.

	x	y	z	U_{eq}
Zr(1)	5356(1)	9878(1)	8771(1)	33(1)
O(1)	4028(2)	11687(2)	8853(1)	38(1)
O(2)	6619(2)	11491(2)	7929(1)	44(1)
N(1)	3456(2)	9727(2)	10006(1)	33(1)
N(2)	7405(2)	9162(2)	8023(2)	41(1)
F(1)	5546(2)	6125(1)	8811(1)	63(1)
F(2)	3111(2)	4864(2)	9568(1)	67(1)
F(3)	745(2)	5945(2)	10551(1)	70(1)
F(4)	829(2)	8282(2)	10827(1)	57(1)
F(5)	9873(2)	8003(2)	8737(1)	67(1)
F(6)	10972(2)	5828(2)	8346(1)	77(1)
F(7)	9640(2)	4546(2)	7292(2)	88(1)
F(8)	7306(2)	5577(2)	6557(2)	91(1)
F(9)	6245(2)	7789(2)	6886(1)	80(1)
C(1)	4529(3)	7945(2)	9400(2)	35(1)
C(2)	4426(3)	6731(2)	9308(2)	42(1)
C(3)	3182(3)	6049(2)	9686(2)	46(1)
C(4)	1982(3)	6586(3)	10187(2)	46(1)
C(5)	2040(3)	7789(2)	10316(2)	39(1)
C(6)	3292(3)	8468(2)	9934(2)	33(1)
C(7)	2143(3)	10522(2)	9843(2)	38(1)
C(8)	2679(3)	11794(2)	9521(2)	41(1)
C(9)	4651(3)	12842(2)	8462(2)	44(1)
C(10)	5808(3)	12601(2)	7668(2)	49(1)
C(11)	7887(3)	11205(3)	7268(2)	57(1)
C(12)	8590(3)	10069(3)	7656(2)	55(1)
C(13)	7951(3)	7982(3)	7863(2)	42(1)
C(14)	9179(3)	7416(3)	8203(2)	48(1)
C(15)	9765(3)	6297(3)	8010(2)	54(1)
C(16)	9120(4)	5664(3)	7473(2)	57(1)
C(17)	7933(4)	6183(3)	7108(2)	58(1)
C(18)	7382(3)	7314(3)	7291(2)	52(1)
C(19)	3688(3)	9581(3)	7828(2)	46(1)
C(20)	3541(3)	10537(3)	7075(2)	45(1)
C(21)	2451(3)	11475(3)	7152(2)	53(1)
C(22)	2361(4)	12382(3)	6469(3)	78(1)
C(23)	3359(5)	12396(4)	5681(3)	92(1)
C(24)	4451(5)	11488(4)	5583(2)	82(1)
C(25)	4539(4)	10573(3)	6266(2)	61(1)

C(26)	6395(7)	4217(7)	3594(5)	211(4)
C(27)	7455(6)	3506(7)	4025(4)	131(2)
C(28)	7829(9)	2282(8)	3823(5)	154(4)
C(29)	8856(11)	1641(9)	4284(6)	184(5)
C(30)	9521(9)	2068(9)	4837(5)	173(3)
C(31)	9135(9)	3244(7)	5020(4)	139(2)
C(32)	8134(7)	3955(5)	4631(4)	120(2)

U_{eq} is defined as one third of the trace of the orthogonalized U_{ij} tensor.

Table X. Bond Distances (Å) and Angles (deg) for 6.

Bond Lengths

Zr(1)-N(2)	2.163(2)
Zr(1)-O(2)	2.285(2)
Zr(1)-O(1)	2.286(2)
Zr(1)-N(1)	2.308(2)
Zr(1)-C(19)	2.314(3)
Zr(1)-C(1)	2.326(3)
Zr(1)-N(1)[1]	2.401(2)
O(1)-C(9)	1.434(3)
O(1)-C(8)	1.452(3)
O(2)-C(11)	1.437(3)
O(2)-C(10)	1.446(3)
N(1)-C(6)	1.423(3)
N(1)-C(7)	1.478(3)
N(2)-C(13)	1.406(3)
N(2)-C(12)	1.482(3)
F(1)-C(2)	1.355(3)
F(2)-C(3)	1.348(3)
F(3)-C(4)	1.343(3)
F(4)-C(5)	1.358(3)
F(5)-C(14)	1.348(3)
F(6)-C(15)	1.338(3)
F(7)-C(16)	1.343(3)
F(8)-C(17)	1.346(3)
F(9)-C(18)	1.341(3)
C(1)-C(2)	1.373(4)
C(1)-C(6)	1.405(3)
C(2)-C(3)	1.376(4)
C(3)-C(4)	1.366(4)
C(4)-C(5)	1.370(4)
C(5)-C(6)	1.381(3)
C(7)-C(8)	1.501(4)
C(9)-C(10)	1.495(4)
C(11)-C(12)	1.485(4)
C(13)-C(18)	1.384(4)
C(13)-C(14)	1.393(4)
C(14)-C(15)	1.367(4)
C(15)-C(16)	1.356(4)
C(16)-C(17)	1.362(4)
C(17)-C(18)	1.365(4)
C(19)-C(20)	1.482(4)
C(20)-C(25)	1.392(4)
C(20)-C(21)	1.395(4)
C(21)-C(22)	1.366(4)
C(22)-C(23)	1.368(5)
C(23)-C(24)	1.374(5)
C(24)-C(25)	1.372(5)
C(26)-C(27)	1.409(8)
C(27)-C(32)	1.347(7)
C(27)-C(28)	1.435(9)
C(28)-C(29)	1.377(11)
C(29)-C(30)	1.262(10)
C(30)-C(31)	1.378(9)
C(31)-C(32)	1.338(7)

Bond Angles

N(2)-Zr(1)-O(2)	72.40(7)

N(2)-Zr(1)-O(1)	138.92(7)	F(3)-C(4)-C(5)	119.8(3)
O(2)-Zr(1)-O(1)	66.89(6)	C(3)-C(4)-C(5)	119.7(3)
N(2)-Zr(1)-N(1)	150.29(8)	F(4)-C(5)-C(4)	117.7(2)
O(2)-Zr(1)-N(1)	133.18(7)	F(4)-C(5)-C(6)	121.7(2)
O(1)-Zr(1)-N(1)	69.70(7)	C(4)-C(5)-C(6)	120.6(2)
N(2)-Zr(1)-C(19)	99.30(9)	C(5)-C(6)-C(1)	120.9(2)
O(2)-Zr(1)-C(19)	98.44(9)	C(5)-C(6)-N(1)	125.2(2)
O(1)-Zr(1)-C(19)	81.81(8)	C(1)-C(6)-N(1)	113.8(2)
N(1)-Zr(1)-C(19)	91.93(9)	N(1)-C(7)-C(8)	108.8(2)
N(2)-Zr(1)-C(1)	93.08(9)	O(1)-C(8)-C(7)	106.9(2)
O(2)-Zr(1)-C(1)	165.23(8)	O(1)-C(9)-C(10)	106.9(2)
O(1)-Zr(1)-C(1)	127.20(8)	O(2)-C(10)-C(9)	106.7(2)
N(1)-Zr(1)-C(1)	61.51(8)	O(2)-C(11)-C(12)	105.8(2)
C(19)-Zr(1)-C(1)	80.89(9)	N(2)-C(12)-C(11)	109.6(2)
N(2)-Zr(1)-N(1)^{1}	94.10(7)	C(18)-C(13)-C(14)	113.8(3)
O(2)-Zr(1)-N(1)^{1}	88.34(7)	C(18)-C(13)-N(2)	122.4(3)
O(1)-Zr(1)-N(1)^{1}	90.02(6)	C(14)-C(13)-N(2)	123.6(2)
N(1)-Zr(1)-N(1)^{1}	74.85(7)	F(5)-C(14)-C(15)	117.0(3)
C(19)-Zr(1)-N(1)^{1}	166.28(8)	F(5)-C(14)-C(13)	119.2(3)
C(1)-Zr(1)-N(1)^{1}	95.56(8)	C(15)-C(14)-C(13)	123.8(3)
C(9)-O(1)-C(8)	113.4(2)	F(6)-C(15)-C(16)	120.1(3)
C(9)-O(1)-Zr(1)	123.2(2)	F(6)-C(15)-C(14)	120.2(3)
C(8)-O(1)-Zr(1)	121.03(14)	C(16)-C(15)-C(14)	119.7(3)
C(11)-O(2)-C(10)	113.5(2)	F(7)-C(16)-C(15)	121.2(3)
C(11)-O(2)-Zr(1)	116.8(2)	F(7)-C(16)-C(17)	119.8(3)
C(10)-O(2)-Zr(1)	120.5(2)	C(15)-C(16)-C(17)	119.0(3)
C(7)-N(1)-Zr(1)	111.2(2)	F(8)-C(17)-C(16)	119.6(3)
C(7)-N(1)-Zr(1)^{1}	116.3(2)	F(8)-C(17)-C(18)	119.8(3)
Zr(1)-N(1)-Zr(1)^{1}	105.15(7)	C(16)-C(17)-C(18)	120.6(3)
Zr(1)-N(1)-C(6)	90.8(2)	F(9)-C(18)-C(17)	117.5(3)
C(6)-N(1)-C(7)	115.0(2)	F(9)-C(18)-C(13)	119.4(3)
C(6)-N(1)-Zr(1)^{1}	114.8(2)	C(17)-C(18)-C(13)	123.1(3)
C(13)-N(2)-C(12)	110.1(2)	C(20)-C(19)-Zr(1)	118.5(2)
C(13)-N(2)-Zr(1)	134.1(2)	C(25)-C(20)-C(21)	116.6(3)
C(12)-N(2)-Zr(1)	115.5(2)	C(25)-C(20)-C(19)	121.3(3)
C(2)-C(1)-C(6)	116.1(2)	C(21)-C(20)-C(19)	122.1(3)
C(2)-C(1)-Zr(1)	148.5(2)	C(22)-C(21)-C(20)	121.8(3)
C(6)-C(1)-Zr(1)	90.5(2)	C(21)-C(22)-C(23)	120.4(4)
F(1)-C(2)-C(1)	121.7(2)	C(22)-C(23)-C(24)	119.4(4)
F(1)-C(2)-C(3)	115.1(2)	C(25)-C(24)-C(23)	120.4(4)
C(1)-C(2)-C(3)	123.3(3)	C(24)-C(25)-C(20)	121.5(3)
F(2)-C(3)-C(4)	119.0(3)	C(32)-C(27)-C(26)	121.1(8)
F(2)-C(3)-C(2)	121.6(3)	C(32)-C(27)-C(28)	118.8(6)
C(4)-C(3)-C(2)	119.4(3)	C(26)-C(27)-C(28)	120.2(7)
F(3)-C(4)-C(3)	120.5(3)	C(29)-C(28)-C(27)	116.6(7)

C(30)-C(29)-C(28)	124.9(11)	C(31)-C(32)-C(27)	118.7(6)
C(29)-C(30)-C(31)	117.2(10)		
C(32)-C(31)-C(30)	123.8(7)		

Symmetry Code: 1 = -x + 1, -y + 2, -z + 2

Table XI. Anisotropic Displacement Parameters ($Å^2$ x 10^3) for 6.

	U11	U22	U33	U23	U13	U12
Zr(1)	32(1)	34(1)	34(1)	-9(1)	-4(1)	0(1)
O(1)	39(1)	33(1)	42(1)	-6(1)	-3(1)	2(1)
O(2)	45(1)	39(1)	46(1)	-5(1)	3(1)	-1(1)
N(1)	29(1)	31(1)	40(1)	-10(1)	-7(1)	1(1)
N(2)	37(1)	39(1)	46(1)	-12(1)	3(1)	-4(1)
F(1)	68(1)	42(1)	72(1)	-16(1)	10(1)	10(1)
F(2)	82(1)	34(1)	87(1)	-15(1)	-10(1)	-5(1)
F(3)	58(1)	54(1)	96(2)	-11(1)	2(1)	-25(1)
F(4)	38(1)	54(1)	76(1)	-17(1)	8(1)	-7(1)
F(5)	54(1)	75(1)	82(1)	-36(1)	-20(1)	12(1)
F(6)	64(1)	73(1)	94(2)	-16(1)	-18(1)	25(1)
F(7)	100(2)	54(1)	111(2)	-30(1)	-11(1)	21(1)
F(8)	105(2)	75(1)	109(2)	-56(1)	-37(1)	13(1)
F(9)	85(1)	78(1)	93(2)	-45(1)	-42(1)	25(1)
C(1)	36(1)	35(2)	35(2)	-5(1)	-8(1)	2(1)
C(2)	45(2)	38(2)	42(2)	-11(1)	-5(1)	7(1)
C(3)	59(2)	30(2)	53(2)	-9(1)	-16(2)	-2(1)
C(4)	44(2)	40(2)	54(2)	-5(1)	-9(2)	-13(1)
C(5)	31(1)	42(2)	43(2)	-10(1)	-3(1)	-1(1)
C(6)	31(1)	34(2)	35(2)	-8(1)	-9(1)	1(1)
C(7)	30(1)	40(2)	45(2)	-11(1)	-5(1)	4(1)
C(8)	33(1)	44(2)	47(2)	-14(1)	-6(1)	8(1)
C(9)	50(2)	32(2)	51(2)	-5(1)	-9(1)	1(1)
C(10)	60(2)	35(2)	52(2)	2(1)	-7(2)	-5(1)
C(11)	53(2)	56(2)	54(2)	-7(2)	15(2)	-8(2)
C(12)	44(2)	53(2)	63(2)	-16(2)	11(2)	-7(2)
C(13)	39(2)	44(2)	42(2)	-14(1)	5(1)	-1(1)
C(14)	43(2)	50(2)	52(2)	-17(2)	-2(1)	2(2)
C(15)	47(2)	53(2)	60(2)	-10(2)	-2(2)	9(2)
C(16)	58(2)	41(2)	67(2)	-17(2)	4(2)	12(2)
C(17)	63(2)	55(2)	60(2)	-30(2)	-7(2)	1(2)

C(18)	48(2)	53(2)	55(2)	-17(2)	-7(2)	10(2)
C(19)	46(2)	47(2)	47(2)	-15(1)	-12(1)	2(1)
C(20)	45(2)	50(2)	44(2)	-13(1)	-13(1)	-5(1)
C(21)	50(2)	63(2)	47(2)	-10(2)	-10(2)	6(2)
C(22)	87(3)	75(3)	70(3)	-5(2)	-20(2)	24(2)
C(23)	129(4)	77(3)	65(3)	12(2)	-19(3)	15(3)
C(24)	104(3)	85(3)	49(2)	-8(2)	6(2)	-4(3)
C(25)	71(2)	63(2)	47(2)	-14(2)	-3(2)	4(2)
C(26)	134(6)	269(10)	226(9)	-3(7)	-24(6)	-69(6)
C(27)	95(4)	193(7)	105(4)	-6(4)	-7(3)	-66(4)
C(28)	173(7)	186(8)	108(5)	-84(5)	40(4)	-119(6)
C(29)	217(11)	207(10)	115(7)	-70(7)	64(6)	-81(8)
C(30)	193(8)	176(8)	123(7)	4(6)	37(6)	-37(7)
C(31)	194(7)	136(6)	90(4)	-4(4)	-29(4)	-47(5)
C(32)	153(5)	119(5)	93(4)	-26(3)	-19(4)	-43(4)

The anisotropic displacement factor exponent takes the form:

$-2\pi^2[h^2 a^{*2} U_{11} + \ldots + 2 h k a^* U_{12}]$

Table XII. Hydrogen Coordinates (x 10^4) and Isotropic Displacement Parameters ($Å^2$ x 10^3) for 6.

	x	y	z	U(eq)
H(7A)	1413	10524	10391	45
H(7B)	1658	10218	9397	45
H(8A)	1905	12279	9260	49
H(8B)	2909	12186	10014	49
H(9A)	5116	13207	8890	53
H(9B)	3865	13396	8279	53
H(10A)	5323	12500	7164	59
H(10B)	6495	13276	7499	59
H(11A)	8601	11864	7142	68
H(11B)	7556	11078	6716	68
H(12A)	9325	9736	7198	66
H(12B)	9110	10249	8129	66
H(19A)	3979	8821	7577	55
H(19B)	2694	9468	8191	55
H(21A)	1766	11483	7683	63
H(22A)	1618	12992	6539	93
H(23A)	3299	13015	5217	110
H(24A)	5134	11494	5050	98
H(25A)	5281	9963	6187	73
H(26A)	6274	5005	3806	316
H(26B)	5442	3816	3723	316
H(26C)	6746	4313	2960	316
H(28A)	7399	1938	3403	185
H(29A)	9075	834	4181	221
H(30A)	10242	1608	5109	207
H(31A)	9598	3562	5438	167
H(32A)	7911	4745	4777	144

Figure IV. ORTEP3 Drawings of 11.

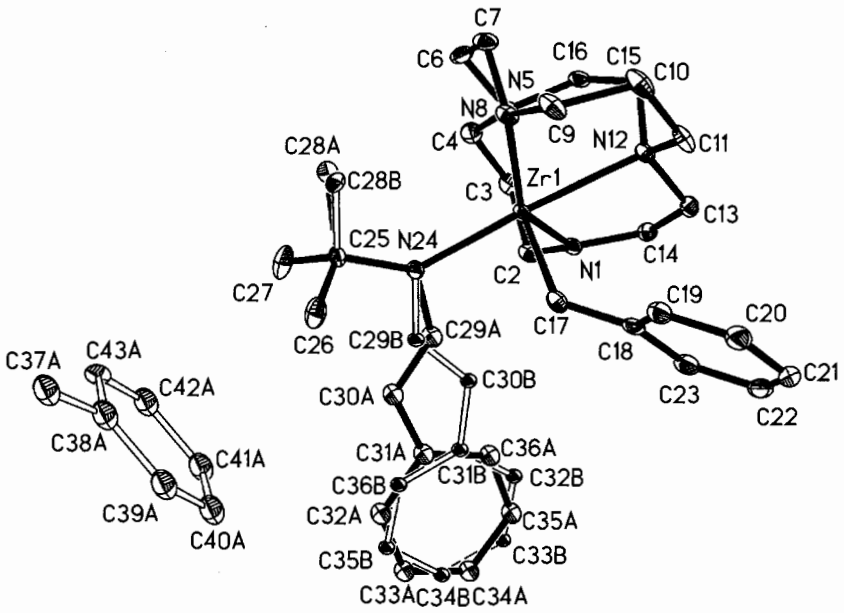

Table XIII. Atomic Coordinates (x 10^4) and Equivalent Isotropic Displacement Parameters ($Å^2$ x 10^3) for 11.

	x	y	z	U(eq)
C(2)	7800(2)	1726(1)	6883(2)	23(1)
C(3)	8820(2)	2009(2)	7563(2)	26(1)
C(4)	9091(2)	2821(2)	7412(2)	27(1)
C(6)	8650(2)	4146(2)	7343(2)	27(1)
C(7)	7754(3)	4709(2)	7146(2)	30(1)
C(9)	5844(3)	4805(2)	6513(2)	29(1)
C(10)	5415(3)	4700(2)	7426(2)	33(1)
C(11)	5173(2)	3895(2)	7662(2)	28(1)
C(13)	5680(2)	2587(2)	7907(2)	23(1)
C(14)	6462(2)	1991(1)	7777(2)	21(1)
C(15)	6954(2)	3587(2)	8546(2)	23(1)
C(16)	8039(2)	3320(2)	8479(2)	23(1)
C(17)	4935(2)	3217(2)	5247(2)	23(1)
C(18)	3879(2)	3150(2)	5439(2)	22(1)
C(19)	3148(2)	3747(2)	5307(2)	26(1)
C(20)	2167(3)	3659(2)	5512(2)	34(1)
C(21)	1873(3)	2982(2)	5850(2)	39(1)
C(22)	2578(3)	2391(2)	5980(2)	35(1)
C(23)	3545(3)	2476(2)	5773(2)	28(1)
C(25)	7673(2)	3466(2)	4263(2)	23(1)
C(26)	6846(2)	3596(2)	3310(2)	34(1)
C(27)	8674(2)	3124(2)	4064(3)	41(1)
C(28A)	8171(6)	4169(3)	4813(6)	31(2)
C(28B)	7751(6)	4275(2)	4640(6)	26(2)
N(1)	6861(2)	2169(1)	6926(2)	19(1)
N(5)	8263(2)	3387(1)	7499(2)	20(1)
N(8)	6808(2)	4371(1)	6534(2)	22(1)
N(12)	6059(2)	3348(1)	7734(2)	19(1)
N(24)	7224(2)	2991(1)	4932(2)	19(1)
Zr(1)	6657(1)	3223(1)	6243(1)	14(1)
C(29A)	6902(4)	2261(2)	4649(3)	23(1)
C(30A)	6927(3)	1847(2)	3875(2)	23(1)
C(31A)	6559(3)	1070(2)	3766(4)	23(1)
C(32A)	6514(3)	724(2)	2875(3)	23(1)
C(33A)	6177(3)	-9(2)	2693(3)	23(1)
C(34A)	5890(3)	-437(2)	3396(3)	23(1)
C(35A)	5957(3)	-111(2)	4305(3)	23(1)
C(36A)	6280(3)	633(3)	4481(3)	23(1)

C(29B)	6992(12)	2295(4)	4479(8)	15(1)
C(30B)	6486(8)	1693(4)	4682(7)	15(1)
C(31B)	6343(9)	966(7)	4148(10)	15(1)
C(32B)	6020(9)	333(7)	4558(8)	15(1)
C(33B)	5896(9)	-353(6)	4019(9)	15(1)
C(34B)	6074(9)	-369(7)	3108(9)	15(1)
C(35B)	6449(9)	256(7)	2730(8)	15(1)
C(36B)	6546(9)	915(6)	3275(10)	15(1)
C(37A)	4832(4)	6179(2)	-639(3)	31(1)
C(38A)	4956(3)	5460(2)	-200(3)	31(1)
C(39A)	4085(3)	4987(2)	-326(3)	31(1)
C(40A)	4210(3)	4264(2)	44(3)	31(1)
C(41A)	5203(3)	4013(2)	539(3)	31(1)
C(42A)	6071(3)	4486(2)	665(3)	31(1)
C(43A)	5946(3)	5210(2)	296(3)	21(1)

U(eq) is defined as one third of the trace of the orthogonalized U^{ij} tensor.

Table XIV. Bond Lengths (Å) and Angles (deg) for 11.

Bond Lengths			
		C(10)-C(11)	1.526(4)
		C(10)-H(10A)	0.9900
C(2)-N(1)	1.471(3)	C(10)-H(10B)	0.9900
C(2)-C(3)	1.530(4)	C(11)-N(12)	1.498(3)
C(2)-H(2A)	0.9900	C(11)-H(11A)	0.9900
C(2)-H(2B)	0.9900	C(11)-H(11B)	0.9900
C(3)-C(4)	1.520(4)	C(13)-N(12)	1.488(3)
C(3)-H(3A)	0.9900	C(13)-C(14)	1.516(4)
C(3)-H(3B)	0.9900	C(13)-H(13A)	0.9900
C(4)-N(5)	1.506(4)	C(13)-H(13B)	0.9900
C(4)-H(4A)	0.9900	C(14)-N(1)	1.456(3)
C(4)-H(4B)	0.9900	C(14)-H(14A)	0.9900
C(6)-N(5)	1.483(3)	C(14)-H(14B)	0.9900
C(6)-C(7)	1.516(4)	C(15)-N(12)	1.492(3)
C(6)-H(6A)	0.9900	C(15)-C(16)	1.517(4)
C(6)-H(6B)	0.9900	C(15)-H(15A)	0.9900
C(7)-N(8)	1.459(4)	C(15)-H(15B)	0.9900
C(7)-H(7A)	0.9900	C(16)-N(5)	1.487(3)
C(7)-H(7B)	0.9900	C(16)-H(16A)	0.9900
C(9)-N(8)	1.471(4)	C(16)-H(16B)	0.9900
C(9)-C(10)	1.536(4)	C(17)-C(18)	1.469(4)
C(9)-H(9A)	0.9900	C(17)-Zr(1)	2.349(3)
C(9)-H(9B)	0.9900	C(17)-H(17A)	0.9900

C(17)-H(17B)	0.9900	C(33A)-H(33A)	0.9500
C(18)-C(23)	1.401(4)	C(34A)-C(35A)	1.394(6)
C(18)-C(19)	1.413(4)	C(34A)-H(34A)	0.9500
C(19)-C(20)	1.385(4)	C(35A)-C(36A)	1.400(6)
C(19)-H(19A)	0.9500	C(35A)-H(35A)	0.9500
C(20)-C(21)	1.388(5)	C(36A)-H(36A)	0.9500
C(20)-H(20A)	0.9500	C(29B)-C(30B)	1.328(5)
C(21)-C(22)	1.383(5)	C(29B)-H(29B)	0.9500
C(21)-H(21A)	0.9500	C(30B)-C(31B)	1.492(13)
C(22)-C(23)	1.369(4)	C(30B)-H(30B)	0.9500
C(22)-H(22A)	0.9500	C(31B)-C(36B)	1.325(16)
C(23)-H(23A)	0.9500	C(31B)-C(32B)	1.383(16)
C(25)-N(24)	1.491(3)	C(32B)-C(33B)	1.431(15)
C(25)-C(27)	1.527(4)	C(32B)-H(32B)	0.9500
C(25)-C(26)	1.530(4)	C(33B)-C(34B)	1.362(15)
C(25)-C(28A)	1.537(4)	C(33B)-H(33B)	0.9500
C(25)-C(28B)	1.537(4)	C(34B)-C(35B)	1.378(16)
C(26)-H(26A)	0.9800	C(34B)-H(34B)	0.9500
C(26)-H(26B)	0.9800	C(35B)-C(36B)	1.397(16)
C(26)-H(26C)	0.9800	C(35B)-H(35B)	0.9500
C(27)-H(27A)	0.9800	C(36B)-H(36B)	0.9500
C(27)-H(27B)	0.9800	C(37A)-C(38A)	1.4189
C(27)-H(27C)	0.9800	C(37A)-H(37A)	0.9800
C(28A)-H(28A)	0.9800	C(37A)-H(37B)	0.9800
C(28A)-H(28B)	0.9800	C(37A)-H(37C)	0.9800
C(28A)-H(28C)	0.9800	C(38A)-C(43A)	1.3887
C(28B)-H(28D)	0.9800	C(38A)-C(39A)	1.3922
C(28B)-H(28E)	0.9800	C(39A)-C(40A)	1.3891
C(28B)-H(28F)	0.9800	C(39A)-H(39A)	0.9500
N(1)-Zr(1)	2.105(2)	C(40A)-C(41A)	1.3907
N(5)-Zr(1)	2.419(2)	C(40A)-H(40A)	0.9500
N(8)-Zr(1)	2.092(2)	C(41A)-C(42A)	1.3900
N(12)-Zr(1)	2.426(2)	C(41A)-H(41A)	0.9500
N(24)-C(29B)	1.3977(14)	C(42A)-C(43A)	1.3903
N(24)-C(29A)	1.3981(10)	C(42A)-H(42A)	0.9500
N(24)-Zr(1)	2.193(2)	C(43A)-H(43A)	0.9500
C(29A)-C(30A)	1.329(4)		
C(29A)-H(29A)	0.9500	**Bond Angles**	
C(30A)-C(31A)	1.465(5)		
C(30A)-H(30A)	0.9500	N(1)-C(2)-C(3)	113.8(2)
C(31A)-C(36A)	1.393(6)	N(1)-C(2)-H(2A)	108.8
C(31A)-C(32A)	1.393(5)	C(3)-C(2)-H(2A)	108.8
C(32A)-C(33A)	1.387(5)	N(1)-C(2)-H(2B)	108.8
C(32A)-H(32A)	0.9500	C(3)-C(2)-H(2B)	108.8
C(33A)-C(34A)	1.375(5)	H(2A)-C(2)-H(2B)	107.7

C(4)-C(3)-C(2)	115.1(2)	N(12)-C(13)-H(13B)	109.4
C(4)-C(3)-H(3A)	108.5	C(14)-C(13)-H(13B)	109.4
C(2)-C(3)-H(3A)	108.5	H(13A)-C(13)-H(13B)	108.0
C(4)-C(3)-H(3B)	108.5	N(1)-C(14)-C(13)	109.2(2)
C(2)-C(3)-H(3B)	108.5	N(1)-C(14)-H(14A)	109.8
H(3A)-C(3)-H(3B)	107.5	C(13)-C(14)-H(14A)	109.8
N(5)-C(4)-C(3)	115.7(2)	N(1)-C(14)-H(14B)	109.8
N(5)-C(4)-H(4A)	108.4	C(13)-C(14)-H(14B)	109.8
C(3)-C(4)-H(4A)	108.4	H(14A)-C(14)-H(14B)	108.3
N(5)-C(4)-H(4B)	108.4	N(12)-C(15)-C(16)	115.6(2)
C(3)-C(4)-H(4B)	108.4	N(12)-C(15)-H(15A)	108.4
H(4A)-C(4)-H(4B)	107.4	C(16)-C(15)-H(15A)	108.4
N(5)-C(6)-C(7)	111.1(2)	N(12)-C(15)-H(15B)	108.4
N(5)-C(6)-H(6A)	109.4	C(16)-C(15)-H(15B)	108.4
C(7)-C(6)-H(6A)	109.4	H(15A)-C(15)-H(15B)	107.4
N(5)-C(6)-H(6B)	109.4	N(5)-C(16)-C(15)	115.2(2)
C(7)-C(6)-H(6B)	109.4	N(5)-C(16)-H(16A)	108.5
H(6A)-C(6)-H(6B)	108.0	C(15)-C(16)-H(16A)	108.5
N(8)-C(7)-C(6)	109.8(2)	N(5)-C(16)-H(16B)	108.5
N(8)-C(7)-H(7A)	109.7	C(15)-C(16)-H(16B)	108.5
C(6)-C(7)-H(7A)	109.7	H(16A)-C(16)-H(16B)	107.5
N(8)-C(7)-H(7B)	109.7	C(18)-C(17)-Zr(1)	133.86(18)
C(6)-C(7)-H(7B)	109.7	C(18)-C(17)-H(17A)	103.7
H(7A)-C(7)-H(7B)	108.2	Zr(1)-C(17)-H(17A)	103.7
N(8)-C(9)-C(10)	113.5(2)	C(18)-C(17)-H(17B)	103.7
N(8)-C(9)-H(9A)	108.9	Zr(1)-C(17)-H(17B)	103.7
C(10)-C(9)-H(9A)	108.9	H(17A)-C(17)-H(17B)	105.4
N(8)-C(9)-H(9B)	108.9	C(23)-C(18)-C(19)	116.0(3)
C(10)-C(9)-H(9B)	108.9	C(23)-C(18)-C(17)	120.8(3)
H(9A)-C(9)-H(9B)	107.7	C(19)-C(18)-C(17)	123.2(3)
C(11)-C(10)-C(9)	115.8(2)	C(20)-C(19)-C(18)	121.0(3)
C(11)-C(10)-H(10A)	108.3	C(20)-C(19)-H(19A)	119.5
C(9)-C(10)-H(10A)	108.3	C(18)-C(19)-H(19A)	119.5
C(11)-C(10)-H(10B)	108.3	C(19)-C(20)-C(21)	121.0(3)
C(9)-C(10)-H(10B)	108.3	C(19)-C(20)-H(20A)	119.5
H(10A)-C(10)-H(10B)	107.4	C(21)-C(20)-H(20A)	119.5
N(12)-C(11)-C(10)	115.7(2)	C(22)-C(21)-C(20)	118.8(3)
N(12)-C(11)-H(11A)	108.3	C(22)-C(21)-H(21A)	120.6
C(10)-C(11)-H(11A)	108.3	C(20)-C(21)-H(21A)	120.6
N(12)-C(11)-H(11B)	108.3	C(23)-C(22)-C(21)	120.3(3)
C(10)-C(11)-H(11B)	108.3	C(23)-C(22)-H(22A)	119.9
H(11A)-C(11)-H(11B)	107.4	C(21)-C(22)-H(22A)	119.9
N(12)-C(13)-C(14)	111.3(2)	C(22)-C(23)-C(18)	122.9(3)
N(12)-C(13)-H(13A)	109.4	C(22)-C(23)-H(23A)	118.5
C(14)-C(13)-H(13A)	109.4	C(18)-C(23)-H(23A)	118.5

N(24)-C(25)-C(27)	111.8(2)	C(13)-N(12)-Zr(1)	104.33(15)
N(24)-C(25)-C(26)	110.1(2)	C(15)-N(12)-Zr(1)	109.91(16)
C(27)-C(25)-C(26)	110.6(3)	C(11)-N(12)-Zr(1)	113.80(15)
N(24)-C(25)-C(28A)	109.1(4)	C(29B)-N(24)-C(25)	106.9(4)
C(27)-C(25)-C(28A)	98.3(4)	C(29A)-N(24)-C(25)	119.1(2)
C(26)-C(25)-C(28A)	116.4(4)	C(29B)-N(24)-Zr(1)	118.4(4)
N(24)-C(25)-C(28B)	108.6(4)	C(29A)-N(24)-Zr(1)	106.3(2)
C(27)-C(25)-C(28B)	116.9(4)	C(25)-N(24)-Zr(1)	133.68(15)
C(26)-C(25)-C(28B)	97.9(4)	N(8)-Zr(1)-N(1)	142.35(9)
C(25)-C(26)-H(26A)	109.5	N(8)-Zr(1)-N(24)	108.53(8)
C(25)-C(26)-H(26B)	109.5	N(1)-Zr(1)-N(24)	100.75(8)
H(26A)-C(26)-H(26B)	109.5	N(8)-Zr(1)-C(17)	98.87(10)
C(25)-C(26)-H(26C)	109.5	N(1)-Zr(1)-C(17)	105.60(9)
H(26A)-C(26)-H(26C)	109.5	N(24)-Zr(1)-C(17)	87.66(9)
H(26B)-C(26)-H(26C)	109.5	N(8)-Zr(1)-N(5)	73.32(8)
C(25)-C(27)-H(27A)	109.5	N(1)-Zr(1)-N(5)	77.21(8)
C(25)-C(27)-H(27B)	109.5	N(24)-Zr(1)-N(5)	103.67(8)
H(27A)-C(27)-H(27B)	109.5	C(17)-Zr(1)-N(5)	167.74(8)
C(25)-C(27)-H(27C)	109.5	N(8)-Zr(1)-N(12)	76.89(8)
H(27A)-C(27)-H(27C)	109.5	N(1)-Zr(1)-N(12)	73.48(8)
H(27B)-C(27)-H(27C)	109.5	N(24)-Zr(1)-N(12)	174.22(7)
C(25)-C(28A)-H(28A)	109.5	C(17)-Zr(1)-N(12)	93.54(8)
C(25)-C(28A)-H(28B)	109.5	N(5)-Zr(1)-N(12)	75.66(8)
C(25)-C(28A)-H(28C)	109.5	C(30A)-C(29A)-N(24)	133.7(4)
C(25)-C(28B)-H(28D)	109.5	C(30A)-C(29A)-H(29A)	113.2
C(25)-C(28B)-H(28E)	109.5	N(24)-C(29A)-H(29A)	113.2
H(28D)-C(28B)-H(28E)	109.5	C(29A)-C(30A)-C(31A)	122.9(4)
C(25)-C(28B)-H(28F)	109.5	C(29A)-C(30A)-H(30A)	118.6
H(28D)-C(28B)-H(28F)	109.5	C(31A)-C(30A)-H(30A)	118.6
H(28E)-C(28B)-H(28F)	109.5	C(36A)-C(31A)-C(32A)	116.5(4)
C(14)-N(1)-C(2)	112.4(2)	C(36A)-C(31A)-C(30A)	126.2(5)
C(14)-N(1)-Zr(1)	122.96(16)	C(32A)-C(31A)-C(30A)	117.3(4)
C(2)-N(1)-Zr(1)	118.56(16)	C(33A)-C(32A)-C(31A)	122.1(4)
C(6)-N(5)-C(16)	111.2(2)	C(33A)-C(32A)-H(32A)	119.0
C(6)-N(5)-C(4)	109.1(2)	C(31A)-C(32A)-H(32A)	119.0
C(16)-N(5)-C(4)	109.0(2)	C(34A)-C(33A)-C(32A)	121.3(4)
C(6)-N(5)-Zr(1)	105.49(16)	C(34A)-C(33A)-H(33A)	119.3
C(16)-N(5)-Zr(1)	110.27(16)	C(32A)-C(33A)-H(33A)	119.3
C(4)-N(5)-Zr(1)	111.80(16)	C(33A)-C(34A)-C(35A)	117.8(4)
C(7)-N(8)-C(9)	113.0(2)	C(33A)-C(34A)-H(34A)	121.1
C(7)-N(8)-Zr(1)	123.35(18)	C(35A)-C(34A)-H(34A)	121.1
C(9)-N(8)-Zr(1)	118.32(19)	C(34A)-C(35A)-C(36A)	120.7(4)
C(13)-N(12)-C(15)	111.4(2)	C(34A)-C(35A)-H(35A)	119.6
C(13)-N(12)-C(11)	109.1(2)	C(36A)-C(35A)-H(35A)	119.6
C(15)-N(12)-C(11)	108.3(2)	C(31A)-C(36A)-C(35A)	121.6(4)

C(31A)-C(36A)-H(36A)	119.2	C(36B)-C(35B)-H(35B)	121.2
C(35A)-C(36A)-H(36A)	119.2	C(31B)-C(36B)-C(35B)	124.0(10)
C(30B)-C(29B)-N(24)	133.3(8)	C(31B)-C(36B)-H(36B)	118.0
C(30B)-C(29B)-H(29B)	113.3	C(35B)-C(36B)-H(36B)	118.0
N(24)-C(29B)-H(29B)	113.3	C(43A)-C(38A)-C(39A)	120.0
C(29B)-C(30B)-C(31B)	127.3(9)	C(43A)-C(38A)-C(37A)	120.5
C(29B)-C(30B)-H(30B)	116.4	C(39A)-C(38A)-C(37A)	119.4
C(31B)-C(30B)-H(30B)	116.4	C(40A)-C(39A)-C(38A)	119.9
C(36B)-C(31B)-C(32B)	118.8(10)	C(40A)-C(39A)-H(39A)	120.0
C(36B)-C(31B)-C(30B)	120.1(13)	C(38A)-C(39A)-H(39A)	120.0
C(32B)-C(31B)-C(30B)	121.0(12)	C(39A)-C(40A)-C(41A)	120.1
C(31B)-C(32B)-C(33B)	119.0(10)	C(39A)-C(40A)-H(40A)	120.0
C(31B)-C(32B)-H(32B)	120.5	C(41A)-C(40A)-H(40A)	120.0
C(33B)-C(32B)-H(32B)	120.5	C(42A)-C(41A)-C(40A)	120.0
C(34B)-C(33B)-C(32B)	120.0(10)	C(42A)-C(41A)-H(41A)	120.0
C(34B)-C(33B)-H(33B)	120.0	C(40A)-C(41A)-H(41A)	120.0
C(32B)-C(33B)-H(33B)	120.0	C(41A)-C(42A)-C(43A)	120.0
C(33B)-C(34B)-C(35B)	120.3(11)	C(41A)-C(42A)-H(42A)	120.0
C(33B)-C(34B)-H(34B)	119.8	C(43A)-C(42A)-H(42A)	120.0
C(35B)-C(34B)-H(34B)	119.8	C(38A)-C(43A)-C(42A)	120.1
C(34B)-C(35B)-C(36B)	117.6(10)	C(38A)-C(43A)-H(43A)	120.0
C(34B)-C(35B)-H(35B)	121.2	C(42A)-C(43A)-H(43A)	120.0

Table XV. Anisotropic Displacement Parameters ($Å^2$ x 10^3) for 11.

	U^{11}	U^{22}	U^{33}	U^{23}	U^{13}	U^{12}
C(2)	33(2)	16(1)	19(1)	1(1)	5(1)	3(1)
C(3)	25(2)	26(1)	23(1)	1(1)	1(1)	10(1)
C(4)	20(2)	34(2)	23(2)	1(1)	1(1)	1(1)
C(6)	33(2)	23(1)	24(2)	-1(1)	3(1)	-13(1)
C(7)	53(2)	15(1)	22(2)	-3(1)	8(1)	-10(1)
C(9)	49(2)	19(1)	20(1)	2(1)	9(1)	13(1)
C(10)	48(2)	30(2)	22(2)	2(1)	10(1)	21(1)
C(11)	33(2)	38(2)	15(1)	1(1)	9(1)	14(1)
C(13)	26(2)	30(2)	14(1)	5(1)	5(1)	-3(1)
C(14)	26(2)	19(1)	17(1)	3(1)	3(1)	-3(1)
C(15)	35(2)	23(1)	11(1)	-2(1)	4(1)	1(1)
C(16)	29(2)	24(1)	14(1)	-3(1)	0(1)	-4(1)
C(17)	28(2)	25(1)	14(1)	2(1)	5(1)	4(1)

C(18)	27(2)	25(1)	12(1)	-4(1)	0(1)	-4(1)
C(19)	29(2)	28(1)	20(1)	-3(1)	3(1)	-1(1)
C(20)	29(2)	39(2)	36(2)	-13(1)	9(1)	-1(1)
C(21)	34(2)	55(2)	31(2)	-18(2)	15(2)	-22(2)
C(22)	46(2)	37(2)	22(2)	-6(1)	8(1)	-21(2)
C(23)	39(2)	26(1)	18(1)	-2(1)	4(1)	-4(1)
C(25)	30(2)	22(1)	17(1)	1(1)	11(1)	-3(1)
C(26)	32(2)	37(2)	34(2)	20(1)	10(1)	2(1)
C(27)	24(2)	51(2)	51(2)	21(2)	16(2)	2(2)
C(28A)	37(4)	31(3)	27(3)	-5(3)	14(3)	-9(3)
C(28B)	35(4)	21(3)	22(3)	1(2)	9(3)	-13(3)
N(1)	25(1)	16(1)	14(1)	1(1)	5(1)	-1(1)
N(5)	25(1)	19(1)	16(1)	-1(1)	3(1)	-4(1)
N(8)	37(1)	13(1)	17(1)	1(1)	7(1)	4(1)
N(12)	24(1)	21(1)	13(1)	1(1)	4(1)	3(1)
N(24)	25(1)	17(1)	15(1)	1(1)	5(1)	-2(1)
Zr(1)	21(1)	12(1)	10(1)	0(1)	3(1)	0(1)
C(29A)	29(1)	18(1)	22(1)	2(1)	8(1)	4(1)
C(30A)	29(1)	18(1)	22(1)	2(1)	8(1)	4(1)
C(31A)	29(1)	18(1)	22(1)	2(1)	8(1)	4(1)
C(32A)	29(1)	18(1)	22(1)	2(1)	8(1)	4(1)
C(33A)	29(1)	18(1)	22(1)	2(1)	8(1)	4(1)
C(34A)	29(1)	18(1)	22(1)	2(1)	8(1)	4(1)
C(35A)	29(1)	18(1)	22(1)	2(1)	8(1)	4(1)
C(36A)	29(1)	18(1)	22(1)	2(1)	8(1)	4(1)
C(29B)	20(2)	11(2)	13(2)	-1(2)	4(2)	-3(2)
C(30B)	20(2)	11(2)	13(2)	-1(2)	4(2)	-3(2)
C(31B)	20(2)	11(2)	13(2)	-1(2)	4(2)	-3(2)
C(32B)	20(2)	11(2)	13(2)	-1(2)	4(2)	-3(2)
C(33B)	20(2)	11(2)	13(2)	-1(2)	4(2)	-3(2)
C(34B)	20(2)	11(2)	13(2)	-1(2)	4(2)	-3(2)
C(35B)	20(2)	11(2)	13(2)	-1(2)	4(2)	-3(2)
C(36B)	20(2)	11(2)	13(2)	-1(2)	4(2)	-3(2)
C(37A)	30(1)	42(2)	24(1)	0(1)	10(1)	3(1)
C(38A)	30(1)	42(2)	24(1)	0(1)	10(1)	3(1)
C(39A)	30(1)	42(2)	24(1)	0(1)	10(1)	3(1)
C(40A)	30(1)	42(2)	24(1)	0(1)	10(1)	3(1)
C(41A)	30(1)	42(2)	24(1)	0(1)	10(1)	3(1)
C(42A)	30(1)	42(2)	24(1)	0(1)	10(1)	3(1)
C(43A)	6(2)	33(3)	20(3)	-7(2)	-2(2)	4(2)

The anisotropic displacement factor exponent takes the form:

$-2\pi^2[\, h^2 a^{*2} U^{11} + \ldots + 2\, h\, k\, a^*\, b^*\, U^{12} \,]$

Table XVI. Hydrogen Coordinates (x 10^4) and Isotropic Displacement Parameters ($Å^2$ x 10^3) for 11.

	x	y	z	U(eq)
H(2A)	7886	1732	6206	28
H(2B)	7682	1201	7052	28
H(3A)	8762	1947	8244	31
H(3B)	9411	1691	7475	31
H(4A)	9753	2947	7895	32
H(4B)	9232	2869	6757	32
H(6A)	8984	4136	6784	33
H(6B)	9191	4301	7927	33
H(7A)	7608	4874	7770	36
H(7B)	7958	5154	6816	36
H(9A)	5292	4656	5933	35
H(9B)	5997	5342	6444	35
H(10A)	5937	4908	7991	40
H(10B)	4760	4998	7345	40
H(11A)	4959	3894	8288	34
H(11B)	4562	3718	7153	34
H(13A)	4991	2493	7447	28
H(13B)	5574	2559	8577	28
H(14A)	7055	1969	8363	25
H(14B)	6111	1496	7691	25
H(15A)	6820	3404	9166	28
H(15B)	6962	4141	8573	28
H(16A)	8578	3610	8948	28
H(16B)	8117	2789	8681	28
H(17A)	4895	3687	4871	27
H(17B)	4951	2812	4773	27
H(19A)	3331	4215	5075	31
H(20A)	1689	4068	5420	41
H(21A)	1200	2925	5990	46
H(22A)	2391	1925	6213	42
H(23A)	4010	2059	5859	34
H(26A)	6648	3115	2983	51
H(26B)	7140	3924	2886	51
H(26C)	6220	3831	3450	51
H(27A)	8493	2668	3675	61
H(27B)	9168	3000	4683	61
H(27C)	9005	3484	3706	61
H(28A)	8779	4024	5335	46
H(28B)	7647	4422	5095	46

H(28C)	8403	4507	4361	46
H(28D)	7066	4432	4745	38
H(28E)	7950	4606	4160	38
H(28F)	8287	4305	5257	38
H(29A)	6600	2008	5108	28
H(30A)	7196	2064	3370	28
H(32A)	6721	999	2375	28
H(33A)	6144	-220	2070	28
H(34A)	5655	-938	3268	28
H(35A)	5780	-397	4810	28
H(36A)	6309	845	5103	28
H(29B)	7249	2242	3908	18
H(30B)	6182	1729	5227	18
H(32B)	5881	352	5187	18
H(33B)	5691	-796	4296	18
H(34B)	5938	-814	2731	18
H(35B)	6636	239	2121	18
H(36B)	6770	1354	3003	18
H(37A)	5529	6391	-623	47
H(37B)	4454	6506	-282	47
H(37C)	4428	6134	-1317	47
H(39A)	3407	5158	-663	38
H(40A)	3617	3940	-42	38
H(41A)	5287	3518	791	38
H(42A)	6749	4315	1004	38
H(43A)	6539	5534	384	25

Figure V. ORTEP3 Drawing of 14.

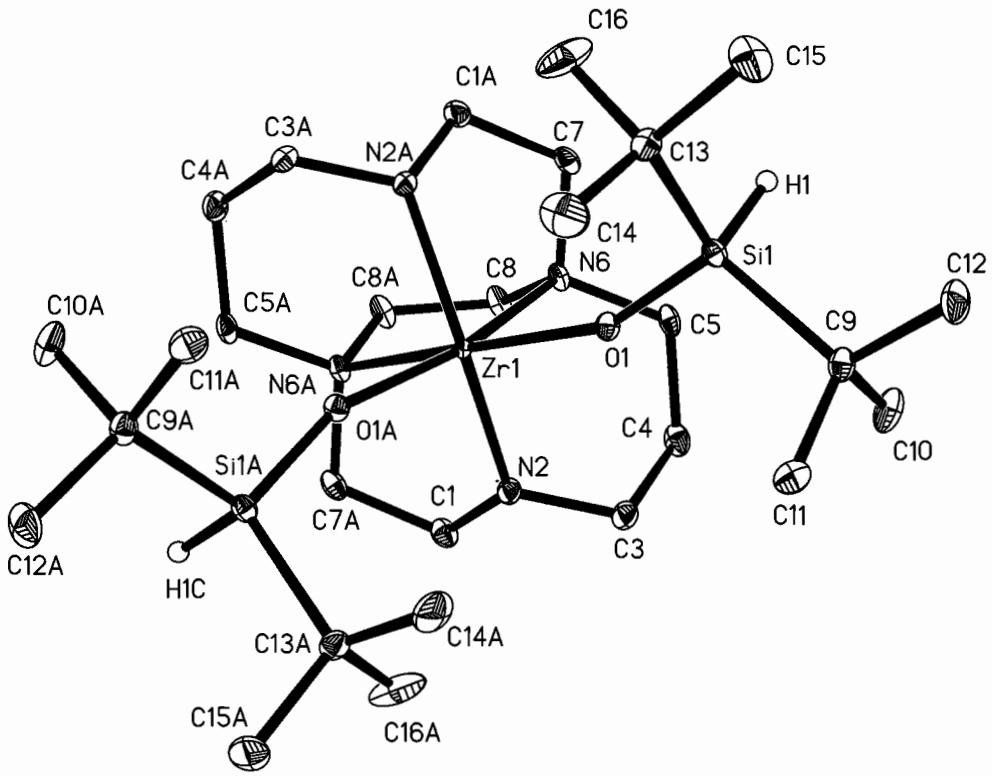

Table XVII. Atomic Coordinates (x 10^4) and Equivalent Isotropic Displacement Parameters ($Å^2$ x 10^3) for 14.

	x	y	z	U(eq)
C(1)	-1955(2)	3931(1)	2185(2)	21(1)
C(3)	-1595(2)	3361(1)	651(2)	22(1)
C(4)	-1072(2)	3946(1)	130(2)	24(1)
C(5)	53(2)	3971(1)	434(2)	18(1)
C(7)	1532(2)	4021(1)	1697(2)	18(1)
C(8)	49(2)	4712(1)	1939(2)	21(1)
C(9)	273(2)	1463(1)	-330(2)	18(1)
C(10)	-255(2)	2040(1)	-1049(2)	29(1)
C(11)	-500(2)	996(1)	55(2)	25(1)
C(12)	884(2)	1006(1)	-949(2)	30(1)
C(13)	2011(2)	1409(1)	1647(2)	19(1)
C(14)	1535(2)	888(2)	2292(2)	44(1)
C(15)	2724(2)	1008(2)	1084(2)	35(1)
C(16)	2632(2)	1964(2)	2320(2)	47(1)
N(2)	-1385(1)	3391(1)	1758(1)	16(1)
N(6)	438(1)	4043(1)	1549(1)	14(1)
O(1)	354(1)	2383(1)	1413(1)	14(1)
Si(1)	1067(1)	1951(1)	758(1)	14(1)
Zr(1)	0	3027(1)	2500	8(1)

U(eq) is defined as one third of the trace of the orthogonalized U^{ij} tensor.

Table XVIII. Bond Lengths (Å) and Angles (deg) for 14.

Bond Lengths

C(1)-N(2)	1.449(3)	C(4)-H(4A)	0.9900
C(1)-C(7)#1	1.520(3)	C(4)-H(4B)	0.9900
C(1)-H(1A)	0.9900	C(5)-N(6)	1.500(3)
C(1)-H(1B)	0.9900	C(5)-H(5A)	0.9900
C(3)-N(2)	1.459(3)	C(5)-H(5B)	0.9900
C(3)-C(4)	1.536(3)	C(7)-N(6)	1.486(3)
C(3)-H(3A)	0.9900	C(7)-C(1)#1	1.520(3)
C(3)-H(3B)	0.9900	C(7)-H(7A)	0.9900
C(4)-C(5)	1.537(3)	C(7)-H(7B)	0.9900
		C(8)-N(6)	1.486(3)
		C(8)-C(8)#1	1.525(4)

C(8)-H(8A)	0.9900
C(8)-H(8B)	0.9900
C(9)-C(11)	1.527(3)
C(9)-C(12)	1.531(3)
C(9)-C(10)	1.543(3)
C(9)-Si(1)	1.899(2)
C(10)-H(10A)	0.9800
C(10)-H(10B)	0.9800
C(10)-H(10C)	0.9800
C(11)-H(11A)	0.9800
C(11)-H(11B)	0.9800
C(11)-H(11C)	0.9800
C(12)-H(12A)	0.9800
C(12)-H(12B)	0.9800
C(12)-H(12C)	0.9800
C(13)-C(14)	1.516(3)
C(13)-C(15)	1.526(3)
C(13)-C(16)	1.536(3)
C(13)-Si(1)	1.901(2)
C(14)-H(14A)	0.9800
C(14)-H(14B)	0.9800
C(14)-H(14C)	0.9800
C(15)-H(15A)	0.9800
C(15)-H(15B)	0.9800
C(15)-H(15C)	0.9800
C(16)-H(16A)	0.9800
C(16)-H(16B)	0.9800
C(16)-H(16C)	0.9800
N(2)-Zr(1)	2.1108(18)
N(6)-Zr(1)	2.4113(17)
O(1)-Si(1)	1.6298(15)
O(1)-Zr(1)	2.0039(14)
Si(1)-H(1)	1.35(2)
Zr(1)-O(1)#1	2.0039(14)
Zr(1)-N(2)#1	2.1108(18)
Zr(1)-N(6)#1	2.4113(17)

Bond Angles

N(2)-C(1)-C(7)#1	108.47(17)
N(2)-C(1)-H(1A)	110.0
C(7)#1-C(1)-H(1A)	110.0
N(2)-C(1)-H(1B)	110.0
C(7)#1-C(1)-H(1B)	110.0
H(1A)-C(1)-H(1B)	108.4
N(2)-C(3)-C(4)	113.59(19)
N(2)-C(3)-H(3A)	108.8
C(4)-C(3)-H(3A)	108.8
N(2)-C(3)-H(3B)	108.8
C(4)-C(3)-H(3B)	108.8
H(3A)-C(3)-H(3B)	107.7
C(3)-C(4)-C(5)	115.33(18)
C(3)-C(4)-H(4A)	108.4
C(5)-C(4)-H(4A)	108.4
C(3)-C(4)-H(4B)	108.4
C(5)-C(4)-H(4B)	108.4
H(4A)-C(4)-H(4B)	107.5
N(6)-C(5)-C(4)	116.21(17)
N(6)-C(5)-H(5A)	108.2
C(4)-C(5)-H(5A)	108.2
N(6)-C(5)-H(5B)	108.2
C(4)-C(5)-H(5B)	108.2
H(5A)-C(5)-H(5B)	107.4
N(6)-C(7)-C(1)#1	110.53(17)
N(6)-C(7)-H(7A)	109.5
C(1)#1-C(7)-H(7A)	109.5
N(6)-C(7)-H(7B)	109.5
C(1)#1-C(7)-H(7B)	109.5
H(7A)-C(7)-H(7B)	108.1
N(6)-C(8)-C(8)#1	115.96(13)
N(6)-C(8)-H(8A)	108.3
C(8)#1-C(8)-H(8A)	108.3
N(6)-C(8)-H(8B)	108.3
C(8)#1-C(8)-H(8B)	108.3
H(8A)-C(8)-H(8B)	107.4
C(11)-C(9)-C(12)	109.70(19)
C(11)-C(9)-C(10)	108.95(19)
C(12)-C(9)-C(10)	107.30(18)
C(11)-C(9)-Si(1)	111.25(15)
C(12)-C(9)-Si(1)	112.40(16)
C(10)-C(9)-Si(1)	107.08(15)
C(9)-C(10)-H(10A)	109.5
C(9)-C(10)-H(10B)	109.5
H(10A)-C(10)-H(10B)	109.5
C(9)-C(10)-H(10C)	109.5
H(10A)-C(10)-H(10C)	109.5
H(10B)-C(10)-H(10C)	109.5
C(9)-C(11)-H(11A)	109.5
C(9)-C(11)-H(11B)	109.5
H(11A)-C(11)-H(11B)	109.5

C(9)-C(11)-H(11C)	109.5	H(16B)-C(16)-H(16C)	109.5
H(11A)-C(11)-H(11C)	109.5	C(1)-N(2)-C(3)	113.23(17)
H(11B)-C(11)-H(11C)	109.5	C(1)-N(2)-Zr(1)	123.06(13)
C(9)-C(12)-H(12A)	109.5	C(3)-N(2)-Zr(1)	118.41(14)
C(9)-C(12)-H(12B)	109.5	C(8)-N(6)-C(7)	113.04(17)
H(12A)-C(12)-H(12B)	109.5	C(8)-N(6)-C(5)	109.42(16)
C(9)-C(12)-H(12C)	109.5	C(7)-N(6)-C(5)	108.31(16)
H(12A)-C(12)-H(12C)	109.5	C(8)-N(6)-Zr(1)	110.00(12)
H(12B)-C(12)-H(12C)	109.5	C(7)-N(6)-Zr(1)	104.09(12)
C(14)-C(13)-C(15)	109.7(2)	C(5)-N(6)-Zr(1)	111.91(12)
C(14)-C(13)-C(16)	110.6(2)	Si(1)-O(1)-Zr(1)	157.42(9)
C(15)-C(13)-C(16)	106.2(2)	O(1)-Si(1)-C(9)	108.96(9)
C(14)-C(13)-Si(1)	112.33(16)	O(1)-Si(1)-C(13)	109.85(9)
C(15)-C(13)-Si(1)	112.51(15)	C(9)-Si(1)-C(13)	118.09(10)
C(16)-C(13)-Si(1)	105.30(16)	O(1)-Si(1)-H(1)	110.0(10)
C(13)-C(14)-H(14A)	109.5	C(9)-Si(1)-H(1)	104.3(10)
C(13)-C(14)-H(14B)	109.5	C(13)-Si(1)-H(1)	105.3(10)
H(14A)-C(14)-H(14B)	109.5	O(1)-Zr(1)-O(1)#1	106.27(8)
C(13)-C(14)-H(14C)	109.5	O(1)-Zr(1)-N(2)#1	103.00(7)
H(14A)-C(14)-H(14C)	109.5	O(1)#1-Zr(1)-N(2)#1	99.29(6)
H(14B)-C(14)-H(14C)	109.5	O(1)-Zr(1)-N(2)	99.29(6)
C(13)-C(15)-H(15A)	109.5	O(1)#1-Zr(1)-N(2)	103.00(7)
C(13)-C(15)-H(15B)	109.5	N(2)#1-Zr(1)-N(2)	142.42(10)
H(15A)-C(15)-H(15B)	109.5	O(1)-Zr(1)-N(6)	88.86(6)
C(13)-C(15)-H(15C)	109.5	O(1)#1-Zr(1)-N(6)	164.42(6)
H(15A)-C(15)-H(15C)	109.5	N(2)#1-Zr(1)-N(6)	73.10(7)
H(15B)-C(15)-H(15C)	109.5	N(2)-Zr(1)-N(6)	77.54(6)
C(13)-C(16)-H(16A)	109.5	O(1)-Zr(1)-N(6)#1	164.42(6)
C(13)-C(16)-H(16B)	109.5	O(1)#1-Zr(1)-N(6)#1	88.86(6)
H(16A)-C(16)-H(16B)	109.5	N(2)#1-Zr(1)-N(6)#1	77.54(7)
C(13)-C(16)-H(16C)	109.5	N(2)-Zr(1)-N(6)#1	73.10(7)
H(16A)-C(16)-H(16C)	109.5	N(6)-Zr(1)-N(6)#1	76.33(8)

Symmetry transformations used to generate equivalent atoms: #1 -x,y,-z+1/2

Table XIX. Anisotropic Displacement Parameters ($Å^2$ x 10^3) for 14.

	U^{11}	U^{22}	U^{33}	U^{23}	U^{13}	U^{12}
C(1)	20(1)	24(1)	21(1)	6(1)	7(1)	7(1)
C(3)	18(1)	29(1)	16(1)	1(1)	-1(1)	4(1)
C(4)	27(1)	29(1)	17(1)	7(1)	5(1)	9(1)
C(5)	27(1)	16(1)	14(1)	5(1)	9(1)	6(1)
C(7)	22(1)	15(1)	21(1)	-1(1)	11(1)	-5(1)
C(8)	34(1)	9(1)	22(1)	2(1)	16(1)	2(1)
C(9)	23(1)	15(1)	15(1)	-1(1)	3(1)	3(1)
C(10)	43(1)	24(1)	16(1)	0(1)	-4(1)	6(1)
C(11)	23(1)	26(1)	26(1)	-3(1)	0(1)	-4(1)
C(12)	38(1)	29(1)	23(1)	-11(1)	8(1)	2(1)
C(13)	21(1)	17(1)	18(1)	-2(1)	0(1)	5(1)
C(14)	34(2)	63(2)	35(2)	32(1)	5(1)	8(1)
C(15)	37(2)	34(1)	34(1)	9(1)	10(1)	22(1)
C(16)	33(2)	38(2)	58(2)	-19(1)	-23(1)	17(1)
N(2)	16(1)	19(1)	14(1)	1(1)	2(1)	3(1)
N(6)	21(1)	9(1)	14(1)	1(1)	8(1)	2(1)
O(1)	18(1)	12(1)	14(1)	-2(1)	3(1)	2(1)
Si(1)	16(1)	11(1)	15(1)	-1(1)	5(1)	1(1)
Zr(1)	9(1)	7(1)	7(1)	0	1(1)	0

The anisotropic displacement factor exponent takes the form:

$-2\pi^2[\, h^2\, a^{*2} U^{11} + \ldots + 2\, h\, k\, a^*\, b^*\, U^{12} \,]$

Table XX. Hydrogen Coordinates (x 10^4) and Isotropic Displacement Parameters(Å^2 x 10^3) for 14.

	x	y	z	U(eq)
H(1A)	-2654	3781	2109	25
H(1B)	-1923	4391	1823	25
H(3A)	-2314	3406	428	26
H(3B)	-1391	2886	426	26
H(4A)	-1344	4417	286	29
H(4B)	-1231	3876	-615	29
H(5A)	330	3528	186	22
H(5B)	305	4379	78	22
H(7A)	1783	4471	1439	22
H(7B)	1747	3617	1304	22
H(8A)	-608	4809	1536	25
H(8B)	487	5112	1817	25
H(10A)	-671	1808	-1624	43
H(10B)	237	2342	-1301	43
H(10C)	-665	2337	-679	43
H(11A)	-941	791	-525	38
H(11B)	-883	1289	459	38
H(11C)	-172	609	478	38
H(12A)	1172	601	-536	44
H(12B)	1412	1299	-1149	44
H(12C)	459	826	-1559	44
H(14A)	1187	516	1855	66
H(14B)	1067	1145	2640	66
H(14C)	2044	666	2796	66
H(15A)	3278	826	1574	52
H(15B)	2971	1334	607	52
H(15C)	2381	606	707	52
H(16A)	2211	2226	2721	70
H(16B)	2923	2302	1890	70
H(16C)	3158	1720	2778	70
H(1)	1597(18)	2418(13)	296(18)	21(6)

Figure VI. ORTEP3 Drawing of 15.

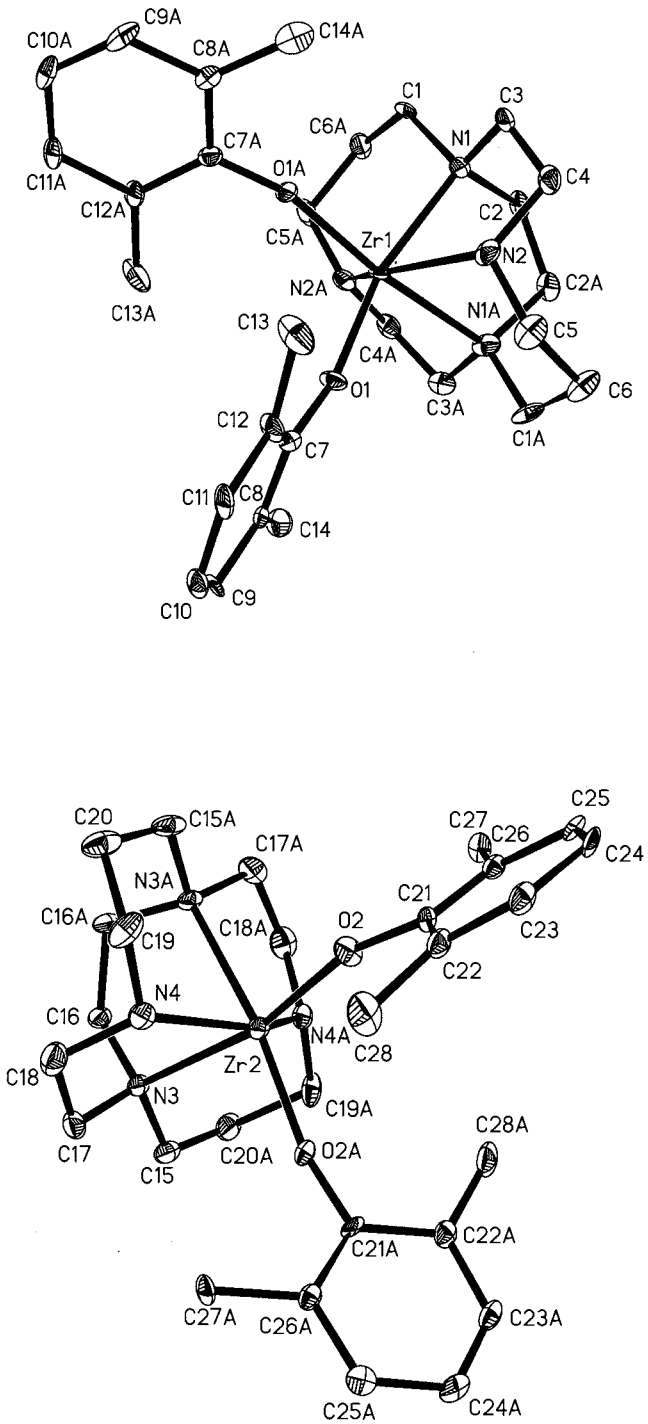

Table XXI. Atomic Coordinates (x 10^4) and Equivalent Isotropic Displacement Parameters ($Å^2$ x 10^3) for 15.

	x	y	z	U(eq)
C(1)	11748(4)	-1522(4)	5262(3)	30(1)
C(2)	10502(5)	-369(6)	5998(3)	31(1)
C(3)	12037(3)	512(4)	5333(3)	27(1)
C(4)	11511(4)	1651(5)	5244(3)	29(1)
C(5)	9884(4)	2543(5)	4693(4)	35(1)
C(6)	9003(4)	2567(4)	5255(3)	36(1)
C(7)	8395(4)	1029(4)	3150(3)	22(1)
C(8)	7285(4)	732(4)	3017(3)	20(1)
C(9)	6765(4)	1205(4)	2434(3)	30(1)
C(10)	7296(4)	1935(4)	2019(3)	29(1)
C(11)	8423(4)	2197(4)	2136(3)	27(1)
C(12)	8980(4)	1737(5)	2708(3)	27(1)
C(13)	10200(5)	1964(7)	2803(4)	49(2)
C(14)	6707(6)	-29(4)	3491(5)	39(2)
C(15)	6766(4)	3515(4)	3721(3)	34(1)
C(16)	5448(4)	4520(4)	3026(3)	25(1)
C(17)	4826(4)	2896(4)	3700(3)	33(1)
C(18)	3623(4)	3258(5)	3801(3)	36(1)
C(19)	2474(4)	4701(5)	4324(3)	36(1)
C(20)	2361(4)	5598(4)	3742(3)	39(1)
C(21)	3968(4)	6638(4)	5886(2)	21(1)
C(22)	3246(4)	6084(4)	6364(3)	24(1)
C(23)	2854(4)	6722(4)	6907(3)	27(1)
C(24)	3175(4)	7790(4)	7034(3)	28(1)
C(25)	3932(4)	8307(4)	6582(3)	26(1)
C(26)	4337(3)	7729(4)	6008(3)	21(1)
C(27)	5110(4)	8315(5)	5505(4)	23(1)
C(28)	2938(7)	4879(5)	6255(4)	45(2)
N(1)	11168(3)	-401(4)	5342(3)	28(1)
N(2)	10642(3)	1576(3)	4710(3)	28(1)
N(3)	5556(3)	3888(3)	3680(2)	23(1)
N(4)	3559(3)	4143(3)	4327(2)	26(1)
O(1)	8889(2)	613(3)	3710(2)	27(1)
O(2)	4283(3)	6069(3)	5304(2)	29(1)
Zr(1)	10000	0	4382(1)	20(1)
Zr(2)	5000	5000	4649(1)	21(1)

U(eq) is defined as one third of the trace of the orthogonalized U_{ij} tensor.

Table XXII. Bond Lengths (Å) and Angles (deg) for 15.

Bond Lengths

C(1)-N(1)	1.512(6)	C(15)-C(20)#2	1.484(7)
C(1)-C(6)#1	1.533(7)	C(15)-N(3)	1.512(6)
C(1)-H(1A)	0.9900	C(15)-H(15A)	0.9900
C(1)-H(1B)	0.9900	C(15)-H(15B)	0.9900
C(2)-C(2)#1	1.485(12)	C(16)-N(3)	1.482(7)
C(2)-N(1)	1.502(7)	C(16)-C(16)#2	1.565(9)
C(2)-H(2A)	0.9900	C(16)-H(16A)	0.9900
C(2)-H(2B)	0.9900	C(16)-H(16B)	0.9900
C(3)-N(1)	1.502(6)	C(17)-N(3)	1.469(7)
C(3)-C(4)	1.504(7)	C(17)-C(18)	1.510(7)
C(3)-H(3A)	0.9900	C(17)-H(17A)	0.9900
C(3)-H(3B)	0.9900	C(17)-H(17B)	0.9900
C(4)-N(2)	1.469(6)	C(18)-N(4)	1.471(7)
C(4)-H(4A)	0.9900	C(18)-H(18A)	0.9900
C(4)-H(4B)	0.9900	C(18)-H(18B)	0.9900
C(5)-N(2)	1.464(7)	C(19)-N(4)	1.454(7)
C(5)-C(6)	1.516(7)	C(19)-C(20)	1.562(7)
C(5)-H(5A)	0.9900	C(19)-H(19A)	0.9900
C(5)-H(5B)	0.9900	C(19)-H(19B)	0.9900
C(6)-C(1)#1	1.533(7)	C(20)-C(15)#2	1.484(7)
C(6)-H(6A)	0.9900	C(20)-H(20A)	0.9900
C(6)-H(6B)	0.9900	C(20)-H(20B)	0.9900
C(7)-O(1)	1.333(6)	C(21)-O(2)	1.370(5)
C(7)-C(12)	1.392(7)	C(21)-C(26)	1.392(7)
C(7)-C(8)	1.393(6)	C(21)-C(22)	1.428(7)
C(8)-C(9)	1.409(6)	C(22)-C(23)	1.381(7)
C(8)-C(14)	1.464(9)	C(22)-C(28)	1.498(8)
C(9)-C(10)	1.344(8)	C(23)-C(24)	1.351(7)
C(9)-H(9)	0.9500	C(23)-H(23)	0.9500
C(10)-C(11)	1.398(7)	C(24)-C(25)	1.401(8)
C(10)-H(10)	0.9500	C(24)-H(24)	0.9500
C(11)-C(12)	1.405(7)	C(25)-C(26)	1.397(7)
C(11)-H(11)	0.9500	C(25)-H(25)	0.9500
C(12)-C(13)	1.490(8)	C(26)-C(27)	1.514(7)
C(13)-H(13A)	0.9800	C(27)-H(27A)	0.9800
C(13)-H(13B)	0.9800	C(27)-H(27B)	0.9800
C(13)-H(13C)	0.9800	C(27)-H(27C)	0.9800
C(14)-H(14A)	0.9800	C(28)-H(28A)	0.9800
C(14)-H(14B)	0.9800	C(28)-H(28B)	0.9800
C(14)-H(14C)	0.9800	C(28)-H(28C)	0.9800
		N(1)-Zr(1)	2.377(4)
		N(2)-Zr(1)	2.125(4)

N(3)-Zr(2)	2.394(4)
N(4)-Zr(2)	2.094(4)
O(1)-Zr(1)	1.997(3)
O(2)-Zr(2)	1.994(4)
Zr(1)-O(1)#1	1.997(3)
Zr(1)-N(2)#1	2.125(4)
Zr(1)-N(1)#1	2.377(4)
Zr(2)-O(2)#2	1.994(4)
Zr(2)-N(4)#2	2.094(4)
Zr(2)-N(3)#2	2.394(4)

Bond Angles

N(1)-C(1)-C(6)#1	116.8(4)
N(1)-C(1)-H(1A)	108.1
C(6)#1-C(1)-H(1A)	108.1
N(1)-C(1)-H(1B)	108.1
C(6)#1-C(1)-H(1B)	108.1
H(1A)-C(1)-H(1B)	107.3
C(2)#1-C(2)-N(1)	116.2(3)
C(2)#1-C(2)-H(2A)	108.2
N(1)-C(2)-H(2A)	108.2
C(2)#1-C(2)-H(2B)	108.2
N(1)-C(2)-H(2B)	108.2
H(2A)-C(2)-H(2B)	107.4
N(1)-C(3)-C(4)	111.6(4)
N(1)-C(3)-H(3A)	109.3
C(4)-C(3)-H(3A)	109.3
N(1)-C(3)-H(3B)	109.3
C(4)-C(3)-H(3B)	109.3
H(3A)-C(3)-H(3B)	108.0
N(2)-C(4)-C(3)	108.6(4)
N(2)-C(4)-H(4A)	110.0
C(3)-C(4)-H(4A)	110.0
N(2)-C(4)-H(4B)	110.0
C(3)-C(4)-H(4B)	110.0
H(4A)-C(4)-H(4B)	108.3
N(2)-C(5)-C(6)	115.2(5)
N(2)-C(5)-H(5A)	108.5
C(6)-C(5)-H(5A)	108.5
N(2)-C(5)-H(5B)	108.5
C(6)-C(5)-H(5B)	108.5
H(5A)-C(5)-H(5B)	107.5
C(5)-C(6)-C(1)#1	113.3(5)
C(5)-C(6)-H(6A)	108.9
C(1)#1-C(6)-H(6A)	108.9
C(5)-C(6)-H(6B)	108.9
C(1)#1-C(6)-H(6B)	108.9
H(6A)-C(6)-H(6B)	107.7
O(1)-C(7)-C(12)	120.5(4)
O(1)-C(7)-C(8)	118.5(4)
C(12)-C(7)-C(8)	121.0(5)
C(7)-C(8)-C(9)	117.7(5)
C(7)-C(8)-C(14)	119.2(5)
C(9)-C(8)-C(14)	123.1(5)
C(10)-C(9)-C(8)	122.2(4)
C(10)-C(9)-H(9)	118.9
C(8)-C(9)-H(9)	118.9
C(9)-C(10)-C(11)	120.0(5)
C(9)-C(10)-H(10)	120.0
C(11)-C(10)-H(10)	120.0
C(10)-C(11)-C(12)	119.7(5)
C(10)-C(11)-H(11)	120.1
C(12)-C(11)-H(11)	120.1
C(7)-C(12)-C(11)	119.2(5)
C(7)-C(12)-C(13)	121.5(5)
C(11)-C(12)-C(13)	119.2(5)
C(12)-C(13)-H(13A)	109.5
C(12)-C(13)-H(13B)	109.5
H(13A)-C(13)-H(13B)	109.5
C(12)-C(13)-H(13C)	109.5
H(13A)-C(13)-H(13C)	109.5
H(13B)-C(13)-H(13C)	109.5
C(8)-C(14)-H(14A)	109.5
C(8)-C(14)-H(14B)	109.5
H(14A)-C(14)-H(14B)	109.5
C(8)-C(14)-H(14C)	109.5
H(14A)-C(14)-H(14C)	109.5
H(14B)-C(14)-H(14C)	109.5
C(20)#2-C(15)-N(3)	117.4(4)
C(20)#2-C(15)-H(15A)	107.9
N(3)-C(15)-H(15A)	107.9
C(20)#2-C(15)-H(15B)	107.9
N(3)-C(15)-H(15B)	107.9
H(15A)-C(15)-H(15B)	107.2
N(3)-C(16)-C(16)#2	115.5(3)
N(3)-C(16)-H(16A)	108.4
C(16)#2-C(16)-H(16A)	108.4
N(3)-C(16)-H(16B)	108.4
C(16)#2-C(16)-H(16B)	108.4

H(16A)-C(16)-H(16B)	107.5	H(27A)-C(27)-H(27B)	109.5
N(3)-C(17)-C(18)	109.6(4)	C(26)-C(27)-H(27C)	109.5
N(3)-C(17)-H(17A)	109.7	H(27A)-C(27)-H(27C)	109.5
C(18)-C(17)-H(17A)	109.7	H(27B)-C(27)-H(27C)	109.5
N(3)-C(17)-H(17B)	109.7	C(22)-C(28)-H(28A)	109.5
C(18)-C(17)-H(17B)	109.7	C(22)-C(28)-H(28B)	109.5
H(17A)-C(17)-H(17B)	108.2	H(28A)-C(28)-H(28B)	109.5
N(4)-C(18)-C(17)	110.2(4)	C(22)-C(28)-H(28C)	109.5
N(4)-C(18)-H(18A)	109.6	H(28A)-C(28)-H(28C)	109.5
C(17)-C(18)-H(18A)	109.6	H(28B)-C(28)-H(28C)	109.5
N(4)-C(18)-H(18B)	109.6	C(2)-N(1)-C(3)	110.8(4)
C(17)-C(18)-H(18B)	109.6	C(2)-N(1)-C(1)	110.6(4)
H(18A)-C(18)-H(18B)	108.1	C(3)-N(1)-C(1)	108.9(4)
N(4)-C(19)-C(20)	113.1(4)	C(2)-N(1)-Zr(1)	110.6(3)
N(4)-C(19)-H(19A)	109.0	C(3)-N(1)-Zr(1)	104.4(3)
C(20)-C(19)-H(19A)	109.0	C(1)-N(1)-Zr(1)	111.4(3)
N(4)-C(19)-H(19B)	109.0	C(5)-N(2)-C(4)	113.7(5)
C(20)-C(19)-H(19B)	109.0	C(5)-N(2)-Zr(1)	117.8(3)
H(19A)-C(19)-H(19B)	107.8	C(4)-N(2)-Zr(1)	121.3(3)
C(15)#2-C(20)-C(19)	116.5(5)	C(17)-N(3)-C(16)	112.3(4)
C(15)#2-C(20)-H(20A)	108.2	C(17)-N(3)-C(15)	109.1(4)
C(19)-C(20)-H(20A)	108.2	C(16)-N(3)-C(15)	106.1(4)
C(15)#2-C(20)-H(20B)	108.2	C(17)-N(3)-Zr(2)	105.2(3)
C(19)-C(20)-H(20B)	108.2	C(16)-N(3)-Zr(2)	111.6(3)
H(20A)-C(20)-H(20B)	107.3	C(15)-N(3)-Zr(2)	112.7(3)
O(2)-C(21)-C(26)	121.0(4)	C(19)-N(4)-C(18)	111.8(4)
O(2)-C(21)-C(22)	118.2(4)	C(19)-N(4)-Zr(2)	120.5(3)
C(26)-C(21)-C(22)	120.8(4)	C(18)-N(4)-Zr(2)	121.0(3)
C(23)-C(22)-C(21)	116.5(4)	C(7)-O(1)-Zr(1)	164.2(3)
C(23)-C(22)-C(28)	123.6(5)	C(21)-O(2)-Zr(2)	163.8(3)
C(21)-C(22)-C(28)	119.9(5)	O(1)-Zr(1)-O(1)#1	98.4(2)
C(24)-C(23)-C(22)	124.2(5)	O(1)-Zr(1)-N(2)	96.42(15)
C(24)-C(23)-H(23)	117.9	O(1)#1-Zr(1)-N(2)	106.28(14)
C(22)-C(23)-H(23)	117.9	O(1)-Zr(1)-N(2)#1	106.28(14)
C(23)-C(24)-C(25)	118.8(5)	O(1)#1-Zr(1)-N(2)#1	96.42(15)
C(23)-C(24)-H(24)	120.6	N(2)-Zr(1)-N(2)#1	145.1(3)
C(25)-C(24)-H(24)	120.6	O(1)-Zr(1)-N(1)#1	92.91(14)
C(26)-C(25)-C(24)	120.4(4)	O(1)#1-Zr(1)-N(1)#1	167.12(16)
C(26)-C(25)-H(25)	119.8	N(2)-Zr(1)-N(1)#1	78.32(16)
C(24)-C(25)-H(25)	119.8	N(2)#1-Zr(1)-N(1)#1	74.41(17)
C(21)-C(26)-C(25)	119.1(4)	O(1)-Zr(1)-N(1)	167.12(16)
C(21)-C(26)-C(27)	120.9(4)	O(1)#1-Zr(1)-N(1)	92.91(14)
C(25)-C(26)-C(27)	119.9(5)	N(2)-Zr(1)-N(1)	74.41(17)
C(26)-C(27)-H(27A)	109.5	N(2)#1-Zr(1)-N(1)	78.32(16)
C(26)-C(27)-H(27B)	109.5	N(1)#1-Zr(1)-N(1)	76.6(2)

O(2)#2-Zr(2)-O(2)	100.6(2)	N(4)-Zr(2)-N(3)	73.90(16)
O(2)#2-Zr(2)-N(4)	103.36(14)	N(4)#2-Zr(2)-N(3)	78.95(16)
O(2)-Zr(2)-N(4)	98.64(15)	O(2)#2-Zr(2)-N(3)#2	166.89(16)
O(2)#2-Zr(2)-N(4)#2	98.64(15)	O(2)-Zr(2)-N(3)#2	91.72(14)
O(2)-Zr(2)-N(4)#2	103.36(14)	N(4)-Zr(2)-N(3)#2	78.95(16)
N(4)-Zr(2)-N(4)#2	145.3(3)	N(4)#2-Zr(2)-N(3)#2	73.90(16)
O(2)#2-Zr(2)-N(3)	91.72(14)	N(3)-Zr(2)-N(3)#2	76.4(2)
O(2)-Zr(2)-N(3)	166.89(16)		

Symmetry transformations used to generate equivalent atoms:

#1 -x+2, -y, z #2 -x+1, -y+1, z

Table XXIII. Anisotropic Displacement Parameters ($Å^2$ x 10^3) for 15.

	U_{11}	U_{22}	U_{33}	U_{23}	U_{13}	U_{12}
C(1)	20(2)	38(3)	30(2)	-11(2)	-18(2)	14(2)
C(2)	41(3)	45(3)	6(2)	-2(2)	-3(2)	0(2)
C(3)	23(2)	42(3)	17(2)	-11(2)	-4(2)	0(2)
C(4)	32(2)	39(3)	17(2)	-6(2)	5(2)	-4(2)
C(5)	42(3)	33(3)	29(2)	9(2)	15(2)	-1(2)
C(6)	45(2)	28(2)	34(2)	9(2)	17(2)	14(2)
C(7)	18(2)	26(2)	21(2)	-3(2)	0(2)	5(2)
C(8)	25(2)	18(2)	18(3)	-10(2)	-4(2)	7(2)
C(9)	31(2)	31(2)	27(3)	-17(2)	-23(2)	9(2)
C(10)	48(3)	23(2)	15(2)	-2(2)	-11(2)	10(2)
C(11)	45(3)	25(2)	10(2)	-1(2)	-1(2)	0(2)
C(12)	28(2)	44(3)	10(2)	1(2)	-3(2)	-1(2)
C(13)	33(3)	92(6)	21(3)	4(4)	4(2)	-23(3)
C(14)	38(3)	32(3)	46(5)	-13(2)	-9(3)	2(2)
C(15)	47(3)	39(3)	17(2)	-7(2)	-5(2)	24(2)
C(16)	27(3)	28(3)	19(3)	-5(2)	-2(2)	13(2)
C(17)	51(3)	24(2)	23(2)	-5(2)	-7(2)	-1(2)
C(18)	42(3)	40(3)	26(2)	2(2)	-7(2)	-6(2)
C(19)	34(2)	53(3)	19(2)	15(3)	-1(2)	-3(2)
C(20)	41(2)	48(3)	27(2)	12(2)	5(2)	19(2)
C(21)	30(2)	27(3)	5(2)	-5(2)	1(2)	8(2)
C(22)	31(2)	28(3)	14(2)	2(2)	-3(2)	-1(2)
C(23)	29(2)	40(3)	13(2)	1(2)	2(2)	2(2)
C(24)	33(2)	41(3)	9(2)	-7(2)	-10(2)	9(2)
C(25)	28(2)	31(2)	18(2)	1(2)	-15(2)	3(2)
C(26)	20(2)	27(2)	15(2)	1(2)	0(2)	1(2)

C(27)	30(3)	20(3)	20(3)	4(2)	1(2)	-14(2)
C(28)	78(4)	41(4)	17(3)	3(2)	12(3)	-9(3)
N(1)	23(2)	42(2)	20(2)	-9(2)	-6(2)	8(2)
N(2)	28(2)	37(2)	19(2)	-2(2)	9(1)	6(1)
N(3)	31(2)	26(2)	11(2)	-4(2)	-1(1)	11(1)
N(4)	38(2)	27(2)	14(2)	3(1)	2(2)	3(1)
O(1)	17(1)	50(2)	15(2)	6(2)	-3(1)	7(1)
O(2)	45(2)	27(2)	14(2)	1(2)	11(2)	3(1)
Zr(1)	7(1)	44(1)	9(1)	0	0	5(1)
Zr(2)	28(1)	23(1)	11(1)	0	0	6(1)

The anisotropic displacement factor exponent takes the form:

$-2\pi^2[\, h^2 a^{*2} U_{11} + \ldots + 2\, h\, k\, a^*\, b^*\, U_{12}\,]$

Table XXIV. Hydrogen coordinates (x 10^4) and Isotropic Displacement Parameters ($Å^2$ x10^3) for 15.

	x	y	z	U(eq)
H(1A)	12295	-1604	5642	35
H(1B)	12180	-1508	4827	35
H(2A)	10257	-1143	6107	37
H(2B)	11006	-121	6374	37
H(3A)	12569	374	4951	33
H(3B)	12465	496	5769	33
H(4A)	11174	1901	5684	35
H(4B)	12089	2204	5107	35
H(5A)	9500	2555	4242	42
H(5B)	10340	3236	4727	42
H(6A)	8527	3240	5193	43
H(6B)	9381	2634	5707	43
H(9)	6013	1000	2330	35
H(10)	6906	2272	1646	35
H(11)	8810	2685	1831	32
H(13A)	10343	2172	3283	73
H(13B)	10428	2581	2500	73
H(13C)	10630	1289	2687	73
H(14A)	6472	386	3902	58
H(14B)	7217	-637	3625	58
H(14C)	6046	-347	3263	58
H(15A)	6852	3045	4138	41
H(15B)	6920	3028	3319	41

H(16A)	5258	3983	2655	30
H(16B)	6187	4852	2913	30
H(17A)	5056	2397	4082	39
H(17B)	4896	2472	3263	39
H(18A)	3317	3543	3360	43
H(18B)	3166	2606	3946	43
H(19A)	2356	5069	4775	43
H(19B)	1878	4130	4265	43
H(20A)	2365	5203	3293	46
H(20B)	1621	5966	3790	46
H(23)	2326	6388	7210	33
H(24)	2892	8183	7422	33
H(25)	4172	9054	6667	31
H(27A)	5670	7781	5334	35
H(27B)	5489	8939	5737	35
H(27C)	4671	8605	5117	35
H(28A)	2637	4567	6684	68
H(28B)	3606	4455	6118	68
H(28C)	2370	4826	5892	68

Figure VII. ORTEP3 Drawing of 19.

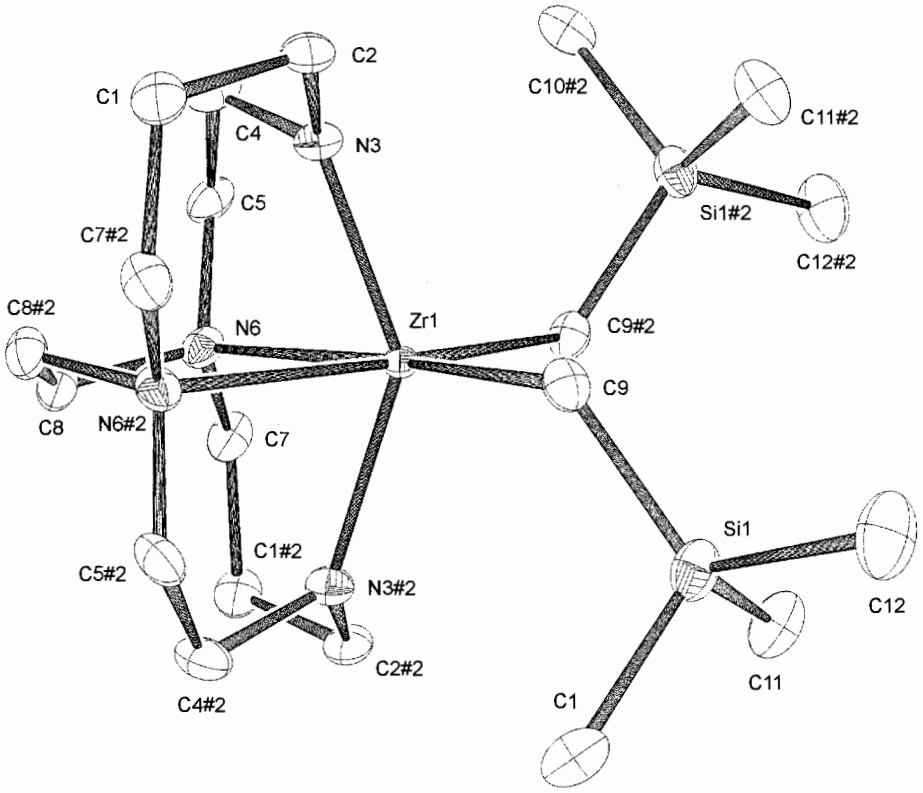

Table XXV. Atomic Coordinates (x 10^4) and Equivalent Isotropic Displacement Parameters ($Å^2$ x 10^3) for 19.

	x	y	z	U(eq)
C(1)	8061(2)	1236(1)	5174(3)	22(1)
C(2)	8629(2)	1850(1)	4694(3)	20(1)
C(4)	10107(2)	1268(1)	4757(3)	22(1)
C(5)	11039(2)	1165(1)	5736(3)	21(1)
C(7)	11904(2)	1190(1)	8199(3)	20(1)
C(8)	10524(2)	462(1)	7647(3)	21(1)
C(9)	8871(2)	2994(1)	7772(3)	18(1)
C(10)	8731(2)	3008(2)	10995(3)	27(1)
C(11)	10147(2)	3950(2)	10042(3)	28(1)
C(12)	8150(2)	4335(2)	9107(4)	34(1)
N(3)	9603(1)	1826(1)	5359(2)	16(1)
N(6)	10962(1)	1139(1)	7275(2)	17(1)
Si(1)	8975(1)	3550(1)	9435(1)	20(1)
Zr(1)	10000	2194(1)	7500	10(1)

U(eq) is defined as one third of the trace of the orthogonalized U_{ij} tensor.

Table XXVI. Bond Lengths (Å) and Angles (deg) for 19.

Bond Lengths		C(5)-H(5B)	0.9900
		C(7)-N(6)	1.502(3)
C(1)-C(7)#1	1.526(4)	C(7)-C(1)#1	1.526(4)
C(1)-C(2)	1.534(4)	C(7)-H(7A)	0.9900
C(1)-H(1A)	0.9900	C(7)-H(7B)	0.9900
C(1)-H(1B)	0.9900	C(8)-N(6)	1.483(3)
C(2)-N(3)	1.464(3)	C(8)-C(8)#1	1.531(5)
C(2)-H(2A)	0.9900	C(8)-H(8A)	0.9900
C(2)-H(2B)	0.9900	C(8)-H(8B)	0.9900
C(4)-N(3)	1.452(3)	C(9)-Si(1)	1.855(3)
C(4)-C(5)	1.521(4)	C(9)-Zr(1)	2.290(2)
C(4)-H(4A)	0.9900	C(9)-H(9A)	0.9900
C(4)-H(4B)	0.9900	C(9)-H(9B)	0.9900
C(5)-N(6)	1.479(3)	C(10)-Si(1)	1.872(3)
C(5)-H(5A)	0.9900	C(10)-H(10A)	0.9800

C(10)-H(10B)	0.9800
C(10)-H(10C)	0.9800
C(11)-Si(1)	1.878(3)
C(11)-H(11A)	0.9800
C(11)-H(11B)	0.9800
C(11)-H(11C)	0.9800
C(12)-Si(1)	1.885(3)
C(12)-H(12A)	0.9800
C(12)-H(12B)	0.9800
C(12)-H(12C)	0.9800
N(3)-Zr(1)	2.103(2)
N(6)-Zr(1)	2.452(2)
Zr(1)-N(3)#1	2.103(2)
Zr(1)-C(9)#1	2.290(2)
Zr(1)-N(6)#1	2.452(2)

Bond Angles

C(7)#1-C(1)-C(2)	115.1(2)
C(7)#1-C(1)-H(1A)	108.5
C(2)-C(1)-H(1A)	108.5
C(7)#1-C(1)-H(1B)	108.5
C(2)-C(1)-H(1B)	108.5
H(1A)-C(1)-H(1B)	107.5
N(3)-C(2)-C(1)	114.1(2)
N(3)-C(2)-H(2A)	108.7
C(1)-C(2)-H(2A)	108.7
N(3)-C(2)-H(2B)	108.7
C(1)-C(2)-H(2B)	108.7
H(2A)-C(2)-H(2B)	107.6
N(3)-C(4)-C(5)	109.4(2)
N(3)-C(4)-H(4A)	109.8
C(5)-C(4)-H(4A)	109.8
N(3)-C(4)-H(4B)	109.8
C(5)-C(4)-H(4B)	109.8
H(4A)-C(4)-H(4B)	108.2
N(6)-C(5)-C(4)	111.3(2)
N(6)-C(5)-H(5A)	109.4
C(4)-C(5)-H(5A)	109.4
N(6)-C(5)-H(5B)	109.4
C(4)-C(5)-H(5B)	109.4
H(5A)-C(5)-H(5B)	108.0
N(6)-C(7)-C(1)#1	115.5(2)
N(6)-C(7)-H(7A)	108.4
C(1)#1-C(7)-H(7A)	108.4
N(6)-C(7)-H(7B)	108.4
C(1)#1-C(7)-H(7B)	108.4
H(7A)-C(7)-H(7B)	107.5
N(6)-C(8)-C(8)#1	115.91(14)
N(6)-C(8)-H(8A)	108.3
C(8)#1-C(8)-H(8A)	108.3
N(6)-C(8)-H(8B)	108.3
C(8)#1-C(8)-H(8B)	108.3
H(8A)-C(8)-H(8B)	107.4
Si(1)-C(9)-Zr(1)	120.69(12)
Si(1)-C(9)-H(9A)	107.2
Zr(1)-C(9)-H(9A)	107.2
Si(1)-C(9)-H(9B)	107.2
Zr(1)-C(9)-H(9B)	107.2
H(9A)-C(9)-H(9B)	106.8
Si(1)-C(10)-H(10A)	109.5
Si(1)-C(10)-H(10B)	109.5
H(10A)-C(10)-H(10B)	109.5
Si(1)-C(10)-H(10C)	109.5
H(10A)-C(10)-H(10C)	109.5
H(10B)-C(10)-H(10C)	109.5
Si(1)-C(11)-H(11A)	109.5
Si(1)-C(11)-H(11B)	109.5
H(11A)-C(11)-H(11B)	109.5
Si(1)-C(11)-H(11C)	109.5
H(11A)-C(11)-H(11C)	109.5
H(11B)-C(11)-H(11C)	109.5
Si(1)-C(12)-H(12A)	109.5
Si(1)-C(12)-H(12B)	109.5
H(12A)-C(12)-H(12B)	109.5
Si(1)-C(12)-H(12C)	109.5
H(12A)-C(12)-H(12C)	109.5
H(12B)-C(12)-H(12C)	109.5
C(4)-N(3)-C(2)	113.50(19)
C(4)-N(3)-Zr(1)	122.27(15)
C(2)-N(3)-Zr(1)	118.04(16)
C(5)-N(6)-C(8)	112.4(2)
C(5)-N(6)-C(7)	109.0(2)
C(8)-N(6)-C(7)	108.68(19)
C(5)-N(6)-Zr(1)	102.53(14)
C(8)-N(6)-Zr(1)	110.94(15)
C(7)-N(6)-Zr(1)	113.23(14)
C(9)-Si(1)-C(10)	111.80(12)
C(9)-Si(1)-C(11)	113.18(13)
C(10)-Si(1)-C(11)	106.35(14)

C(9)-Si(1)-C(12)	110.02(13)	N(3)-Zr(1)-N(6)#1	76.52(8)
C(10)-Si(1)-C(12)	108.65(14)	C(9)-Zr(1)-N(6)#1	92.80(8)
C(11)-Si(1)-C(12)	106.57(13)	C(9)#1-Zr(1)-N(6)#1	167.59(8)
N(3)#1-Zr(1)-N(3)	142.29(11)	N(3)#1-Zr(1)-N(6)	76.52(8)
N(3)#1-Zr(1)-C(9)	100.12(9)	N(3)-Zr(1)-N(6)	73.72(7)
N(3)-Zr(1)-C(9)	103.97(9)	C(9)-Zr(1)-N(6)	167.59(8)
N(3)#1-Zr(1)-C(9)#1	103.97(9)	C(9)#1-Zr(1)-N(6)	92.80(8)
N(3)-Zr(1)-C(9)#1	100.12(9)	N(6)#1-Zr(1)-N(6)	74.78(10)
C(9)-Zr(1)-C(9)#1	99.61(12)		
N(3)#1-Zr(1)-N(6)#1	73.72(7)		

Symmetry transformations used to generate equivalent atoms: #1 -x+2, y, -z+3/2

Table XXVII. Anisotropic Displacement Parameters ($Å^2$ x 10^3) for 19.

	U_{11}	U_{22}	U_{33}	U_{23}	U_{13}	U_{12}
C(1)	18(1)	22(1)	22(1)	1(1)	-8(1)	-2(1)
C(2)	20(1)	22(1)	14(1)	1(1)	-5(1)	-1(1)
C(4)	24(1)	26(1)	15(1)	-5(1)	1(1)	0(1)
C(5)	23(1)	20(1)	21(1)	-8(1)	4(1)	4(1)
C(7)	14(1)	19(1)	25(1)	-4(1)	-2(1)	4(1)
C(8)	21(1)	14(1)	23(1)	-1(1)	-6(1)	1(1)
C(9)	14(1)	17(1)	22(1)	3(1)	1(1)	1(1)
C(10)	25(1)	32(1)	24(1)	-10(1)	5(1)	-1(1)
C(11)	24(1)	25(1)	35(2)	-10(1)	5(1)	-2(1)
C(12)	28(2)	26(2)	49(2)	-5(1)	7(1)	10(1)
N(3)	16(1)	20(1)	13(1)	-1(1)	1(1)	0(1)
N(6)	15(1)	17(1)	16(1)	-3(1)	-2(1)	1(1)
Si(1)	16(1)	18(1)	27(1)	-4(1)	3(1)	2(1)
Zr(1)	10(1)	11(1)	9(1)	0	0(1)	0

The anisotropic displacement factor exponent takes the form:

$-2\pi^2[\, h^2\, a^{*2} U_{11} + \ldots + 2\, h\, k\, a^*\, b^*\, U_{12}\,]$

Table XXVIII. Hydrogen Coordinates (x 10^4) and Isotropic Displacement Parameters (Å^2 x 10^3) for 19.

	x	y	z	U(eq)
H(1A)	7415	1298	4681	27
H(1B)	8278	770	4846	27
H(2A)	8566	1828	3630	24
H(2B)	8374	2319	4935	24
H(4A)	10186	1412	3778	27
H(4B)	9761	807	4676	27
H(5A)	11316	709	5475	25
H(5B)	11447	1569	5586	25
H(7A)	12210	1624	7899	24
H(7B)	12261	761	8005	24
H(8A)	10748	361	8688	25
H(8B)	10730	58	7097	25
H(9A)	8793	3333	6944	21
H(9B)	8295	2715	7674	21
H(10A)	8122	2789	10732	40
H(10B)	8752	3326	11834	40
H(10C)	9192	2625	11237	40
H(11A)	10595	3559	10300	42
H(11B)	10150	4259	10887	42
H(11C)	10307	4239	9257	42
H(12A)	8312	4652	8363	52
H(12B)	8182	4608	10006	52
H(12C)	7526	4151	8780	52

Figure VIII. ORTEP3 Drawing of 20.

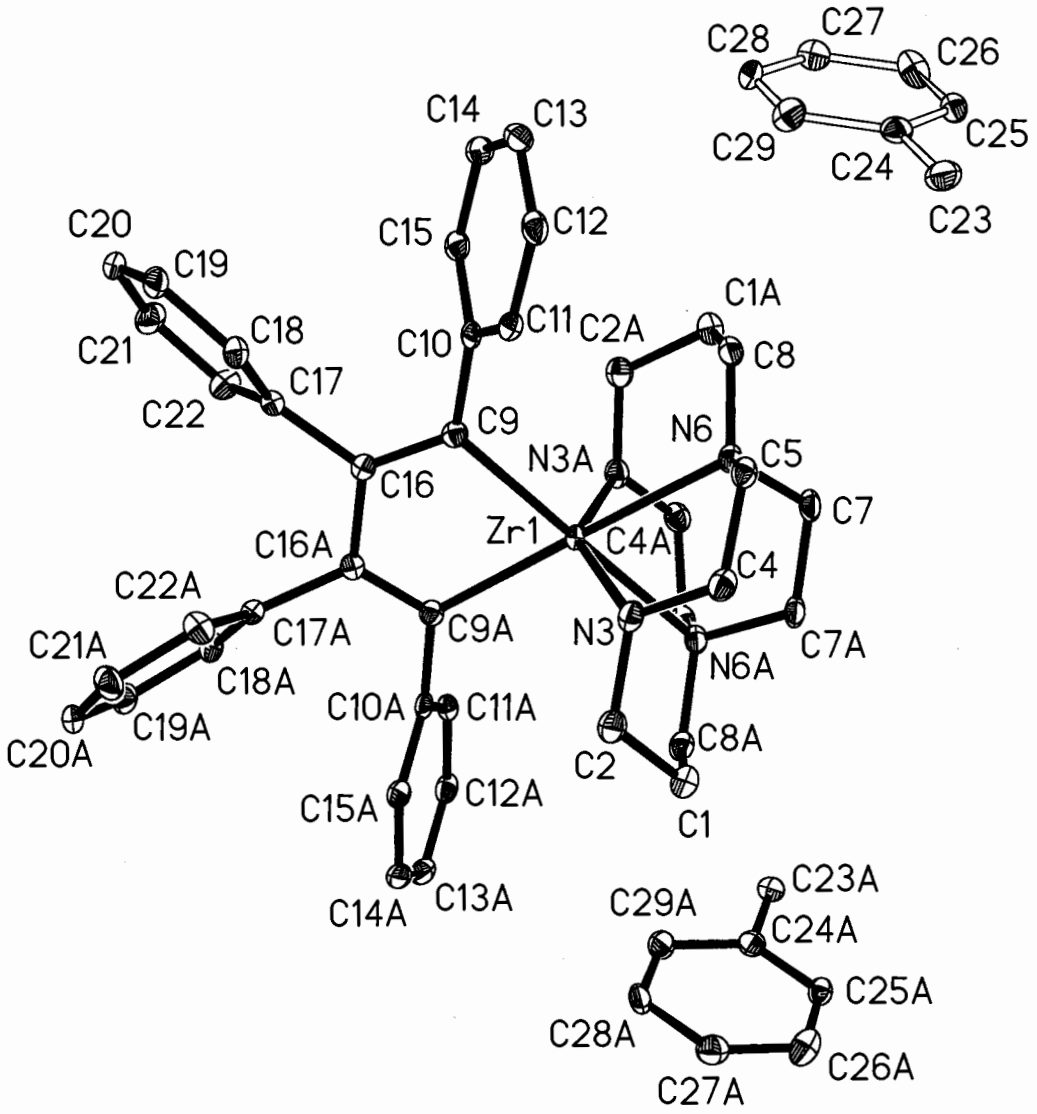

Table XXIX. Atomic Coordinates (x 10^4) and Equivalent Isotropic Displacement Parameters ($Å^2$ x 10^3) for 20.

	x	y	z	U(eq)
C(1)	-301(1)	3591(2)	4247(1)	28(1)
C(2)	290(1)	4499(2)	4099(1)	27(1)
C(4)	1296(1)	3582(2)	3361(1)	28(1)
C(5)	1509(1)	3432(2)	2566(1)	24(1)
C(7)	295(2)	2423(2)	2190(1)	28(1)
C(8)	999(1)	3501(2)	1309(1)	24(1)
C(9)	726(1)	6411(2)	2091(1)	20(1)
C(10)	1430(1)	6370(2)	1617(1)	20(1)
C(11)	2168(1)	6036(2)	1915(1)	22(1)
C(12)	2835(1)	5924(2)	1485(1)	26(1)
C(13)	2783(1)	6140(2)	742(1)	28(1)
C(14)	2059(2)	6466(2)	437(1)	27(1)
C(15)	1392(1)	6581(2)	867(1)	23(1)
C(16)	354(1)	7347(2)	2251(1)	18(1)
C(17)	558(1)	8390(2)	1891(1)	19(1)
C(18)	1327(1)	8817(2)	1895(1)	23(1)
C(19)	1507(2)	9722(2)	1486(1)	28(1)
C(20)	924(2)	10222(2)	1059(1)	29(1)
C(21)	152(2)	9827(2)	1061(1)	31(1)
C(22)	-28(1)	8936(2)	1478(1)	28(1)
N(3)	675(1)	4415(2)	3399(1)	25(1)
N(6)	773(1)	3423(1)	2094(1)	22(1)
Zr(1)	0	4955(1)	2500	15(1)
C(23)	3349(5)	1891(6)	1038(4)	36(2)
C(24)	2852(3)	2224(4)	391(3)	27(1)
C(25)	2500(6)	1498(9)	-72(6)	23(2)
C(26)	2033(3)	1789(5)	-674(4)	33(1)
C(27)	1890(5)	2863(6)	-797(4)	34(2)
C(28)	2239(4)	3633(4)	-336(4)	33(1)
C(29)	2707(7)	3322(9)	267(6)	31(2)

U(eq) is defined as one third of the trace of the orthogonalized U_{ij} tensor.

Table XXX. Bond Lengths (Å) and Angles (deg) for 20.

Bond Lengths

C(1)-C(2)	1.529(3)
C(1)-C(8)#1	1.536(3)
C(1)-H(1A)	0.9900
C(1)-H(1B)	0.9900
C(2)-N(3)	1.449(3)
C(2)-H(2A)	0.9900
C(2)-H(2B)	0.9900
C(4)-N(3)	1.470(3)
C(4)-C(5)	1.513(3)
C(4)-H(4A)	0.9900
C(4)-H(4B)	0.9900
C(5)-N(6)	1.488(3)
C(5)-H(5A)	0.9900
C(5)-H(5B)	0.9900
C(7)-N(6)	1.491(3)
C(7)-C(7)#1	1.520(5)
C(7)-H(7A)	0.9900
C(7)-H(7B)	0.9900
C(8)-N(6)	1.495(3)
C(8)-C(1)#1	1.536(3)
C(8)-H(8A)	0.9900
C(8)-H(8B)	0.9900
C(9)-C(16)	1.354(3)
C(9)-C(10)	1.480(3)
C(9)-Zr(1)	2.313(2)
C(10)-C(15)	1.395(3)
C(10)-C(11)	1.402(3)
C(11)-C(12)	1.389(3)
C(11)-H(11)	0.9500
C(12)-C(13)	1.384(3)
C(12)-H(12)	0.9500
C(13)-C(14)	1.383(4)
C(13)-H(13)	0.9500
C(14)-C(15)	1.388(3)
C(14)-H(14)	0.9500
C(15)-H(15)	0.9500
C(16)-C(17)	1.496(3)
C(16)-C(16)#1	1.511(4)
C(17)-C(18)	1.395(3)
C(17)-C(22)	1.398(3)
C(18)-C(19)	1.387(3)
C(18)-H(18)	0.9500
C(19)-C(20)	1.383(4)
C(19)-H(19)	0.9500
C(20)-C(21)	1.384(4)
C(20)-H(20)	0.9500
C(21)-C(22)	1.380(3)
C(21)-H(21)	0.9500
C(22)-H(22)	0.9500
N(3)-Zr(1)	2.0820(19)
N(6)-Zr(1)	2.4269(19)
Zr(1)-N(3)#1	2.0820(19)
Zr(1)-C(9)#1	2.313(2)
Zr(1)-N(6)#1	2.4269(19)
C(23)-C(24)	1.487(8)
C(23)-H(23A)	0.9800
C(23)-H(23B)	0.9800
C(23)-H(23C)	0.9800
C(24)-C(25)	1.362(12)
C(24)-C(29)	1.402(12)
C(25)-C(26)	1.381(9)
C(25)-H(25A)	0.9500
C(26)-C(27)	1.373(10)
C(26)-H(26A)	0.9500
C(27)-C(28)	1.393(10)
C(27)-H(27A)	0.9500
C(28)-C(29)	1.392(9)
C(28)-H(28A)	0.9500
C(29)-H(29A)	0.9500

Bond Angles

C(2)-C(1)-C(8)#1	115.13(19)
C(2)-C(1)-H(1A)	108.5
C(8)#1-C(1)-H(1A)	108.5
C(2)-C(1)-H(1B)	108.5
C(8)#1-C(1)-H(1B)	108.5
H(1A)-C(1)-H(1B)	107.5

N(3)-C(2)-C(1)	114.0(2)	C(13)-C(14)-C(15)	121.0(2)
N(3)-C(2)-H(2A)	108.8	C(13)-C(14)-H(14)	119.5
C(1)-C(2)-H(2A)	108.8	C(15)-C(14)-H(14)	119.5
N(3)-C(2)-H(2B)	108.8	C(14)-C(15)-C(10)	121.1(2)
C(1)-C(2)-H(2B)	108.8	C(14)-C(15)-H(15)	119.5
H(2A)-C(2)-H(2B)	107.6	C(10)-C(15)-H(15)	119.5
N(3)-C(4)-C(5)	108.33(18)	C(9)-C(16)-C(17)	122.51(19)
N(3)-C(4)-H(4A)	110.0	C(9)-C(16)-C(16)#1	120.13(13)
C(5)-C(4)-H(4A)	110.0	C(17)-C(16)-C(16)#1	117.05(12)
N(3)-C(4)-H(4B)	110.0	C(18)-C(17)-C(22)	117.2(2)
C(5)-C(4)-H(4B)	110.0	C(18)-C(17)-C(16)	123.19(19)
H(4A)-C(4)-H(4B)	108.4	C(22)-C(17)-C(16)	119.46(19)
N(6)-C(5)-C(4)	110.16(18)	C(19)-C(18)-C(17)	121.2(2)
N(6)-C(5)-H(5A)	109.6	C(19)-C(18)-H(18)	119.4
C(4)-C(5)-H(5A)	109.6	C(17)-C(18)-H(18)	119.4
N(6)-C(5)-H(5B)	109.6	C(20)-C(19)-C(18)	120.5(2)
C(4)-C(5)-H(5B)	109.6	C(20)-C(19)-H(19)	119.7
H(5A)-C(5)-H(5B)	108.1	C(18)-C(19)-H(19)	119.7
N(6)-C(7)-C(7)#1	116.62(15)	C(19)-C(20)-C(21)	119.2(2)
N(6)-C(7)-H(7A)	108.1	C(19)-C(20)-H(20)	120.4
C(7)#1-C(7)-H(7A)	108.1	C(21)-C(20)-H(20)	120.4
N(6)-C(7)-H(7B)	108.1	C(22)-C(21)-C(20)	120.1(2)
C(7)#1-C(7)-H(7B)	108.1	C(22)-C(21)-H(21)	119.9
H(7A)-C(7)-H(7B)	107.3	C(20)-C(21)-H(21)	119.9
N(6)-C(8)-C(1)#1	115.55(19)	C(21)-C(22)-C(17)	121.8(2)
N(6)-C(8)-H(8A)	108.4	C(21)-C(22)-H(22)	119.1
C(1)#1-C(8)-H(8A)	108.4	C(17)-C(22)-H(22)	119.1
N(6)-C(8)-H(8B)	108.4	C(2)-N(3)-C(4)	114.96(18)
C(1)#1-C(8)-H(8B)	108.4	C(2)-N(3)-Zr(1)	115.23(14)
H(8A)-C(8)-H(8B)	107.5	C(4)-N(3)-Zr(1)	124.24(15)
C(16)-C(9)-C(10)	122.24(19)	C(5)-N(6)-C(7)	112.26(18)
C(16)-C(9)-Zr(1)	110.62(15)	C(5)-N(6)-C(8)	109.21(17)
C(10)-C(9)-Zr(1)	126.47(15)	C(7)-N(6)-C(8)	108.36(17)
C(15)-C(10)-C(11)	117.1(2)	C(5)-N(6)-Zr(1)	105.05(12)
C(15)-C(10)-C(9)	123.3(2)	C(7)-N(6)-Zr(1)	108.95(13)
C(11)-C(10)-C(9)	119.5(2)	C(8)-N(6)-Zr(1)	113.05(13)
C(12)-C(11)-C(10)	121.8(2)	N(3)#1-Zr(1)-N(3)	142.43(10)
C(12)-C(11)-H(11)	119.1	N(3)#1-Zr(1)-C(9)	106.17(8)
C(10)-C(11)-H(11)	119.1	N(3)-Zr(1)-C(9)	102.99(8)
C(13)-C(12)-C(11)	120.0(2)	N(3)#1-Zr(1)-C(9)#1	102.99(8)
C(13)-C(12)-H(12)	120.0	N(3)-Zr(1)-C(9)#1	106.17(8)
C(11)-C(12)-H(12)	120.0	C(9)-Zr(1)-C(9)#1	77.19(11)
C(14)-C(13)-C(12)	119.1(2)	N(3)#1-Zr(1)-N(6)	78.00(7)
C(14)-C(13)-H(13)	120.5	N(3)-Zr(1)-N(6)	72.74(7)
C(12)-C(13)-H(13)	120.5	C(9)-Zr(1)-N(6)	103.01(7)

C(9)#1-Zr(1)-N(6)	178.91(7)	C(27)-C(26)-H(26A)	120.7
N(3)#1-Zr(1)-N(6)#1	72.74(7)	C(25)-C(26)-H(26A)	120.7
N(3)-Zr(1)-N(6)#1	78.00(7)	C(26)-C(27)-C(28)	119.9(7)
C(9)-Zr(1)-N(6)#1	178.91(7)	C(26)-C(27)-H(27A)	120.0
C(9)#1-Zr(1)-N(6)#1	103.01(7)	C(28)-C(27)-H(27A)	120.0
N(6)-Zr(1)-N(6)#1	76.81(9)	C(29)-C(28)-C(27)	120.5(8)
C(25)-C(24)-C(29)	118.2(6)	C(29)-C(28)-H(28A)	119.8
C(25)-C(24)-C(23)	122.4(7)	C(27)-C(28)-H(28A)	119.8
C(29)-C(24)-C(23)	119.3(7)	C(28)-C(29)-C(24)	119.4(10)
C(24)-C(25)-C(26)	123.3(9)	C(28)-C(29)-H(29A)	120.3
C(24)-C(25)-H(25A)	118.3	C(24)-C(29)-H(29A)	120.3
C(26)-C(25)-H(25A)	118.3		
C(27)-C(26)-C(25)	118.6(7)		

Symmetry transformations used to generate equivalent atoms: #1 -x, y, -z+1/2

Table XXXI. Anisotropic Displacement Parameters ($Å^2$ x 10^3) for 20.

	U_{11}	U_{22}	U_{33}	U_{23}	U_{13}	U_{12}
C(1)	28(1)	24(1)	33(1)	3(1)	-2(1)	-1(1)
C(2)	27(1)	24(1)	29(1)	3(1)	-3(1)	2(1)
C(4)	27(1)	24(1)	32(1)	5(1)	1(1)	2(1)
C(5)	19(1)	20(1)	33(1)	4(1)	1(1)	4(1)
C(7)	28(1)	13(1)	42(2)	-2(1)	8(1)	-2(1)
C(8)	22(1)	20(1)	31(1)	-3(1)	3(1)	1(1)
C(9)	19(1)	20(1)	22(1)	-1(1)	0(1)	-3(1)
C(10)	23(1)	11(1)	26(1)	-4(1)	3(1)	-5(1)
C(11)	24(1)	16(1)	25(1)	0(1)	3(1)	-3(1)
C(12)	21(1)	18(1)	39(1)	-5(1)	3(1)	-3(1)
C(13)	26(1)	23(1)	36(1)	-10(1)	13(1)	-9(1)
C(14)	36(1)	22(1)	24(1)	-6(1)	6(1)	-11(1)
C(15)	26(1)	18(1)	25(1)	-4(1)	-2(1)	-5(1)
C(16)	17(1)	19(1)	18(1)	0(1)	-4(1)	-2(1)
C(17)	20(1)	18(1)	20(1)	-2(1)	1(1)	1(1)
C(18)	23(1)	19(1)	29(1)	-3(1)	-2(1)	-1(1)
C(19)	29(1)	19(1)	36(1)	-4(1)	7(1)	-5(1)
C(20)	43(2)	15(1)	29(1)	2(1)	11(1)	0(1)
C(21)	33(1)	28(1)	33(1)	10(1)	1(1)	6(1)
C(22)	22(1)	30(1)	31(1)	6(1)	-1(1)	-1(1)
N(3)	29(1)	19(1)	27(1)	3(1)	-3(1)	1(1)
N(6)	19(1)	17(1)	31(1)	1(1)	4(1)	0(1)
Zr(1)	15(1)	11(1)	18(1)	0	-2(1)	0
C(23)	52(5)	31(4)	27(4)	-2(3)	10(3)	-10(3)
C(24)	24(3)	28(3)	30(3)	-2(2)	10(2)	-5(2)
C(25)	19(5)	21(4)	28(6)	-2(4)	1(4)	-1(3)
C(26)	18(3)	33(3)	49(4)	-13(3)	-2(3)	-1(2)
C(27)	36(4)	36(4)	31(5)	0(3)	5(3)	1(3)
C(28)	44(4)	16(3)	40(4)	4(3)	17(3)	-1(2)
C(29)	40(7)	27(5)	25(5)	-3(4)	-3(4)	-11(4)

The anisotropic displacement factor exponent takes the form:

$-2\pi^2[\, h^2\, a^{*2} U_{11} + \ldots + 2\, h\, k\, a^*\, b^*\, U_{12}\,]$

Table XXXII. Hydrogen Coordinates (x 10^4) and Isotropic Displacement Parameters ($Å^2$ x 10^3) for 20.

	x	y	z	U(eq)
H(1A)	-520	3698	4741	34
H(1B)	-7	2899	4254	34
H(2A)	5	5195	4120	32
H(2B)	706	4501	4494	32
H(4A)	1097	2896	3565	33
H(4B)	1773	3805	3652	33
H(5A)	1863	4024	2413	29
H(5B)	1799	2744	2509	29
H(7A)	669	1815	2270	33
H(7B)	-4	2281	1726	33
H(8A)	1317	2856	1186	29
H(8B)	1348	4137	1252	29
H(11)	2212	5882	2424	26
H(12)	3328	5699	1702	31
H(13)	3237	6066	444	34
H(14)	2018	6614	-73	33
H(15)	902	6808	645	27
H(18)	1735	8481	2184	28
H(19)	2035	10000	1498	34
H(20)	1051	10830	768	35
H(21)	-255	10170	776	38
H(22)	-563	8685	1484	33
H(23A)	3292	1114	1116	54
H(23B)	3174	2279	1473	54
H(23C)	3910	2061	951	54
H(25A)	2580	753	22	27
H(26A)	1816	1258	-995	40
H(27A)	1553	3081	-1196	41
H(28A)	2156	4377	-434	40
H(29A)	2926	3848	592	37

Figure IX. ORTEP3 Drawing of 24.

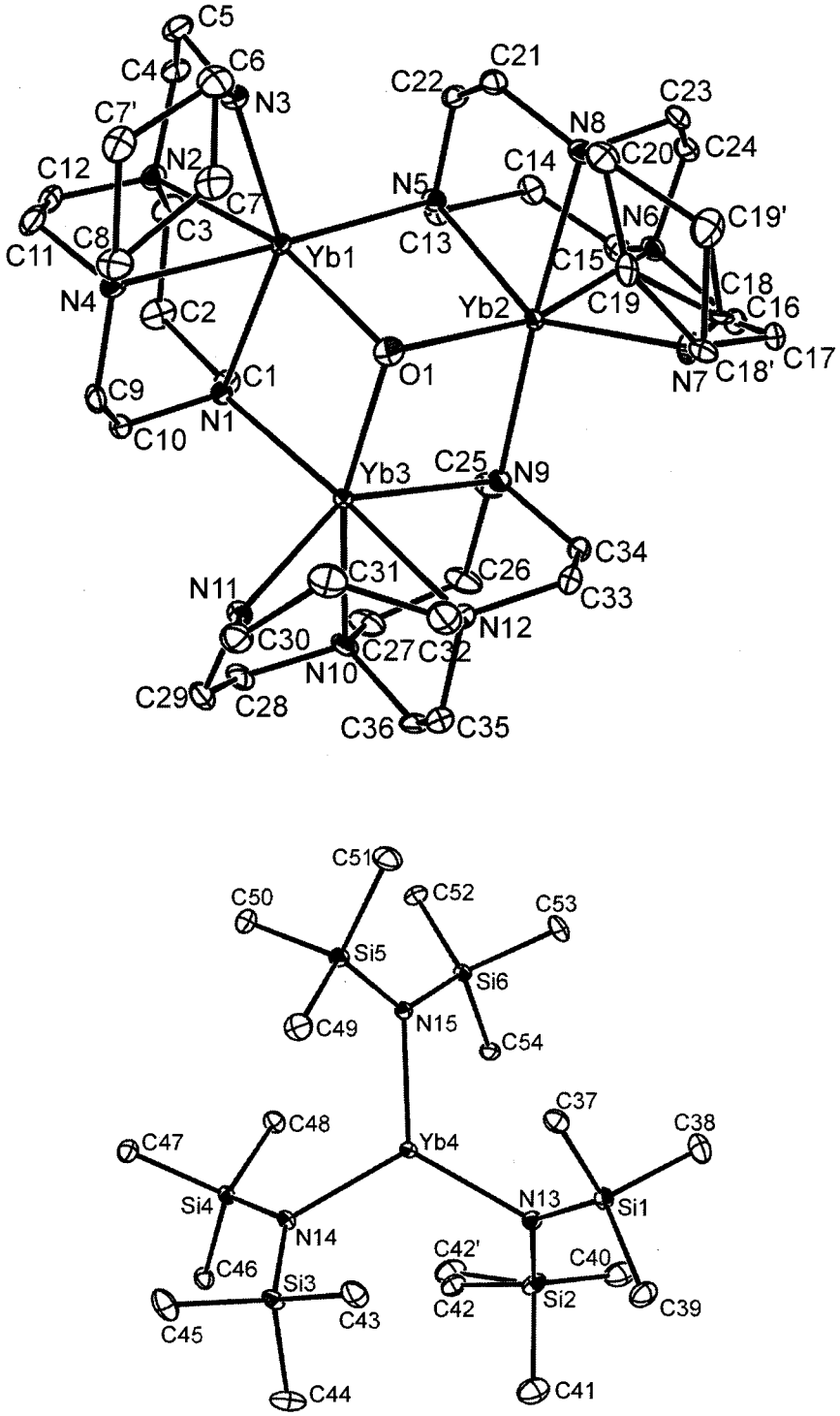

Table XXXIII. Atomic Coordinates (x 10^4) and Equivalent Isotropic Displacement Parameters ($Å^2$ x 10^3) for 24.

	x	y	z	U(eq)
C(1)	2319(2)	6423(2)	419(2)	24(1)
C(2)	2099(2)	5926(2)	852(2)	34(1)
C(3)	2566(2)	6004(2)	1530(2)	31(1)
C(4)	3805(2)	6078(2)	2382(2)	29(1)
C(5)	4728(2)	6104(2)	2599(2)	31(1)
C(6)	5826(2)	6355(2)	2232(2)	34(1)
C(7)	5962(5)	6340(4)	1662(4)	33(2)
C(18)	5405(3)	9588(5)	891(4)	15(2)
C(19)	5856(4)	8940(3)	1165(3)	21(2)
C(7')	5978(5)	5749(4)	1877(4)	30(2)
C(18')	5363(3)	9469(6)	705(4)	27(3)
C(19')	5941(5)	9454(4)	1393(3)	37(2)
C(8)	5511(2)	5711(2)	1212(2)	32(1)
C(9)	4219(2)	5547(2)	418(2)	23(1)
C(10)	3316(2)	5687(2)	207(2)	23(1)
C(11)	4439(3)	5128(2)	1460(2)	34(1)
C(12)	3655(3)	5205(2)	1590(2)	30(1)
C(13)	2745(2)	7966(2)	1500(2)	24(1)
C(14)	2461(2)	8688(2)	1638(2)	28(1)
C(15)	2549(2)	9296(2)	1254(2)	26(1)
C(16)	3341(2)	10006(2)	809(2)	25(1)
C(17)	4154(2)	10142(2)	744(2)	26(1)
C(20)	5827(2)	8824(2)	1792(2)	29(1)
C(21)	4974(2)	8217(2)	2258(2)	24(1)
C(22)	4116(2)	8019(2)	2199(2)	23(1)
C(23)	4802(2)	9471(2)	2048(2)	24(1)
C(24)	3909(2)	9649(2)	1876(2)	25(1)
C(25)	2163(2)	8326(2)	-249(2)	30(1)
C(26)	1572(3)	8155(2)	-889(2)	37(1)
C(27)	1637(2)	7433(2)	-1137(2)	36(1)
C(28)	2399(2)	6500(2)	-1366(2)	28(1)
C(29)	3208(2)	6239(2)	-1375(2)	27(1)
C(30)	4642(2)	6465(2)	-892(2)	30(1)
C(31)	5166(3)	7037(2)	-540(2)	36(1)
C(32)	4913(3)	7781(2)	-773(2)	34(1)
C(33)	4002(3)	8687(2)	-665(2)	34(1)
C(34)	3213(3)	8842(2)	-560(2)	31(1)
C(35)	3543(3)	7821(2)	-1490(2)	35(1)

C(36)	2649(3)	7701(2)	-1621(2)	35(1)
N(1)	3145(2)	6386(1)	393(1)	17(1)
N(2)	3449(2)	5917(2)	1724(1)	22(1)
N(3)	4990(2)	6482(2)	2173(1)	23(1)
N(4)	4621(2)	5673(2)	1076(1)	22(1)
N(5)	3608(2)	7883(1)	1568(1)	19(1)
N(6)	3379(2)	9444(1)	1258(1)	21(1)
N(7)	4533(2)	9495(2)	695(2)	24(1)
N(8)	5000(2)	8785(2)	1842(1)	22(1)
N(9)	3029(2)	8324(1)	-161(1)	21(1)
N(10)	2431(2)	7239(2)	-1182(1)	26(1)
N(11)	3839(2)	6491(1)	-843(1)	21(1)
N(12)	4048(2)	7961(2)	-856(1)	27(1)
O(1)	4497(2)	7494(1)	685(1)	31(1)
Yb(1)	4109(1)	6794(1)	1305(1)	15(1)
Yb(2)	3989(1)	8521(1)	847(1)	15(1)
Yb(3)	3563(1)	7206(1)	-220(1)	14(1)
C(37)	2143(2)	6941(2)	4670(2)	26(1)
C(38)	2686(3)	6727(2)	3590(2)	37(1)
C(39)	1791(2)	8022(2)	3676(2)	35(1)
C(40)	4527(5)	7702(4)	3828(4)	30(1)
C(41)	3573(5)	9001(4)	3788(4)	30(1)
C(42)	4931(8)	8588(7)	4950(6)	30(1)
Si(2)	4072(6)	8254(4)	4286(4)	18(1)
C(40')	4393(7)	7988(5)	3741(5)	46(2)
C(41')	3579(6)	9176(4)	4110(5)	46(2)
C(42')	5020(9)	8484(8)	5008(8)	46(2)
Si(2')	4053(7)	8309(4)	4369(4)	25(2)
C(43)	2487(2)	8795(2)	5589(2)	34(1)
C(44)	3751(3)	9914(2)	5819(2)	44(1)
C(45)	3226(2)	9405(2)	6837(2)	37(1)
C(46)	5683(2)	9284(2)	6833(2)	25(1)
C(47)	5058(2)	8391(2)	7633(2)	26(1)
C(48)	5712(2)	7734(2)	6735(2)	26(1)
C(49)	2928(3)	6922(2)	6601(2)	33(1)
C(50)	4453(3)	6186(2)	7330(2)	30(1)
C(51)	3121(3)	5379(2)	6431(2)	35(1)
C(52)	5356(2)	5371(2)	6276(2)	25(1)
C(53)	3926(2)	5314(2)	5122(2)	29(1)
C(54)	5142(2)	6468(2)	5308(2)	24(1)
N(13)	3453(2)	7775(1)	4565(1)	19(1)
N(14)	4162(2)	8476(1)	6298(1)	19(1)
N(15)	4048(2)	6449(1)	6005(1)	18(1)
Si(1)	2580(1)	7399(1)	4143(1)	21(1)
Si(3)	3469(1)	9112(1)	6155(1)	22(1)

Si(4)	5084(1)	8479(1)	6840(1)	17(1)
Si(5)	3670(1)	6238(1)	6552(1)	20(1)
Si(6)	4582(1)	5926(1)	5706(1)	17(1)
Yb(4)	3969(1)	7561(1)	5617(1)	24(1)
Yb(4')	3719(1)	7567(1)	5600(1)	18(1)

U(eq) is defined as one third of the trace of the orthogonalized U^{ij} tensor.

Table XXXIV. Bond Lengths (Å) and Angles (deg) for 24.

Bond Lengths			
		C(18)-H(18A)	0.9900
		C(18)-H(18B)	0.9900
C(1)-N(1)	1.481(4)	C(19)-C(20)	1.504(7)
C(1)-C(2)	1.540(5)	C(19)-H(19A)	0.9900
C(1)-H(1A)	0.9900	C(19)-H(19B)	0.9900
C(1)-H(1B)	0.9900	C(7')-C(8)	1.497(9)
C(2)-C(3)	1.527(6)	C(7')-H(7'A)	0.9900
C(2)-H(2A)	0.9900	C(7')-H(7'B)	0.9900
C(2)-H(2B)	0.9900	C(18')-N(7)	1.457(5)
C(3)-N(2)	1.475(5)	C(18')-C(19')	1.587(6)
C(3)-H(3A)	0.9900	C(18')-Yb(2)	3.142(8)
C(3)-H(3B)	0.9900	C(18')-H(18C)	0.9900
C(4)-N(2)	1.486(5)	C(18')-H(18D)	0.9900
C(4)-C(5)	1.531(6)	C(19')-C(20)	1.588(6)
C(4)-H(4A)	0.9900	C(19')-H(19C)	0.9900
C(4)-H(4B)	0.9900	C(19')-H(19D)	0.9900
C(5)-N(3)	1.434(5)	C(8)-N(4)	1.493(5)
C(5)-H(5A)	0.9900	C(8)-H(8A)	0.9616
C(5)-H(5B)	0.9900	C(8)-H(8B)	0.9762
C(6)-C(7)	1.435(9)	C(8)-H(8C)	0.9717
C(6)-N(3)	1.454(5)	C(8)-H(8D)	0.9699
C(6)-C(7')	1.512(9)	C(9)-N(4)	1.482(5)
C(6)-H(6A)	0.9703	C(9)-C(10)	1.522(5)
C(6)-H(6B)	0.9638	C(9)-H(9A)	0.9900
C(6)-H(6C)	0.9607	C(9)-H(9B)	0.9900
C(6)-H(6D)	0.9719	C(10)-N(1)	1.480(4)
C(7)-C(8)	1.627(9)	C(10)-H(10A)	0.9900
C(7)-H(7A)	0.9900	C(10)-H(10B)	0.9900
C(7)-H(7B)	0.9900	C(11)-N(4)	1.489(5)
C(18)-N(7)	1.457(5)	C(11)-C(12)	1.521(6)
C(18)-C(19)	1.504(7)	C(11)-H(11A)	0.9900

C(11)-H(11B)	0.9900	C(26)-H(26A)	0.9900
C(12)-N(2)	1.482(5)	C(26)-H(26B)	0.9900
C(12)-H(12A)	0.9900	C(27)-N(10)	1.487(5)
C(12)-H(12B)	0.9900	C(27)-H(27A)	0.9900
C(13)-N(5)	1.482(4)	C(27)-H(27B)	0.9900
C(13)-C(14)	1.551(5)	C(28)-N(10)	1.486(4)
C(13)-H(13A)	0.9900	C(28)-C(29)	1.520(5)
C(13)-H(13B)	0.9900	C(28)-H(28A)	0.9900
C(14)-C(15)	1.520(5)	C(28)-H(28B)	0.9900
C(14)-H(14A)	0.9900	C(29)-N(11)	1.442(5)
C(14)-H(14B)	0.9900	C(29)-H(29A)	0.9900
C(15)-N(6)	1.487(5)	C(29)-H(29B)	0.9900
C(15)-H(15A)	0.9900	C(30)-N(11)	1.460(5)
C(15)-H(15B)	0.9900	C(30)-C(31)	1.494(6)
C(16)-N(6)	1.497(5)	C(30)-H(30A)	0.9900
C(16)-C(17)	1.515(5)	C(30)-H(30B)	0.9900
C(16)-H(16A)	0.9900	C(31)-C(32)	1.546(6)
C(16)-H(16B)	0.9900	C(31)-H(31A)	0.9900
C(17)-N(7)	1.439(4)	C(31)-H(31B)	0.9900
C(17)-H(17A)	0.9900	C(32)-N(12)	1.510(5)
C(17)-H(17B)	0.9900	C(32)-H(32A)	0.9900
C(20)-N(8)	1.504(5)	C(32)-H(32B)	0.9900
C(20)-H(20A)	0.9616	C(33)-N(12)	1.481(5)
C(20)-H(20B)	0.9754	C(33)-C(34)	1.522(6)
C(20)-H(20C)	0.9721	C(33)-H(33A)	0.9900
C(20)-H(20D)	0.9673	C(33)-H(33B)	0.9900
C(21)-N(8)	1.479(5)	C(34)-N(9)	1.479(5)
C(21)-C(22)	1.519(5)	C(34)-H(34A)	0.9900
C(21)-H(21A)	0.9900	C(34)-H(34B)	0.9900
C(21)-H(21B)	0.9900	C(35)-N(12)	1.474(5)
C(22)-N(5)	1.468(4)	C(35)-C(36)	1.516(6)
C(22)-H(22A)	0.9900	C(35)-H(35A)	0.9900
C(22)-H(22B)	0.9900	C(35)-H(35B)	0.9900
C(23)-N(8)	1.490(4)	C(36)-N(10)	1.507(5)
C(23)-C(24)	1.525(5)	C(36)-H(36A)	0.9900
C(23)-H(23A)	0.9900	C(36)-H(36B)	0.9900
C(23)-H(23B)	0.9900	N(1)-Yb(1)	2.367(3)
C(24)-N(6)	1.485(4)	N(1)-Yb(3)	2.416(3)
C(24)-H(24A)	0.9900	N(2)-Yb(1)	2.442(3)
C(24)-H(24B)	0.9900	N(3)-Yb(1)	2.181(3)
C(25)-N(9)	1.470(5)	N(4)-Yb(1)	2.473(3)
C(25)-C(26)	1.543(5)	N(5)-Yb(2)	2.367(3)
C(25)-H(25A)	0.9900	N(5)-Yb(1)	2.439(3)
C(25)-H(25B)	0.9900	N(6)-Yb(2)	2.443(3)
C(26)-C(27)	1.528(6)	N(7)-Yb(2)	2.194(3)

N(8)-Yb(2)	2.457(3)	C(42')-Si(2')	1.876(3)
N(9)-Yb(3)	2.376(3)	C(42')-H(42D)	0.9800
N(9)-Yb(2)	2.421(3)	C(42')-H(42E)	0.9800
N(10)-Yb(3)	2.449(3)	C(42')-H(42F)	0.9800
N(11)-Yb(3)	2.181(3)	Si(2')-N(13)	1.649(12)
N(12)-Yb(3)	2.439(3)	C(43)-Si(3)	1.888(4)
O(1)-Yb(1)	2.255(3)	C(43)-H(43A)	0.9800
O(1)-Yb(2)	2.259(3)	C(43)-H(43B)	0.9800
O(1)-Yb(3)	2.266(3)	C(43)-H(43C)	0.9800
Yb(1)-Yb(3)	3.4642(9)	C(44)-Si(3)	1.879(4)
Yb(1)-Yb(2)	3.4875(7)	C(44)-H(44A)	0.9800
Yb(2)-Yb(3)	3.4605(6)	C(44)-H(44B)	0.9800
C(37)-Si(1)	1.884(4)	C(44)-H(44C)	0.9800
C(37)-H(37A)	0.9800	C(45)-Si(3)	1.878(4)
C(37)-H(37B)	0.9800	C(45)-H(45A)	0.9800
C(37)-H(37C)	0.9800	C(45)-H(45B)	0.9800
C(38)-Si(1)	1.888(4)	C(45)-H(45C)	0.9800
C(38)-H(38A)	0.9800	C(46)-Si(4)	1.882(4)
C(38)-H(38B)	0.9800	C(46)-H(46A)	0.9800
C(38)-H(38C)	0.9800	C(46)-H(46B)	0.9800
C(39)-Si(1)	1.882(4)	C(46)-H(46C)	0.9800
C(39)-H(39A)	0.9800	C(47)-Si(4)	1.881(4)
C(39)-H(39B)	0.9800	C(47)-H(47A)	0.9800
C(39)-H(39C)	0.9800	C(47)-H(47B)	0.9800
C(40)-Si(2)	1.876(3)	C(47)-H(47C)	0.9800
C(40)-H(40A)	0.9800	C(48)-Si(4)	1.882(4)
C(40)-H(40B)	0.9800	C(48)-H(48A)	0.9800
C(40)-H(40C)	0.9800	C(48)-H(48B)	0.9800
C(41)-Si(2)	1.876(3)	C(48)-H(48C)	0.9800
C(41)-H(41A)	0.9800	C(49)-Si(5)	1.888(4)
C(41)-H(41B)	0.9800	C(49)-H(49A)	0.9800
C(41)-H(41C)	0.9800	C(49)-H(49B)	0.9800
C(42)-Si(2)	1.877(3)	C(49)-H(49C)	0.9800
C(42)-H(42A)	0.9800	C(50)-Si(5)	1.877(4)
C(42)-H(42B)	0.9800	C(50)-H(50A)	0.9800
C(42)-H(42C)	0.9800	C(50)-H(50B)	0.9800
Si(2)-N(13)	1.720(10)	C(50)-H(50C)	0.9800
C(40')-Si(2')	1.876(3)	C(51)-Si(5)	1.893(4)
C(40')-H(40D)	0.9800	C(51)-H(51A)	0.9800
C(40')-H(40E)	0.9800	C(51)-H(51B)	0.9800
C(40')-H(40F)	0.9800	C(51)-H(51C)	0.9800
C(41')-Si(2')	1.876(3)	C(52)-Si(6)	1.884(4)
C(41')-H(41D)	0.9800	C(52)-H(52A)	0.9800
C(41')-H(41E)	0.9800	C(52)-H(52B)	0.9800
C(41')-H(41F)	0.9800	C(52)-H(52C)	0.9800

C(53)-Si(6)	1.878(4)
C(53)-H(53A)	0.9800
C(53)-H(53B)	0.9800
C(53)-H(53C)	0.9800
C(54)-Si(6)	1.888(4)
C(54)-H(54A)	0.9800
C(54)-H(54B)	0.9800
C(54)-H(54C)	0.9800
N(13)-Si(1)	1.683(3)
N(13)-Yb(4')	2.343(3)
N(13)-Yb(4)	2.357(3)
N(14)-Si(3)	1.684(3)
N(14)-Si(4)	1.687(3)
N(14)-Yb(4)	2.326(3)
N(14)-Yb(4')	2.345(3)
N(15)-Si(5)	1.686(3)
N(15)-Si(6)	1.688(3)
N(15)-Yb(4)	2.317(3)
N(15)-Yb(4')	2.349(3)

Bond Angles

N(1)-C(1)-C(2)	118.0(3)
N(1)-C(1)-H(1A)	107.8
C(2)-C(1)-H(1A)	107.8
N(1)-C(1)-H(1B)	107.8
C(2)-C(1)-H(1B)	107.8
H(1A)-C(1)-H(1B)	107.1
C(3)-C(2)-C(1)	117.1(3)
C(3)-C(2)-H(2A)	108.0
C(1)-C(2)-H(2A)	108.0
C(3)-C(2)-H(2B)	108.0
C(1)-C(2)-H(2B)	108.0
H(2A)-C(2)-H(2B)	107.3
N(2)-C(3)-C(2)	116.6(3)
N(2)-C(3)-H(3A)	108.1
C(2)-C(3)-H(3A)	108.1
N(2)-C(3)-H(3B)	108.1
C(2)-C(3)-H(3B)	108.1
H(3A)-C(3)-H(3B)	107.3
N(2)-C(4)-C(5)	112.2(3)
N(2)-C(4)-H(4A)	109.2
C(5)-C(4)-H(4A)	109.2
N(2)-C(4)-H(4B)	109.2
C(5)-C(4)-H(4B)	109.2
H(4A)-C(4)-H(4B)	107.9
N(3)-C(5)-C(4)	110.0(3)
N(3)-C(5)-H(5A)	109.7
C(4)-C(5)-H(5A)	109.7
N(3)-C(5)-H(5B)	109.7
C(4)-C(5)-H(5B)	109.7
H(5A)-C(5)-H(5B)	108.2
C(7)-C(6)-N(3)	113.7(4)
N(3)-C(6)-C(7')	116.3(4)
C(7)-C(6)-H(6A)	108.8
N(3)-C(6)-H(6A)	108.7
C(7')-C(6)-H(6A)	134.9
C(7)-C(6)-H(6B)	109.6
N(3)-C(6)-H(6B)	109.1
C(7')-C(6)-H(6B)	61.9
H(6A)-C(6)-H(6B)	106.7
C(7)-C(6)-H(6C)	62.9
N(3)-C(6)-H(6C)	108.7
C(7')-C(6)-H(6C)	108.9
H(6A)-C(6)-H(6C)	50.4
H(6B)-C(6)-H(6C)	140.8
C(7)-C(6)-H(6D)	138.1
N(3)-C(6)-H(6D)	108.1
C(7')-C(6)-H(6D)	108.0
H(6A)-C(6)-H(6D)	58.2
H(6B)-C(6)-H(6D)	51.2
H(6C)-C(6)-H(6D)	106.5
C(6)-C(7)-C(8)	114.8(6)
C(6)-C(7)-H(7A)	108.6
C(8)-C(7)-H(7A)	108.6
C(6)-C(7)-H(7B)	108.6
C(8)-C(7)-H(7B)	108.6
H(7A)-C(7)-H(7B)	107.5
C(8)-C(7)-H(6C)	152.4
H(7A)-C(7)-H(6C)	94.3
H(7B)-C(7)-H(6C)	77.6
C(6)-C(7)-H(8D)	145.7
H(7A)-C(7)-H(8D)	100.6
H(7B)-C(7)-H(8D)	78.4
H(6C)-C(7)-H(8D)	154.7
N(7)-C(18)-C(19)	112.3(6)
N(7)-C(18)-H(18A)	109.1
C(19)-C(18)-H(18A)	109.1
N(7)-C(18)-H(18B)	109.1
C(19)-C(18)-H(18B)	109.1

H(18A)-C(18)-H(18B)	107.9	C(7)-C(8)-H(8A)	109.0
C(20)-C(19)-C(18)	110.6(6)	N(4)-C(8)-H(8B)	108.8
C(20)-C(19)-H(19A)	109.5	C(7')-C(8)-H(8B)	137.6
C(18)-C(19)-H(19A)	109.5	C(7)-C(8)-H(8B)	107.8
C(20)-C(19)-H(19B)	109.5	H(8A)-C(8)-H(8B)	106.2
C(18)-C(19)-H(19B)	109.5	N(4)-C(8)-H(8C)	109.7
H(19A)-C(19)-H(19B)	108.1	C(7')-C(8)-H(8C)	108.8
C(18)-C(19)-H(20D)	144.2	C(7)-C(8)-H(8C)	134.9
H(19A)-C(19)-H(20D)	78.7	H(8B)-C(8)-H(8C)	62.1
H(19B)-C(19)-H(20D)	100.0	N(4)-C(8)-H(8D)	109.7
C(8)-C(7')-C(6)	118.2(5)	C(7')-C(8)-H(8D)	109.2
C(8)-C(7')-H(6B)	148.5	C(7)-C(8)-H(8D)	65.0
C(6)-C(7')-H(8A)	153.4	H(8A)-C(8)-H(8D)	138.2
H(6B)-C(7')-H(8A)	150.2	H(8C)-C(8)-H(8D)	106.3
C(8)-C(7')-H(7'A)	107.8	N(4)-C(9)-C(10)	112.7(3)
C(6)-C(7')-H(7'A)	107.8	N(4)-C(9)-H(9A)	109.1
H(6B)-C(7')-H(7'A)	101.5	C(10)-C(9)-H(9A)	109.1
H(8A)-C(7')-H(7'A)	94.7	N(4)-C(9)-H(9B)	109.1
C(8)-C(7')-H(7'B)	107.8	C(10)-C(9)-H(9B)	109.1
C(6)-C(7')-H(7'B)	107.8	H(9A)-C(9)-H(9B)	107.8
H(6B)-C(7')-H(7'B)	73.5	N(1)-C(10)-C(9)	111.1(3)
H(8A)-C(7')-H(7'B)	77.9	N(1)-C(10)-H(10A)	109.4
H(7'A)-C(7')-H(7'B)	107.1	C(9)-C(10)-H(10A)	109.4
N(7)-C(18')-C(19')	108.1(5)	N(1)-C(10)-H(10B)	109.4
C(19')-C(18')-Yb(2)	97.6(5)	C(9)-C(10)-H(10B)	109.4
N(7)-C(18')-H(18C)	110.1	H(10A)-C(10)-H(10B)	108.0
C(19')-C(18')-H(18C)	110.1	N(4)-C(11)-C(12)	116.7(3)
Yb(2)-C(18')-H(18C)	144.9	N(4)-C(11)-H(11A)	108.1
N(7)-C(18')-H(18D)	110.1	C(12)-C(11)-H(11A)	108.1
C(19')-C(18')-H(18D)	110.1	N(4)-C(11)-H(11B)	108.1
Yb(2)-C(18')-H(18D)	80.2	C(12)-C(11)-H(11B)	108.1
H(18C)-C(18')-H(18D)	108.4	H(11A)-C(11)-H(11B)	107.3
C(18')-C(19')-C(20)	116.5(7)	N(2)-C(12)-C(11)	116.0(3)
C(18')-C(19')-H(20A)	149.4	N(2)-C(12)-H(12A)	108.3
C(18')-C(19')-H(19C)	108.2	C(11)-C(12)-H(12A)	108.3
C(20)-C(19')-H(19C)	108.2	N(2)-C(12)-H(12B)	108.3
H(20A)-C(19')-H(19C)	80.6	C(11)-C(12)-H(12B)	108.3
C(18')-C(19')-H(19D)	108.2	H(12A)-C(12)-H(12B)	107.4
C(20)-C(19')-H(19D)	108.2	N(5)-C(13)-C(14)	117.9(3)
H(20A)-C(19')-H(19D)	96.4	N(5)-C(13)-H(13A)	107.8
H(19C)-C(19')-H(19D)	107.3	C(14)-C(13)-H(13A)	107.8
N(4)-C(8)-C(7')	112.9(4)	N(5)-C(13)-H(13B)	107.8
N(4)-C(8)-C(7)	114.9(4)	C(14)-C(13)-H(13B)	107.8
N(4)-C(8)-H(8A)	109.8	H(13A)-C(13)-H(13B)	107.2
C(7')-C(8)-H(8A)	66.3	C(15)-C(14)-C(13)	117.7(3)

C(15)-C(14)-H(14A)	107.9	C(22)-C(21)-H(21B)	109.1
C(13)-C(14)-H(14A)	107.9	H(21A)-C(21)-H(21B)	107.9
C(15)-C(14)-H(14B)	107.9	N(5)-C(22)-C(21)	112.5(3)
C(13)-C(14)-H(14B)	107.9	N(5)-C(22)-H(22A)	109.1
H(14A)-C(14)-H(14B)	107.2	C(21)-C(22)-H(22A)	109.1
N(6)-C(15)-C(14)	116.3(3)	N(5)-C(22)-H(22B)	109.1
N(6)-C(15)-H(15A)	108.2	C(21)-C(22)-H(22B)	109.1
C(14)-C(15)-H(15A)	108.2	H(22A)-C(22)-H(22B)	107.8
N(6)-C(15)-H(15B)	108.2	N(8)-C(23)-C(24)	116.7(3)
C(14)-C(15)-H(15B)	108.2	N(8)-C(23)-H(23A)	108.1
H(15A)-C(15)-H(15B)	107.4	C(24)-C(23)-H(23A)	108.1
N(6)-C(16)-C(17)	112.4(3)	N(8)-C(23)-H(23B)	108.1
N(6)-C(16)-H(16A)	109.1	C(24)-C(23)-H(23B)	108.1
C(17)-C(16)-H(16A)	109.1	H(23A)-C(23)-H(23B)	107.3
N(6)-C(16)-H(16B)	109.1	N(6)-C(24)-C(23)	116.6(3)
C(17)-C(16)-H(16B)	109.1	N(6)-C(24)-H(24A)	108.1
H(16A)-C(16)-H(16B)	107.9	C(23)-C(24)-H(24A)	108.1
N(7)-C(17)-C(16)	109.7(3)	N(6)-C(24)-H(24B)	108.1
N(7)-C(17)-H(17A)	109.7	C(23)-C(24)-H(24B)	108.1
C(16)-C(17)-H(17A)	109.7	H(24A)-C(24)-H(24B)	107.3
N(7)-C(17)-H(17B)	109.7	N(9)-C(25)-C(26)	117.4(3)
C(16)-C(17)-H(17B)	109.7	N(9)-C(25)-H(25A)	108.0
H(17A)-C(17)-H(17B)	108.2	C(26)-C(25)-H(25A)	108.0
N(8)-C(20)-C(19)	116.1(4)	N(9)-C(25)-H(25B)	108.0
N(8)-C(20)-C(19')	113.9(4)	C(26)-C(25)-H(25B)	108.0
N(8)-C(20)-H(20A)	108.8	H(25A)-C(25)-H(25B)	107.2
C(19)-C(20)-H(20A)	108.8	C(27)-C(26)-C(25)	116.9(3)
C(19')-C(20)-H(20A)	70.6	C(27)-C(26)-H(26A)	108.1
N(8)-C(20)-H(20B)	108.1	C(25)-C(26)-H(26A)	108.1
C(19)-C(20)-H(20B)	108.5	C(27)-C(26)-H(26B)	108.1
C(19')-C(20)-H(20B)	136.6	C(25)-C(26)-H(26B)	108.1
H(20A)-C(20)-H(20B)	106.1	H(26A)-C(26)-H(26B)	107.3
N(8)-C(20)-H(20C)	108.8	N(10)-C(27)-C(26)	116.8(3)
C(19)-C(20)-H(20C)	133.8	N(10)-C(27)-H(27A)	108.1
C(19')-C(20)-H(20C)	109.2	C(26)-C(27)-H(27A)	108.1
H(20B)-C(20)-H(20C)	65.3	N(10)-C(27)-H(27B)	108.1
N(8)-C(20)-H(20D)	109.1	C(26)-C(27)-H(27B)	108.1
C(19)-C(20)-H(20D)	69.5	H(27A)-C(27)-H(27B)	107.3
C(19')-C(20)-H(20D)	109.4	N(10)-C(28)-C(29)	112.3(3)
H(20A)-C(20)-H(20D)	137.7	N(10)-C(28)-H(28A)	109.2
H(20C)-C(20)-H(20D)	106.2	C(29)-C(28)-H(28A)	109.2
N(8)-C(21)-C(22)	112.4(3)	N(10)-C(28)-H(28B)	109.2
N(8)-C(21)-H(21A)	109.1	C(29)-C(28)-H(28B)	109.2
C(22)-C(21)-H(21A)	109.1	H(28A)-C(28)-H(28B)	107.9
N(8)-C(21)-H(21B)	109.1	N(11)-C(29)-C(28)	109.1(3)

N(11)-C(29)-H(29A)	109.9	C(35)-C(36)-H(36B)	108.2
C(28)-C(29)-H(29A)	109.9	H(36A)-C(36)-H(36B)	107.4
N(11)-C(29)-H(29B)	109.9	C(10)-N(1)-C(1)	111.0(3)
C(28)-C(29)-H(29B)	109.9	C(10)-N(1)-Yb(1)	114.5(2)
H(29A)-C(29)-H(29B)	108.3	C(1)-N(1)-Yb(1)	111.0(2)
N(11)-C(30)-C(31)	111.4(3)	C(10)-N(1)-Yb(3)	106.8(2)
N(11)-C(30)-H(30A)	109.4	C(1)-N(1)-Yb(3)	119.8(2)
C(31)-C(30)-H(30A)	109.4	Yb(1)-N(1)-Yb(3)	92.81(9)
N(11)-C(30)-H(30B)	109.4	C(3)-N(2)-C(12)	110.5(3)
C(31)-C(30)-H(30B)	109.4	C(3)-N(2)-C(4)	108.9(3)
H(30A)-C(30)-H(30B)	108.0	C(12)-N(2)-C(4)	111.5(3)
C(30)-C(31)-C(32)	116.1(4)	C(3)-N(2)-Yb(1)	113.2(2)
C(30)-C(31)-H(31A)	108.3	C(12)-N(2)-Yb(1)	111.9(2)
C(32)-C(31)-H(31A)	108.3	C(4)-N(2)-Yb(1)	100.4(2)
C(30)-C(31)-H(31B)	108.3	C(5)-N(3)-C(6)	113.9(3)
C(32)-C(31)-H(31B)	108.3	C(5)-N(3)-Yb(1)	119.6(2)
H(31A)-C(31)-H(31B)	107.4	C(6)-N(3)-Yb(1)	120.7(3)
N(12)-C(32)-C(31)	114.7(3)	C(9)-N(4)-C(11)	112.9(3)
N(12)-C(32)-H(32A)	108.6	C(9)-N(4)-C(8)	108.9(3)
C(31)-C(32)-H(32A)	108.6	C(11)-N(4)-C(8)	109.5(3)
N(12)-C(32)-H(32B)	108.6	C(9)-N(4)-Yb(1)	106.8(2)
C(31)-C(32)-H(32B)	108.6	C(11)-N(4)-Yb(1)	108.5(2)
H(32A)-C(32)-H(32B)	107.6	C(8)-N(4)-Yb(1)	110.2(2)
N(12)-C(33)-C(34)	112.5(3)	C(22)-N(5)-C(13)	109.9(3)
N(12)-C(33)-H(33A)	109.1	C(22)-N(5)-Yb(2)	113.7(2)
C(34)-C(33)-H(33A)	109.1	C(13)-N(5)-Yb(2)	113.4(2)
N(12)-C(33)-H(33B)	109.1	C(22)-N(5)-Yb(1)	105.0(2)
C(34)-C(33)-H(33B)	109.1	C(13)-N(5)-Yb(1)	120.9(2)
H(33A)-C(33)-H(33B)	107.8	Yb(2)-N(5)-Yb(1)	93.03(10)
N(9)-C(34)-C(33)	112.2(3)	C(24)-N(6)-C(15)	110.4(3)
N(9)-C(34)-H(34A)	109.2	C(24)-N(6)-C(16)	110.8(3)
C(33)-C(34)-H(34A)	109.2	C(15)-N(6)-C(16)	109.0(3)
N(9)-C(34)-H(34B)	109.2	C(24)-N(6)-Yb(2)	111.4(2)
C(33)-C(34)-H(34B)	109.2	C(15)-N(6)-Yb(2)	115.0(2)
H(34A)-C(34)-H(34B)	107.9	C(16)-N(6)-Yb(2)	99.9(2)
N(12)-C(35)-C(36)	117.5(3)	C(17)-N(7)-C(18')	121.3(5)
N(12)-C(35)-H(35A)	107.9	C(17)-N(7)-C(18)	109.6(4)
C(36)-C(35)-H(35A)	107.9	C(17)-N(7)-Yb(2)	119.4(2)
N(12)-C(35)-H(35B)	107.9	C(18')-N(7)-Yb(2)	117.4(5)
C(36)-C(35)-H(35B)	107.9	C(18)-N(7)-Yb(2)	121.7(4)
H(35A)-C(35)-H(35B)	107.2	C(21)-N(8)-C(23)	112.4(3)
N(10)-C(36)-C(35)	116.2(3)	C(21)-N(8)-C(20)	109.7(3)
N(10)-C(36)-H(36A)	108.2	C(23)-N(8)-C(20)	108.7(3)
C(35)-C(36)-H(36A)	108.2	C(21)-N(8)-Yb(2)	107.2(2)
N(10)-C(36)-H(36B)	108.2	C(23)-N(8)-Yb(2)	108.6(2)

C(20)-N(8)-Yb(2)	110.2(2)	N(4)-Yb(1)-Yb(3)	88.32(7)
C(25)-N(9)-C(34)	110.5(3)	N(3)-Yb(1)-Yb(2)	120.03(8)
C(25)-N(9)-Yb(3)	114.1(2)	O(1)-Yb(1)-Yb(2)	39.47(7)
C(34)-N(9)-Yb(3)	113.6(2)	N(1)-Yb(1)-Yb(2)	95.16(7)
C(25)-N(9)-Yb(2)	118.9(2)	N(5)-Yb(1)-Yb(2)	42.67(7)
C(34)-N(9)-Yb(2)	106.3(2)	N(2)-Yb(1)-Yb(2)	143.11(7)
Yb(3)-N(9)-Yb(2)	92.33(10)	N(4)-Yb(1)-Yb(2)	139.27(7)
C(28)-N(10)-C(27)	108.6(3)	Yb(3)-Yb(1)-Yb(2)	59.71(3)
C(28)-N(10)-C(36)	111.3(3)	N(7)-Yb(2)-O(1)	120.34(11)
C(27)-N(10)-C(36)	111.4(3)	N(7)-Yb(2)-N(5)	143.90(11)
C(28)-N(10)-Yb(3)	100.4(2)	O(1)-Yb(2)-N(5)	83.58(10)
C(27)-N(10)-Yb(3)	115.6(2)	N(7)-Yb(2)-N(9)	100.07(11)
C(36)-N(10)-Yb(3)	109.1(2)	O(1)-Yb(2)-N(9)	83.30(10)
C(29)-N(11)-C(30)	113.7(3)	N(5)-Yb(2)-N(9)	109.93(10)
C(29)-N(11)-Yb(3)	120.7(2)	N(7)-Yb(2)-N(6)	73.39(11)
C(30)-N(11)-Yb(3)	121.2(2)	O(1)-Yb(2)-N(6)	163.51(10)
C(35)-N(12)-C(33)	113.7(3)	N(5)-Yb(2)-N(6)	80.05(10)
C(35)-N(12)-C(32)	108.9(3)	N(9)-Yb(2)-N(6)	104.15(10)
C(33)-N(12)-C(32)	109.7(3)	N(7)-Yb(2)-N(8)	76.14(11)
C(35)-N(12)-Yb(3)	106.8(2)	O(1)-Yb(2)-N(8)	98.12(10)
C(33)-N(12)-Yb(3)	108.2(2)	N(5)-Yb(2)-N(8)	73.80(10)
C(32)-N(12)-Yb(3)	109.4(2)	N(9)-Yb(2)-N(8)	176.18(10)
Yb(1)-O(1)-Yb(2)	101.15(11)	N(6)-Yb(2)-N(8)	75.41(10)
Yb(1)-O(1)-Yb(3)	100.01(11)	N(7)-Yb(2)-C(18')	24.3(2)
Yb(2)-O(1)-Yb(3)	99.75(11)	O(1)-Yb(2)-C(18')	97.5(2)
N(3)-Yb(1)-O(1)	119.41(11)	N(5)-Yb(2)-C(18')	142.71(18)
N(3)-Yb(1)-N(1)	144.52(10)	N(9)-Yb(2)-C(18')	107.19(18)
O(1)-Yb(1)-N(1)	84.16(10)	N(6)-Yb(2)-C(18')	94.35(19)
N(3)-Yb(1)-N(5)	101.91(10)	N(8)-Yb(2)-C(18')	69.14(18)
O(1)-Yb(1)-N(5)	82.04(10)	N(7)-Yb(2)-Yb(3)	120.70(9)
N(1)-Yb(1)-N(5)	107.75(10)	O(1)-Yb(2)-Yb(3)	40.20(7)
N(3)-Yb(1)-N(2)	73.66(11)	N(5)-Yb(2)-Yb(3)	95.16(7)
O(1)-Yb(1)-N(2)	164.90(10)	N(9)-Yb(2)-Yb(3)	43.31(7)
N(1)-Yb(1)-N(2)	80.77(10)	N(6)-Yb(2)-Yb(3)	143.48(7)
N(5)-Yb(1)-N(2)	103.47(10)	N(8)-Yb(2)-Yb(3)	138.30(7)
N(3)-Yb(1)-N(4)	76.38(10)	C(18')-Yb(2)-Yb(3)	109.62(16)
O(1)-Yb(1)-N(4)	99.86(10)	N(7)-Yb(2)-Yb(1)	152.33(8)
N(1)-Yb(1)-N(4)	73.46(10)	O(1)-Yb(2)-Yb(1)	39.38(7)
N(5)-Yb(1)-N(4)	177.89(10)	N(5)-Yb(2)-Yb(1)	44.30(7)
N(2)-Yb(1)-N(4)	74.92(10)	N(9)-Yb(2)-Yb(1)	95.69(7)
N(3)-Yb(1)-Yb(3)	152.26(8)	N(6)-Yb(2)-Yb(1)	124.34(7)
O(1)-Yb(1)-Yb(3)	40.11(7)	N(8)-Yb(2)-Yb(1)	87.60(7)
N(1)-Yb(1)-Yb(3)	44.14(7)	C(18')-Yb(2)-Yb(1)	128.44(19)
N(5)-Yb(1)-Yb(3)	93.74(7)	Yb(3)-Yb(2)-Yb(1)	59.812(15)
N(2)-Yb(1)-Yb(3)	124.88(8)	N(11)-Yb(3)-O(1)	121.69(11)

N(11)-Yb(3)-N(9)	142.80(11)	Si(2)-C(40)-H(40A)	109.5
O(1)-Yb(3)-N(9)	84.19(10)	Si(2)-C(40)-H(40B)	109.5
N(11)-Yb(3)-N(1)	99.53(10)	H(40A)-C(40)-H(40B)	109.5
O(1)-Yb(3)-N(1)	82.83(10)	Si(2)-C(40)-H(40C)	109.5
N(9)-Yb(3)-N(1)	110.71(10)	H(40A)-C(40)-H(40C)	109.5
N(11)-Yb(3)-N(12)	76.38(11)	H(40B)-C(40)-H(40C)	109.5
O(1)-Yb(3)-N(12)	97.59(11)	Si(2)-C(41)-H(41A)	109.5
N(9)-Yb(3)-N(12)	73.82(11)	Si(2)-C(41)-H(41B)	109.5
N(1)-Yb(3)-N(12)	175.46(10)	H(41A)-C(41)-H(41B)	109.5
N(11)-Yb(3)-N(10)	72.40(11)	Si(2)-C(41)-H(41C)	109.5
O(1)-Yb(3)-N(10)	163.51(10)	H(41A)-C(41)-H(41C)	109.5
N(9)-Yb(3)-N(10)	79.39(10)	H(41B)-C(41)-H(41C)	109.5
N(1)-Yb(3)-N(10)	104.26(10)	Si(2)-C(42)-H(42A)	109.5
N(12)-Yb(3)-N(10)	76.53(11)	Si(2)-C(42)-H(42B)	109.5
N(11)-Yb(3)-Yb(2)	154.80(8)	H(42A)-C(42)-H(42B)	109.5
O(1)-Yb(3)-Yb(2)	40.05(7)	Si(2)-C(42)-H(42C)	109.5
N(9)-Yb(3)-Yb(2)	44.36(7)	H(42A)-C(42)-H(42C)	109.5
N(1)-Yb(3)-Yb(2)	94.95(7)	H(42B)-C(42)-H(42C)	109.5
N(12)-Yb(3)-Yb(2)	88.21(7)	N(13)-Si(2)-C(40)	111.3(5)
N(10)-Yb(3)-Yb(2)	123.66(7)	N(13)-Si(2)-C(41)	115.3(6)
N(11)-Yb(3)-Yb(1)	119.90(8)	C(40)-Si(2)-C(41)	106.3(5)
O(1)-Yb(3)-Yb(1)	39.88(7)	N(13)-Si(2)-C(42)	107.9(7)
N(9)-Yb(3)-Yb(1)	97.17(7)	C(40)-Si(2)-C(42)	106.8(9)
N(1)-Yb(3)-Yb(1)	43.04(7)	C(41)-Si(2)-C(42)	109.0(6)
N(12)-Yb(3)-Yb(1)	137.45(8)	Si(2')-C(40')-H(40D)	109.5
N(10)-Yb(3)-Yb(1)	143.94(8)	Si(2')-C(40')-H(40E)	109.5
Yb(2)-Yb(3)-Yb(1)	60.48(3)	H(40D)-C(40')-H(40E)	109.5
Si(1)-C(37)-H(37A)	109.5	Si(2')-C(40')-H(40F)	109.5
Si(1)-C(37)-H(37B)	109.5	H(40D)-C(40')-H(40F)	109.5
H(37A)-C(37)-H(37B)	109.5	H(40E)-C(40')-H(40F)	109.5
Si(1)-C(37)-H(37C)	109.5	Si(2')-C(41')-H(41D)	109.5
H(37A)-C(37)-H(37C)	109.5	Si(2')-C(41')-H(41E)	109.5
H(37B)-C(37)-H(37C)	109.5	H(41D)-C(41')-H(41E)	109.5
Si(1)-C(38)-H(38A)	109.5	Si(2')-C(41')-H(41F)	109.5
Si(1)-C(38)-H(38B)	109.5	H(41D)-C(41')-H(41F)	109.5
H(38A)-C(38)-H(38B)	109.5	H(41E)-C(41')-H(41F)	109.5
Si(1)-C(38)-H(38C)	109.5	Si(2')-C(42')-H(42D)	109.5
H(38A)-C(38)-H(38C)	109.5	Si(2')-C(42')-H(42E)	109.5
H(38B)-C(38)-H(38C)	109.5	H(42D)-C(42')-H(42E)	109.5
Si(1)-C(39)-H(39A)	109.5	Si(2')-C(42')-H(42F)	109.5
Si(1)-C(39)-H(39B)	109.5	H(42D)-C(42')-H(42F)	109.5
H(39A)-C(39)-H(39B)	109.5	H(42E)-C(42')-H(42F)	109.5
Si(1)-C(39)-H(39C)	109.5	N(13)-Si(2')-C(40')	114.7(7)
H(39A)-C(39)-H(39C)	109.5	N(13)-Si(2')-C(41')	113.1(7)
H(39B)-C(39)-H(39C)	109.5	C(40')-Si(2')-C(41')	105.4(6)

N(13)-Si(2')-C(42')	112.7(8)	Si(5)-C(50)-H(50A)	109.5
C(40')-Si(2')-C(42')	103.8(11)	Si(5)-C(50)-H(50B)	109.5
C(41')-Si(2')-C(42')	106.3(7)	H(50A)-C(50)-H(50B)	109.5
Si(3)-C(43)-H(43A)	109.5	Si(5)-C(50)-H(50C)	109.5
Si(3)-C(43)-H(43B)	109.5	H(50A)-C(50)-H(50C)	109.5
H(43A)-C(43)-H(43B)	109.5	H(50B)-C(50)-H(50C)	109.5
Si(3)-C(43)-H(43C)	109.5	Si(5)-C(51)-H(51A)	109.5
H(43A)-C(43)-H(43C)	109.5	Si(5)-C(51)-H(51B)	109.5
H(43B)-C(43)-H(43C)	109.5	H(51A)-C(51)-H(51B)	109.5
Si(3)-C(44)-H(44A)	109.5	Si(5)-C(51)-H(51C)	109.5
Si(3)-C(44)-H(44B)	109.5	H(51A)-C(51)-H(51C)	109.5
H(44A)-C(44)-H(44B)	109.5	H(51B)-C(51)-H(51C)	109.5
Si(3)-C(44)-H(44C)	109.5	Si(6)-C(52)-H(52A)	109.5
H(44A)-C(44)-H(44C)	109.5	Si(6)-C(52)-H(52B)	109.5
H(44B)-C(44)-H(44C)	109.5	H(52A)-C(52)-H(52B)	109.5
Si(3)-C(45)-H(45A)	109.5	Si(6)-C(52)-H(52C)	109.5
Si(3)-C(45)-H(45B)	109.5	H(52A)-C(52)-H(52C)	109.5
H(45A)-C(45)-H(45B)	109.5	H(52B)-C(52)-H(52C)	109.5
Si(3)-C(45)-H(45C)	109.5	Si(6)-C(53)-H(53A)	109.5
H(45A)-C(45)-H(45C)	109.5	Si(6)-C(53)-H(53B)	109.5
H(45B)-C(45)-H(45C)	109.5	H(53A)-C(53)-H(53B)	109.5
Si(4)-C(46)-H(46A)	109.5	Si(6)-C(53)-H(53C)	109.5
Si(4)-C(46)-H(46B)	109.5	H(53A)-C(53)-H(53C)	109.5
H(46A)-C(46)-H(46B)	109.5	H(53B)-C(53)-H(53C)	109.5
Si(4)-C(46)-H(46C)	109.5	Si(6)-C(54)-H(54A)	109.5
H(46A)-C(46)-H(46C)	109.5	Si(6)-C(54)-H(54B)	109.5
H(46B)-C(46)-H(46C)	109.5	H(54A)-C(54)-H(54B)	109.5
Si(4)-C(47)-H(47A)	109.5	Si(6)-C(54)-H(54C)	109.5
Si(4)-C(47)-H(47B)	109.5	H(54A)-C(54)-H(54C)	109.5
H(47A)-C(47)-H(47B)	109.5	H(54B)-C(54)-H(54C)	109.5
Si(4)-C(47)-H(47C)	109.5	Si(2')-N(13)-Si(1)	130.6(4)
H(47A)-C(47)-H(47C)	109.5	Si(1)-N(13)-Si(2)	125.5(4)
H(47B)-C(47)-H(47C)	109.5	Si(2')-N(13)-Yb(4')	118.3(4)
Si(4)-C(48)-H(48A)	109.5	Si(1)-N(13)-Yb(4')	110.74(15)
Si(4)-C(48)-H(48B)	109.5	Si(2)-N(13)-Yb(4')	123.8(3)
H(48A)-C(48)-H(48B)	109.5	Si(2')-N(13)-Yb(4)	110.2(4)
Si(4)-C(48)-H(48C)	109.5	Si(1)-N(13)-Yb(4)	119.23(15)
H(48A)-C(48)-H(48C)	109.5	Si(2)-N(13)-Yb(4)	115.0(3)
H(48B)-C(48)-H(48C)	109.5	Si(3)-N(14)-Si(4)	126.47(17)
Si(5)-C(49)-H(49A)	109.5	Si(3)-N(14)-Yb(4)	119.35(16)
Si(5)-C(49)-H(49B)	109.5	Si(4)-N(14)-Yb(4)	113.46(14)
H(49A)-C(49)-H(49B)	109.5	Si(3)-N(14)-Yb(4')	111.12(15)
Si(5)-C(49)-H(49C)	109.5	Si(4)-N(14)-Yb(4')	122.33(15)
H(49A)-C(49)-H(49C)	109.5	Si(5)-N(15)-Si(6)	126.40(17)
H(49B)-C(49)-H(49C)	109.5	Si(5)-N(15)-Yb(4)	122.35(15)

Si(6)-N(15)-Yb(4)	111.10(14)	C(46)-Si(4)-C(48)	105.87(18)
Si(5)-N(15)-Yb(4')	114.96(14)	N(15)-Si(5)-C(50)	113.67(17)
Si(6)-N(15)-Yb(4')	118.55(15)	N(15)-Si(5)-C(49)	109.80(17)
N(13)-Si(1)-C(37)	108.28(16)	C(50)-Si(5)-C(49)	105.93(19)
N(13)-Si(1)-C(39)	114.36(17)	N(15)-Si(5)-C(51)	114.30(17)
C(37)-Si(1)-C(39)	107.10(19)	C(50)-Si(5)-C(51)	105.50(19)
N(13)-Si(1)-C(38)	114.51(18)	C(49)-Si(5)-C(51)	107.1(2)
C(37)-Si(1)-C(38)	106.64(19)	N(15)-Si(6)-C(53)	112.77(16)
C(39)-Si(1)-C(38)	105.5(2)	N(15)-Si(6)-C(52)	114.60(16)
N(14)-Si(3)-C(45)	114.24(18)	C(53)-Si(6)-C(52)	106.10(18)
N(14)-Si(3)-C(44)	114.01(18)	N(15)-Si(6)-C(54)	109.40(15)
C(45)-Si(3)-C(44)	106.2(2)	C(53)-Si(6)-C(54)	106.53(18)
N(14)-Si(3)-C(43)	109.41(16)	C(52)-Si(6)-C(54)	106.97(17)
C(45)-Si(3)-C(43)	105.9(2)	N(15)-Yb(4)-N(14)	117.34(11)
C(44)-Si(3)-C(43)	106.4(2)	N(15)-Yb(4)-N(13)	121.50(11)
N(14)-Si(4)-C(47)	113.71(17)	N(14)-Yb(4)-N(13)	120.00(11)
N(14)-Si(4)-C(46)	113.26(16)	N(13)-Yb(4')-N(14)	119.75(11)
C(47)-Si(4)-C(46)	106.64(17)	N(13)-Yb(4')-N(15)	120.70(11)
N(14)-Si(4)-C(48)	110.88(16)	N(14)-Yb(4')-N(15)	115.30(11)
C(47)-Si(4)-C(48)	105.90(18)		

Table XXXV. Anisotropic Displacement Parameters ($Å^2$ x 10^3) for 24.

	U^{11}	U^{22}	U^{33}	U^{23}	U^{13}	U^{12}
C(1)	19(2)	26(2)	27(2)	3(2)	8(2)	-4(1)
C(2)	20(2)	48(3)	36(2)	5(2)	10(2)	-10(2)
C(3)	29(2)	38(2)	32(2)	9(2)	17(2)	-2(2)
C(4)	42(2)	29(2)	19(2)	5(2)	15(2)	0(2)
C(5)	35(2)	29(2)	22(2)	9(2)	3(2)	1(2)
C(6)	23(2)	40(2)	33(2)	-1(2)	0(2)	4(2)
C(7)	22(4)	40(5)	35(5)	4(4)	7(4)	13(3)
C(18)	18(4)	23(5)	5(4)	-3(3)	5(3)	-6(3)
C(19)	13(3)	17(3)	32(4)	-2(3)	7(3)	-9(3)
C(7')	19(4)	31(4)	38(5)	6(4)	5(3)	-1(3)
C(18')	41(6)	24(5)	16(6)	-7(4)	12(4)	-5(4)
C(19')	27(4)	35(5)	45(5)	6(4)	9(4)	-6(4)
C(8)	24(2)	40(2)	28(2)	1(2)	4(2)	17(2)
C(9)	33(2)	13(2)	28(2)	-3(1)	15(2)	3(1)
C(10)	31(2)	16(2)	19(2)	-1(1)	6(2)	-7(1)
C(11)	54(3)	24(2)	29(2)	12(2)	20(2)	17(2)
C(12)	47(3)	20(2)	26(2)	8(2)	16(2)	2(2)

C(13)	19(2)	25(2)	30(2)	-2(2)	11(2)	1(1)
C(14)	24(2)	27(2)	35(2)	-5(2)	14(2)	2(2)
C(15)	24(2)	25(2)	29(2)	-6(2)	7(2)	6(2)
C(16)	32(2)	16(2)	22(2)	0(1)	1(2)	8(2)
C(17)	41(2)	13(2)	23(2)	-1(1)	8(2)	-1(2)
C(20)	19(2)	34(2)	29(2)	-4(2)	1(2)	-7(2)
C(21)	24(2)	23(2)	20(2)	-1(2)	0(2)	2(2)
C(22)	26(2)	23(2)	18(2)	2(1)	5(2)	6(2)
C(23)	28(2)	19(2)	19(2)	-6(1)	-1(2)	-5(2)
C(24)	33(2)	19(2)	21(2)	-6(1)	6(2)	2(2)
C(25)	25(2)	35(2)	23(2)	-4(2)	-2(2)	12(2)
C(26)	27(2)	51(3)	24(2)	-11(2)	-5(2)	15(2)
C(27)	24(2)	50(3)	23(2)	-8(2)	-6(2)	5(2)
C(28)	27(2)	27(2)	21(2)	-9(2)	-1(2)	-5(2)
C(29)	35(2)	21(2)	24(2)	-7(2)	7(2)	1(2)
C(30)	33(2)	31(2)	27(2)	-1(2)	13(2)	4(2)
C(31)	31(2)	45(2)	34(2)	-3(2)	13(2)	0(2)
C(32)	41(2)	36(2)	36(2)	-6(2)	26(2)	-11(2)
C(33)	59(3)	18(2)	28(2)	2(2)	18(2)	-6(2)
C(34)	51(3)	15(2)	18(2)	2(1)	2(2)	7(2)
C(35)	61(3)	25(2)	21(2)	2(2)	16(2)	0(2)
C(36)	58(3)	28(2)	10(2)	2(2)	2(2)	9(2)
N(1)	17(1)	15(1)	18(1)	-1(1)	4(1)	-5(1)
N(2)	27(2)	21(2)	22(2)	4(1)	13(1)	-1(1)
N(3)	23(2)	23(2)	19(2)	2(1)	4(1)	1(1)
N(4)	27(2)	21(2)	17(2)	3(1)	5(1)	7(1)
N(5)	18(1)	20(1)	18(1)	-1(1)	6(1)	2(1)
N(6)	23(2)	18(1)	19(2)	-4(1)	4(1)	4(1)
N(7)	21(2)	16(1)	34(2)	3(1)	8(1)	2(1)
N(8)	19(2)	25(2)	18(2)	-4(1)	1(1)	-4(1)
N(9)	25(2)	17(1)	16(1)	0(1)	-1(1)	4(1)
N(10)	31(2)	25(2)	15(2)	-6(1)	1(1)	4(1)
N(11)	23(2)	19(1)	20(2)	-3(1)	7(1)	-2(1)
N(12)	44(2)	20(2)	21(2)	1(1)	14(2)	-4(1)
O(1)	35(2)	29(1)	26(2)	1(1)	7(1)	0(1)
Yb(1)	16(1)	13(1)	13(1)	2(1)	3(1)	1(1)
Yb(2)	18(1)	11(1)	14(1)	-1(1)	3(1)	0(1)
Yb(3)	17(1)	12(1)	12(1)	0(1)	3(1)	0(1)
C(37)	23(2)	23(2)	32(2)	-2(2)	9(2)	1(2)
C(38)	43(3)	38(2)	33(2)	-14(2)	16(2)	-6(2)
C(39)	29(2)	36(2)	31(2)	9(2)	-2(2)	-4(2)
C(40)	30(3)	33(3)	29(3)	8(2)	15(2)	-1(2)
C(41)	30(3)	33(3)	29(3)	8(2)	15(2)	-1(2)
C(42)	30(3)	33(3)	29(3)	8(2)	15(2)	-1(2)
Si(2)	12(2)	28(2)	14(2)	4(1)	5(1)	-4(2)

C(40')	47(4)	43(4)	48(4)	13(3)	17(3)	-3(3)
C(41')	47(4)	43(4)	48(4)	13(3)	17(3)	-3(3)
C(42')	47(4)	43(4)	48(4)	13(3)	17(3)	-3(3)
Si(2')	23(2)	33(2)	24(3)	9(2)	12(2)	8(2)
C(43)	27(2)	29(2)	39(2)	-7(2)	1(2)	11(2)
C(44)	41(3)	22(2)	66(3)	11(2)	16(2)	8(2)
C(45)	26(2)	38(2)	46(3)	-17(2)	11(2)	8(2)
C(46)	27(2)	25(2)	25(2)	-5(2)	11(2)	-7(2)
C(47)	28(2)	30(2)	22(2)	0(2)	10(2)	-2(2)
C(48)	21(2)	25(2)	30(2)	-3(2)	6(2)	3(2)
C(49)	35(2)	34(2)	37(2)	3(2)	21(2)	8(2)
C(50)	39(2)	32(2)	21(2)	2(2)	14(2)	0(2)
C(51)	38(2)	27(2)	44(3)	-1(2)	19(2)	-10(2)
C(52)	25(2)	25(2)	26(2)	8(2)	10(2)	5(2)
C(53)	28(2)	24(2)	33(2)	-14(2)	9(2)	1(2)
C(54)	34(2)	18(2)	24(2)	2(1)	13(2)	4(2)
N(13)	21(2)	18(1)	19(2)	1(1)	7(1)	2(1)
N(14)	23(2)	15(1)	20(2)	-4(1)	8(1)	1(1)
N(15)	23(2)	15(1)	17(1)	-1(1)	9(1)	2(1)
Si(1)	21(1)	22(1)	19(1)	-3(1)	5(1)	0(1)
Si(3)	20(1)	15(1)	29(1)	-3(1)	6(1)	3(1)
Si(4)	18(1)	17(1)	17(1)	-3(1)	8(1)	-1(1)
Si(5)	24(1)	17(1)	21(1)	0(1)	10(1)	-1(1)
Si(6)	19(1)	14(1)	17(1)	-1(1)	6(1)	1(1)
Yb(4)	42(1)	12(1)	17(1)	0(1)	10(1)	1(1)
Yb(4')	24(1)	13(1)	16(1)	-1(1)	6(1)	1(1)

The anisotropic displacement factor exponent takes the form:

$-2\pi^2[\, h^2 a^{*2} U^{11} + \ldots + 2\, h\, k\, a^*\, b^*\, U^{12} \,]$

Table XXXVI. Hydrogen Coordinates (x 10^4) and Isotropic Displacement Parameters ($Å^2$ x 10^3) for 24.

	x	y	z	U(eq)
H(1A)	1934	6342	5	29
H(1B)	2230	6902	533	29
H(2A)	1517	5984	788	41
H(2B)	2175	5446	733	41

H(3A)	2452	6471	1657	38
H(3B)	2352	5662	1751	38
H(4A)	3633	5722	2616	35
H(4B)	3597	6531	2462	35
H(5A)	4935	6331	3002	37
H(5B)	4946	5627	2642	37
H(6A)	6159	6716	2484	41
H(6B)	6000	5924	2443	41
H(8A)	5757	5279	1383	41
H(8B)	5615	5768	831	41
H(20A)	6127	9186	2054	41
H(20B)	6109	8393	1951	41
H(7A)	6550	6302	1743	40
H(7B)	5778	6785	1450	40
H(18A)	5564	9966	1193	18
H(18B)	5557	9727	538	18
H(19A)	5613	8538	905	25
H(19B)	6425	8981	1186	25
H(6C)	6041	6768	2115	25
H(6D)	6132	6279	2658	25
H(8C)	5690	5308	1044	25
H(8D)	5639	6111	1012	25
H(20C)	6224	8859	2198	25
H(20D)	5939	8394	1624	25
H(7'A)	6560	5748	1928	36
H(7'B)	5870	5319	2067	36
H(18C)	5482	9880	498	32
H(18D)	5447	9049	491	32
H(19C)	5863	9890	1588	44
H(19D)	6506	9449	1400	44
H(9A)	4310	5060	326	28
H(9B)	4468	5849	189	28
H(10A)	3088	5647	-241	27
H(10B)	3051	5334	382	27
H(11A)	4889	5114	1853	41
H(11B)	4429	4674	1260	41
H(12A)	3208	5029	1235	36
H(12B)	3684	4905	1940	36
H(13A)	2618	7625	1769	29
H(13B)	2419	7842	1078	29
H(14A)	1885	8650	1597	33
H(14B)	2764	8799	2068	33
H(15A)	2199	9210	829	32
H(15B)	2342	9716	1394	32
H(16A)	3145	10437	941	30

H(16B)	2949	9873	409	30
H(17A)	4082	10426	377	32
H(17B)	4502	10403	1101	32
H(21A)	5268	8362	2681	29
H(21B)	5252	7806	2169	29
H(22A)	4130	7599	2446	27
H(22B)	3873	8398	2363	27
H(23A)	5063	9835	1882	29
H(23B)	5048	9490	2496	29
H(24A)	3702	9426	2174	30
H(24B)	3861	10156	1917	30
H(25A)	2022	8790	-135	36
H(25B)	2069	7990	39	36
H(26A)	1016	8214	-887	45
H(26B)	1652	8500	-1176	45
H(27A)	1499	7089	-875	43
H(27B)	1224	7395	-1547	43
H(28A)	1990	6445	-1775	33
H(28B)	2228	6215	-1080	33
H(29A)	3212	5726	-1378	33
H(29B)	3301	6405	-1745	33
H(30A)	4594	6504	-1324	35
H(30B)	4896	6014	-738	35
H(31A)	5722	6957	-537	43
H(31B)	5180	7008	-115	43
H(32A)	5271	8113	-483	41
H(32B)	4997	7840	-1167	41
H(33A)	4056	9003	-981	41
H(33B)	4458	8777	-286	41
H(34A)	3246	9307	-375	37
H(34B)	2767	8850	-956	37
H(35A)	3764	7407	-1628	42
H(35B)	3600	8216	-1741	42
H(36A)	2388	8156	-1629	42
H(36B)	2418	7497	-2032	42
H(37A)	2076	7272	4966	39
H(37B)	2508	6569	4883	39
H(37C)	1617	6744	4435	39
H(38A)	3092	6384	3807	56
H(38B)	2855	6953	3278	56
H(38C)	2166	6496	3398	56
H(39A)	1708	8387	3940	53
H(39B)	1283	7774	3484	53
H(39C)	1971	8230	3363	53
H(40A)	4798	7303	4070	44

H(40B)	4921	7976	3712	44
H(40C)	4101	7541	3461	44
H(41A)	3322	9305	4007	44
H(41B)	3159	8827	3420	44
H(41C)	3978	9263	3676	44
H(42A)	5195	8200	5212	44
H(42B)	4724	8915	5181	44
H(42C)	5321	8824	4803	44
H(40D)	3921	7898	3379	69
H(40E)	4702	7559	3868	69
H(40F)	4734	8339	3646	69
H(41D)	3077	9113	3766	69
H(41E)	3952	9463	3983	69
H(41F)	3462	9404	4444	69
H(42D)	5299	8045	5153	69
H(42E)	4901	8714	5340	69
H(42F)	5365	8784	4863	69
H(43A)	2314	8375	5746	51
H(43B)	2564	8690	5204	51
H(43C)	2074	9155	5525	51
H(44A)	4260	10100	6098	66
H(44B)	3324	10262	5752	66
H(44C)	3816	9799	5431	66
H(45A)	3070	9004	7029	56
H(45B)	2779	9737	6711	56
H(45C)	3701	9627	7127	56
H(46A)	5711	9352	6426	38
H(46B)	6229	9235	7127	38
H(46C)	5419	9685	6941	38
H(47A)	4737	8768	7714	40
H(47B)	5609	8412	7925	40
H(47C)	4814	7945	7673	40
H(48A)	5745	7754	6326	39
H(48B)	5461	7296	6786	39
H(48C)	6255	7764	7037	39
H(49A)	3192	7377	6664	50
H(49B)	2744	6817	6941	50
H(49C)	2465	6928	6222	50
H(50A)	4761	6619	7420	45
H(50B)	4819	5799	7345	45
H(50C)	4188	6112	7631	45
H(51A)	3489	5009	6405	53
H(51B)	2657	5395	6053	53
H(51C)	2934	5287	6772	53
H(52A)	5088	5080	6493	38

H(52B)	5754	5669	6567	38
H(52C)	5629	5076	6066	38
H(53A)	3622	5020	5308	43
H(53B)	4264	5023	4963	43
H(53C)	3549	5580	4789	43
H(54A)	4759	6765	5006	37
H(54B)	5416	6163	5105	37
H(54C)	5542	6756	5606	37

Figure X. ORTEP3 Drawing of the Cation of 25.

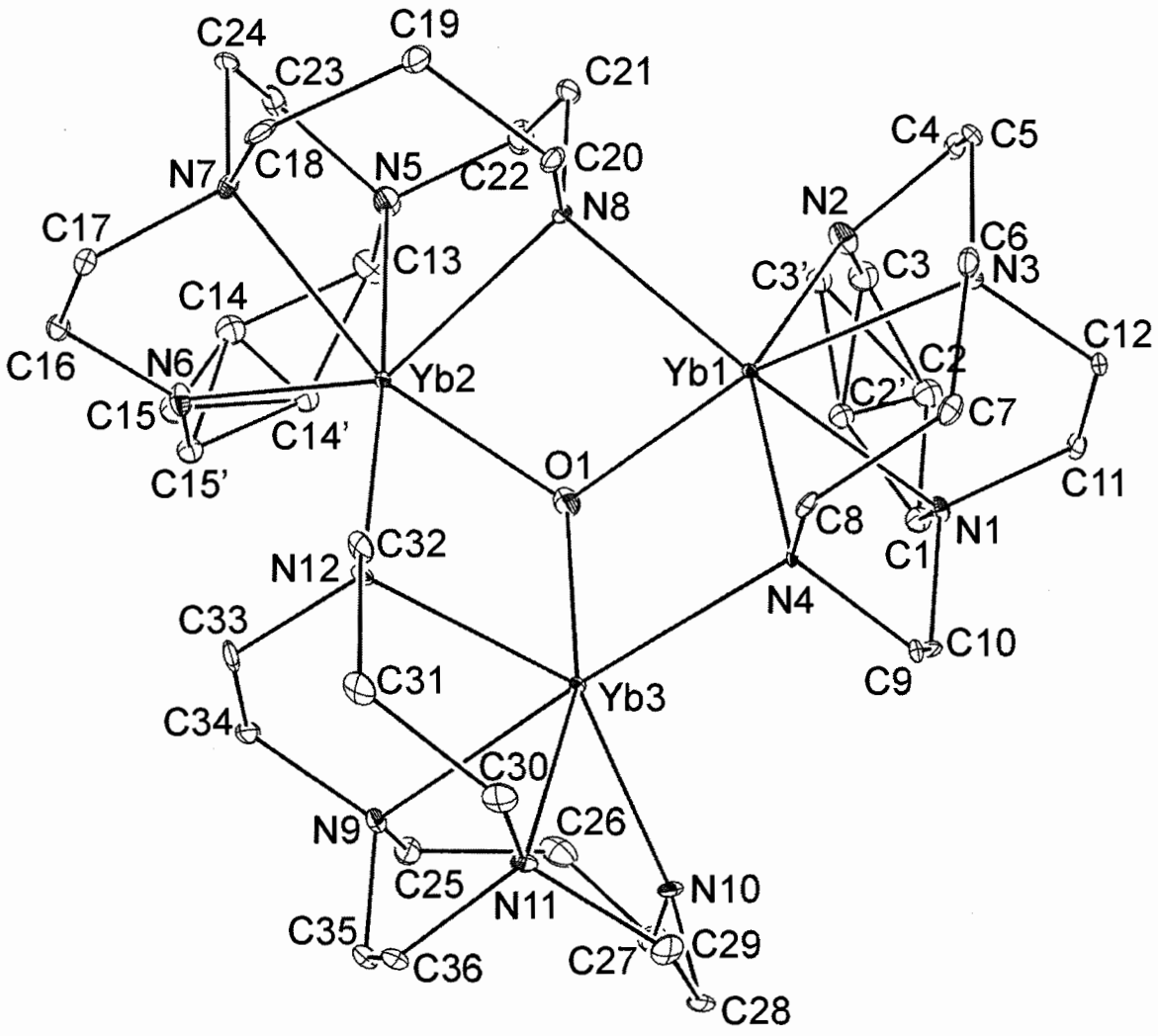

Table XXXVII. Atomic Coordinates (x 10^4) and Equivalent Isotropic Displacement Parameters ($Å^2$ x 10^3) for 25.

	x	y	z	U(eq)
C(2)	7451(11)	3993(10)	1417(3)	28(2)
C(3)	7183(12)	3402(11)	1770(4)	28(2)
C(14)	2302(11)	4442(10)	2475(4)	28(2)
C(15)	1488(13)	4251(12)	2227(4)	28(2)
O(2)	5146(9)	5911(7)	1643(3)	39(2)
C(37)	3988(11)	6162(11)	1651(5)	39(2)
C(38)	3876(13)	7200(11)	1477(5)	39(2)
C(39)	4958(14)	7326(12)	1231(5)	39(2)
C(40)	5480(30)	6321(18)	1259(10)	39(2)
C(2')	6703(16)	4116(12)	1457(4)	20(3)
C(3')	6859(17)	3507(15)	1824(6)	20(3)
C(14')	2659(15)	4575(13)	2184(6)	20(3)
C(15')	1450(17)	4298(15)	2079(6)	20(3)
O(2')	4402(13)	7686(11)	1422(5)	44(4)
C(37')	3758(17)	6826(15)	1537(8)	44(4)
C(38')	4590(20)	6006(15)	1575(8)	44(4)
C(39')	5510(40)	6310(30)	1283(17)	44(4)
C(40')	5200(20)	7318(18)	1129(7)	44(4)
C(1)	6748(6)	3953(5)	1005(2)	20(2)
C(4)	7580(6)	1694(6)	1761(2)	23(2)
C(5)	7178(6)	711(6)	1574(2)	21(2)
C(6)	6083(6)	-136(5)	1022(2)	18(2)
C(7)	5339(6)	-120(5)	620(2)	17(2)
C(8)	4308(5)	574(5)	605(2)	13(1)
C(9)	5195(5)	2043(5)	311(2)	14(1)
C(10)	5784(5)	3004(5)	443(2)	13(1)
C(11)	7474(5)	2331(6)	805(2)	19(2)
C(12)	7367(6)	1204(5)	839(2)	17(2)
C(13)	3523(7)	3969(7)	2444(2)	34(2)
C(16)	460(6)	2742(6)	2291(2)	22(2)
C(17)	565(6)	1620(6)	2223(2)	22(2)
C(18)	1788(6)	194(5)	2132(2)	23(2)
C(19)	2958(6)	-270(6)	2102(2)	25(2)
C(20)	3730(6)	195(5)	1782(2)	19(2)
C(21)	4690(6)	1391(6)	2251(2)	22(2)
C(22)	4625(6)	2453(7)	2393(3)	32(2)
C(23)	2861(6)	2434(7)	2755(2)	31(2)
C(24)	2280(6)	1430(6)	2683(2)	25(2)
C(25)	1764(6)	4992(5)	684(2)	24(2)

C(26)	2969(7)	5137(6)	535(3)	33(2)
C(27)	3193(7)	4732(6)	111(2)	26(2)
C(28)	2750(6)	3258(6)	-302(2)	21(2)
C(29)	2317(6)	2183(6)	-250(2)	24(2)
C(30)	1317(6)	1021(6)	164(2)	22(2)
C(31)	671(6)	749(6)	545(2)	22(2)
C(32)	1244(6)	972(5)	975(2)	19(2)
C(33)	471(6)	2602(6)	1072(2)	24(2)
C(34)	639(6)	3721(6)	1018(2)	22(2)
C(35)	697(6)	3797(6)	247(2)	24(2)
C(36)	591(6)	2741(5)	69(2)	20(2)
O(3)	8829(5)	7544(7)	1398(2)	65(2)
C(41)	9488(8)	6714(8)	1293(3)	54(3)
C(42)	10622(8)	6889(6)	1496(4)	52(3)
C(43)	10695(7)	8013(6)	1563(2)	32(2)
C(44)	9574(8)	8372(8)	1395(3)	56(3)
N(1)	6438(4)	2921(4)	847(2)	14(1)
N(2)	6686(5)	2442(5)	1726(2)	23(1)
N(3)	6595(5)	834(4)	1156(2)	13(1)
N(4)	4501(4)	1660(4)	648(2)	8(1)
N(5)	3484(5)	2862(5)	2405(2)	27(2)
N(6)	1253(5)	3253(4)	2044(2)	21(1)
N(7)	1758(5)	1279(5)	2250(2)	20(1)
N(8)	4063(5)	1256(4)	1837(2)	14(1)
N(9)	1321(5)	3944(4)	656(2)	19(1)
N(10)	3119(5)	3650(4)	102(2)	17(1)
N(11)	1622(5)	2104(5)	118(2)	18(1)
N(12)	1513(4)	2025(4)	1081(2)	13(1)
O(1)	3725(4)	3175(4)	1304(2)	27(1)
Yb(1)	5185(1)	2097(1)	1327(1)	9(1)
Yb(2)	2540(1)	2400(1)	1729(1)	11(1)
Yb(3)	2904(1)	2762(1)	667(1)	9(1)
I(1)	2249(1)	8199(1)	450(1)	20(1)

U(eq) is defined as one third of the trace of the orthogonalized U^{ij} tensor.

Table XXXVIII. Bond Lengths and Angles for 25.

Bond Lengths

C(2)-C(3)	1.427(14)	C(14')-H(14D)	0.9900
C(2)-C(1)	1.521(11)	C(15')-N(6)	1.42(2)
C(2)-H(2A)	0.9900	C(15')-Yb(2)	3.09(2)
C(2)-H(2B)	0.9900	C(15')-H(15C)	0.9900
C(3)-N(2)	1.418(16)	C(15')-H(15D)	0.9900
C(3)-H(3A)	0.9900	O(2')-C(37')	1.440(16)
C(3)-H(3B)	0.9900	O(2')-C(40')	1.449(17)
C(14)-C(15)	1.246(19)	C(37')-C(38')	1.481(17)
C(14)-C(13)	1.590(15)	C(37')-H(37C)	0.9900
C(14)-H(14A)	0.9900	C(37')-H(37D)	0.9900
C(14)-H(14B)	0.9900	C(38')-C(39')	1.528(19)
C(15)-N(6)	1.478(16)	C(38')-H(38C)	0.9900
C(15)-H(15A)	0.9900	C(38')-H(38D)	0.9900
C(15)-H(15B)	0.9900	C(39')-C(40')	1.479(16)
O(2)-C(40)	1.418(17)	C(39')-H(39C)	0.9900
O(2)-C(37)	1.418(13)	C(39')-H(39D)	0.9900
C(37)-C(38)	1.500(15)	C(40')-H(40C)	0.9900
C(37)-H(37A)	0.9900	C(40')-H(40D)	0.9900
C(37)-H(37B)	0.9900	C(1)-N(1)	1.509(9)
C(38)-C(39)	1.549(16)	C(1)-H(1A)	0.9721
C(38)-H(38A)	0.9900	C(1)-H(1B)	0.9669
C(38)-H(38B)	0.9900	C(1)-H(1C)	0.9640
C(39)-C(40)	1.480(14)	C(1)-H(1D)	0.9738
C(39)-H(39A)	0.9900	C(4)-N(2)	1.460(9)
C(39)-H(39B)	0.9900	C(4)-C(5)	1.513(10)
C(40)-H(40A)	0.9900	C(4)-Yb(1)	3.147(7)
C(40)-H(40B)	0.9900	C(4)-H(4A)	0.9900
C(2')-C(3')	1.43(2)	C(4)-H(4B)	0.9900
C(2')-C(1)	1.464(13)	C(5)-N(3)	1.482(8)
C(2')-H(2'1)	0.9900	C(5)-Yb(1)	3.078(7)
C(2')-H(2'2)	0.9900	C(5)-H(5A)	0.9900
C(3')-N(2)	1.47(2)	C(5)-H(5B)	0.9900
C(3')-Yb(1)	3.12(2)	C(6)-N(3)	1.486(9)
C(3')-H(3'1)	0.9900	C(6)-C(7)	1.522(9)
C(3')-H(3'2)	0.9900	C(6)-H(6A)	0.9900
C(14')-C(15')	1.50(3)	C(6)-H(6B)	0.9900
C(14')-C(13)	1.521(19)	C(7)-C(8)	1.536(9)
C(14')-H(14C)	0.9900	C(7)-H(7A)	0.9900
		C(7)-H(7B)	0.9900
		C(8)-N(4)	1.477(8)

C(8)-H(8A)	0.9900	C(21)-H(21A)	0.9900
C(8)-H(8B)	0.9900	C(21)-H(21B)	0.9900
C(9)-N(4)	1.482(8)	C(22)-N(5)	1.465(10)
C(9)-C(10)	1.513(9)	C(22)-Yb(2)	3.178(8)
C(9)-Yb(3)	3.154(6)	C(22)-H(22A)	0.9900
C(9)-H(9A)	0.9900	C(22)-H(22B)	0.9900
C(9)-H(9B)	0.9900	C(23)-N(5)	1.487(10)
C(10)-N(1)	1.475(7)	C(23)-C(24)	1.522(11)
C(10)-Yb(1)	3.187(6)	C(23)-H(23A)	0.9900
C(10)-H(10A)	0.9900	C(23)-H(23B)	0.9900
C(10)-H(10B)	0.9900	C(24)-N(7)	1.501(8)
C(11)-N(1)	1.475(8)	C(24)-H(24A)	0.9900
C(11)-C(12)	1.518(10)	C(24)-H(24B)	0.9900
C(11)-H(11A)	0.9900	C(25)-N(9)	1.499(9)
C(11)-H(11B)	0.9900	C(25)-C(26)	1.543(11)
C(12)-N(3)	1.486(8)	C(25)-H(25A)	0.9900
C(12)-H(12A)	0.9900	C(25)-H(25B)	0.9900
C(12)-H(12B)	0.9900	C(26)-C(27)	1.495(11)
C(13)-N(5)	1.488(11)	C(26)-Yb(3)	3.208(8)
C(13)-H(13A)	0.9737	C(26)-H(26A)	0.9900
C(13)-H(13B)	0.9775	C(26)-H(26B)	0.9900
C(13)-H(13C)	0.9592	C(27)-N(10)	1.451(9)
C(13)-H(13D)	0.9847	C(27)-Yb(3)	3.207(7)
C(16)-N(6)	1.433(9)	C(27)-H(27A)	0.9900
C(16)-C(17)	1.523(10)	C(27)-H(27B)	0.9900
C(16)-Yb(2)	3.163(7)	C(28)-N(10)	1.440(8)
C(16)-H(16A)	0.9900	C(28)-C(29)	1.540(10)
C(16)-H(16B)	0.9900	C(28)-Yb(3)	3.162(7)
C(17)-N(7)	1.487(9)	C(28)-H(28A)	0.9900
C(17)-Yb(2)	3.079(7)	C(28)-H(28B)	0.9900
C(17)-H(17A)	0.9900	C(29)-N(11)	1.475(8)
C(17)-H(17B)	0.9900	C(29)-Yb(3)	3.074(6)
C(18)-N(7)	1.500(9)	C(29)-H(29A)	0.9900
C(18)-C(19)	1.531(10)	C(29)-H(29B)	0.9900
C(18)-H(18A)	0.9900	C(30)-N(11)	1.503(9)
C(18)-H(18B)	0.9900	C(30)-C(31)	1.518(10)
C(19)-C(20)	1.541(9)	C(30)-H(30A)	0.9900
C(19)-H(19A)	0.9900	C(30)-H(30B)	0.9900
C(19)-H(19B)	0.9900	C(31)-C(32)	1.530(9)
C(20)-N(8)	1.482(9)	C(31)-H(31A)	0.9900
C(20)-H(20A)	0.9900	C(31)-H(31B)	0.9900
C(20)-H(20B)	0.9900	C(32)-N(12)	1.480(9)
C(21)-N(8)	1.495(8)	C(32)-H(32A)	0.9900
C(21)-C(22)	1.495(11)	C(32)-H(32B)	0.9900
C(21)-Yb(1)	3.184(7)	C(33)-N(12)	1.458(8)

C(33)-C(34)	1.522(10)	O(1)-Yb(3)	2.279(5)
C(33)-Yb(2)	3.159(7)	Yb(1)-Yb(3)	3.4626(11)
C(33)-H(33A)	0.9900	Yb(2)-Yb(3)	3.4756(8)
C(33)-H(33B)	0.9900		
C(34)-N(9)	1.477(8)	**Bond Angles**	
C(34)-H(34A)	0.9900		
C(34)-H(34B)	0.9900	C(3)-C(2)-C(1)	121.9(10)
C(35)-N(9)	1.481(9)	C(3)-C(2)-H(2A)	106.9
C(35)-C(36)	1.526(10)	C(1)-C(2)-H(2A)	106.9
C(35)-Yb(3)	3.198(7)	C(3)-C(2)-H(2B)	106.9
C(35)-H(35A)	0.9900	C(1)-C(2)-H(2B)	106.9
C(35)-H(35B)	0.9900	H(2A)-C(2)-H(2B)	106.7
C(36)-N(11)	1.495(9)	N(2)-C(3)-C(2)	122.2(12)
C(36)-H(36A)	0.9900	N(2)-C(3)-H(3A)	106.8
C(36)-H(36B)	0.9900	C(2)-C(3)-H(3A)	106.8
O(3)-C(41)	1.410(11)	N(2)-C(3)-H(3B)	106.8
O(3)-C(44)	1.420(11)	C(2)-C(3)-H(3B)	106.8
C(41)-C(42)	1.483(12)	H(3A)-C(3)-H(3B)	106.6
C(41)-H(41A)	0.9900	C(15)-C(14)-C(13)	124.0(12)
C(41)-H(41B)	0.9900	C(15)-C(14)-H(14A)	106.3
C(42)-C(43)	1.522(11)	C(13)-C(14)-H(14A)	106.3
C(42)-H(42A)	0.9900	C(15)-C(14)-H(14B)	106.3
C(42)-H(42B)	0.9900	C(13)-C(14)-H(14B)	106.3
C(43)-C(44)	1.489(11)	H(14A)-C(14)-H(14B)	106.4
C(43)-H(43A)	0.9900	C(14)-C(15)-N(6)	124.2(14)
C(43)-H(43B)	0.9900	C(14)-C(15)-H(15A)	106.3
C(44)-H(44A)	0.9900	N(6)-C(15)-H(15A)	106.3
C(44)-H(44B)	0.9900	C(14)-C(15)-H(15B)	106.3
N(1)-Yb(1)	2.453(5)	N(6)-C(15)-H(15B)	106.3
N(2)-Yb(1)	2.186(6)	H(15A)-C(15)-H(15B)	106.4
N(3)-Yb(1)	2.461(5)	C(40)-O(2)-C(37)	103.6(13)
N(4)-Yb(1)	2.349(5)	O(2)-C(37)-C(38)	106.3(10)
N(4)-Yb(3)	2.406(5)	O(2)-C(37)-H(37A)	110.5
N(5)-Yb(2)	2.460(6)	C(38)-C(37)-H(37A)	110.5
N(6)-Yb(2)	2.194(6)	O(2)-C(37)-H(37B)	110.5
N(7)-Yb(2)	2.459(6)	C(38)-C(37)-H(37B)	110.5
N(8)-Yb(2)	2.382(5)	H(37A)-C(37)-H(37B)	108.7
N(8)-Yb(1)	2.435(5)	C(37)-C(38)-C(39)	103.2(11)
N(9)-Yb(3)	2.457(6)	C(37)-C(38)-H(38A)	111.1
N(10)-Yb(3)	2.187(5)	C(39)-C(38)-H(38A)	111.1
N(11)-Yb(3)	2.427(5)	C(37)-C(38)-H(38B)	111.1
N(12)-Yb(3)	2.383(5)	C(39)-C(38)-H(38B)	111.1
N(12)-Yb(2)	2.400(5)	H(38A)-C(38)-H(38B)	109.1
O(1)-Yb(1)	2.255(5)	C(40)-C(39)-C(38)	103.0(12)
O(1)-Yb(2)	2.257(5)	C(40)-C(39)-H(39A)	111.2

C(38)-C(39)-H(39A)	111.2	H(15C)-C(15')-H(15D)	107.6
C(40)-C(39)-H(39B)	111.2	C(37')-O(2')-C(40')	105.4(14)
C(38)-C(39)-H(39B)	111.2	O(2')-C(37')-C(38')	104.5(14)
H(39A)-C(39)-H(39B)	109.1	O(2')-C(37')-H(37C)	110.8
O(2)-C(40)-C(39)	105.7(14)	C(38')-C(37')-H(37C)	110.8
O(2)-C(40)-H(40A)	110.6	O(2')-C(37')-H(37D)	110.8
C(39)-C(40)-H(40A)	110.6	C(38')-C(37')-H(37D)	110.8
O(2)-C(40)-H(40B)	110.6	H(37C)-C(37')-H(37D)	108.9
C(39)-C(40)-H(40B)	110.6	C(37')-C(38')-C(39')	104.4(15)
H(40A)-C(40)-H(40B)	108.7	C(37')-C(38')-H(38C)	110.9
C(3')-C(2')-C(1)	135.4(14)	C(39')-C(38')-H(38C)	110.9
C(3')-C(2')-H(1B)	149.4	C(37')-C(38')-H(38D)	110.9
C(3')-C(2')-H(2'1)	103.3	C(39')-C(38')-H(38D)	110.9
C(1)-C(2')-H(2'1)	103.3	H(38C)-C(38')-H(38D)	108.9
H(1B)-C(2')-H(2'1)	107.2	C(40')-C(39')-C(38')	105.6(16)
C(3')-C(2')-H(2'2)	103.3	C(40')-C(39')-H(39C)	110.6
C(1)-C(2')-H(2'2)	103.3	C(38')-C(39')-H(39C)	110.6
H(1B)-C(2')-H(2'2)	66.3	C(40')-C(39')-H(39D)	110.6
H(2'1)-C(2')-H(2'2)	105.2	C(38')-C(39')-H(39D)	110.6
C(2')-C(3')-N(2)	111.5(15)	H(39C)-C(39')-H(39D)	108.8
C(2')-C(3')-Yb(1)	82.9(11)	O(2')-C(40')-C(39')	105.0(17)
C(2')-C(3')-H(3'1)	109.3	O(2')-C(40')-H(40C)	110.8
N(2)-C(3')-H(3'1)	109.3	C(39')-C(40')-H(40C)	110.8
Yb(1)-C(3')-H(3'1)	95.7	O(2')-C(40')-H(40D)	110.8
C(2')-C(3')-H(3'2)	109.3	C(39')-C(40')-H(40D)	110.8
N(2)-C(3')-H(3'2)	109.3	H(40C)-C(40')-H(40D)	108.8
Yb(1)-C(3')-H(3'2)	147.0	C(2')-C(1)-N(1)	116.5(8)
H(3'1)-C(3')-H(3'2)	108.0	N(1)-C(1)-C(2)	115.8(7)
C(15')-C(14')-C(13)	126.9(15)	C(2')-C(1)-H(1A)	131.9
C(15')-C(14')-H(13B)	147.5	N(1)-C(1)-H(1A)	108.4
C(15')-C(14')-H(14C)	105.6	C(2)-C(1)-H(1A)	108.6
C(13)-C(14')-H(14C)	105.6	C(2')-C(1)-H(1B)	75.5
H(13B)-C(14')-H(14C)	106.6	N(1)-C(1)-H(1B)	108.8
C(15')-C(14')-H(14D)	105.6	C(2)-C(1)-H(1B)	108.8
C(13)-C(14')-H(14D)	105.6	H(1A)-C(1)-H(1B)	106.0
H(13B)-C(14')-H(14D)	69.3	C(2')-C(1)-H(1C)	108.8
H(14C)-C(14')-H(14D)	106.1	N(1)-C(1)-H(1C)	108.7
N(6)-C(15')-C(14')	114.3(15)	C(2)-C(1)-H(1C)	76.2
C(14')-C(15')-Yb(2)	82.5(11)	H(1B)-C(1)-H(1C)	134.6
N(6)-C(15')-H(15C)	108.7	C(2')-C(1)-H(1D)	108.1
C(14')-C(15')-H(15C)	108.7	N(1)-C(1)-H(1D)	108.2
Yb(2)-C(15')-H(15C)	145.4	C(2)-C(1)-H(1D)	132.7
N(6)-C(15')-H(15D)	108.7	H(1A)-C(1)-H(1D)	71.3
C(14')-C(15')-H(15D)	108.7	H(1C)-C(1)-H(1D)	106.0
Yb(2)-C(15')-H(15D)	98.9	N(2)-C(4)-C(5)	110.6(5)

C(5)-C(4)-Yb(1)	73.4(3)	N(1)-C(10)-C(9)	113.3(5)
N(2)-C(4)-H(4A)	109.5	C(9)-C(10)-Yb(1)	78.6(3)
C(5)-C(4)-H(4A)	109.5	N(1)-C(10)-H(10A)	108.9
Yb(1)-C(4)-H(4A)	130.7	C(9)-C(10)-H(10A)	108.9
N(2)-C(4)-H(4B)	109.5	Yb(1)-C(10)-H(10A)	154.8
C(5)-C(4)-H(4B)	109.5	N(1)-C(10)-H(10B)	108.9
Yb(1)-C(4)-H(4B)	117.2	C(9)-C(10)-H(10B)	108.9
H(4A)-C(4)-H(4B)	108.1	Yb(1)-C(10)-H(10B)	91.6
N(3)-C(5)-C(4)	112.6(6)	H(10A)-C(10)-H(10B)	107.7
N(3)-C(5)-Yb(1)	52.0(3)	N(1)-C(11)-C(12)	116.9(5)
C(4)-C(5)-Yb(1)	78.5(4)	N(1)-C(11)-H(11A)	108.1
N(3)-C(5)-H(5A)	109.1	C(12)-C(11)-H(11A)	108.1
C(4)-C(5)-H(5A)	109.1	N(1)-C(11)-H(11B)	108.1
Yb(1)-C(5)-H(5A)	160.5	C(12)-C(11)-H(11B)	108.1
N(3)-C(5)-H(5B)	109.1	H(11A)-C(11)-H(11B)	107.3
C(4)-C(5)-H(5B)	109.1	N(3)-C(12)-C(11)	115.9(5)
Yb(1)-C(5)-H(5B)	85.6	N(3)-C(12)-H(12A)	108.3
H(5A)-C(5)-H(5B)	107.8	C(11)-C(12)-H(12A)	108.3
N(3)-C(6)-C(7)	116.2(6)	N(3)-C(12)-H(12B)	108.3
N(3)-C(6)-H(6A)	108.2	C(11)-C(12)-H(12B)	108.3
C(7)-C(6)-H(6A)	108.2	H(12A)-C(12)-H(12B)	107.4
N(3)-C(6)-H(6B)	108.2	N(5)-C(13)-C(14')	117.9(9)
C(7)-C(6)-H(6B)	108.2	N(5)-C(13)-C(14)	112.1(8)
H(6A)-C(6)-H(6B)	107.4	N(5)-C(13)-H(13A)	109.9
C(6)-C(7)-C(8)	117.5(5)	C(14')-C(13)-H(13A)	130.3
C(6)-C(7)-H(7A)	107.9	C(14)-C(13)-H(13A)	109.8
C(8)-C(7)-H(7A)	107.9	N(5)-C(13)-H(13B)	109.6
C(6)-C(7)-H(7B)	107.9	C(14')-C(13)-H(13B)	71.1
C(8)-C(7)-H(7B)	107.9	C(14)-C(13)-H(13B)	109.6
H(7A)-C(7)-H(7B)	107.2	H(13A)-C(13)-H(13B)	105.6
N(4)-C(8)-C(7)	118.2(5)	N(5)-C(13)-H(13C)	109.4
N(4)-C(8)-H(8A)	107.8	C(14')-C(13)-H(13C)	108.5
C(7)-C(8)-H(8A)	107.8	C(14)-C(13)-H(13C)	74.8
N(4)-C(8)-H(8B)	107.8	H(13B)-C(13)-H(13C)	134.9
C(7)-C(8)-H(8B)	107.8	N(5)-C(13)-H(13D)	107.8
H(8A)-C(8)-H(8B)	107.1	C(14')-C(13)-H(13D)	107.1
N(4)-C(9)-C(10)	111.0(5)	C(14)-C(13)-H(13D)	137.4
C(10)-C(9)-Yb(3)	92.0(4)	H(13A)-C(13)-H(13D)	68.3
N(4)-C(9)-H(9A)	109.4	H(13C)-C(13)-H(13D)	105.4
C(10)-C(9)-H(9A)	109.4	N(6)-C(16)-C(17)	109.4(6)
Yb(3)-C(9)-H(9A)	76.6	C(17)-C(16)-Yb(2)	72.8(4)
N(4)-C(9)-H(9B)	109.4	N(6)-C(16)-H(16A)	109.8
C(10)-C(9)-H(9B)	109.4	C(17)-C(16)-H(16A)	109.8
Yb(3)-C(9)-H(9B)	154.1	Yb(2)-C(16)-H(16A)	129.4
H(9A)-C(9)-H(9B)	108.0	N(6)-C(16)-H(16B)	109.8

C(17)-C(16)-H(16B)	109.8	N(5)-C(22)-H(22B)	108.5
Yb(2)-C(16)-H(16B)	118.3	C(21)-C(22)-H(22B)	108.5
H(16A)-C(16)-H(16B)	108.3	Yb(2)-C(22)-H(22B)	91.0
N(7)-C(17)-C(16)	112.3(6)	H(22A)-C(22)-H(22B)	107.5
N(7)-C(17)-Yb(2)	51.9(3)	N(5)-C(23)-C(24)	117.7(6)
C(16)-C(17)-Yb(2)	79.0(4)	N(5)-C(23)-H(23A)	107.9
N(7)-C(17)-H(17A)	109.1	C(24)-C(23)-H(23A)	107.9
C(16)-C(17)-H(17A)	109.1	N(5)-C(23)-H(23B)	107.9
Yb(2)-C(17)-H(17A)	160.7	C(24)-C(23)-H(23B)	107.9
N(7)-C(17)-H(17B)	109.1	H(23A)-C(23)-H(23B)	107.2
C(16)-C(17)-H(17B)	109.1	N(7)-C(24)-C(23)	114.9(6)
Yb(2)-C(17)-H(17B)	84.9	N(7)-C(24)-H(24A)	108.5
H(17A)-C(17)-H(17B)	107.9	C(23)-C(24)-H(24A)	108.5
N(7)-C(18)-C(19)	116.2(6)	N(7)-C(24)-H(24B)	108.5
N(7)-C(18)-H(18A)	108.2	C(23)-C(24)-H(24B)	108.5
C(19)-C(18)-H(18A)	108.2	H(24A)-C(24)-H(24B)	107.5
N(7)-C(18)-H(18B)	108.2	N(9)-C(25)-C(26)	115.4(6)
C(19)-C(18)-H(18B)	108.2	N(9)-C(25)-H(25A)	108.4
H(18A)-C(18)-H(18B)	107.4	C(26)-C(25)-H(25A)	108.4
C(18)-C(19)-C(20)	116.8(6)	N(9)-C(25)-H(25B)	108.4
C(18)-C(19)-H(19A)	108.1	C(26)-C(25)-H(25B)	108.4
C(20)-C(19)-H(19A)	108.1	H(25A)-C(25)-H(25B)	107.5
C(18)-C(19)-H(19B)	108.1	C(27)-C(26)-C(25)	116.4(7)
C(20)-C(19)-H(19B)	108.1	C(27)-C(26)-Yb(3)	76.5(4)
H(19A)-C(19)-H(19B)	107.3	C(25)-C(26)-Yb(3)	78.8(4)
N(8)-C(20)-C(19)	118.2(6)	C(27)-C(26)-H(26A)	108.2
N(8)-C(20)-H(20A)	107.8	C(25)-C(26)-H(26A)	108.2
C(19)-C(20)-H(20A)	107.8	Yb(3)-C(26)-H(26A)	167.6
N(8)-C(20)-H(20B)	107.8	C(27)-C(26)-H(26B)	108.2
C(19)-C(20)-H(20B)	107.8	C(25)-C(26)-H(26B)	108.2
H(20A)-C(20)-H(20B)	107.1	Yb(3)-C(26)-H(26B)	60.3
N(8)-C(21)-C(22)	110.6(6)	H(26A)-C(26)-H(26B)	107.3
C(22)-C(21)-Yb(1)	90.8(4)	N(10)-C(27)-C(26)	111.5(6)
N(8)-C(21)-H(21A)	109.5	C(26)-C(27)-Yb(3)	76.6(4)
C(22)-C(21)-H(21A)	109.5	N(10)-C(27)-H(27A)	109.3
Yb(1)-C(21)-H(21A)	77.2	C(26)-C(27)-H(27A)	109.3
N(8)-C(21)-H(21B)	109.5	Yb(3)-C(27)-H(27A)	127.1
C(22)-C(21)-H(21B)	109.5	N(10)-C(27)-H(27B)	109.3
Yb(1)-C(21)-H(21B)	154.8	C(26)-C(27)-H(27B)	109.3
H(21A)-C(21)-H(21B)	108.1	Yb(3)-C(27)-H(27B)	119.6
N(5)-C(22)-C(21)	115.1(7)	H(27A)-C(27)-H(27B)	108.0
C(21)-C(22)-Yb(2)	80.0(4)	N(10)-C(28)-C(29)	109.3(5)
N(5)-C(22)-H(22A)	108.5	C(29)-C(28)-Yb(3)	72.6(3)
C(21)-C(22)-H(22A)	108.5	N(10)-C(28)-H(28A)	109.8
Yb(2)-C(22)-H(22A)	155.0	C(29)-C(28)-H(28A)	109.8

Yb(3)-C(28)-H(28A)	126.2	N(9)-C(34)-H(34B)	109.3
N(10)-C(28)-H(28B)	109.8	C(33)-C(34)-H(34B)	109.3
C(29)-C(28)-H(28B)	109.8	H(34A)-C(34)-H(34B)	108.0
Yb(3)-C(28)-H(28B)	121.5	N(9)-C(35)-C(36)	118.6(6)
H(28A)-C(28)-H(28B)	108.3	C(36)-C(35)-Yb(3)	78.7(4)
N(11)-C(29)-C(28)	110.9(6)	N(9)-C(35)-H(35A)	107.7
N(11)-C(29)-Yb(3)	50.8(3)	C(36)-C(35)-H(35A)	107.7
C(28)-C(29)-Yb(3)	78.9(4)	Yb(3)-C(35)-H(35A)	98.6
N(11)-C(29)-H(29A)	109.5	N(9)-C(35)-H(35B)	107.7
C(28)-C(29)-H(29A)	109.5	C(36)-C(35)-H(35B)	107.7
Yb(3)-C(29)-H(29A)	159.8	Yb(3)-C(35)-H(35B)	149.7
N(11)-C(29)-H(29B)	109.5	H(35A)-C(35)-H(35B)	107.1
C(28)-C(29)-H(29B)	109.5	N(11)-C(36)-C(35)	116.0(6)
Yb(3)-C(29)-H(29B)	85.2	N(11)-C(36)-H(36A)	108.3
H(29A)-C(29)-H(29B)	108.0	C(35)-C(36)-H(36A)	108.3
N(11)-C(30)-C(31)	116.3(6)	N(11)-C(36)-H(36B)	108.3
N(11)-C(30)-H(30A)	108.2	C(35)-C(36)-H(36B)	108.3
C(31)-C(30)-H(30A)	108.2	H(36A)-C(36)-H(36B)	107.4
N(11)-C(30)-H(30B)	108.2	C(41)-O(3)-C(44)	105.0(7)
C(31)-C(30)-H(30B)	108.2	O(3)-C(41)-C(42)	105.9(7)
H(30A)-C(30)-H(30B)	107.4	O(3)-C(41)-H(41A)	110.5
C(30)-C(31)-C(32)	117.0(6)	C(42)-C(41)-H(41A)	110.5
C(30)-C(31)-H(31A)	108.0	O(3)-C(41)-H(41B)	110.5
C(32)-C(31)-H(31A)	108.0	C(42)-C(41)-H(41B)	110.5
C(30)-C(31)-H(31B)	108.0	H(41A)-C(41)-H(41B)	108.7
C(32)-C(31)-H(31B)	108.0	C(41)-C(42)-C(43)	105.2(7)
H(31A)-C(31)-H(31B)	107.3	C(41)-C(42)-H(42A)	110.7
N(12)-C(32)-C(31)	118.2(6)	C(43)-C(42)-H(42A)	110.7
N(12)-C(32)-H(32A)	107.8	C(41)-C(42)-H(42B)	110.7
C(31)-C(32)-H(32A)	107.8	C(43)-C(42)-H(42B)	110.7
N(12)-C(32)-H(32B)	107.8	H(42A)-C(42)-H(42B)	108.8
C(31)-C(32)-H(32B)	107.8	C(44)-C(43)-C(42)	103.0(7)
H(32A)-C(32)-H(32B)	107.1	C(44)-C(43)-H(43A)	111.2
N(12)-C(33)-C(34)	114.1(6)	C(42)-C(43)-H(43A)	111.2
C(34)-C(33)-Yb(2)	93.3(4)	C(44)-C(43)-H(43B)	111.2
N(12)-C(33)-H(33A)	108.7	C(42)-C(43)-H(43B)	111.2
C(34)-C(33)-H(33A)	108.7	H(43A)-C(43)-H(43B)	109.1
Yb(2)-C(33)-H(33A)	78.0	O(3)-C(44)-C(43)	107.0(8)
N(12)-C(33)-H(33B)	108.7	O(3)-C(44)-H(44A)	110.3
C(34)-C(33)-H(33B)	108.7	C(43)-C(44)-H(44A)	110.3
Yb(2)-C(33)-H(33B)	153.3	O(3)-C(44)-H(44B)	110.3
H(33A)-C(33)-H(33B)	107.6	C(43)-C(44)-H(44B)	110.3
N(9)-C(34)-C(33)	111.6(6)	H(44A)-C(44)-H(44B)	108.6
N(9)-C(34)-H(34A)	109.3	C(11)-N(1)-C(10)	111.4(5)
C(33)-C(34)-H(34A)	109.3	C(11)-N(1)-C(1)	109.3(5)

C(10)-N(1)-C(1)	109.4(5)	C(34)-N(9)-C(25)	110.4(6)
C(11)-N(1)-Yb(1)	110.6(4)	C(35)-N(9)-C(25)	109.6(6)
C(10)-N(1)-Yb(1)	105.7(4)	C(34)-N(9)-Yb(3)	108.0(4)
C(1)-N(1)-Yb(1)	110.4(4)	C(35)-N(9)-Yb(3)	105.9(4)
C(3)-N(2)-C(4)	108.4(8)	C(25)-N(9)-Yb(3)	109.6(4)
C(4)-N(2)-C(3')	123.7(9)	C(28)-N(10)-C(27)	113.4(5)
C(3)-N(2)-Yb(1)	124.9(7)	C(28)-N(10)-Yb(3)	119.9(4)
C(4)-N(2)-Yb(1)	117.9(4)	C(27)-N(10)-Yb(3)	122.4(4)
C(3')-N(2)-Yb(1)	115.5(9)	C(29)-N(11)-C(36)	111.4(5)
C(5)-N(3)-C(12)	112.0(5)	C(29)-N(11)-C(30)	107.1(6)
C(5)-N(3)-C(6)	109.1(5)	C(36)-N(11)-C(30)	111.1(5)
C(12)-N(3)-C(6)	110.7(5)	C(29)-N(11)-Yb(3)	101.2(4)
C(5)-N(3)-Yb(1)	99.7(4)	C(36)-N(11)-Yb(3)	110.4(4)
C(12)-N(3)-Yb(1)	111.9(4)	C(30)-N(11)-Yb(3)	115.2(4)
C(6)-N(3)-Yb(1)	113.0(4)	C(33)-N(12)-C(32)	109.1(5)
C(8)-N(4)-C(9)	111.2(5)	C(33)-N(12)-Yb(3)	112.4(4)
C(8)-N(4)-Yb(1)	112.1(4)	C(32)-N(12)-Yb(3)	114.5(4)
C(9)-N(4)-Yb(1)	113.9(4)	C(33)-N(12)-Yb(2)	107.4(4)
C(8)-N(4)-Yb(3)	119.1(4)	C(32)-N(12)-Yb(2)	119.4(4)
C(9)-N(4)-Yb(3)	106.0(4)	Yb(3)-N(12)-Yb(2)	93.20(18)
Yb(1)-N(4)-Yb(3)	93.47(17)	Yb(1)-O(1)-Yb(2)	100.9(2)
C(22)-N(5)-C(23)	111.9(6)	Yb(1)-O(1)-Yb(3)	99.6(2)
C(22)-N(5)-C(13)	110.4(6)	Yb(2)-O(1)-Yb(3)	100.0(2)
C(23)-N(5)-C(13)	109.6(6)	N(2)-Yb(1)-O(1)	119.1(2)
C(22)-N(5)-Yb(2)	105.3(4)	N(2)-Yb(1)-N(4)	145.4(2)
C(23)-N(5)-Yb(2)	110.0(4)	O(1)-Yb(1)-N(4)	84.28(18)
C(13)-N(5)-Yb(2)	109.5(4)	N(2)-Yb(1)-N(8)	99.5(2)
C(15')-N(6)-C(16)	122.5(10)	O(1)-Yb(1)-N(8)	82.59(18)
C(16)-N(6)-C(15)	109.3(8)	N(4)-Yb(1)-N(8)	109.15(18)
C(15')-N(6)-Yb(2)	115.6(9)	N(2)-Yb(1)-N(1)	76.5(2)
C(16)-N(6)-Yb(2)	119.9(4)	O(1)-Yb(1)-N(1)	100.50(18)
C(15)-N(6)-Yb(2)	121.9(7)	N(4)-Yb(1)-N(1)	74.19(17)
C(17)-N(7)-C(18)	108.5(6)	N(8)-Yb(1)-N(1)	175.77(17)
C(17)-N(7)-C(24)	110.9(5)	N(2)-Yb(1)-N(3)	74.4(2)
C(18)-N(7)-C(24)	110.3(6)	O(1)-Yb(1)-N(3)	164.52(18)
C(17)-N(7)-Yb(2)	99.6(4)	N(4)-Yb(1)-N(3)	80.28(17)
C(18)-N(7)-Yb(2)	114.1(4)	N(8)-Yb(1)-N(3)	103.51(18)
C(24)-N(7)-Yb(2)	112.9(4)	N(1)-Yb(1)-N(3)	74.24(18)
C(20)-N(8)-C(21)	109.9(5)	N(2)-Yb(1)-C(5)	52.0(2)
C(20)-N(8)-Yb(2)	113.7(4)	O(1)-Yb(1)-C(5)	166.96(18)
C(21)-N(8)-Yb(2)	113.0(4)	N(4)-Yb(1)-C(5)	108.16(18)
C(20)-N(8)-Yb(1)	121.0(4)	N(8)-Yb(1)-C(5)	89.44(18)
C(21)-N(8)-Yb(1)	105.8(4)	N(1)-Yb(1)-C(5)	87.00(18)
Yb(2)-N(8)-Yb(1)	92.46(19)	N(3)-Yb(1)-C(5)	28.34(18)
C(34)-N(9)-C(35)	113.2(6)	N(2)-Yb(1)-C(3')	25.2(4)

O(1)-Yb(1)-C(3')	95.6(4)	N(6)-Yb(2)-N(8)	144.1(2)
N(4)-Yb(1)-C(3')	143.3(4)	O(1)-Yb(2)-N(8)	83.73(18)
N(8)-Yb(1)-C(3')	107.2(4)	N(6)-Yb(2)-N(12)	99.7(2)
N(1)-Yb(1)-C(3')	69.8(4)	O(1)-Yb(2)-N(12)	83.27(18)
N(3)-Yb(1)-C(3')	96.1(4)	N(8)-Yb(2)-N(12)	109.82(18)
C(5)-Yb(1)-C(3')	76.8(4)	N(6)-Yb(2)-N(7)	73.2(2)
N(2)-Yb(1)-C(4)	24.2(2)	O(1)-Yb(2)-N(7)	163.06(18)
O(1)-Yb(1)-C(4)	143.15(19)	N(8)-Yb(2)-N(7)	79.60(19)
N(4)-Yb(1)-C(4)	128.78(18)	N(12)-Yb(2)-N(7)	105.19(19)
N(8)-Yb(1)-C(4)	97.98(18)	N(6)-Yb(2)-N(5)	76.3(2)
N(1)-Yb(1)-C(4)	77.81(18)	O(1)-Yb(2)-N(5)	98.2(2)
N(3)-Yb(1)-C(4)	50.98(19)	N(8)-Yb(2)-N(5)	74.08(19)
C(5)-Yb(1)-C(4)	28.1(2)	N(12)-Yb(2)-N(5)	176.00(19)
C(3')-Yb(1)-C(4)	48.7(4)	N(7)-Yb(2)-N(5)	74.3(2)
N(2)-Yb(1)-C(21)	72.9(2)	N(6)-Yb(2)-C(17)	51.2(2)
O(1)-Yb(1)-C(21)	92.37(18)	O(1)-Yb(2)-C(17)	168.49(18)
N(4)-Yb(1)-C(21)	135.28(18)	N(8)-Yb(2)-C(17)	107.47(19)
N(8)-Yb(1)-C(21)	26.86(18)	N(12)-Yb(2)-C(17)	90.24(19)
N(1)-Yb(1)-C(21)	149.30(18)	N(7)-Yb(2)-C(17)	28.44(18)
N(3)-Yb(1)-C(21)	99.37(17)	N(5)-Yb(2)-C(17)	87.7(2)
C(5)-Yb(1)-C(21)	76.12(18)	N(6)-Yb(2)-C(15')	24.5(4)
C(3')-Yb(1)-C(21)	81.4(4)	O(1)-Yb(2)-C(15')	97.2(4)
C(4)-Yb(1)-C(21)	75.28(18)	N(8)-Yb(2)-C(15')	143.7(4)
N(2)-Yb(1)-C(10)	102.9(2)	N(12)-Yb(2)-C(15')	106.3(4)
O(1)-Yb(1)-C(10)	86.22(18)	N(7)-Yb(2)-C(15')	94.4(4)
N(4)-Yb(1)-C(10)	50.20(16)	N(5)-Yb(2)-C(15')	69.9(4)
N(8)-Yb(1)-C(10)	157.60(17)	C(17)-Yb(2)-C(15')	75.4(4)
N(1)-Yb(1)-C(10)	26.46(16)	N(6)-Yb(2)-C(33)	73.9(2)
N(3)-Yb(1)-C(10)	83.06(17)	O(1)-Yb(2)-C(33)	92.82(18)
C(5)-Yb(1)-C(10)	104.62(18)	N(8)-Yb(2)-C(33)	135.28(19)
C(3')-Yb(1)-C(10)	93.1(4)	N(12)-Yb(2)-C(33)	26.14(19)
C(4)-Yb(1)-C(10)	102.58(17)	N(7)-Yb(2)-C(33)	101.13(19)
C(21)-Yb(1)-C(10)	174.20(18)	N(5)-Yb(2)-C(33)	149.9(2)
N(2)-Yb(1)-Yb(3)	152.77(16)	C(17)-Yb(2)-C(33)	77.42(18)
O(1)-Yb(1)-Yb(3)	40.47(13)	C(15')-Yb(2)-C(33)	81.0(4)
N(4)-Yb(1)-Yb(3)	43.91(12)	N(6)-Yb(2)-C(16)	23.1(2)
N(8)-Yb(1)-Yb(3)	95.08(13)	O(1)-Yb(2)-C(16)	143.60(19)
N(1)-Yb(1)-Yb(3)	89.14(12)	N(8)-Yb(2)-C(16)	128.32(18)
N(3)-Yb(1)-Yb(3)	124.16(12)	N(12)-Yb(2)-C(16)	98.19(18)
C(5)-Yb(1)-Yb(3)	151.45(14)	N(7)-Yb(2)-C(16)	50.96(19)
C(3')-Yb(1)-Yb(3)	127.8(4)	N(5)-Yb(2)-C(16)	78.39(19)
C(4)-Yb(1)-Yb(3)	166.87(13)	C(17)-Yb(2)-C(16)	28.21(19)
C(21)-Yb(1)-Yb(3)	117.70(13)	C(15')-Yb(2)-C(16)	47.2(4)
C(10)-Yb(1)-Yb(3)	64.30(11)	C(33)-Yb(2)-C(16)	76.16(18)
N(6)-Yb(2)-O(1)	120.5(2)	N(6)-Yb(2)-C(22)	102.7(2)

O(1)-Yb(2)-C(22)	84.44(19)	N(12)-Yb(3)-C(9)	135.22(18)
N(8)-Yb(2)-C(22)	50.0(2)	N(4)-Yb(3)-C(9)	26.85(16)
N(12)-Yb(2)-C(22)	157.55(19)	N(11)-Yb(3)-C(9)	98.63(18)
N(7)-Yb(2)-C(22)	82.6(2)	N(9)-Yb(3)-C(9)	149.95(18)
N(5)-Yb(2)-C(22)	26.4(2)	C(29)-Yb(3)-C(9)	74.77(18)
C(17)-Yb(2)-C(22)	104.7(2)	N(10)-Yb(3)-C(28)	23.3(2)
C(15')-Yb(2)-C(22)	93.8(4)	O(1)-Yb(3)-C(28)	145.44(19)
C(33)-Yb(2)-C(22)	173.8(2)	N(12)-Yb(3)-C(28)	128.61(18)
C(16)-Yb(2)-C(22)	102.84(19)	N(4)-Yb(3)-C(28)	96.34(18)
N(6)-Yb(2)-Yb(3)	120.02(16)	N(11)-Yb(3)-C(28)	50.73(19)
O(1)-Yb(2)-Yb(3)	40.22(13)	N(9)-Yb(3)-C(28)	81.09(19)
N(8)-Yb(2)-Yb(3)	95.73(12)	C(29)-Yb(3)-C(28)	28.55(19)
N(12)-Yb(2)-Yb(3)	43.21(13)	C(9)-Yb(3)-C(28)	73.66(18)
N(7)-Yb(2)-Yb(3)	144.66(14)	N(10)-Yb(3)-C(35)	63.1(2)
N(5)-Yb(2)-Yb(3)	138.43(16)	O(1)-Yb(3)-C(35)	124.96(19)
C(17)-Yb(2)-Yb(3)	133.20(14)	N(12)-Yb(3)-C(35)	80.54(18)
C(15')-Yb(2)-Yb(3)	108.3(4)	N(4)-Yb(3)-C(35)	152.31(18)
C(33)-Yb(2)-Yb(3)	58.11(13)	N(11)-Yb(3)-C(35)	52.0(2)
C(16)-Yb(2)-Yb(3)	132.41(13)	N(9)-Yb(3)-C(35)	26.44(19)
C(22)-Yb(2)-Yb(3)	121.14(14)	C(29)-Yb(3)-C(35)	64.5(2)
N(10)-Yb(3)-O(1)	122.8(2)	C(9)-Yb(3)-C(35)	133.24(17)
N(10)-Yb(3)-N(12)	142.89(19)	C(28)-Yb(3)-C(35)	59.58(19)
O(1)-Yb(3)-N(12)	83.20(18)	N(10)-Yb(3)-C(26)	49.3(2)
N(10)-Yb(3)-N(4)	100.75(19)	O(1)-Yb(3)-C(26)	82.2(2)
O(1)-Yb(3)-N(4)	82.48(17)	N(12)-Yb(3)-C(26)	120.4(2)
N(12)-Yb(3)-N(4)	109.28(17)	N(4)-Yb(3)-C(26)	125.41(19)
N(10)-Yb(3)-N(11)	72.4(2)	N(11)-Yb(3)-C(26)	106.5(2)
O(1)-Yb(3)-N(11)	163.05(19)	N(9)-Yb(3)-C(26)	51.9(2)
N(12)-Yb(3)-N(11)	79.86(18)	C(29)-Yb(3)-C(26)	97.5(2)
N(4)-Yb(3)-N(11)	103.04(18)	C(9)-Yb(3)-C(26)	103.15(19)
N(10)-Yb(3)-N(9)	76.1(2)	C(28)-Yb(3)-C(26)	70.3(2)
O(1)-Yb(3)-N(9)	98.53(19)	C(35)-Yb(3)-C(26)	62.6(2)
N(12)-Yb(3)-N(9)	73.90(19)	N(10)-Yb(3)-C(27)	22.5(2)
N(4)-Yb(3)-N(9)	176.79(18)	O(1)-Yb(3)-C(27)	103.98(19)
N(11)-Yb(3)-N(9)	76.8(2)	N(12)-Yb(3)-C(27)	138.17(19)
N(10)-Yb(3)-C(29)	51.8(2)	N(4)-Yb(3)-C(27)	112.50(19)
O(1)-Yb(3)-C(29)	167.76(19)	N(11)-Yb(3)-C(27)	88.9(2)
N(12)-Yb(3)-C(29)	107.18(19)	N(9)-Yb(3)-C(27)	64.31(19)
N(4)-Yb(3)-C(29)	87.83(19)	C(29)-Yb(3)-C(27)	72.9(2)
N(11)-Yb(3)-C(29)	28.09(18)	C(9)-Yb(3)-C(27)	86.09(19)
N(9)-Yb(3)-C(29)	90.8(2)	C(28)-Yb(3)-C(27)	44.57(19)
N(10)-Yb(3)-C(9)	74.23(19)	C(35)-Yb(3)-C(27)	61.4(2)
O(1)-Yb(3)-C(9)	93.33(17)	C(26)-Yb(3)-C(27)	27.0(2)

Table XXXIX. Anisotropic Displacement Parameters ($Å^2$ x10^3) for 25.

	U^{11}	U^{22}	U^{33}	U^{23}	U^{13}	U^{12}
C(4)	7(3)	45(4)	16(3)	4(3)	-1(3)	-3(3)
C(5)	11(3)	33(4)	18(4)	9(3)	1(3)	11(3)
C(6)	18(4)	16(4)	21(4)	1(3)	9(3)	4(3)
C(7)	23(4)	13(3)	16(3)	-4(3)	8(3)	-2(3)
C(8)	16(3)	17(3)	6(3)	-4(3)	4(2)	-4(3)
C(9)	6(3)	23(4)	14(3)	2(3)	3(2)	4(3)
C(10)	10(3)	21(4)	7(3)	3(3)	-3(2)	-3(3)
C(11)	6(3)	38(4)	14(3)	-4(3)	0(2)	-4(3)
C(12)	12(3)	25(4)	15(3)	5(3)	6(3)	9(3)
C(13)	40(5)	38(5)	24(4)	-18(4)	-9(4)	11(4)
C(16)	20(4)	34(4)	13(3)	-1(3)	5(3)	10(3)
C(17)	16(4)	32(4)	19(4)	7(3)	6(3)	2(3)
C(18)	33(4)	20(4)	16(4)	10(3)	10(3)	1(3)
C(19)	28(4)	22(4)	24(4)	8(3)	10(3)	7(3)
C(20)	26(4)	19(4)	15(3)	4(3)	11(3)	8(3)
C(21)	20(4)	33(4)	13(3)	0(3)	2(3)	12(3)
C(22)	20(4)	50(6)	27(4)	0(4)	4(3)	-1(4)
C(23)	17(4)	65(6)	11(3)	-8(4)	-3(3)	14(4)
C(24)	18(4)	47(5)	10(3)	8(3)	0(3)	14(4)
C(25)	26(4)	18(4)	28(4)	8(3)	7(3)	9(3)
C(26)	29(5)	21(4)	47(5)	13(4)	-8(4)	-3(4)
C(27)	24(4)	27(4)	26(4)	11(3)	1(3)	-3(3)
C(28)	15(4)	36(4)	12(3)	7(3)	-5(3)	0(3)
C(29)	25(4)	36(5)	11(3)	-10(3)	-2(3)	-4(3)
C(30)	22(4)	24(4)	18(4)	-4(3)	-7(3)	-5(3)
C(31)	13(4)	24(4)	27(4)	-2(3)	-7(3)	-8(3)
C(32)	8(3)	19(4)	29(4)	2(3)	-2(3)	-6(3)
C(33)	7(3)	31(4)	35(4)	10(3)	7(3)	6(3)
C(34)	21(4)	32(4)	13(3)	3(3)	3(3)	14(3)
C(35)	14(4)	34(4)	23(4)	9(3)	-1(3)	8(3)
C(36)	13(3)	31(3)	16(3)	5(3)	-5(2)	2(3)
O(3)	27(4)	121(7)	49(4)	19(5)	6(3)	-2(4)
C(41)	55(7)	78(8)	29(5)	-6(5)	3(5)	-16(6)
C(42)	60(7)	19(5)	75(7)	1(5)	-9(6)	11(4)
C(43)	36(5)	31(5)	31(4)	-2(4)	17(4)	-2(4)
C(44)	51(7)	64(7)	54(6)	11(6)	17(5)	13(6)
N(1)	7(3)	15(3)	18(3)	-4(2)	-1(2)	-2(2)
N(2)	18(3)	25(3)	26(3)	-10(3)	-7(3)	0(3)
N(3)	14(3)	15(3)	12(3)	2(2)	1(2)	3(2)
N(4)	5(2)	10(3)	8(2)	-1(2)	3(2)	2(2)

N(5)	23(3)	41(4)	15(3)	-9(3)	-1(2)	8(3)
N(6)	16(3)	18(3)	31(3)	-4(3)	7(3)	2(3)
N(7)	18(3)	29(4)	11(3)	1(2)	7(2)	6(3)
N(8)	15(3)	22(3)	6(2)	1(2)	3(2)	6(2)
N(9)	12(3)	24(3)	22(3)	6(3)	3(2)	6(2)
N(10)	16(3)	24(3)	10(3)	9(2)	-1(2)	0(2)
N(11)	14(3)	30(3)	9(3)	2(2)	-5(2)	1(3)
N(12)	7(3)	16(3)	16(3)	4(2)	-4(2)	-1(2)
O(1)	21(3)	34(3)	25(3)	0(2)	1(2)	8(2)
Yb(1)	6(1)	15(1)	7(1)	-1(1)	-1(1)	2(1)
Yb(2)	8(1)	16(1)	8(1)	1(1)	2(1)	4(1)
Yb(3)	5(1)	13(1)	8(1)	2(1)	-1(1)	0(1)
I(1)	17(1)	24(1)	17(1)	-1(1)	0(1)	-4(1)

The anisotropic displacement factor exponent takes the form:

$-2\pi^2[\, h^2\, a^{*2} U^{11} + \ldots + 2\, h\, k\, a^*\, b^*\, U^{12}\,]$

Table XL. Hydrogen Coordinates and Isotropic Displacement Parameters ($Å^2$ x 10^3) for 25.

	x	y	z	U(eq)
H(2A)	8234	3824	1352	33
H(2B)	7459	4698	1510	33
H(3A)	7891	3317	1944	33
H(3B)	6673	3808	1937	33
H(14A)	2057	4279	2758	33
H(14B)	2404	5176	2468	33
H(15A)	1545	4714	1987	33
H(15B)	803	4447	2370	33
H(1A)	7158	4293	792	33
H(1B)	6065	4332	1035	33
H(13A)	3998	4158	2689	33
H(13B)	3887	4254	2204	33
H(37A)	3736	6140	1941	47
H(37B)	3525	5689	1477	47
H(38A)	3846	7700	1704	47
H(38B)	3191	7265	1288	47
H(39A)	4773	7516	936	47
H(39B)	5464	7837	1363	47
H(40A)	5201	5901	1020	47

H(40B)	6307	6370	1257	47
H(2'1)	7238	4674	1512	24
H(2'2)	5946	4410	1486	24
H(3'1)	6321	3716	2034	24
H(3'2)	7632	3605	1948	24
H(14C)	2633	5236	2321	24
H(14D)	2998	4688	1911	24
H(15C)	978	4570	2299	24
H(15D)	1205	4620	1810	24
H(1C)	7495	4111	921	24
H(1D)	6245	4432	862	24
H(13C)	3475	4153	2733	24
H(13D)	4274	4193	2366	24
H(37C)	3162	6673	1318	53
H(37D)	3402	6939	1807	53
H(38C)	4247	5361	1487	53
H(38D)	4904	5943	1867	53
H(39C)	6258	6323	1436	53
H(39D)	5542	5834	1046	53
H(40C)	5867	7757	1127	53
H(40D)	4842	7285	842	53
H(4A)	7815	1596	2060	27
H(4B)	8242	1933	1614	27
H(5A)	7834	262	1549	25
H(5B)	6658	390	1765	25
H(6A)	5628	-386	1251	22
H(6B)	6699	-622	986	22
H(7A)	5068	-810	564	20
H(7B)	5815	69	387	20
H(8A)	3880	459	335	16
H(8B)	3817	365	830	16
H(9A)	4708	2165	56	17
H(9B)	5765	1536	244	17
H(10A)	6298	3203	224	16
H(10B)	5213	3538	465	16
H(11A)	8039	2558	1023	23
H(11B)	7776	2488	529	23
H(12A)	7105	940	561	21
H(12B)	8127	924	906	21
H(16A)	-315	2963	2208	27
H(16B)	611	2902	2591	27
H(17A)	144	1264	2438	27
H(17B)	219	1445	1945	27
H(18A)	1371	110	1858	27
H(18B)	1378	-188	2342	27

H(19A)	2861	-987	2033	30
H(19B)	3353	-231	2383	30
H(20A)	4427	-209	1782	23
H(20B)	3347	127	1500	23
H(21A)	5489	1200	2227	26
H(21B)	4364	949	2462	26
H(22A)	4994	2505	2678	39
H(22B)	5061	2873	2204	39
H(23A)	2281	2925	2831	37
H(23B)	3398	2366	3001	37
H(24A)	2839	893	2742	30
H(24B)	1685	1360	2886	30
H(25A)	1750	5216	979	28
H(25B)	1248	5431	514	28
H(26A)	3137	5861	536	39
H(26B)	3503	4818	743	39
H(27A)	2639	5015	-98	31
H(27B)	3955	4940	34	31
H(28A)	3384	3262	-491	26
H(28B)	2139	3683	-428	26
H(29A)	1863	1984	-505	29
H(29B)	2967	1721	-216	29
H(30A)	2021	624	171	26
H(30B)	860	816	-90	26
H(31A)	502	25	532	26
H(31B)	-59	1108	526	26
H(32A)	753	711	1191	23
H(32B)	1955	587	998	23
H(33A)	93	2485	1337	29
H(33B)	-37	2355	840	29
H(34A)	-106	4050	978	26
H(34B)	1019	3998	1276	26
H(35A)	1063	4216	38	29
H(35B)	-75	4062	273	29
H(36A)	-30	2398	207	24
H(36B)	372	2791	-233	24
H(41A)	9534	6662	985	65
H(41B)	9159	6088	1398	65
H(42A)	11218	6658	1313	63
H(42B)	10705	6531	1767	63
H(43A)	10817	8178	1864	39
H(43B)	11312	8308	1406	39
H(44A)	9299	8918	1572	67
H(44B)	9629	8628	1106	67